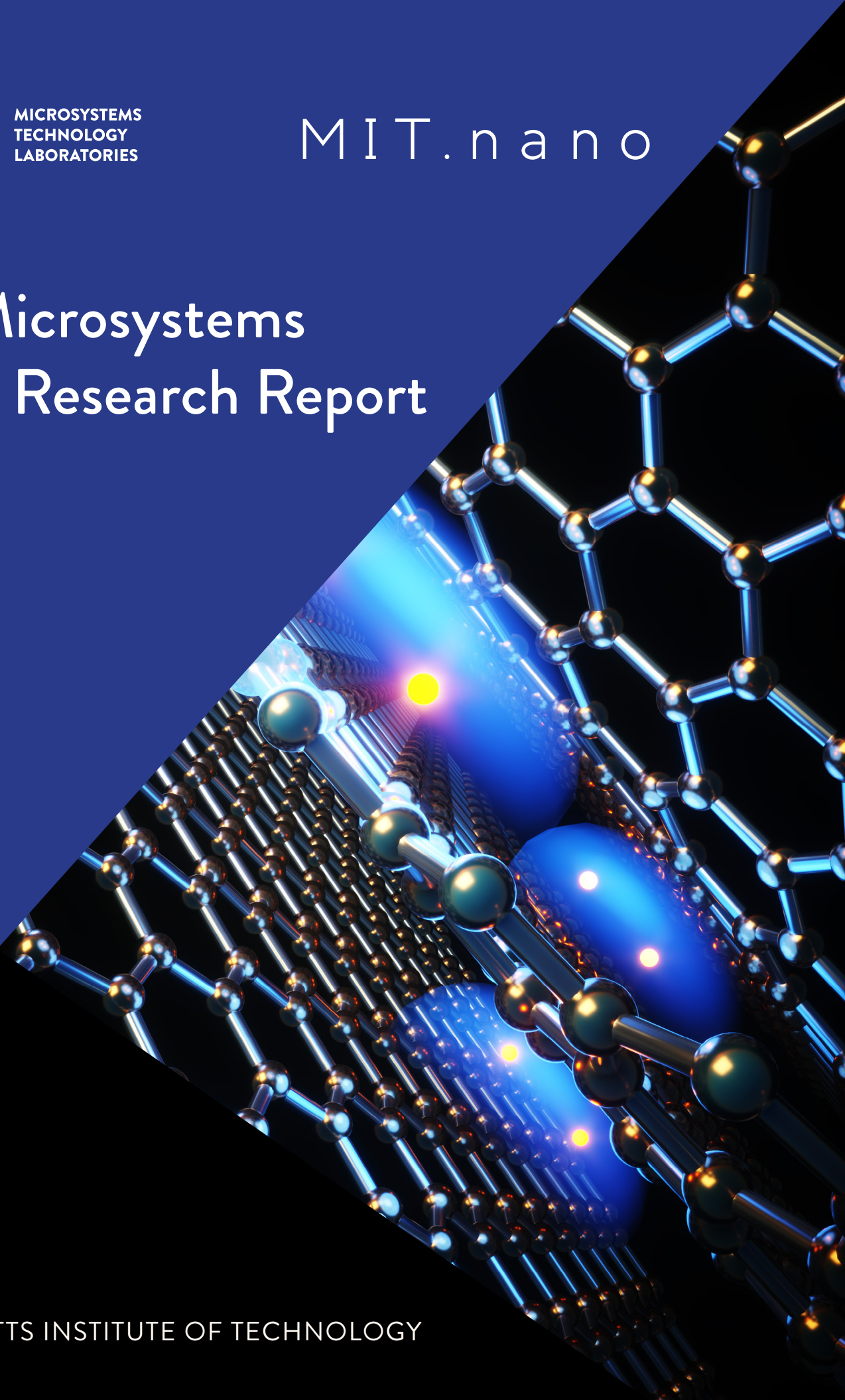


2021 Microsystems Annual Research Report



CONTENTS

Foreword	i
Acknowledgments	iii
RESEARCH ABSTRACTS	
Biological, Medical Devices, and Systems	1
Circuits & Systems for Communications, IoT, and Machine Learning	20
Electronic, Magnetic, Superconducting, and Neuromorphic Devices	42
Machine Learning, Neural Networks, AI	64
MEMS, Field-Emitter, Thermal, and Fluidic Devices	75
Nanotechnology, Nanostructures, Nanomaterials	92
Photonics and Optoelectronics	107
Nano Explorations Videos	126
Research Centers	127
Faculty Profiles	132
Theses Awarded	174
Glossary	178

Foreword

We are pleased to bring to you the 2021 Microsystems Annual Research Report.

The core mission of Microsystems Technology Laboratories (MTL) has always been to foster interdisciplinary research and education as well as strong industrial relation in microsystems and technology. MTL has maintained a wide footprint of research that encompasses broad areas of disciplines. They include nanoscale technology and materials as well as nano and microscale devices and systems. MTL's research portfolio includes a diverse array of novel devices including electronic, magnetic, field emitter, thermal, fluidic, superconducting and quantum devices, as well as integrated circuits and systems, machine learning and neuromorphic computing, biological and medical devices and systems, photonics, and energy.

Since MTL's research has been at the forefront of technology, an advanced, flexible fabrication facility has always been a central element of MTL. The ultramodern MIT.nano facility was completed in 2018, replacing the aging facility at MTL. The availability of such an advanced, grand-scale fabrication facility is dramatically improving not only MTL's position in cutting-edge research but also that of the entire MIT community. MTL has been closely collaborating with and financially supporting MIT.nano since 2016. The Microsystems Annual Research Conference (MARC), MTL's flagship student-organized technical conference, was administered and sponsored jointly by MTL and MIT.nano for the first time in 2020, then again in 2021. Also, since 2020, Microsystems Annual Research Report has become a joint effort between MTL and MIT.nano.

This year's MTL/MIT.nano joint Microsystems Annual Research Report represents a broad cross-section of the MIT community, with 37+ faculty, 118 students, postdoctoral associates, and research staff participating. As the pages ahead demonstrate, an astonishing range of insights and innovations emerge from the MTL community and users of MIT's shared facilities. It is a privilege to serve these remarkable communities. On behalf MTL and MIT.nano, we thank every contributor to this year's Microsystems Annual Research Report, as well as the staff of both organizations who worked tirelessly to produce such a beautiful volume. We hope you thoroughly enjoy the 2021 Microsystems Annual Research Report.

Hae-Seung Lee
Director, Microsystems Technology Laboratories

Vladimir Bulović
Director, MIT.nano

August 2021

Acknowledgments

MICROSYSTEMS INDUSTRIAL GROUP

Analog Devices, Inc.
Applied Materials
Draper
Edwards
HARTING
Hitachi High-Tech Corporation
IBM
Lam Research Co.
NEC
TSMC
Texas Instruments

MTL LEADERSHIP TEAM

Hae-Seung Lee, Director
Duane S. Boning, Associate Director, Computation
Vicky Diadiuk, Associate Director, Facilities
Jing Kong, Associate Director,
Diversity, Equity and Inclusion
Jeffrey H. Lang, Associate Director
Stacy McDaid, Administrative Officer

MTL POLICY BOARD

Vladimir Bulović
Vicky Diadiuk
Hae-Seung Lee
Tomás Palacios
Charles G. Sodini
Carl V. Thompson

MTL TECHNICAL STAFF

Michael J. Hobbs, Systems Administrator
Thomas J. Lohman, Project Leader, Computation
William T. Maloney, Systems Manager
Paul J. McGrath, Research Specialist
Michael McIlrath, Research Scientist

MTL ADMINISTRATIVE STAFF

Joseph Baylon, Administrative Assistant
Kathleen Brody, Administrative Assistant
Kristin Cook, Financial Officer
Elizabeth Green, Senior Administrative Assistant
Elizabeth Kubicki, Administrative Assistant
Ludmila Leoparde, Financial Officer
Meghan Melvin, Communications Administrator
Jami L. Mitchell, Administrative Assistant
Steven O'Hearn, Administrative Assistant
Jessie-Leigh Thomas, Administrative Assistant

PROCESS TECHNOLOGY COMMITTEE

Vicky Diadiuk, Chair
Akintunde I. Akinwande
Xiaowei Cai
Winston Chern
Nadim Chowdhury
Jeffrey H. Lang
Derek Kita
Eveline Postelnicu
Jörg Scholvin
Max Shulaker
Saima Afroz Siddiqui
Tathagata Srimani

MTL SEMINAR SERIES COMMITTEE

Luis Velásquez-García, Chair
Jeffrey H. Lang
Jami L. Mitchell
Vivienne Sze

MARC2021 CONFERENCE ORGANIZERS

STEERING COMMITTEE

Hae-Seung (Harry) Lee, MTL Director
Vladimir Bulović, MIT.nano Director
Stacy McDaid, Administrative Officer
Meghan Melvin, Proceedings / Design
Amanda Stoll, Proceedings / Design
Jami L. Mitchell, Logistics
Shereece Beckford, Logistics
Catherine Bourgeois, Logistics
Jessica Boles, Conference Co-Chair
Qingyun Xie, Conference Co-Chair

CORE COMMITTEE

Jatin Patil, Website / Proceedings
Haoquan (Tony) Zhang, Conference Platform
Sarah Muschinske, Outreach
Nili Persits, Communications Training
Kaidong Peng, Social / Networking Activities
John Niroula, Conference Package

SESSION CHAIRS

Eric Bersin, Quantum Technologies
Benjamin Cary, Power
Nadim Chowdhury, Electronic Devices
Kruthika Kikkeri, Biotechnologies
Jane Lai, Energy-Efficient AI
Ting-An Lin, COVID-19-Applicable Technologies
Elaine McVay, Nanostructures and Nanomaterials
Rishabh Mittal, Integrated Circuits
Milica Notaros, Optics and Photonics
Haozhe Wang, Materials and Manufacturing

MIT.NANO CONSORTIUM

Agilent Technologies
Analog Devices, Inc.
Dow
Draper
DSM
Edwards
Fujikura
IBM
Lam Research
NCSOFT
NEC
Oxford Instruments Asylum Research
Raith
Waters

MIT.NANO LEADERSHIP TEAM

Vladimir Bulović, Director, MIT.nano
Brian Anthony, Associate Director
Kathleen Boisvert, Administrative Officer
Tom Gearty, Communications and Initiatives Director
Tina Gilman, Assistant Director of
Programs and Member Relations
Dennis Grimard, Managing Director
Whitney R. Hess, Manager, Safety
Systems and Programs
Nicholas Menounos, Assistant
Director of Infrastructure
Anna Osharov, Assistant Director of User
Services for Characterization
Jorg Scholvin, Assistant Director of
User Services for Fabrication

MIT.NANO STAFF

Daniel A. Adams, Research Specialist
Shereece Beckford, Events and Projects Coordinator
Robert J. Bicchieri, Research Specialist
Kurt A. Broderick, Research Associate
David Dunham, EHS DLC Officer
Samantha Farrell, Senior Administrative Assistant
Donal Jamieson, Research Specialist
Ludmila Leoparde, Financial Officer
Gongqin Li, Sponsored Research Technical Staff
Eric Lim, Research Engineer
Paul J. McGrath, Research Specialist
Kristofor R. Payer, Research Specialist
Aubrey Penn, Research Specialist
Scott J. Poesse, Research Specialist
and Technical Instructor
Gary Riggott, Research Specialist
Amanda Stoll, Communications
and Marketing Assistant
David M. Terry, Sponsored Research Technical Staff
Paul S. Tierney, Research Specialist

Timothy K. Turner, Project Technician
Electro - Mechanical
Annie I. Wang, Research Scientist
Dennis J. Ward, Research Specialist

AFFILIATED STAFF FROM OTHER DLCS

Anuradha Murthy Agarwal, Principal
Research Scientist
Edward Brignole, Assistant Director, Dept. of Biology
Jim Daley, Research Specialist
Rami Dana, Research Scientist
Vicky Diadiuk, MTL Associate Director
Phat Vinh Dip, Research Scientist, Dept. of Biology
Michael Hobbs, Systems Manager
Thomas Lohman, Senior Software
Developer/Systems Manager
Bill Maloney, Systems Manager
Mark K. Mondol, Assistant Director,
NanoStructures Laboratory
Praneeth Namburi, Postdoctoral Associate
Mark Rapoza, Area Manager, Dept. of Facilities
Travis Wanat, Project Manager, Dept. of Facilities
Samantha Young, Administrative
Assistant II/Mech Eng

MIT.NANO LEADERSHIP COUNCIL

Brian Anthony, MIT.nano
Robert Atkins, Lincoln Laboratory
Karl Berggren, NSL, EECS
Kathy Boisvert, MIT.nano
Vladimir Bulović, MIT.nano
Dennis Grimard, MIT.nano
Pablo Jarillo-Herrero, Physics
James LeBeau, DMSE
Hae-Seung Lee, MTL, EECS
Will Oliver, RLE, Physics
Tomás Palacios, EECS
Katharina Ribbeck, BioEng
Frances Ross, DMSE
Thomas Schwartz, Biology
Carl Thompson, MRL, DMSE

MIT.NANO FACULTY ADVOCATES WORKING GROUP - CHARACTERIZATION.NANO

Jim LeBeau, Faculty Lead, DMSE
Anna Osharov, Technical Lead, MIT.nano
Karl Berggren, NSL, EECS
A. John Hart, MechE
Long Ju, Physics
Benedetto Marelli, CEE
Yogesh Surendranath, Chemistry

MIT.NANO FACULTY ADVOCATES WORKING GROUP - FAB.NANO

Tomás Palacios – Faculty Lead, EECS
Jorg Scholvin – Technical Lead, MIT.nano
Vicky Diadiuk – Technical Lead, MTL
Tayo Akinwande, EECS
Karl Berggren, EECS
Jesus A. del Alamo, EECS
Dirk Englund, EECS
Juejun Hu, MechE
Pablo Jarillo-Herrero, Physics
Jeehwan Kim, MechE/DMSE
Jing Kong, EECS
Farnaz Niroui, EECS
Will Oliver, EECS
Caroline Ross, DMSE
Max Shulaker, EECS

MIT.NANO INTERNAL ADVISORY BOARD

Marc Baldo – Director, RLE; EECS
Anantha Chandrakasan – Dean,
School of Engineering; EECS
John Deutch – Chemistry
Elazer Edelman – Director, IMES
Jeff Grossman – Department Head, DMSE
Paula T. Hammond – Department Head, ChemE
Susan Hockfield – President Emerita
and Professor of Neuroscience
Craig Keast – Lincoln Laboratory
Nergis Mavalvala, Dean, School of Science; Physics
Chris Schuh – DMSE
Michael Sipser – Math
Krystyn Van Vliet – Associate Provost, DMSE
Evelyn Wang – Department Head, MechE

Biological, Medical Devices, and Systems

Rethinking Plant-Based Materials Production: Selective Growth of Tunable Materials via Cell Culture	3
Absolute Blood Pressure Waveform Monitoring using Philips Ultrasound Probe	4
Electrochemical Neuromodulation Using Electrodes Coated with Ion-Selective Membranes	5
Ultrasound-Based Cerebral Arterial Blood Flow Measurement	6
Force-Coupled Ultrasound for Noninvasive Venous Pressure Assessment	7
An Electrokinetic-Based Concentrator for Ultra-Low Abundant Target Detection.....	8
Micro/Nanofluidic Technologies for Next-Generation Biomanufacturing.....	9
Measuring Eye Movement Features using Mobile Devices to Track Neurodegenerative Diseases.....	10
A Comparison of Microfluidic Methods for High-Throughput Cell Deformability Measurements	11
Electronics for Transparent, Long-Lasting Respirators	12
Self-Editing or “Lamarckian” Genomes Using the Bio/Nano TERCOM Approach.....	13
Balancing Actuation Energy and Computing Energy in Motion Planning.....	14
Absolute Blood Pressure Measurement using Machine Learning Algorithms on Ultrasound-based Signals	15
Analytical and Numerical Modeling of an Intracochlear Hydrophone for Fully Implantable Assistive Hearing Devices.....	16
Fluorescent Janus Droplet and Its Application in Biosensing of <i>Listeria Monocytogenes</i>	17
Dance-Inspired Investigation of Human Movement	18
Nanoscale Insights into the Mechanisms of Cellular Growth and Proliferation	19

Rethinking Plant-Based Materials Production: Selective Growth of Tunable Materials via Cell Culture

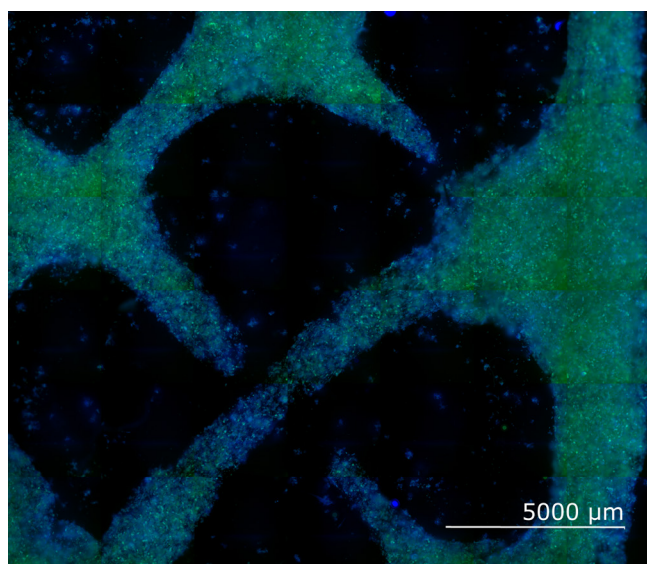
A. L. Beckwith, J. T. Borenstein, L. F. Velásquez-García
Sponsorship: Draper Fellowship Program

Current systems for plant-based materials production are inefficient and place unsustainable demands on environmental resources. Traditionally cultivated crops present low yields of industrially useful components and require extensive post-harvest processing to remove extraneous portions of the plants. Large-scale monoculture remains the unchallenged standard for biomass production despite the negative impacts of the practice to the surrounding biome as well as a susceptibility to season, climate, and local resource availability. This work proposes a novel solution to these shortcomings based on the selective cultivation of useful, tunable plant tissues using scalable, land-free techniques. By limiting biomass cultivation to only desirable plant tissues, *ex planta* farming promises to improve yields while reducing plant waste and competition for arable land.

Employing a *Zinnia elegans* model system, we provide the first proof-of-concept demonstration of isolated, tissue-like plant material production by way of gel-mediated cell culture. Parameters governing

cell development and morphology including hormone concentrations, medium pH, and initial cell density are optimized and implemented to demonstrate the tunability of cultured biomaterials at cellular and macroscopic scales. Targeted deposition of cell-doped, nutrient-rich gel scaffolds via injection molding and 3D bioprinting enable biomaterial growth in near-final form (Figure 1), reducing downstream processing requirements. These investigations demonstrate the implementation of plant cell culture in a new application space, propose novel methods for quantification and evaluation of cell development, and characterize morphological developments in response to critical culture parameters—illustrating the feasibility and potential of the proposed techniques.

The proposed concept of selectively grown, tunable plant materials via gel-mediated cell culture is believed to be the first of its kind. This work uniquely quantifies and modulates cell development of cultured primary plant products to optimize and direct growth of plant materials.



▲ Figure 1: Bioprinted culture, with vascular cell types, grown to confluency.

FURTHER READING

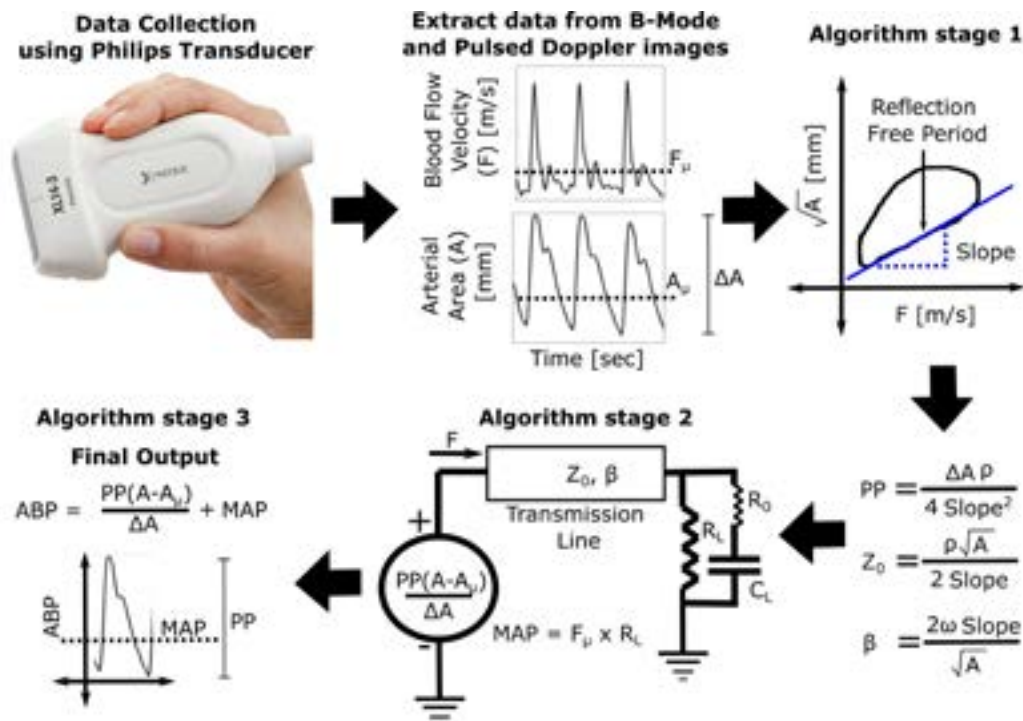
- A. L. Beckwith, J. T. Borenstein, and L. F. Velásquez-García, "Tunable Plant-based Materials via *In Vitro* Cell Culture Using a *Zinnia Elegans* Model," *J Cleaner Production*, vol. 288, pp. 125571, Mar. 2021., DOI: 10.1016/j.jclepro.2020.125571.
- A. L. Beckwith, J. T. Borenstein, and L. F. Velásquez-García, "Monolithic, 3D-printed Microfluidic Platform for Recapitulation of Dynamic Tumor Microenvironments," *J Microelectromech Syst*, vol. 27, 6, pp.1009-1022, Oct. 2018, DOI: 10.1109/JMEMS.2018.2869327.
- A. L. Beckwith, L. F. Velásquez-García, and J. T. Borenstein, "Microfluidic Model for Evaluation of Immune Checkpoint Inhibitors in Human Tumors," *Advanced Healthcare Materials*, vol. 8, 11, pp. 1900289, Jun. 2019, DOI: 10.1002/adhm.201900289.

Absolute Blood Pressure Waveform Monitoring using Philips Ultrasound Probe

A. Chandrasekhar, A. Aguirre, C. G. Sodini, H.-S. Lee
Sponsorship: MEDRC-Philips, MIT J-Clinic, CICS

In an Intensive Care Unit (ICU), physicians use an invasive radial catheter to measure blood pressure (BP) to track the hemodynamic status of the subject, and these measurements are neither easy nor feasible to perform outside an ICU environment. In such non-ICU settings as a step-down clinical ward or an outpatient clinic, clinicians prefer to use a non-invasive arm-cuff device to measure BP. Even though these measurements are convenient, these devices cannot record the absolute BP (ABP) waveform. Hence, strong interest exists in developing a non-invasive device to monitor the ABP waveform as a quantitative option to perform rapid hemodynamic profiling of patients who cannot undergo invasive BP measurements.

This project uses a Philips ultrasound-based transducer (XL-143) to measure BP from superficial arteries (carotid and brachial) proximal to the heart. We measure the arterial diameter and blood flow velocity waveforms from these arteries; an algorithm computes BP from this data in three stages, as illustrated in Figure 1. The algorithm uses the arterial area (A) calculated from arterial diameter and the blood flow velocity (F) waveforms to estimate the height of the ABP waveform, known as pulse pressure (PP), via standard fluid dynamics principles. Further, the algorithm uses a transmission line model of the human vasculature to estimate the mean arterial pressure (MAP).



▲ Figure 1: An algorithm to estimate absolute blood pressure waveform from ultrasound signals.

FURTHER READING

- J. Seo, "A Non-invasive Central Arterial Pressure Waveform Estimation System using Ultrasonography for Real-time Monitoring," Ph.D. dissertation, Massachusetts Institute of Technology, Cambridge, 2018.

Electrochemical Neuromodulation Using Electrodes Coated with Ion-Selective Membranes

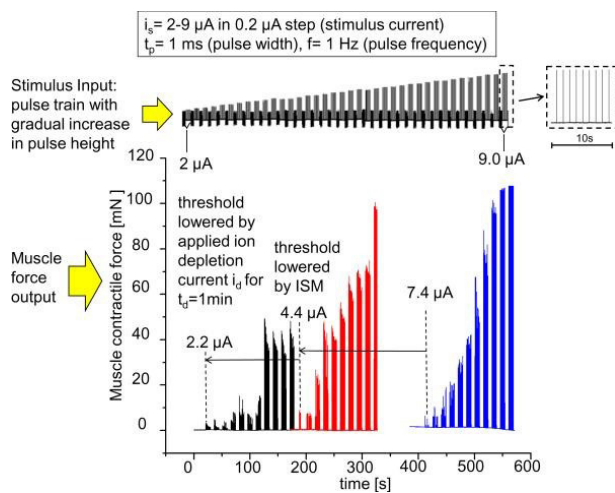
M. T. Flavin, C. Lissandrello, J. Han
Sponsorship: Draper Laboratory

Developing precise and effective means of modulating the nervous system is a major challenge in neural prostheses. While modalities such as deep brain stimulation (DBS), vagus nerve stimulation, and electric acoustic stimulation (EAS) for cochlear implants are finally being realized on the clinical level, there still remains work to be done with respect to our ultimate goal. In the Micro/Nanofluidic BioMEMS research group, we are developing a type of electrode modified with an ion-selective material that can change the concentration of chemicals around a nerve, which will enhance the level of control compared to traditional electrical stimulation.

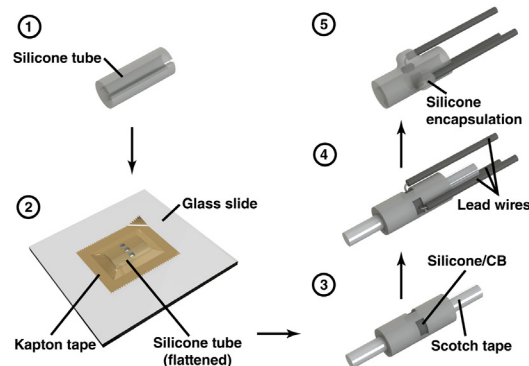
A type of material called the ion-selective membrane (ISM) has been used in the field of analytical chemistry for decades to measure ion concentrations. These membranes are composed of a polymer matrix modified with a chemical called an ionophore, which

makes them selective to a particular ion species. In work published by our group, the functionality of these electrodes was inverted, using them for electrochemical stimulation in *ex vivo* studies of a frog sciatic nerve (see Figure 1 from Song et al.).

As a continuation of this work, we are: (1) developing computational models that describe and predict physical behavior of chemical transport from galvanostatic operation of polymeric neutral-carrier based ion-selective membrane electrodes, (2) fabricating and characterizing practical devices for implementing ISM-based neuromodulation (see Figure 2 from Flavin et al.), and (3) employing prototype devices in *in vitro* and *in vivo* animal models. A successful implementation of this work will pave the way for more advanced operations such as central nervous system (CNS) intervention.



▲ Figure 1: Comparison of excitability of the frog sciatic nerve without and with modulating Ca^{2+} ion concentration. This represents one of the current applications of the ion-selective membrane (see Song et al.).



▲ Figure 2: Step-by-step fabrication of rapid manufactured cuff electrodes (Flavin et al.). We developed this technology to support our *in vivo* work.

FURTHER READING

- Y. A. Song, R. Melik, A. N. Rabie, et al. "Electrochemical activation and inhibition of neuromuscular systems through modulation of ion concentrations with ion-selective membranes," *Nature Materials*, vol. 10, pp. 980-986, Oct. 2011.
- M. T. Flavin, M. A. Paul, A. S. Lim, et al. "Rapid and low cost manufacturing of cuff electrodes," *Frontiers in Neuroscience*, vol. 15, p.

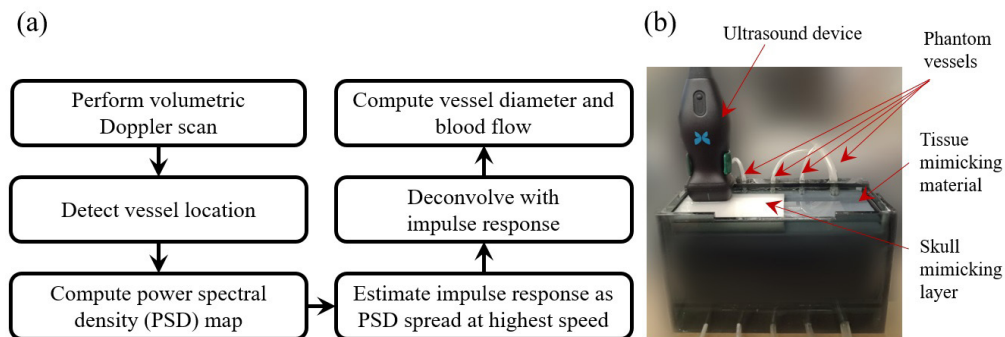
Ultrasound-Based Cerebral Arterial Blood Flow Measurement

S. M. Imaduddin, T. Heldt
Sponsorship: Analog Devices, Inc.

Ultrasound-based cerebral blood flow (CBF) monitoring is vital in the diagnosis and treatment of a variety of acute neurologic conditions. While flow velocity can be measured using Doppler ultrasound, accurate CBF measurement is difficult as vessel diameters cannot be determined reliably due to acoustic aberrations introduced by the skull and because cranial attenuation necessitates low frequency (1-2 MHz) insonation with poor spatial resolution.

We have developed a CBF estimation technique that achieves the spatial resolution required for

CBF determination by estimating the point spread function of the imaging system. The received data are then deconvolved to increase spatial resolution, and a correction is applied to account for cranial aberrations. Doppler data were collected from phantom blood vessels with diameters between 2 and 6 mm over a 150-mL/min range using a clinical ultrasound device. Our method achieved an RMSE of 26 mL/min, within acceptable range for cerebral perfusion monitoring at the bedside.



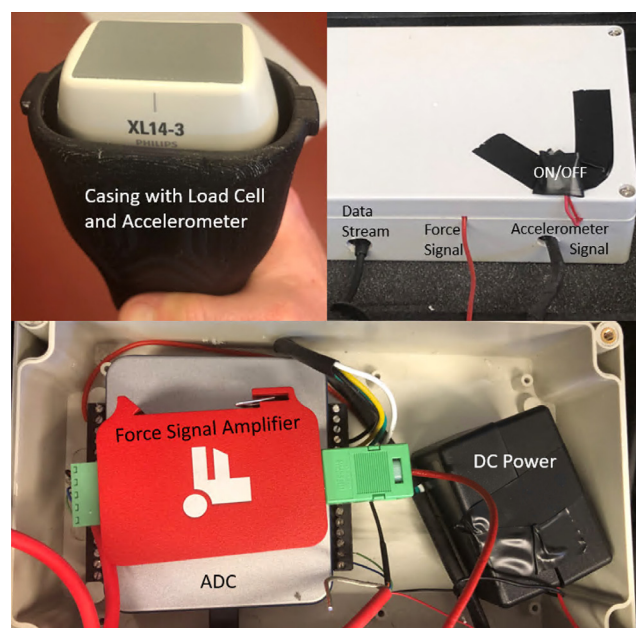
▲ Figure 1: (a) Flow chart of proposed measurement technique, and (b) Flow phantom used to test our method.

Force-Coupled Ultrasound for Noninvasive Venous Pressure Assessment

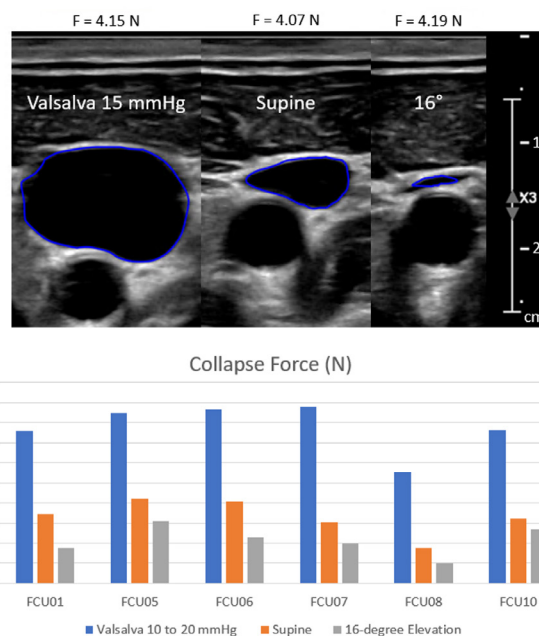
A. Jaffe, B. Anthony
Sponsorship: MEDRC-Philips

Congestive heart failure is a clinical syndrome that affects about 6 million people and accounts for about 1 in 9 deaths in the United States. In this condition, the pumping ability of the heart decreases, causing a buildup of blood volume and pressure in the venous system as it returns blood to the heart. This buildup further decreases the pumping ability of the heart by over-stretching its ventricles. Additionally, increased venous pressure can lead to fluid migrating from the veins to the interstitial space, which is called edema. Left unchecked, edema can lead to death. Proper administration of diuretic drugs can allow venous pressure to drop back down by lowering intravascular volume, which will improve a patient's condition. However, thus far, only invasive catheterization can produce an accurate and reliable venous pressure measurement.

Our goal is to produce an accurate, noninvasive means of assessing venous pressure by means of force-coupled ultrasound. By positioning our force-coupled ultrasound probe at the base of the neck, we can observe the compression of the internal jugular vein, which returns blood from the cerebral vasculature to the heart. Unlike in the case of an artery, we can safely observe compression from zero force all the way to complete occlusion of the vein. We can also observe compression of the internal jugular vein while increasing its pressure with the Valsalva maneuver, exhalation against a closed airway, and while decreasing its pressure by elevating it above the supine position. We expect these observations to give us excellent insight for our computational models to accurately assess venous pressure.



▲ Figure 1: Top left: Custom-made force-coupled ultrasound casing for Philips XL14-3 xMATRIX ultrasound probe. Top right: Closed electronics box with force and accelerometer analog inputs from the casing and data streaming to a tablet for data collection and display. Bottom: Electronics box components consisting of the DC power source of two series 9V batteries, the force signal amplifier, and the multi-channel analog-to-digital converter.



▲ Figure 2: Top: Merged force-coupled ultrasound images of the segmented internal jugular vein in the same individual during a Valsalva maneuver with an airway pressure of 15 mmHg (left), during normal breathing while lying flat (middle), and during normal breathing while elevated at an angle of 16 degrees above horizontal or supine position (right). Bar graph showing the force necessary to occlude different individuals' internal jugular veins at different venous pressures.

An Electrokinetic-Based Concentrator for Ultra-Low Abundant Target Detection

H. J. Kwon, E. Wynne, J. Han

Sponsorship: Federal Drug Administration, SMART CAMP

The recent COVID-19 outbreak has sparked urgent interest in rapid and reliable viral identification. In fact, this is a recurring challenge in many other pathogen detection and diagnostics, where only a few target viruses or bacterial cells are present in milliliters or even liters of volume, necessitating that a large volume of the sample must be concentrated for the targets to be introduced into the downstream detection system. Unfortunately, due to the size of the virus or biomolecule, concentrating or retrieving the virus or biomolecule with a filter, ultracentrifuge, or any kind of method is extremely hard.

Figure 1 (a) shows the purpose of this work and the overall concept. This technology is based on microfluidic devices that couple microchannel and cation exchange membrane (CEM) to play an electrophoretic force off a hydraulic drag force to enable charge-based concentration, without any physical filter. Under the electric field, the virus experiences the electrophoretic

force and hydraulic drag force at the same time. The electrophoretic force is driven by the intensive electric field focused near the CEM while drag force is driven simply by the hydraulic flow.

Efforts are being made to build electrokinetic concentrators using materials and processes that are more robust and scalable than those of traditional microfluidics. Instead of using polydimethylsiloxane (PDMS) that is patterned using photolithography, one can laser etch channels and ports into acrylic polymethyl methacrylate (PMMA). Thin adhesive films can have custom patterns cut into them using a digital die cutter and then be used to bond PMMA layers and seal channels. Designing the device in manner seen in Figure 1b also allows the use of ion-exchange membranes that are commonly used in electro dialysis and fuel cell systems, meaning these materials are robust and relatively inexpensive.

FURTHER READING

- H. J. Kwon, B. Lenneman, T. K. Lu, K. Choi, and J. Han, "An Electrokinetic-Based Large Volume Concentrator for Ultra-Low Abundant Target Detection," *uTAS*, pp. 35–36, 2020.

Micro/Nanofluidic Technologies for Next-Generation Biomanufacturing

T. Kwon, K. Choi, Z. Sun, J. Han

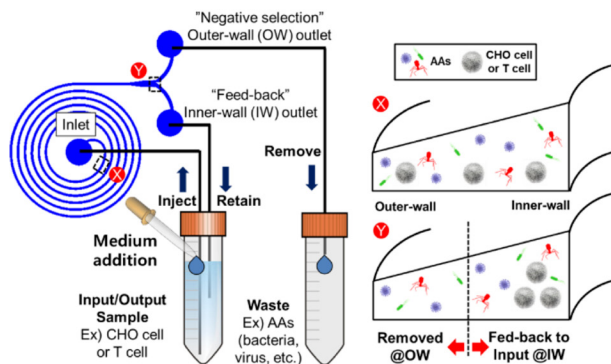
Sponsorship: The National Institute for Innovation in Manufacturing Biopharmaceuticals, U.S. Food and Drug Administration

Biomanufacturing of therapeutic proteins and vaccines is crucial for modern medicine. Recently, the biopharmaceutical industry started to focus more on process intensification through continuous biomanufacturing. New therapeutic modalities such as cell and gene therapies are rapidly emerging as well. Accordingly, it has become increasingly important for biomanufacturers to improve manufacturing efficiency, quality, and safety. Compared to conventional biomanufacturing technologies, micro/nanofluidic technologies can contribute to the improvement with their unique advantages. Here, we introduce our new micro/nanofluidic technologies for efficient, high-quality, and safe biomanufacturing.

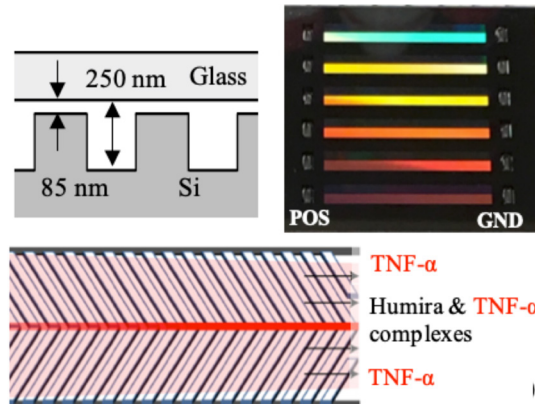
First, we developed spiral microfluidic devices for reliable and efficient perfusion culture and adventitious agent (AA) clearance. The devices enable size-based cell sorting without any physical barriers, so that mammalian cells can be continuously separated from cell culture. Using this feature, the spiral device was used for 1) cell retention for perfusion culture

and 2) rapid AA clearance (Figure 1). This microfluidic technology could overcome the limitations (biofouling, cell damage) of conventional cell separation techniques (e.g., membrane-based filtration, centrifugation).

Second, we introduce a new nanofluidic device for monitoring critical quality attributes (purity, binding affinity, glycosylation, etc.) of antibody therapeutics during biomanufacturing. The device has a nanofilter array and enables continuous-flow size or charge-based protein separation. Using this device, we demonstrated a fully automated continuous online protein-size monitoring during continuous perfusion culture. We are currently expanding the capability of the nanofluidic device to monitor binding affinity and glycosylation of antibodies at real-time speed (Figure 2). The technology could complement conventional protein-quality-monitoring equipment while producing a large amount of information about biologics quality.



▲ Figure 1: AA clearance using a spiral microfluidic device. AAs are removed towards the waste stream constantly while CHO cells or T-cells are retained and fed back to the input.



▲ Figure 2: Continuous monitoring of protein quality using a nanofluidic device. The device has a nanofilter array (85-nm shallow and 250-nm deep regions). It can concentrate Humira and TNF- α bound complexes.

FURTHER READING

- T. Kwon, H. Prentice, J. D. Oliveira, N. Madziva, M. E. Warkiani, J.-F. P. Hamel, and J. Han, "Microfluidic Cell Retention Device for Perfusion of Mammalian Suspension Culture," *Scientific Reports*, vol. 7, 6703, Jul. 2017.
- K. Choi, H. Ryu, K. J. Siddle, A. Piantadosi, L. Freimark, D. J. Park, P. Sabeti, and J. Han, "Negative Selection by Spiral Inertial Microfluidics Improves Viral Recovery and Sequencing from Blood," *Analytical Chemistry*, vol. 90, no. 7, pp. 4657–4662, Mar. 2018.
- T. Kwon, S. H. Ko, J.-F. P. Hamel, and J. Han, "Continuous Online Protein Quality Monitoring during Perfusion Culture Production Using an Integrated Micro/Nanofluidic System," *Analytical Chemistry*, vol. 92, no. 7, pp. 5267–5275, Mar. 2020.

Measuring Eye Movement Features using Mobile Devices to Track Neurodegenerative Diseases

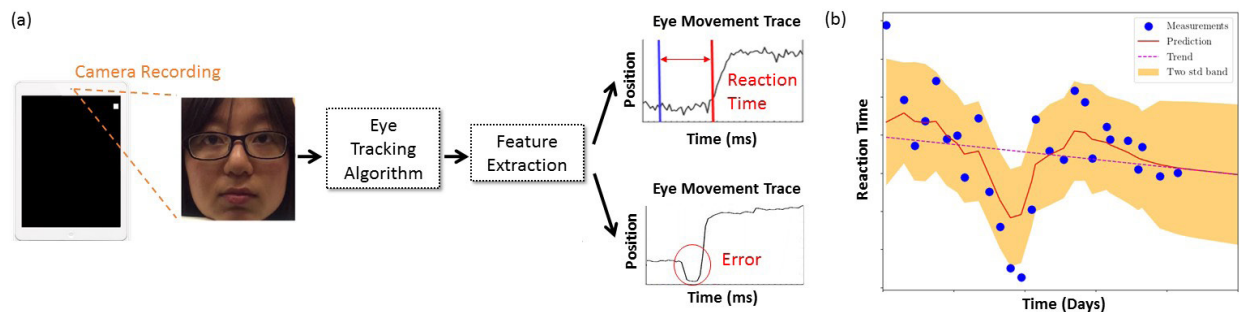
H.-Y. Lai, C. G. Sodini, T. Heldt, V. Sze
Sponsorship: MIT-IBM Watson AI Lab

Current clinical assessment of neurodegenerative diseases (e.g., Alzheimer's disease) requires trained specialists, is mostly qualitative, and is commonly done only intermittently. Therefore, these assessments are affected by an individual physician's clinical acumen and by a host of confounding factors, such as a patient's level of attention. Quantitative, objective, and more frequent measurements are needed to mitigate the influence of these factors.

A promising candidate for a quantitative and accessible diseases progression monitor is eye movement. In the clinical literature, an eye movement is often measured through a pro/anti-saccade task, where a subject is asked to look towards/away from a visual stimulus. Two features are observed to differ significantly between healthy subjects and patients: reaction time (time difference between a stimulus presentation and the initiation of the corresponding eye movement) and error rate (the proportion of eye movements towards the wrong direction).

However, these features are commonly measured with high-speed, IR-illuminated cameras, which limits accessibility. A portable measurement system is required to track them longitudinally.

Previously, we enabled ubiquitous tracking of eye-movement features by enabling app-based measurements of visual reaction time and error rates. In this work, we further show how we learn potential trends in these eye-movement features using Gaussian process modeling. Such modeling has allowed us to discover subjects' task-performing strategies such as trading off between speed and accuracy. We hope that once we have collected data from patients, we can use the model to a) compare the trends of the features with the clinical assessments, b) distinguish the effect of strategies from the effect of disease progression, and c) evaluate the potential to use our system to track disease progression more frequently and widely than previously possible.



▲ Figure 1: (a) Our measurement system includes the tablet-based video recording, an eye tracking algorithm, and feature extraction algorithms. (b) Example reaction-time measurements from a subject and the trend learned from the data.

FURTHER READING

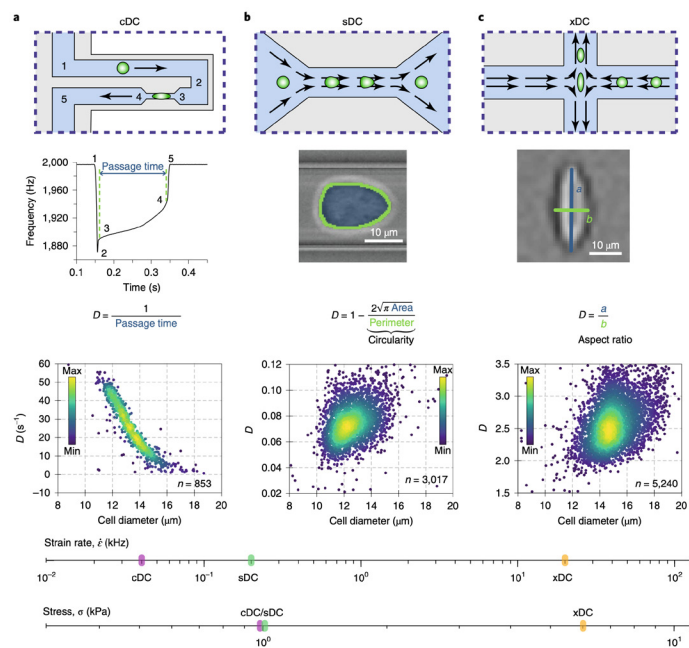
- H.-Y. Lai, G. Saavedra-Peña, C. G. Sodini, T. Heldt, and V. Sze, "App-based Saccade Latency and Error Determination Across the Adult Age Spectrum," *arXiv:2012.09723 [q-bio.NC]*, 2020.
- H.-Y. Lai, G. Saavedra-Peña, C. G. Sodini, V. Sze, and T. Heldt, "Measuring Saccade Latency Using Smartphone Cameras," *IEEE Journal of Biomedical and Health Informatics*, vol. 24, no. 3, pp. 885-897, 2020.
- H.-Y. Lai, G. Saavedra-Peña, C. G. Sodini, T. Heldt, and V. Sze, "Enabling Saccade Latency Measurements with Consumer-grade Cameras," *Proc. IEEE International Conference on Image Processing (ICIP)*, pp. 3169-3173, 2018.

A Comparison of Microfluidic Methods for High-Throughput Cell Deformability Measurements

M. Urbanska, H. Muñoz, J. Bagnall, O. Otto, S. R. Manalis, D. Di Carlo, J. Guck
Sponsorship: NIH, German Federal Ministry of Research and Education

The mechanical phenotype of a cell is an inherent biophysical marker of its state and function, with many applications in basic and applied biological research. Microfluidics-based methods have enabled single-cell mechanophenotyping at throughputs comparable to those of flow cytometry. As shown in Figure 1, we present a standardized cross-laboratory study comparing three microfluidics-based approaches for measuring cell mechanical phenotype: constriction-based deformability cytometry (cDC), shear flow deformability cytometry (sDC), and extensional flow deformability cytometry (xDC). All three methods detect cell

deformability changes induced by exposure to altered osmolarity. However, a dose-dependent deformability increase upon latrunculin B-induced actin disassembly was detected only with cDC and sDC, which suggests that when cells are exposed to the higher strain rate imposed by xDC, cellular components other than the actin cytoskeleton dominate the response. The direct comparison presented here furthers our understanding of the applicability of the different deformability cytometry methods and provides context for the interpretation of deformability measurements performed using different platforms.



▲ Figure 1: Comparison of the microfluidics-based approaches for the determination of cell deformability used in this study. a–c, Operation principle of cDC (a), sDC (b), and xDC (c). Schematic representation of the chip geometries used in the respective methods (top row). Overview of how the deformability, D , is defined for each method (middle row). The numbers 1–5 in the plot of frequency versus time correspond to the cell positions in the cDC microchannel indicated in the scheme above. Representative scatter plots of D versus cell diameter from the measurements of untreated HL60 cells (bottom row); n indicates number of cells; the measurements were repeated a total of 10, 9, and 8 times for cDC, sDC, and xDC, respectively. The color map corresponds to event density. The strain rate and stress applied to the cells in cDC, sDC, and xDC are indicated on the corresponding axes at the bottom of the panel.

FURTHER READING

- M. Urbanska, H. Muñoz, J. Bagnall, O. Otto, S. R. Manalis, D. Di Carlo and J. Guck, "A Comparison of Microfluidic Methods for High-throughput Cell Deformability Measurements," *Nature Methods*, vol. 17, no. 6, pp. 587–593, Jun. 2020.

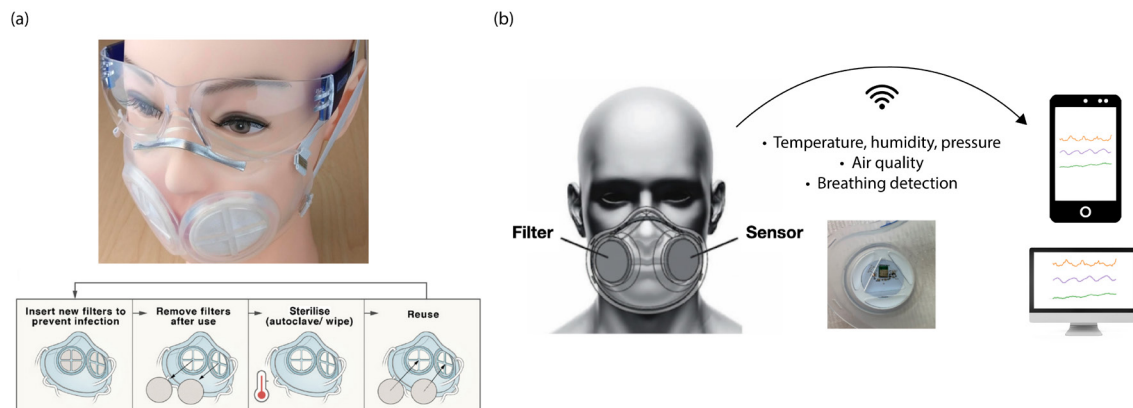
Electronics for Transparent, Long-Lasting Respirators

S. Orguc, A. Wentworth, J. Byrne, J. Sands, S. Maji, C. Tov, S. Babae, H. Huang, H. Boyce, P. R. Chai, S. Min, C. Li, J. N. Chu, A. Som, S. L. Becker, M. Gala, A. P. Chandrakasan, G. Traverso
Sponsorship: NIH

The use of personal protective equipment (PPE), including the N95 respirators and surgical masks, is essential in reducing airborne disease transmission, particularly during the COVID-19 pandemic. Unfortunately, there has been a shortage of PPE since the beginning of the pandemic. Also, the available N95 masks have major limitations, including masking facial features, waste, and lack of integrity after decontamination, forcing researchers to find alternatives.

This work presents a transparent, elastomeric, adaptable, long-lasting respirator with an integrated

biometric interface. The mask is made mostly of silicon rubber and comes with two replaceable filter cartridges. The electronic interface uses one of the filter insert locations to measure temperature, humidity, pressure, and air quality. The system uses Bluetooth Low Energy and sends real-time sensor data to a phone or a computer. The data can be used to inform the user regarding mask fit, fatigue, mask condition, and potential diagnostic information.



▲ Figure 1: (a) The respirator prototype. (b) System overview for the biometric sensor interface and the wireless operation.

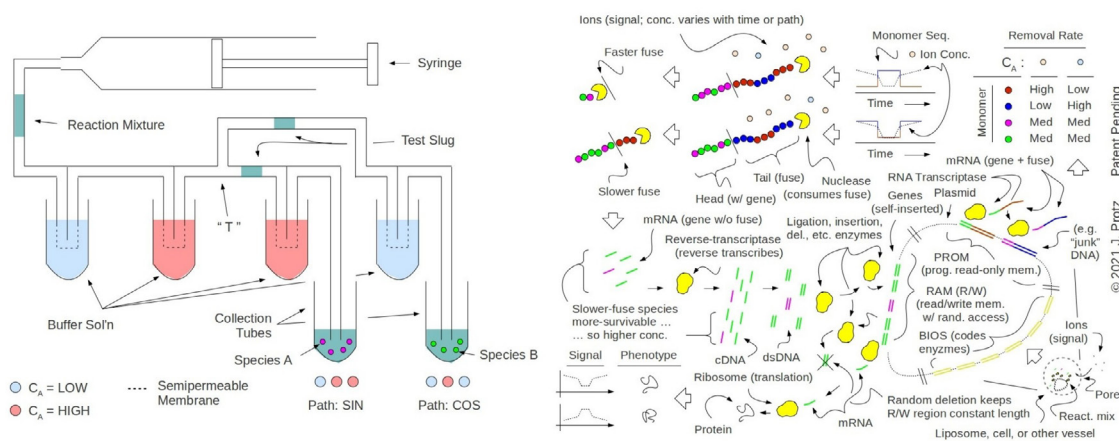
Self-Editing or “Lamarckian” Genomes Using the Bio/Nano TERCOM Approach

J. Protz

Sponsorship: Protz Lab Group; BioMolecular Nanodevices, LLC

Gene editing has been an area of active investigation for many decades. Some approaches introduce permanent edits; others modify expression. In this work, conceptually, cells or cell-free reactions estimate their location by correlating the evolution of their sensed fluid environment (e.g., temp., salinity, sugar, pH, ion concentration, etc.) against an embodied map and then self-edit the content of their genomes in a way that depends on said estimate; editing the genome shifts the expressed phenotype and the heritable genotype. This approach is related to terrain contour matching (TERCOM), a technique used in air navigation. Current efforts focus on a reaction mixture containing a plasmid that experiences path-dependent self-edits while en route to a target site. As envisioned (see Figure 1), a read-only so-called “junk DNA” segment of a plasmid transcribes into mRNA strands having coding heads and consumable tails; the tails are attacked by an exonuclease, the activity of which depends jointly on re-

moved monomer species and local ion concentration (or another environmental variable), causing the tails to function as path-sensitive fuses and the mix of surviving mRNA to depend on the path. The surviving mRNA is reverse-transcribed into DNA and integrated as expressible genes in a read-write portion of the plasmid; concurrent random erasures keep overall length roughly constant. In this process, the genetic composition of the read-write region evolves with the changing environmental path. A related heritage effort explores drug delivery using particles that exhibit path-dependent doses or conformation. The current and heritage efforts build on prior study by the PI and his group of nanoparticles that record the trajectory of their environment. An experimental apparatus has been designed to test these various TERCOM-like reaction mixtures. Progress on the present effort may allow the engineering of organisms that exhibit Lamarckian evolution or gene therapies that confer this ability.



▲ Figure 1: Illustration of concept: (a) apparatus to test sensitivity to path of reaction and delivered genome; (b) nuclease with environmental and substrate sensitivity consumes transcribed RNA's protective tail; RNA with path-matching tails survives and is reverse-transcribed and incorporated into plasmid DNA, causing genetic composition of plasmid to depend on path.

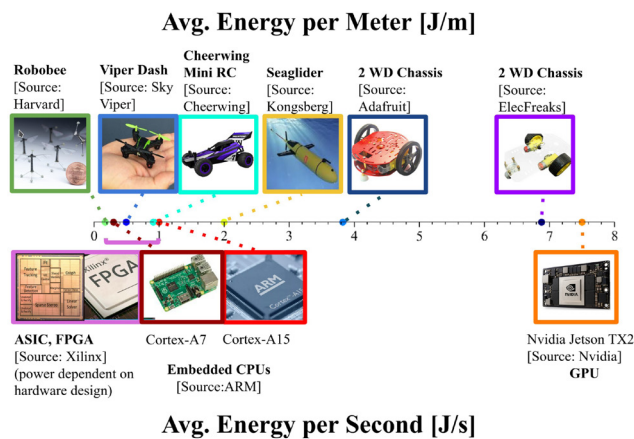
FURTHER READING

- J. Protz, “Methods and Compositions for Targeted Delivery, Release, and/or Activity,” *Int'l. Patent App.* PCT/US2021/016111, 1 Feb 2021. See also *Int'l Patent App.* PCT/US2019/031395 (WO/2019/217601), May 8, 2019.
- J. Protz, M. Tanner, E. Vasievich, A. Lee, A. Jain, and T. LaBean, “Bio-Nanoparticle for Drug Delivery Using TERCOM,” *Proc. MIT MTL Annual Research Conf. (MARC 2021)*, S6.06, p. 32, 2021.
- M. Tanner, E. Vasievich, and J. Protz, “Experimental Demonstration of Lossy Recording of Information into DNA,” *Proc. SPIE 7679, Micro- and Nanotechnology Sensors, Systems, and Applications II*, 767920, doi: 10.1117/12.858775; <https://doi.org/10.1117/12.858775>, 2010.

Balancing Actuation Energy and Computing Energy in Motion Planning

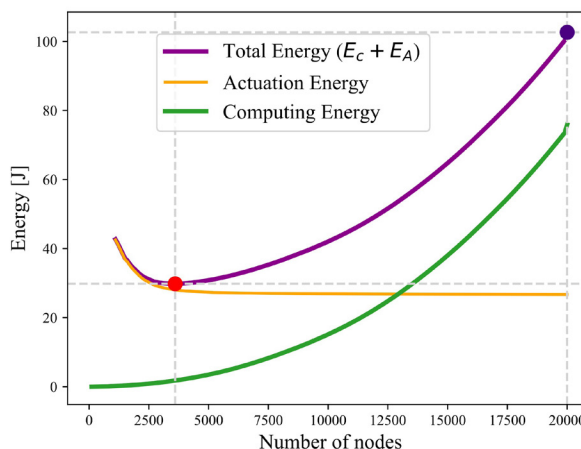
S. Sudhakar, V. Sze, S. Karaman
 Sponsorship: NSF, Cyber-Physical Systems (CPS) Program, grant no. 1837212

Inspired by emerging low-power robotic vehicles such as insect-size flyers, high-endurance autonomous blimps, and chip-size satellites, we identify a new class of motion-planning problems in which the energy consumed by the computer while planning a path can be as large as the energy consumed by the actuators during the execution of the path. Figure 1 shows how the energy to move one meter on various low-powered robotic platforms is of a similar magnitude to the energy to compute one second on various embedded computers. As a result, minimizing energy requires minimizing both actuation energy and computing energy since computing energy is no longer negligible. Figure 2 shows average actuation energy and computing energy curves for a selected robotic platform and a computing platform. Here, minimizing only actuation energy, as is conventionally done, does not minimize total energy. Instead, stopping computing earlier and accepting a higher actuation energy cost for a lower computing energy cost minimizes total energy.



▲ Figure 1: The energy-per-meter various low-power robotic platforms consume to actuate is on a similar magnitude as the energy-per-second that embedded computers consume to compute.

We propose the first algorithm to address this new class of motion planning problems, called Computing Energy Included Motion Planning (CEIMP). CEIMP operates similarly to other anytime planning algorithms, except that it stops when it estimates that while further computing may save actuation energy by finding a shorter path, the additional computing energy spent to find that path will negate those savings. We evaluate CEIMP on realistic computational experiments involving 10 MIT building floor plans, and CEIMP outperforms the average baseline of using maximum computing resources. In one representative experiment on an embedded CPU (ARM Cortex A-15), for a simulated vehicle that uses one Watt to travel one meter per second, CEIMP saves 2.1-8.9x of the total energy on average across the 10 floor plans over the baseline, which translates to missions that can last equivalently longer on the same battery.



▲ Figure 2: Average computing energy, actuation energy, and total energy (computing + actuation) curves vs. nodes in a sampling-based motion planner.

FURTHER READING

- S. Sudhakar, S. Karaman, S., and V. Sze, V. "Balancing Actuation and Computing Energy in Motion Planning," 2020 IEEE International Conference on Robotics and Automation (ICRA) pp. 4259-4265, May 2020.

Absolute Blood Pressure Measurement using Machine Learning Algorithms on Ultrasound-based Signals

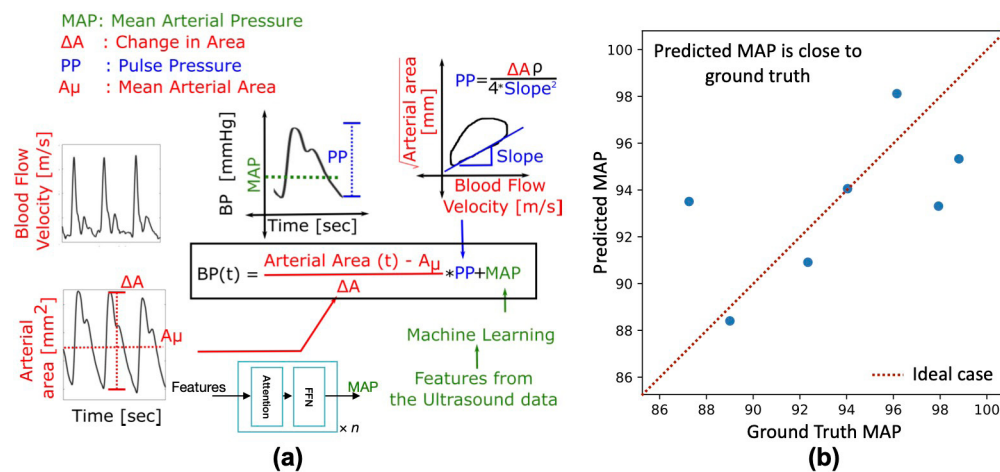
H. Wang, A. Chandrasekhar, A. Aguirre, C. G. Sodini, H.-S. Lee, S. Han

Sponsorship: MIT J-Clinic, MEDRC-Analog Devices, NSF CAREER Award, DARPA Software-Defined Hardware

Hypertension, or high blood pressure (BP), is a major cardiovascular risk factor. Therefore, measuring BP is of significant clinical value. At present, there are a few disadvantages for devices that measure a patient's BP. For instance, in an Intensive Care Unit (ICU), physicians use an invasive radial catheter to measure BP, which is not feasible outside an ICU. In non-ICU settings, clinicians use a non-invasive arm-cuff device to measure BP. This is convenient but can provide only a systolic and a diastolic pressure value and does not output the absolute BP (ABP) waveform. These devices also neglect the dynamic nature of the arterial system as they do not measure the morphology of the BP waveform, which may contain information on the underlying pathophysiology.

In this work, we propose a *non-invasive* way to get BP waveform with blood flow velocity and arterial area obtained from non-invasive ultrasound signals. One

key drawback of the ultrasound-based device is that the output BP waveform has an arbitrary reference, so we have to estimate the mean arterial pressure (MAP). We propose to use a machine learning model containing 1D convolution and Transformer encoder layers to regress the MAP accurately. The input features are arterial area, flow velocity, and several other scalar features such as pulse wave velocity and pulse pressure. They are first embedded into a 512-dimension vector. Then, the convolution layers perform feature extractions, and a transformer models the relationship between time steps. We perform the training on the Pulse Wave Database (PWDB) synthetic dataset and test on seven real patients. The model provides accurate results, with mean absolute error 2.6 mmHg and std 2.1 mmHg. This algorithm has large potential to make affordable BP waveform measurements accessible to everyone.



▲ Figure 1: (a) The whole pipeline of using a machine learning based algorithm to get BP waveforms from ultrasound data, and (b) predictions of the machine learning model are very accurate, with mean absolute error 2.6 mmHg and std 2.1 mmHg.

FURTHER READING

- P. H. Charlton, J. Mariscal Harana, S. Vennin, Y. Li, P. Chowienczyk, and J. Alastruey, "Modeling Arterial Pulse Waves in Healthy Aging: A Database for in Silico Evaluation of Hemodynamics and Pulse Wave Indexes," *Am J Physiol Heart Circ Physiol.*, vol. 317, no. 5, pp. H1062-H1085, 2019.
- H. Wang, Z. Wu, Z. Liu, H. Cai, L. Zhu, C. Gan, and S. Han, "Hat: Hardware-aware Transformers for Efficient Natural Language Processing," *ACL*, pp. 7675-7688, Jul. 2020.

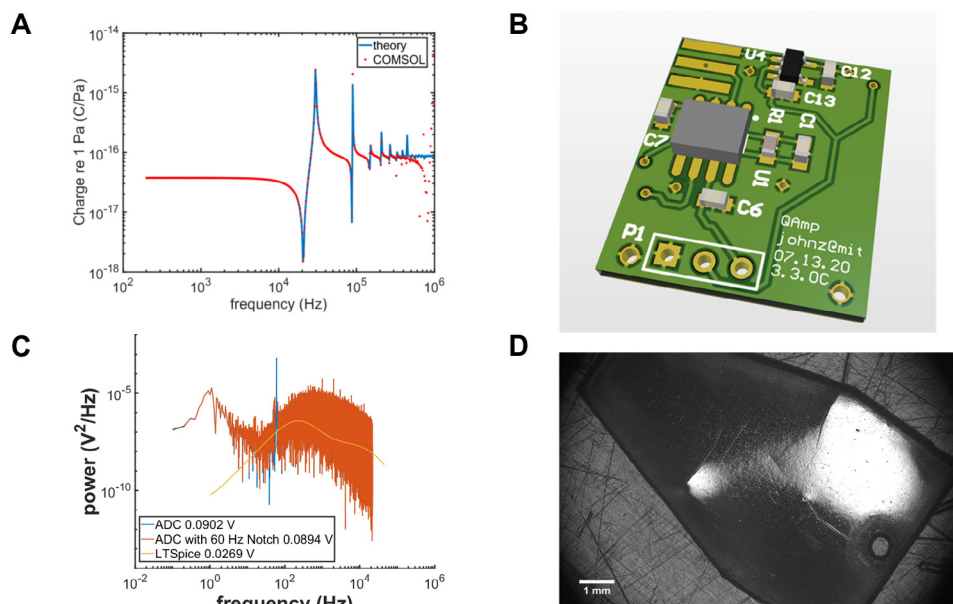
Analytical and Numerical Modeling of an Intracochlear Hydrophone for Fully Implantable Assistive Hearing Devices

J. Z. Zhang, B. G. Cary, E. S. Olson, H. H. Nakajima, J. H. Lang
Sponsorship: NIH/NIDCD, NSF GRFP

Cochlear implants with fully implantable microphones would allow directional and focused hearing by taking advantage of ear mechanics. They would be usable in almost all environmental conditions throughout the day and night. Current implantable microphones suffer from unstable mechanics, poor signal-to-noise ratio (SNR), and low bandwidth.

In this work, we used analytical modeling, a finite element model, and experiments to design a polyvinylidene (PVDF) intracochlear hydrophone for high-bandwidth sensitivity, surgical viability, and improved SNR by electrical shielding and circuit

design. Our analysis shows that the copolymer PVDF-TrFE should be used due to its higher hydrostatic sensitivity, the area of the sensor should be maximized to maximize gain, and the length should not exceed a maximal value determined by the bandwidth requirement. A short-circuit topology charge amplifier maximizes the SNR of the sensor by minimizing noise and attenuating electromagnetic interference by shielding. These advances in sensor performance bring fully implantable systems closer to reality.



▲ Figure 1: Sensor modeling and amplifier design. (a) Frequency response of the device predicted by theory and our finite element model, (b) four-layer charge amplifier PCB, (c) LTSpice and measured noise of the charge amplifier, and (d) laser cut PVDF-TrFE for sensing intracochlear pressure.

FURTHER READING

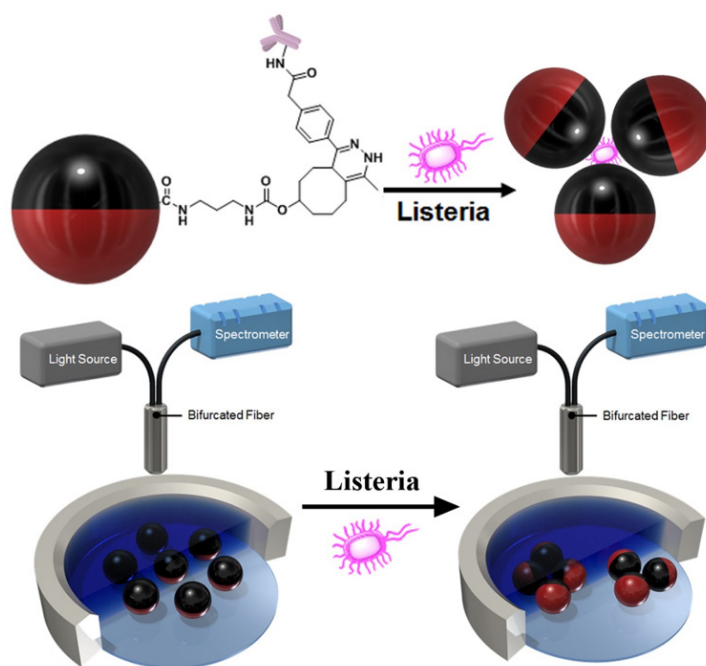
- S. Park et al., "PVDF-Based Piezoelectric Microphone for Sound Detection Inside the Cochlea: Toward Totally Implantable Cochlear Implants," *Trends Hear.*, vol. 22, pp. 1–11, 2018.
- J. S. Yang and X. Zhang, "Extensional Vibration of a Nonuniform Piezoceramic Rod and High Voltage Generation," *Int. J. Appl. Electromagn. Mech.*, vol. 16, no. 1–2, pp. 29–42, 2002.
- J. Sirohi and I. Chopra, "Fundamental Understanding of Piezoelectric Strain Sensors," *J. Intell. Mater. Syst. Struct.*, vol. 11, no. 4, pp. 246–257, 2000.

Fluorescent Janus Droplet and Its Application in Biosensing of *Listeria Monocytogenes*

J. Li, S. Savagatrup, Z. Nelson, K. Yoshinaga, T. M. Swager
Sponsorship: NSF, DOD

Dynamic complex droplets afford versatile platforms for biosensing. The biosensing methods based on droplets enable a combination of advantages including speed, cost-effectiveness, and portability. This research explores a sensing method based on the agglutination of Janus emulsions for *Listeria monocytogenes*, which is a gram-positive bacterium and is responsible for a potentially lethal foodborne bacterial illness. We create a bio-recognition interface between the Janus emulsions that comprises equal volumes of hydrocarbon and fluorocarbon oils in Janus morphology by attaching antibodies to a functional surfactant polymer with a tetrazine/trans-cyclooctene (TCO) click reaction. The *Listeria* antibodies would be on the surface of the hydrocarbon hemisphere since the surfactant will stay at the interface of the hydrocarbon and water phase. Agglutinations of Janus droplets are formed when *Liste-*

ria is added because of the strong binding between *Listeria* and the *Listeria* antibody located at the hydrocarbon surface of the emulsions. By incorporating one emissive dye in the fluorocarbon phase and a blocking dye in the hydrocarbon phase of Janus droplets, we conduct a two-dye assay, which enables the rapid detection of trace *Listeria* in two hours via an emissive signal produced in response to *Listeria* binding. To clarify, the Janus structures are tilted from their equilibrium position as a result of the formation of agglutinations and produce emissions that would ordinarily be obscured by a blocking dye. Overall, this method not only provides rapid and inexpensive *Listeria* detection with high sensitivity but also can be used to create a new class of biosensors by connecting with other related recognition elements.



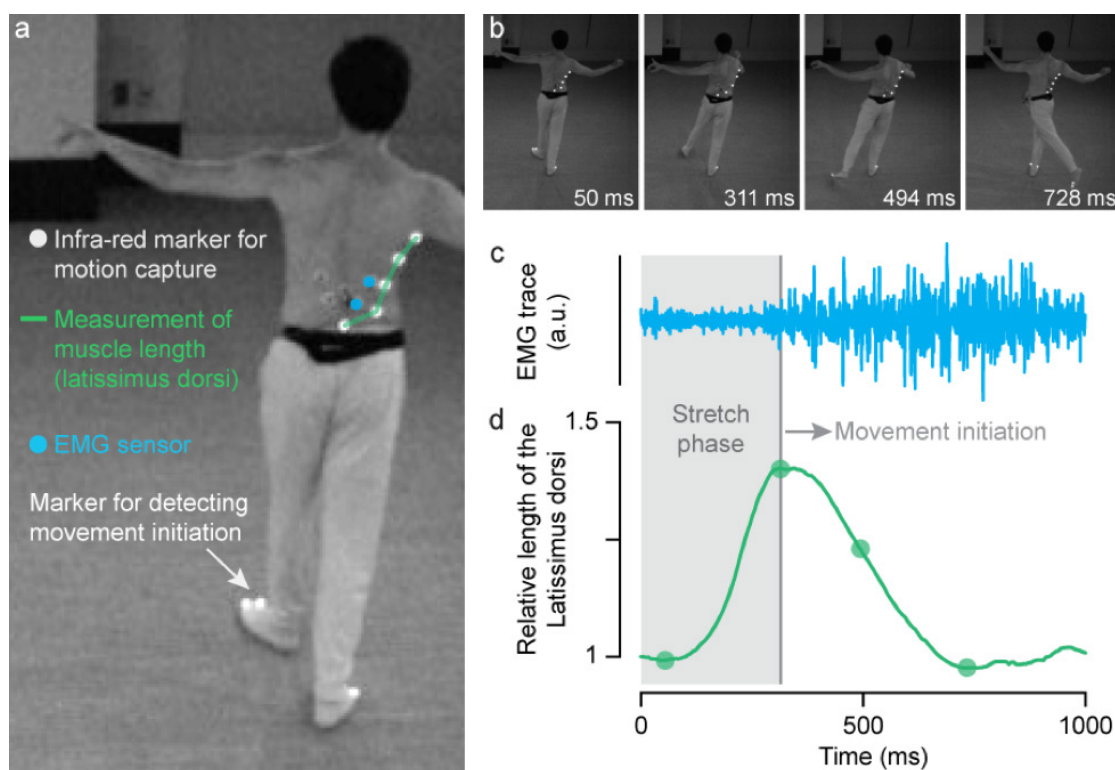
▲ Figure 1: Schematic of the agglutination assay of Janus emulsions for the biosensing of *Listeria Monocytogenes*.

Dance-Inspired Investigation of Human Movement

P. Namburi, L. Daniel, M. Feigin, Almon, B. Anthony, B. Moss, A. Kappacher
Sponsorship: NCSOFT

This research focuses on efforts to formalize a dancer's approach to movement. The overarching hypothesis is that dancers stabilize their joints through stretches – which are observed during common activities such as walking and running. However, most untrained individuals are able to apply this form of stabilization only during activities such as walking that seemingly “just

happen,” much as we “see.” In contrast, the best dancers and athletes are able to generalize this stretch-based joint stabilization beyond walking to their art form. To understand how dancers organize movement through stretches, the researchers use motion tracking and electromyography. This work will potentially benefit several fields, including soft robotics, neuroscience, and AI.



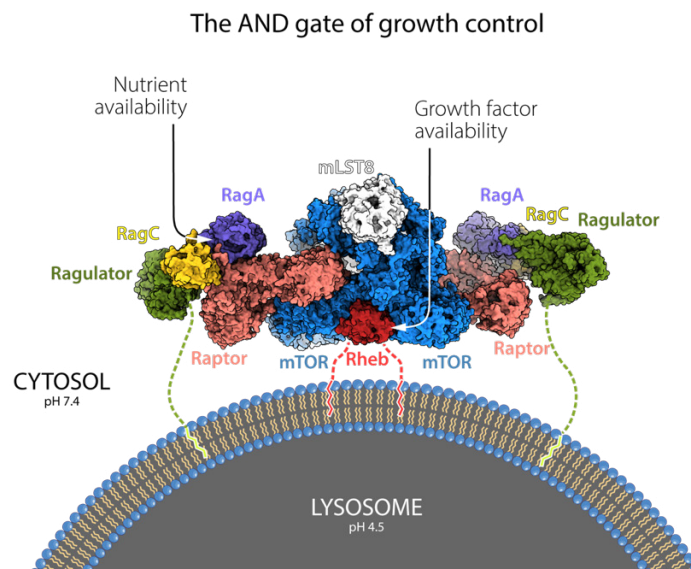
▲ Figure 1: *a-b. Experiment.* A dancer's movements were studied during the execution of a 'back ronde', i.e. a dance move that involves moving the left leg counter-clockwise while maintaining balance on the right leg. Length and activity of the latissimus dorsi muscle were studied. To monitor stretches in the latissimus dorsi muscle, we used 3d motion capture technology at the MIT.nano Immersion Lab. Reflective infra-red markers (bright spots) were placed along the latissimus dorsi muscle to monitor its length (green line), and on the toes to measure initiation of movement. To measure the activation of the latissimus muscle, we used electromyography, and the position of the sensors is shown by blue circles. The four green circles in d correspond to the time points highlighted in the evolution of movement during the ronde, depicted in b.

c-d. Physiological measurements show two distinct phases of movement. An increase in EMG activity is detected starting ~300ms (c). This corresponds to when the movement is initiated (gray vertical line) as monitored by the movement of the big toe. Prior to activation of the latissimus dorsi muscle, we see an increase in its length (d). This 'stretch phase' is marked by the gray rectangle. Within the next 400ms, the leg reaches its destination during the 'execution phase'.

Nanoscale Insights into the Mechanisms of Cellular Growth and Proliferation

K. B. Rogala, X. Gu, J. F. Kedir, M. Abu-Remaileh, L. F. Bianchi, A. M. S. Bottino, R. Dueholm, A. Niehaus, D. Overwijn, A-C. Priso Fils, S. X. Zhou, D. Leary, N. N. Laqtom, E. J. Brignole, D. M. Sabatini
Sponsorship: NIH, DoD, Lustgarten Foundation, Tuberous Sclerosis Association, MIT Koch Institute, Charles A. King Trust, Ibn Khaldun Fellowship, Howard Hughes Medical Institute, American Cancer Society

The growth and proliferation of human cells are controlled by the large molecular machine called mTORC1 that acts as a molecular equivalent of an AND logic gate. mTORC1 integrates multiple environmental signals, such as nutrients and growth factors, and orders the cell to either grow and divide in times of plenty or stand by and recycle when nutrients are scarce. Using electron cryomicroscopy, we revealed how mTORC1 recognizes nutrient signals, which provided a nanoscale-precision blueprint for the design of therapies aimed at deregulated mTORC1 in diseases of cellular growth, such as cancer.



▲ Figure 1: Figure: The mTORC1 kinase fully docked on the lysosomal surface via its association with two classes of GTPase proteins: Rags and Rheb. Together, these two GTPases constitute an AND gate for mTORC1 signaling, relaying the presence or absence of two input signals: (1) nutrients and (2) growth factors.

FURTHER READING

- K.B. Rogala, D. M. Sabatini, et al., "Structural Basis for the Docking of mTORC1 on the Lysosomal Surface", *Science*, 25 Oct 2019 : 468-475 <https://science.sciencemag.org/content/366/6464/468.abstract>
- K. Shen, K. B. Rogala, D. M. Sabatini et al., "Cryo-EM Structure of the Human FLCN-FNIP2-Rag-Ragulator Complex", *Cell*, Volume 179, Issue 6, 2019, <https://doi.org/10.1016/j.cell.2019.10.036>

Circuits & Systems for Communications, IoT, and Machine Learning

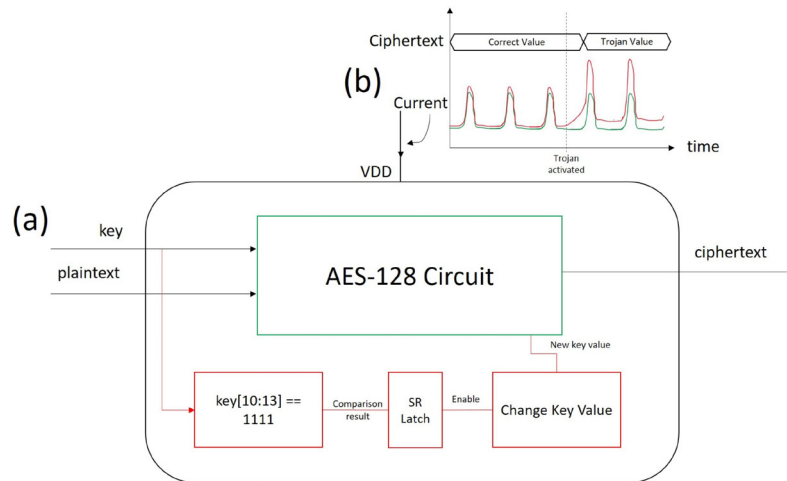
Hardware Trojan Detection using Unsupervised Deep Learning on High Spatial Resolution Magnetic Field Measurements	21
A Low-Power BLS12-381 Elliptic Curve Pairing Crypto-Processor.....	22
Direct Hybrid Encoding for Signed Expressions SAR ADC for Analog Neural Networks.....	23
Efficient Computation of Map-scale Continuous Mutual Information on Chip in Real Time.....	24
Simulation and Analysis of GaN CMOS Logic.....	25
A 0.31 THz CMOS Uniform Circular Antenna Array Enabling Generation/Detection of Waves with Orbital-Angular Momentum.....	26
Stability Improvement of CMOS Molecular Clocks Using an Auxiliary Loop Based on High-Order Detection and Digital Integration	27
A Sampling Jitter Tolerant Continuous-Time Pipelined ADC in 16-nm FinFET.....	28
Bandgap-Less Temperature Sensors for High Untrimmed Accuracy	29
High Angular Resolution THz Beam Steering Antenna Arrays in 22-nm FinFET Technology	30
DC-DC Converter Implementations Based on Piezoelectric Transformers	31
Closed Loop Control for a Piezoelectric-Resonator-Based DC-DC Power Converter	32
Leveraging Multi-Phase and Fractional-Turn Planar Transformers for Power Supply Miniaturization in Data Centers.....	33
Soft-Actuated Micro Aerial Vehicles with High Agility.....	34
Adjusting for Autocorrelated Errors in Neural Networks for Time Series Regression.....	35
Terahertz Wireless Link for Quantum Computing in 22-nm FinFET	36
Energy-Efficient System Design for Video Understanding on the Edge	37
Sparseloop: An Analytical, Energy-Focused Design Space Exploration Methodology for Sparse Tensor Accelerators	38
Multi-Inverter Discrete-Backoff: A High-Efficiency, Very-Wide-Range RF Power Generation Architecture	39
Programming a Quantum Computer with Quantum Instructions.....	40
Silicate-Based Composite as Heterogeneous Integration Packaging Material for Extreme Environments.....	41

Hardware Trojan Detection using Unsupervised Deep Learning on High Spatial Resolution Magnetic Field Measurements

M. Ashok, M. J. Turner, R. L. Walsworth, E. V. Levine, A. P. Chandrakasan
Sponsorship: NSF Graduate Research Fellowship, MITRE Corporation

One major vulnerability of integrated circuits (ICs) is the difficulty of ensuring that an IC fabricated in a third-party foundry is not a maliciously modified version of the original design. Such modifications by attackers, called hardware Trojans (example shown in Figure 1a), can leak private data from an IC, change its functionality, or have other effects. Attackers can design Trojans so that their effects are not visible during simple functional tests, making detection difficult. However, side channel methods (Figure 1b) can measure differences in circuit activity resulting from the modified logic to detect Trojans prior to the presence of functional changes.

In this work, we achieve a method of detecting small footprint hardware Trojans in a field-programmable gate array by performing high spatial resolution and wide field-of-view imaging of the circuit magnetic fields using a quantum diamond microscope. These images are then separated into Trojan-free and Trojan-inserted measurements in an automated framework by using an unsupervised convolutional neural network and clustering. With this framework, we show detection ability comparable to previous literature without requiring any knowledge of the Trojan at test time.



▲ Figure 1: (a) Block diagram of a sample hardware Trojan with malicious effects in a cryptographic circuit. (b) A general method of side channel Trojan detection that measures small differences in IC current prior to the trojan payload activation.

FURTHER READING

- M. J. Turner, N. Langellier, R. Bainbridge, D. Walters, S. Meesala, T. M. Babinec, P. Kehayias, A. Yacoby, et al., "Magnetic Field Fingerprinting of Integrated-Circuit Activity with a Quantum Diamond Microscope," *Physical Rev. Appl.*, vol. 14, no. 1, pp. 014097, Jul. 2020.
- S. Bhunia, M. S. Hsiao, M. Banga, and S. Narasimhan, "Hardware Trojan Attacks: Threat Analysis and Countermeasures," *Proc. IEEE*, vol. 102, no. 8, pp. 1229–1247, Aug. 2014.
- O. Soll, T. Korak, M. Muehlberghuber, and M. Hutter, "EM-based Detection of Hardware Trojans on FPGAs," *2014 IEEE Int. Symposium on Hardware-Oriented Security and Trust (HOST)*, pp. 84–87, May 2014.

A Low-Power BLS12-381 Elliptic Curve Pairing Crypto-Processor

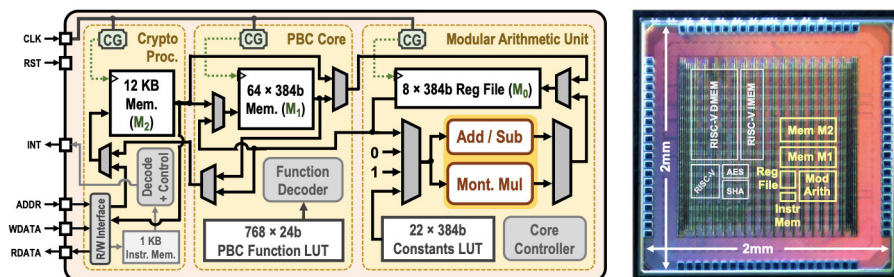
U. Banerjee, A. P. Chandrakasan

Sponsorship: Texas Instruments

Pairing-based cryptography (PBC), a variant of elliptic curve cryptography (ECC), uses bilinear maps between elliptic curves and finite fields to enable novel applications beyond traditional key exchange and signatures, e.g., signature aggregation and functional encryption. These protocols require special pairing-friendly elliptic curves; recent cryptanalysis has compromised the security of commonly used 254b BN curves. Therefore, the new BLS12-381 curve, based on a 381b prime field, is being standardized for PBC applications. However, with strong security, the new curve has higher computational complexity, making implementing low-power embedded devices challenging. To address this challenge, we present the first BLS12-381 elliptic curve pairing crypto-processor, which enables two orders-of-magnitude energy savings through efficient hardware acceleration, implements countermeasures against timing and power side-channel attacks, and provides the flexibility to implement ECC and PBC protocols for securing Internet of Things applications.

Figure 1 shows the architecture of a pairing cryptoprocessor with the chip micrograph. Our test chip was fabricated in TSMC 40-nm low-power

complementary metal-oxide-semiconductor process and supports voltage scaling from 1.1V down to 0.66V. The cryptographic core occupies a 0.2-mm² area consisting of 112k logic gates and 16 KB SRAM. Programming with custom instructions for modular arithmetic, elliptic curve point and line arithmetic, pairing operations, control, and branching is possible. Key building blocks are constant-time and secure against timing and simple power analysis side-channel attacks. For high-security use, our chip can be configured to protect against stronger differential power analysis side-channel attacks at the cost of increased energy consumption. We have evaluated pairing-based public key cryptography protocols on our chip, including signature aggregation, identity-based signatures, identity-based encryption, inner product functional encryption, and multi-party key exchange. Our hardware-accelerated implementations are 130-140× more energy-efficient than software. The programmability of our pairing crypto-processor allows new protocols, algorithm optimizations, and side-channel countermeasures to be easily implemented using one chip.



▲ Figure 1: Architecture of cryptographic core and chip micrograph.

FURTHER READING

- U. Banerjee and A. P. Chandrakasan, "A Low-Power Elliptic Curve Pairing Crypto-Processor for Secure Embedded Blockchain and Functional Encryption," *IEEE Custom Integrated Circuits Conference*, pp. 1-2, Apr. 2021.
- U. Banerjee, T. S. Ukyab, and A. P. Chandrakasan, "Sapphire: A Configurable Crypto-Processor for Post-Quantum Lattice-based Protocols," *IACR Transactions on Cryptographic Hardware and Embedded Systems*, vol. 2019, no. 4, pp. 17-61, Aug. 2019.
- U. Banerjee, A. Wright, C. Juvekar, M. Waller, A. Arvind, and A. P. Chandrakasan, "An Energy-Efficient Reconfigurable DTLS Cryptographic Engine for Securing Internet-of-Things Applications," *IEEE Journal of Solid-State Circuits*, vol. 54, no. 8, pp. 2339-2352, Aug. 2019.

Direct Hybrid Encoding for Signed Expressions SAR ADC for Analog Neural Networks

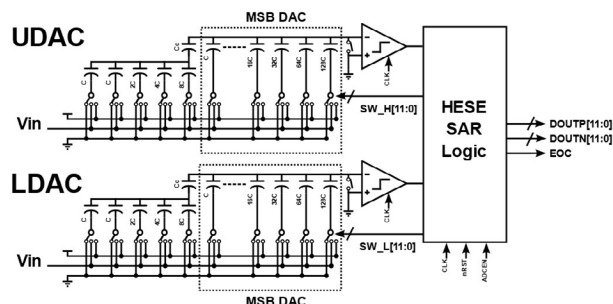
R.-C. Chen, A. P. Chandrakasan, H.-S. Lee
Sponsorship: CICS, DARPA

Artificial intelligence (AI) has proven itself to be one of the most powerful techniques for computer vision, natural language processing, and the automobile industry. Current AI algorithms that are based on deep neural networks (DNNs) are facing a crucial challenge from efficient computing. State-of-the-art DNNs need millions of weights and plenty of computation. The huge energy consumption is neither environmentally friendly nor practical in the battery-constraint edge devices. Conventional DNN hardware is based on fully digital implementation, where data movement is becoming the bottleneck. Data movement typically takes orders of magnitude more energy than the actual computation. Analog neural networks (ANNs) are a promising solution for energy-efficient AI inference. The ANNs perform the in-memory-computing to reduce the energy of data movement. Thus, the analog/digital interface

circuits are a critical part of the ANNs and are often the key bottleneck of the performance, power consumption, and area of the resulting system.

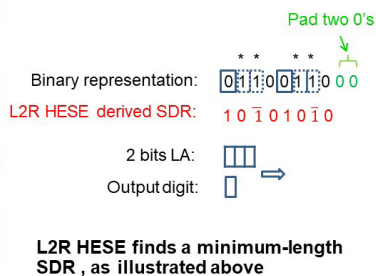
The hybrid encoding for signed expression (HESE) scheme is based on the booth encoding but with additional rules to provide the minimum-length signed-digit-representations (SDR) for efficient encoding for both DNNs including ANNs. This work focuses on a successive approximation register (SAR) analog-to-digital converter (ADC) that produces HESE encoded output on the fly. This ADC has two thresholds for 2-bits look ahead (LA). The proposed SAR ADC can directly encode the analog input to HESE instead of binary encoding. Preliminary results show that in a typical DNN, over 95% of weights can be represented by 5 terms of HESE for a 12-bits resolution.

► Figure 1: Proposed direct hybrid encoding for signed expressions SAR ADC for ANNs. The memory and computation are both inside the PE array. The ADCs are responsible for converting the analog output.



L2R (left-to-right) HESE, starting w/ NOT-IN-A-RUN state

IN-A-RUN (denoted by * in illustration)		
If 2 bit LA is 00 1->	$\bar{1}$	Enter NOT-IN-A-RUN
Else		
0->	$\bar{1}$	Output negative one
1->	0	Output zero
NOT-IN-A-RUN		
If 2 bit LA is 11 0->	1	Enter IN-A-RUN
Else		
0->	0	Output zero
1->	1	Output one



◀ Figure 2: The illustration of direct one-pass HESE. HESE is an efficient one-pass encoding to produce the minimum-length signed-digit-representations (SDR).

FURTHER READING

- Y. Peng, W. Huaqiang, G. Bin, T. Jianshi, Z. Qingtian, Z. Wenqiang, Y. J. Joshua, and Q. He, "Fully Hardware-implemented Memristor Convolutional Neural Network," *Nature*, vol. 577, no. 7792, pp. 641–646, 2020.
- H. T. Kung, B. McDanel, and S. Q. Zhang, "Term Revealing: Furthering Quantization at Run Time on Quantized DNNs," *arXiv preprint arXiv:2007.06389*, 2020.

Efficient Computation of Map-scale Continuous Mutual Information on Chip in Real Time

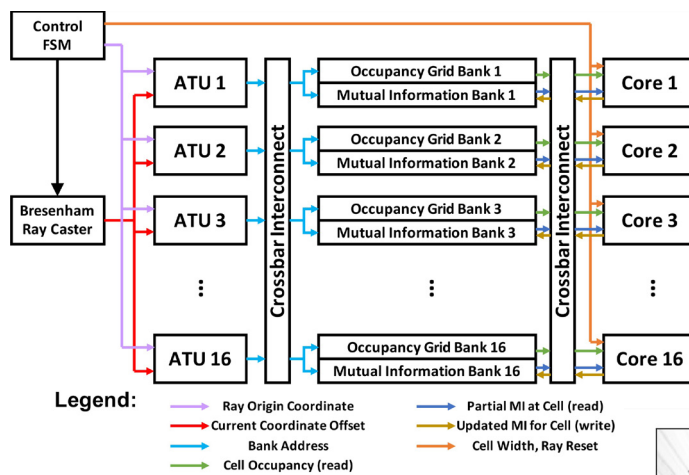
K. Gupta, P. Z. X. Li, S. Karaman, V. Sze
Sponsorship: NSF RTML, NSF CPS

Exploration tasks are essential to many emerging robotics applications, ranging from search and rescue to space exploration. The planning problem for exploration requires determining the best locations for future measurements that will enhance the fidelity of the map, for example, by reducing its total entropy. A widely studied technique involves computing the mutual information (MI) between the current map and future measurements and utilizing this MI metric to decide on the locations for future measurements.

However, computing MI for reasonably sized maps is slow and power-hungry, which has been the bottleneck in fast and efficient robotic exploration. In this paper, we introduce a new hardware accelerator architecture for MI computation that features 16 high-efficiency MI compute cores and an optimized memory subsystem that provides sufficient bandwidth to keep the cores fully utilized. Each core employs interleaving to counter the recursive algorithm and workload

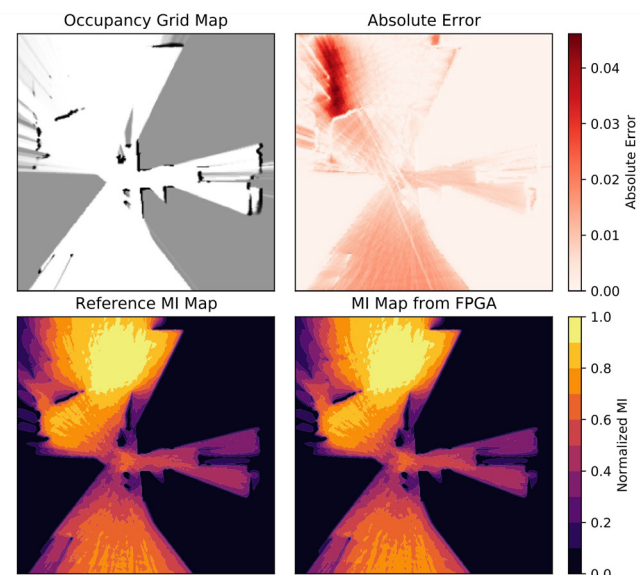
balancing and numerical approximations to reduce latency and energy consumption.

We demonstrate an optimized architecture on a field-programmable gate array (FPGA) implementation, which can compute MI for all cells in an entire 201-by-201 grid (e.g., representing a 20.1-m-by-20.1-m map at 0.1-m resolution) in 1.55 ms while consuming 1.7 mJ of energy, thus finally rendering MI computation for the whole map in real time and at a fraction of the energy cost of traditional compute platforms. For comparison, this particular FPGA implementation running on the Xilinx Zynq-7000 platform is two orders of magnitude faster and consumes three orders of magnitude less energy per MI map compute than a baseline GPU implementation running on an NVIDIA GeForce GTX 980 platform. The improvements are more pronounced when compared to CPU implementations of equivalent algorithms.



◀ Figure 1: Top-level hardware architecture comprised of address translation units (ATU), crossbar interconnects, occupancy grid map, MI map, and 16 FCMI computation cores.

▶ Figure 2: An example input grid and corresponding MI map contours generated from a reference implementation and our FPGA implementation.



Simulation and Analysis of GaN CMOS Logic

J. Jung, N. Chowdhury, Q. Xie, T. Palacios

Sponsorship: MIT Electrical Engineering and Computer Science - Texas Instruments Undergraduate Research and Innovation Scholar

There is an increasing demand for electronics that can operate in high-temperature conditions, such as spacecraft applications and sensors for industrial environments. Electronics based on wide-bandgap materials offer a promising solution, among which gallium nitride (GaN) stands out as a strong candidate due to its excellent material properties and potential for monolithic integration. Most current demonstrations of GaN logic are based on nanometal-oxide-semiconductor (nMOS) technology, which has a high static power consumption. Therefore, we are developing GaN complementary metal-oxide-semiconductor (CMOS) technology, which has lower static power consumption.

This work studies the effect of a p-channel transistor and circuit parameters on the performance of CMOS digital logic circuits. We used the MIT Virtual Source GaN-field-effect transistor (MVSGFET) model to accurately model the behavior of the n-channel and p-channel transistors, which were fabricated on

the developed GaN complementary circuit platform. We simulated and studied several building blocks for digital logic, namely, the logic inverter, multi-stage ring oscillator, and static random-access memory (SRAM) cell, using the developed computer-aided design (CAD) framework. We conducted device-circuit co-design to optimize circuit performance, using a variety of design parameters, including transistor sizing and supply voltage scaling. We projected the high-temperature performance of the circuits through simulations based on experimentally observed device behaviors. The results indicate that GaN CMOS technology based on our monolithically integrated platform has potential for a variety of use cases, including harsh-environment digital computation. We will apply this technique for more complex combinational and sequential logic building blocks, with the eventual goal of realizing a GaN CMOS microprocessor.

FURTHER READING

- N. Chowdhury, J. Jung, Q. Xie, M. Yuan, K. Cheng, and T. Palacios, "Performance Estimation of GaN CMOS Technology," *Proc. Device Research Conference (DRC)*, Jun. 2021.
- N. Chowdhury et al., "Field-induced Acceptor Ionization in Enhancement-mode GaN p-MOSFETs," in *Proc. 2020 IEEE International Electron Devices Meeting (IEDM)*, vol. 4, no. 5, pp. 5.5.1-5.5.4, Dec. 2020. DOI: 10.1109/IEDM13553.2020.9371963.
- N. Chowdhury et al., "Regrowth-Free GaN-Based Complementary Logic on a Si Substrate," *IEEE Electron Device Lett.*, vol. 41, no. 6, pp. 820-823, Jun. 2020. DOI: 10.1109/LED.2020.2987003.

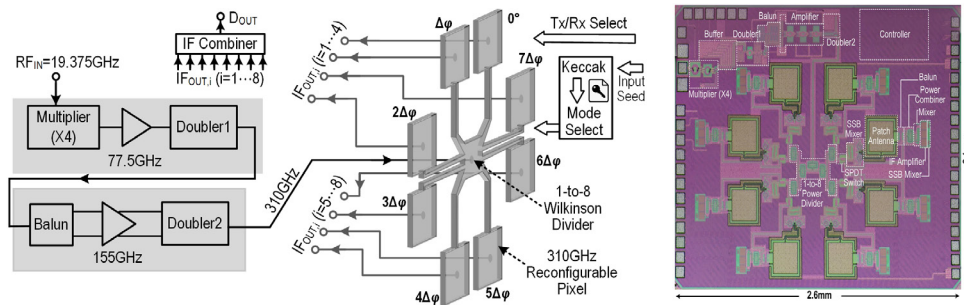
A 0.31 THz CMOS Uniform Circular Antenna Array Enabling Generation/Detection of Waves with Orbital-Angular Momentum

M. I. W. Khan, J. Woo, X. Yi, M. I. Ibrahim, R. T. Yazicigil, A. P. Chandrakasan, R. Han
Sponsorship: NSF EAGER SARE Award

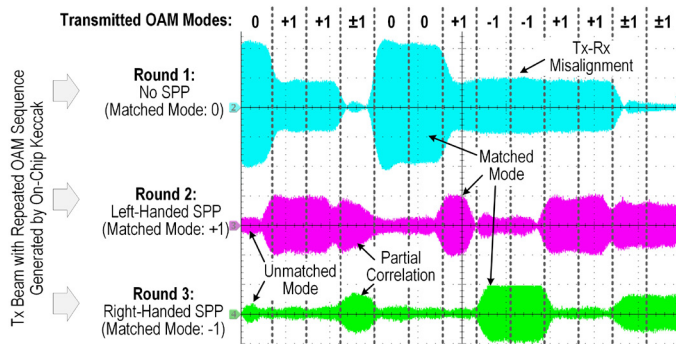
Multiplexing of electromagnetic (EM) waves with different frequencies, polarizations, and coding has been extensively exploited in wireless systems. Recently, another dimension of EM waves—the orbital angular momentum (OAM), is attracting increasing attention. An OAM-based wave possesses a wavefront with a helical phase distribution around the central axis of the beam. Different OAM modes, determined by the handedness and the total phase change ($\Delta\phi$) of the wavefront twist, are orthogonal. Wireless communication uses multi-OAM mode transmission to enhance spectral efficiency and physical-layer security. Conventional OAM-generation approaches incorporate dielectric spiral-phase plates, passive uniform circular antenna arrays, or metasurfaces in conjunction with separate signal drivers. These discrete solutions, however, lead to very bulky and costly systems.

In this project, we demonstrate the first chip-based (at any frequency) CMOS front-end that

generates and receives electromagnetic waves with OAM, shown in Figure 1. The chip, based on a uniform circularly placed patch antenna array at 0.31THz, transmits reconfigurable OAM modes, which are digitally switched among the (plane wave), (left-handed), (right-handed), and superposition states. The chip is also reconfigurable into a receiver mode that identifies different OAM modes with >10dB rejection of unintended modes. The array, driven by only one active path, has a measured EIRP of -4.8dBm and consumes 154mW of DC power in the OAM source mode. In the receiver mode, it has a measured conversion loss of 30dB and consumes 166mW of DC power. The OAM chip output mapped from a repeated Keccak-generated data sequence was verified, and the time-domain outputs of the Rx with different SPP configurations are shown in Figure 2, which shows good correlation with matched modes, partial correlation of multiplexed mode, and rejection of unmatched modes.



▲ Figure 1: The architecture and layout of 0.31 THz chip for OAM generation and reception.



◀ Figure 2: Time-domain output of Rx configured to receive different OAM modes when it is illuminated by same OAM sequence generated by on-chip Keccak.

FURTHER READING

- M. I. W. Khan, J. Woo, X. Yi, M. I. Ibrahim, R. T. Yazicigil, A. P. Chandrakasan, and R. Han, "A 0.31 THz CMOS Uniform Circular Antenna Array Enabling Generation/Detection of Waves with Orbital-Angular Momentum," *2021 IEEE Radio Frequency Integrated Circuits Symposium (RFIC)*, Atlanta, GA, 2021 to be published.
- Y. Yan, G. Xie, M. Lavery, H. Huang, N. Ahmed, C. Bao, Y. Ren, Y. Cao et al. "High-capacity Millimetre-wave Communications with Orbital Angular Momentum Multiplexing." *Nat Commun.* vol. 5, p. 4876, 2014. <https://doi.org/10.1038/ncomms5876>.

Stability Improvement of CMOS Molecular Clocks Using an Auxiliary Loop Based on High-Order Detection and Digital Integration

M. Kim, H. Lee, R. Han

Sponsorship: NASA Jet Propulsion Laboratory, NSF

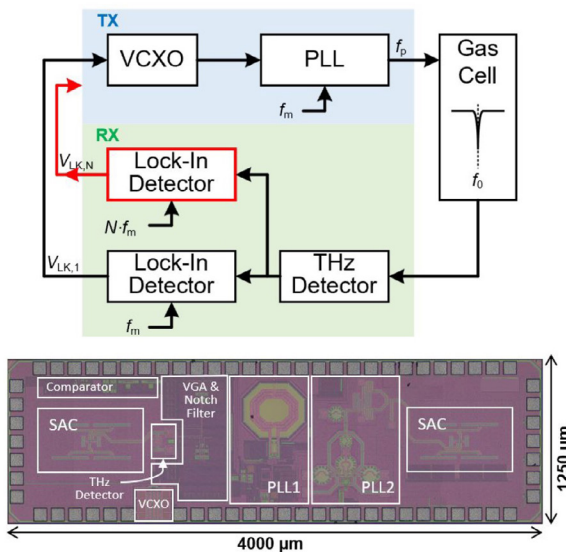
Recently, chip-scaled molecular clocks (CSMC) have achieved high-frequency stability with low power and compact size by using a rotational-mode transition of carbonyl sulfide (OCS) centered around 231.061 GHz as a frequency reference (f_0). In the molecular clock, the probing signal generated from the transmitter is frequency-modulated at f_m around the center frequency (f_c). Since f_c is locked to f_0 in a feedback loop, the output frequency inherits the excellent stability of the OCS transition frequency.

Due to its fully-electronic implementation, CSMC has reduced the cost of high-stability miniaturized clocks. However, the frequency stability is still limited by a finite loop gain of the frequency locked loop and detection non-idealities, which are susceptible to environmental disturbance even though an invariant physical constant is used as the frequency reference. In this work, we propose a new dual-loop CSMC architecture based on both fundamental and high-

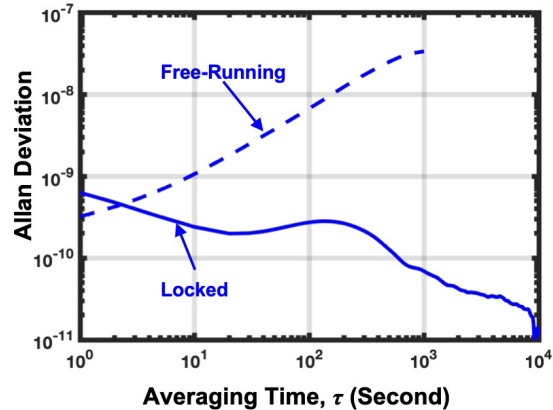
order transition probing as well as digital integration.

In order to achieve a high long-term stability without compromising the signal-to-noise ratio, the fundamental harmonic detection forms the main loop while the higher-order probing is used in an auxiliary loop. The loop fine-tunes the phase-locked loop's frequency multiplication ratio according to the sign of the high-order detection output. With a proper selection of gain and bandwidth in each loop, the main loop enables the fast correction of frequency, and the auxiliary loop responds against long-term frequency variation. Also, the frequency offset between the clock output and the OCS reference can be eliminated when the clock is locked because the auxiliary loop includes a digital integrator to obtain an infinite DC gain.

As a result, the proposed CSMC implemented in 65-nm CMOS process achieved Allan deviation of 5.4×10^{-10} and 2×10^{-11} at 1 s and 10^4 s averaging times, respectively, with 71 mW power consumption.



▲ Figure 1: Simplified block diagram and die micrograph of the proposed CSMC and dispersion curves of the fundamental, third-order, and fifth-order probing.



▲ Figure 2: Measured Allan deviation of the proposed CSMC.

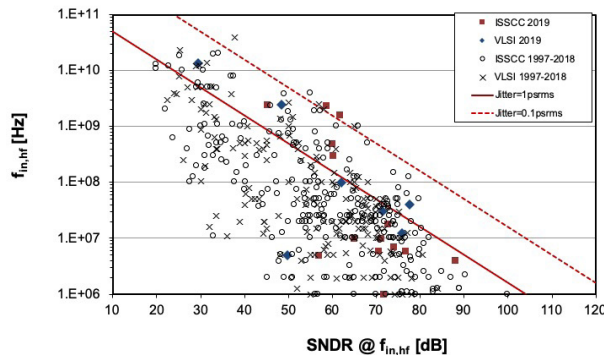
FURTHER READING

- C. Wang, X. Yi, J. Mawdsley, M. Kim, Z. Wang, and R. Han, "An On-chip Fully-electronic Molecular Clock Based on Sub-Terahertz Rotational Spectroscopy," *Nature Electronics*, vol. 1, no. 7, pp. 1-7, Jul. 2018.
- C. Wang, X. Yi, M. Kim, Q. Yang, and R. Han, "A Terahertz Molecular Clock on CMOS using High-harmonic-order Interrogation of Rotational Transition for Medium/long-term Stability Enhancement," *IEEE J. of Solid-State Circuits*, vol. 56, no. 2, pp. 566-580, Feb. 2021.

A Sampling Jitter Tolerant Continuous-Time Pipelined ADC in 16-nm FinFET

R. Mittal, G. Manganaro, A. P. Chandrakasan, H.-S. Lee
Sponsorship: Analog Devices, Inc.

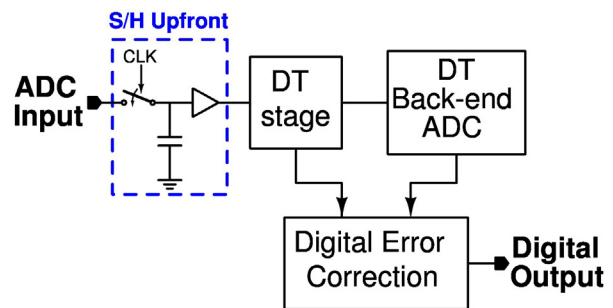
Almost all real-world signals are analog. Yet most of the data is stored and processed digitally due to advances in the integrated circuit technology. Therefore, analog-to-digital converters (ADCs) are an essential part of any electronic system. The advances in modern communication systems including 5G mobile networks and baseband processors require the ADCs to have large dynamic range and bandwidth. Although there have been steady improvements in the performance of ADCs, the improvements in conversion speed have been less significant because the speed-resolution product is limited by the sampling clock jitter (Figure 1). The effect of sampling clock jitter has been considered fundamental. However, continuous-time delta-sigma modulators may reduce the effect of sampling jitter. But since delta-sigma modulators rely on relatively high oversampling, they are unsuitable for high-frequency applications. Therefore, ADCs with low oversampling ratio are desirable for high-speed data conversion.



▲ Figure 1: Performance survey for published ADCs (ISSCC 1997-2019 and VLSI 1997-2019).

In conventional Nyquist-rate ADCs, the input is sampled upfront (Figure 2). Any jitter in the sampling clock directly affects the sampled input and degrades the signal-to-noise ratio (SNR). It is well known that for a given root mean square (rms) sampling jitter σ_t , the maximum achievable SNR is limited to $1/(2\pi f_{in}\sigma_t)$, where f_{in} is the input signal frequency. In an SoC environment, it is difficult to reduce the rms jitter below 100 fs. This limits the maximum SNR to just 44 dB for a 10 GHz input signal. Therefore, unless the effect of sampling jitter is reduced, the performance of an ADC would be greatly limited for high-frequency input signals.

In this project, we propose a continuous-time pipelined ADC having reduced sensitivity to sampling jitter. We are designing this ADC in 16-nm FinFET technology to give a proof-of-concept for improved sensitivity to the sampling clock jitter.



▲ Figure 2: A conventional discrete-time pipelined ADC with a sample-and-hold upfront.

FURTHER READING

- B. Murmann, "ADC Performance Survey 1997-2019," [Online]. Available: <http://web.stanford.edu/~murmann/adcsurvey.html>.
- R. van Veldhoven, "A Tri-mode Continuous-time/spl Sigma/spl Delta/modulator with Switched-capacitor Feedback DAC for a GSM-EDGE/CDMA2000/UMTS Receiver," *Solid-State Circuits Conference, 2003. Digest of Technical Papers. ISSCC. 2003 IEEE International*, pp. 60-477, 2003.

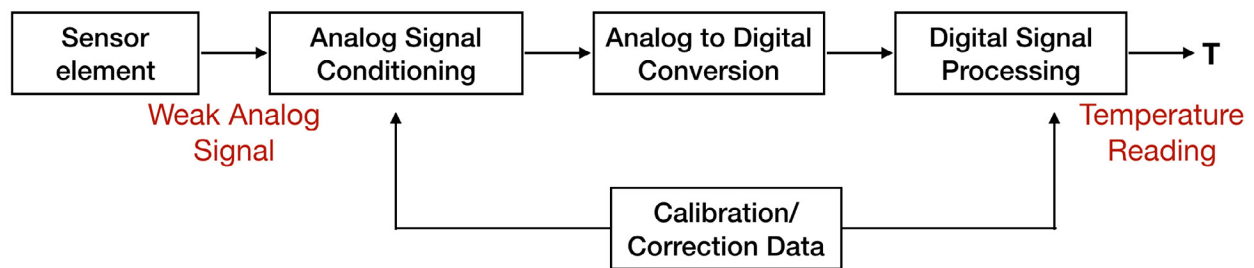
Bandgap-Less Temperature Sensors for High Untrimmed Accuracy

V. Mittal, A. P. Chandrakasan, H.-S. Lee
Sponsorship: Analog Devices Inc.

Temperature sensors are extensively used in measurement, instrumentation, and control systems. A sensor that integrates the sensing element, analog-to-digital converter, and other interface electronics on the same chip is referred to as a smart sensor. Complementary metal-oxide-semiconductor- (CMOS) based smart temperature sensors offer the benefits of low cost and direct digital outputs over conventional sensors. However, they are limited in their absolute accuracy due to the non-ideal behavior of the devices used to design them. Therefore, these sensors require either calibration or gain/offset adjustments in the analog domain to achieve desired accuracies (Figure 1). The latter pro-

cess, also called trimming, needs additional expensive test equipment and valuable production time and is a major contributor to the cost of the sensors. In order to enable high volume production of CMOS-based temperature sensors at low cost, achieving high accuracies without trimming is imperative.

This work proposes the design of a CMOS temperature sensor that uses fundamental physical quantities resilient to process variations, package stress, and manufacturing tolerances to achieve high accuracies without trimming. Simulation results prove that 3σ inaccuracy of less than 10 C can be obtained with the proposed method.



▲ Figure 1: System level diagram of a smart temperature sensor.

FURTHER READING

- G. Meijer, M. Pertijs, and K. Makinwa, "Smart Sensor Systems: Emerging Technologies and Applications," Hoboken, New Jersey: John Wiley & Sons, 2014.
- Y. Li, H. Lakdawala, A. Raychowdhury, G. Taylor, and K. Soumyanath, "A 1.05V 1.6mW 0.450C 3σ -resolution $\Delta\Sigma$ -based Temperature Sensor with Parasitic-resistance Compensation in 32nm CMOS," in *Solid-State Circuits Conference*, 2009. Digest of Technical Papers. 2009 IEEE International, pp. 340-341, Feb. 2009.

High Angular Resolution THz Beam Steering Antenna Arrays in 22-nm FinFET Technology

N. Monroe
Sponsorship: Intel Corp.

THz phased arrays are a promising emerging technology for many applications, including THz imaging, radar, communications, and other sensing applications. This is largely a result of the smaller wavelength at THz frequencies and accordingly smaller array size and weight. However, challenges exist in their design, particularly the design of THz phase shifters, which are often lossy, power hungry, and physically large, precluding their use in dense arrays. These losses often arise from the high-resolution nature of the phase shifters. In addition, lossy on-chip transmission lines significantly degrade system performance. In this work, we apply phased array principles to yield dense THz antenna arrays with only one bit of phase resolution, yielding performance benefits in terms of DC power, THz loss, size, bandwidth, and simplicity. In addition, by distributing radio frequency (RF) power spatially, we mitigate many of the losses with RF signal distribution. This approach is termed reflectarray (reflector array). We demonstrate

our approach on complementary metal-oxide semiconductor silicon in the form of a 4x4 mm² chip containing 7x7 antenna elements, operating at 260 GHz. The chip is designed in Intel 22-nm FinFET process so that multiple chips can be tiled to create large arrays that can be scaled in size based on performance requirements. The use of one-bit phase shifters comes at a cost in system-level performance by introducing sidelobes in the radiation pattern. Our work introduces a number of approaches to mitigate this, allowing the one-bit phased array design to approach the performance of a phased array with a continuous, analog phase shifter. While still in progress, this work pushes towards practical large-scale THz phased arrays.

DC-DC Converter Implementations Based on Piezoelectric Transformers

E. Ng, J. D. Boles, J. H. Lang, D. J. Perreault

Sponsorship: Texas Instruments, UROP, NSF Graduate Research Fellowship

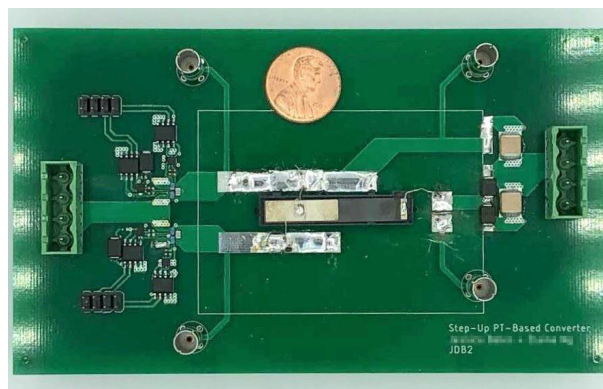
Power converters play major roles in many applications ranging from power generation and distribution in electric grids to everyday devices such as mobile phones and computers. As many applications require small form factors, there has been a significant demand to miniaturize power converters while maintaining high performance. Typical converters rely on magnetic energy storage components, but the achievable power densities of magnetics fundamentally decrease at low volumes and therefore limit converter miniaturization.

Piezoelectrics, which have more favorable power density scaling properties than magnetics, are a promising energy storage alternative to meet the demands for low-volume power electronics. Furthermore, multi-port piezoelectric transformers (PTs) offer the additional benefits of galvanic isolation and inherent voltage conversion ratios. Despite their potential, PTs have seen little use in converters without magnetics, and such design attempts have unreported or limited efficiencies.

In this work, we systematically enumerate isolated and non-isolated converter switching sequences and

topologies that best utilize PTs as their only energy storage components. We constrain this search for (1) high-efficiency behaviors such as zero voltage switching (ZVS) and all-positive instantaneous power transfer and (2) practical characteristics such as voltage regulation capability and control simplicity. To evaluate the selected switching sequences, we also develop a model for estimating the PT's efficiency.

Initial experimental results of these converter designs demonstrate promising high-efficiency behaviors and peak whole-converter efficiencies higher than reported for most magnetic-less PT-based converters in the literature. The prototype displayed in Figure 1 is based on a commercially available PT and achieves a peak efficiency of 89.3%, which is close to our estimation model's predictions. These results suggest that PT-based converters can offer high efficiencies in addition to the low-volume scaling benefits of piezoelectrics. Such characteristics can be advantageous to high-voltage, low-power applications such as portable electronics and biomedical devices, particularly those requiring galvanic isolation.



▲ Figure 1: Photograph of the PT-based converter prototype.

FURTHER READING

- J. D. Boles, J. J. Piel, and D. J. Perreault, "Enumeration and Analysis of DC-DC Converter Implementations Based on Piezoelectric Resonators," *IEEE Transactions on Power Electronics*, vol. 36, no. 1, pp. 129-145, 2021.
- E. Ng, J. D. Boles, J. H. Lang, and D. J. Perreault, "Non-isolated DC-DC Converter Implementations Based on Piezoelectric Transformers," *Proc. IEEE Energy Conversion Congress and Exposition (ECCE)*, Vancouver, Canada, Oct. 2021.
- J. D. Boles, E. Ng, J. H. Lang, and D. J. Perreault, "High-efficiency operating Modes for Isolated Piezoelectric-transformer-based DC-DC Converters," *Proc. IEEE Workshop on Control and Modeling for Power Electronics (COMPEL)*, Aalborg, Denmark, Nov. 2020.

Closed Loop Control for a Piezoelectric-Resonator-Based DC-DC Power Converter

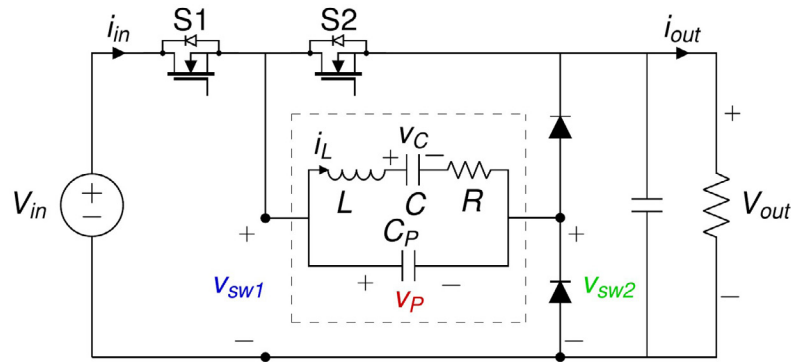
J. Piel, J. Boles, D. Perreault

Sponsorship: Texas Instruments, NSF GRFP, MIT UROP

Electronics such as computers, mobile phones, household appliances, and even electric vehicles can vary greatly in terms of supply requirements; power electronics are necessary to power these devices from standard sources. Reducing the sizes of power converters allows them to be more cost-effective and useful to a wider range of applications. Traditional DC-DC power converters make use of magnetics for energy storage, but these are less efficient and power-dense when scaled down to small sizes. Our prior work has explored the use of piezoelectric resonators (PRs) as alternative energy storage mechanisms for DC-DC converters, and we successfully demonstrated a magnetics-less PR-based converter with >99% efficiency. However, our initial prototypes depended on open-loop switching times that were manually tuned, meaning the converter could not dynamically handle transients or adjust operation when the load or temperature changed.

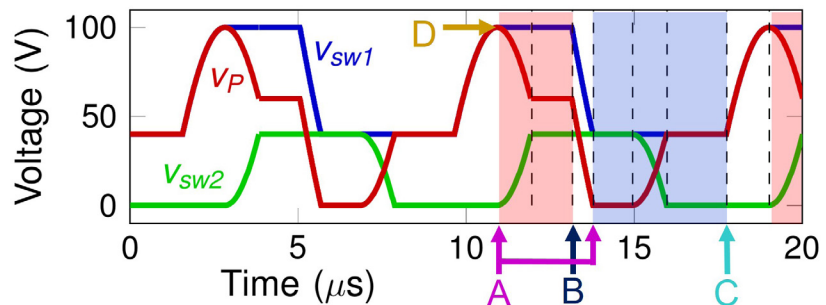
This work presents a closed-loop control scheme

for the PR-based DC-DC converter. For high efficiency, the converter is designed to cycle through a specific 6-stage “switching sequence” during each PR resonant cycle. In this sequence, the PR is switched between fixed-voltage energy transfer stages and resonant transition stages (shown in Figure 1), which is challenging to implement in a simple manner. The converter is controlled by two active switches, as shown in Figure 2. Both switches are triggered to turn on purely by voltage measurements of the PR node voltages. Switch 1’s on-time is modulated to control power output, and switch 2’s on-time is modulated to reach the specific high-efficiency point. Simulation results have shown that this control scheme is effective, and we are currently validating it on hardware. The successful implementation of this closed-loop control scheme will allow the PR-based converter to operate on its own, paving the way for use of these small and efficient DC-DC converters in commercial applications.



◀ Figure 1: Plot of PR voltage waveforms. A indicates voltage-sensed turn-ons. B indicates power-regulating turnoff. C indicates zero voltage switching controlled turnoff. The value of V_p at D is used to control turnoff at C.

▶ Figure 2: The specific converter topology implemented for validation. S1 and S2 are the controlled active switches. The PR equivalent circuit is shown inside the box. This topology steps down to output voltages less than $\frac{1}{2}$ the input voltage.



FURTHER READING

- J. D. Boles, J. J. Piel, and D. J. Perreault, “Enumeration and Analysis of DC-DC Converter Implementations Based on Piezoelectric Resonators,” *IEEE Transactions on Power Electronics*, vol. 36, no. 1, pp. 129-145, 2021.
- J. D. Boles, J. E. Bonavia, P. Acosta, Y. K. Ramadass, J. H. Lang, and D. J. Perreault, “Evaluating Piezoelectric Materials and Vibration Modes for Power Conversion,” (submitted).
- J. D. Boles, J. J. Piel, and D. J. Perreault, “Analysis of high-efficiency operating modes for piezoelectric resonator-based dc-dc converters,” *Proc. IEEE Applied Power Electronics Conference and Exposition (APEC)*, Mar. 2020.

Leveraging Multi-Phase and Fractional-Turn Planar Transformers for Power Supply Miniaturization in Data Centers

M. K. Ranjram, D. J. Perreault

Sponsorship: Cooperative Agreement between the Masdar Institute of Science and Technology and MIT

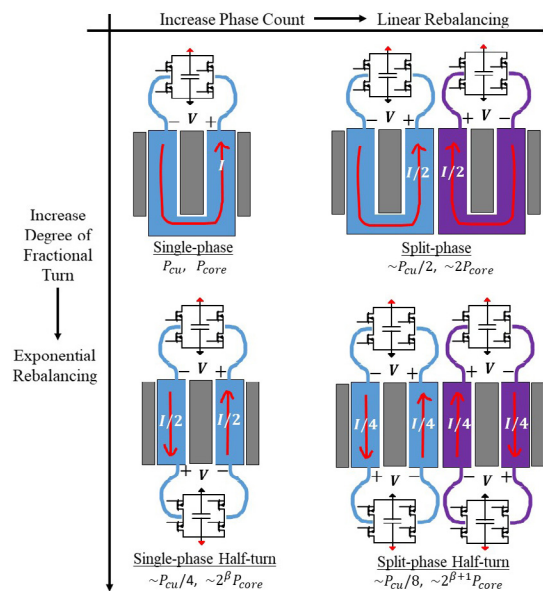
Data centers are the backbone of the Internet. Their servers represent an important and growing electrical load, and there is strong interest in miniaturizing the supplies that power them. Miniaturization is challenging as it requires both a reduction in volume and an increase in efficiency and is bottlenecked in this application by the need for a high-current transformer.

A common approach toward improving the current carrying capability of the transformer is to increase its phase count by employing multiple identical transformers in parallel. Every phase that is added proportionally decreases the “copper loss” (ohmic loss) of the transformer while proportionally increasing its core loss (i.e., loss in the magnetic material). We call this “linear rebalancing.”

In this work, we fundamentally re-think the nature of the transformer to maximally leverage the connecting electronics. In particular, by careful placement of the active switching devices required in a converter around and the passive copper and

magnetic material comprising the transformer, we can create a “fractional turn” transformer. Employing a half-turn fractional transformer reduces copper loss by a factor of four while increasing core loss by a factor of 2^β , where β is between 2 or 3 depending on the core material. Thus, fractional turn transformers yield an “exponential rebalancing” of core and copper loss.

We show that the fractional turn concept can also be combined with the common approach of adding transformer phases, enabling multi-phase fractional-turn transformers. For example, a split-phase half-turn transformer (SPHTT) combines the linear and exponential rebalancing of each of those transformers and allows a designer to get closer to the true optimum loss trade-off for a given application. We show that a SPHTT is optimal for a data center application, yielding 3.1x lower loss than a single-phase transformer in the same volume and demonstrating its clear miniaturization benefit.



▲ Figure 1: Multi-phase and fractional-turn techniques define a “map” to find the optimal loss trade-off.

Soft-Actuated Micro Aerial Vehicles with High Agility

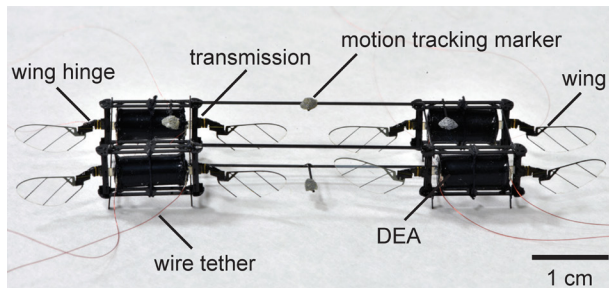
Z. Ren, K. Chen

Sponsorship: Research Laboratory of Electronics, MIT

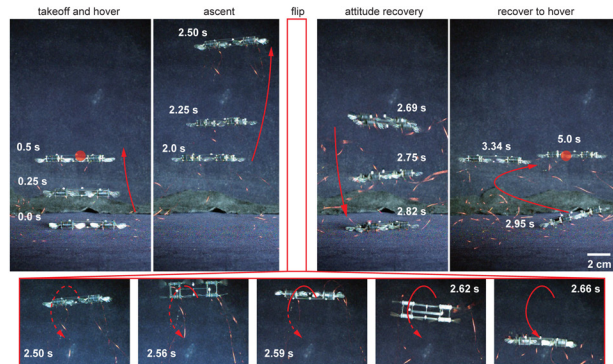
Developing agile and robust micro-aerial-vehicles (MAVs) that can demonstrate insect-like flight capabilities poses significant scientific and engineering challenges. Previously, we chose dielectric elastomer actuators (DEAs) to substitute for rigid actuators and achieved the first take-off and controlled flight of a soft-actuated MAV. In this work, we substantially improve the robot's flight capability through redesigning the actuator, robot wings, and transmission. The new MAV weighs approximately 665 mg and can complete a somersault within 0.16 s. Furthermore, its vertical ascending speed exceeds 70 cm/s, which makes it among the fastest soft mobile robots, and it outperforms rigid-powered subgram MAVs. A major contribution to this excellent performance is that we switch to a less viscoelastic elastomer, Elastosil P7670. Compared to our previously used elastomer (5:4 mixture of Ecoflex 0030 and Sylgard 184), this new elastomer has a higher resonance peak, which implies a larger displacement at

the resonant frequency. In addition, it has higher a dielectric strength and a shorter pot time.

Based on our measurement, the new MAV achieves a high lift-to-weight ratio of 2.2:1, which is 83% better than our previous work. The large lift force enables us to demonstrate hovering flight, ascending flight, in-flight collision recovery, and—more impressively—a somersault. As shown in Figure 2, the MAV takes off and hovers, accelerates upward, flips along its body pitch axis, recovers attitude, and finally returns to hover. The somersault is completed in 0.16 s; during the body flip, the motion capture system loses tracking for approximately 0.1 s. This loss results in the MAV's hitting the ground before recovering its attitude. Despite experiencing disturbance caused by the collision, the MAV quickly stabilizes its attitude and returns to hover. This is the first time that a soft-driven MAV performs agile tasks that rigid-driven MAVs have not yet demonstrated.



▲ Figure 1: Perspective view of a 665-mg MAV that is powered by DEAs. It consists of four identical modules; each module consists of an airframe, a DEA, a pair of wing hinges, wings, and transmissions.



▲ Figure 2: Sequence of composite images that show a 5-s somersault flight. The images illustrate the five flight phases: takeoff, ascent, flip, recovery, and hover.

FURTHER READING

- Y. Chen, S. Xu, Z. Ren, and P. Chirattananon, "Collision Resilient Insect-scale soft-actuated Aerial Robots with High Agility," *IEEE Transactions on Robotics*, to be published, 2021, DOI: 10.1109/TRO.2021.3053647.
- Y. Chen, H. Zhao, J. Mao, P. Chirattananon, E. F. Helbling, N. P. Hyun, D. R. Clarke, R. J. Wood, "Controlled Flight of a Microrobot Powered by Soft Artificial Muscles," *Nature*, vol. 575, no. 7792, pp. 324-329, 2019, DOI: 10.1038/s41586-019-1737-7.
- H. Zhao, A. M. Hussain, M. Duduta, D. M. Vogt, R. J. Wood, and D. R. Clarke, "Compact Dielectric Elastomer Linear Actuators," *Adv. Funct. Mater.*, vol. 28, no. 42, 2018, Art. no. 1804328, DOI: 10.1002/adfm.201804328.

Adjusting for Autocorrelated Errors in Neural Networks for Time Series Regression

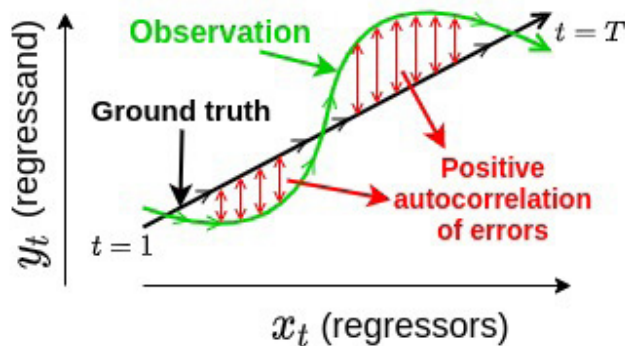
F.-K. Sun, D. S. Boning
Sponsorship: Lam Research

Time series data are ubiquitous. Researchers in many fields, including the social sciences, operations research, and engineering often collect time series data to create models for systems without prior or precise knowledge of the model structure and, in turn, provide insight for such systems. During this process of collection and creation, errors inevitably occur. Usually, the assumption is that the errors are uncorrelated at different time steps. However, in practice, errors can be autocorrelated when (1) the function space of the model and the true underlying system do not intersect, (2) some key explanatory variables are not collected, or (3) a measurement error at a current time step carries over to future time steps.

To solve this issue, previous literature, such as the Cochrane–Orcutt estimation, focuses only on cases where the model is linear or contains only predefined nonlinearity. This focus greatly limits usage, as many systems today (such as in semiconductor manufacturing) are almost certainly nonlinear while

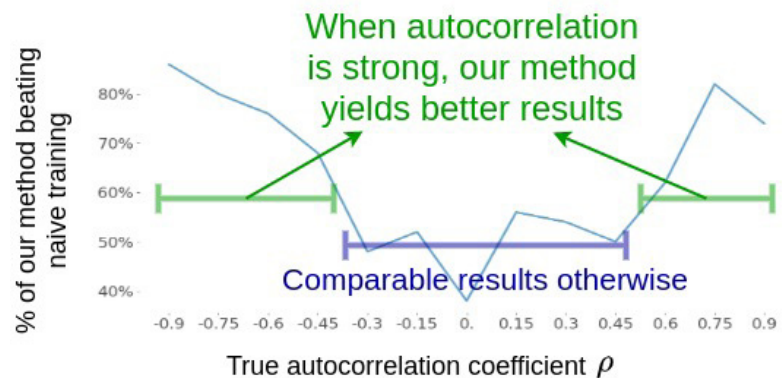
the underlying nonlinearity is unknown.

Here, we propose to use neural networks (NNs) to approximate the unknown nonlinearity and treat the autocorrelation coefficient ρ as a trainable parameter. The input to our model is a vector of features (i.e., regressors) at time t , and the output is the target scalar (i.e., regressand) also at time t . During training, we jointly optimize model parameters with the autocorrelation coefficient to adjust for the autocorrelated errors. This optimization enables us to train a NN that can fit the nonlinearity and adjust correspondingly to its autocorrelated noise. Compared to previous methods, this one has the advantages of (1) fitting unknown nonlinearity with autocorrelated noise and (2) better optimization via joint training of model parameters and autocorrelation coefficient. Our experimental results show that we obtain a better estimate of the autocorrelation coefficient and improve the model performance especially when the autocorrelated errors are substantial.



◀ Figure 1: Schematic illustration of autocorrelated errors.

▶ Figure 2: Applying our method improves the model performance.



FURTHER READING

- F.-K. Sun, C. I. Lang, and D. S. Boning, “Adjusting for Autocorrelated Errors in Neural Networks for Time Series Regression and Forecasting,” *arXiv preprint arXiv:2101.12578*, 2021.

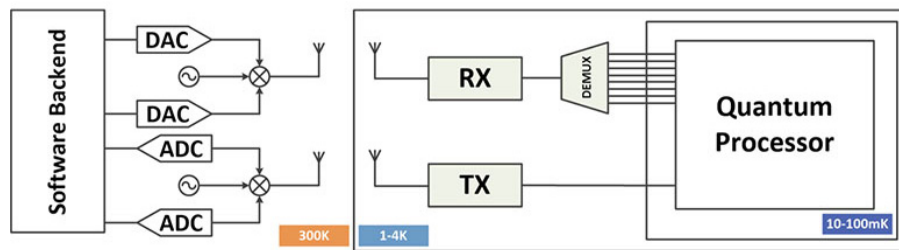
Terahertz Wireless Link for Quantum Computing in 22-nm FinFET

J. Wang, M. I. Ibrahim, R. Han
Sponsorship: Intel University Shuttle

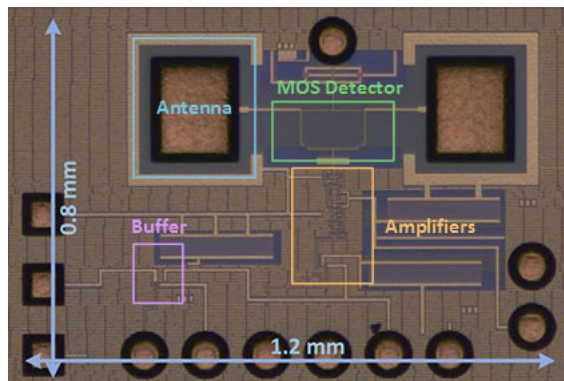
Quantum computing can provide exponential speed-up in solving many of today's intractable problems such as quantum chemistry, RSA encryption, DNA analysis, etc. In order to implement an error-protected quantum computer (QC), we will require approximately a million or thousands of qubits. State-of-the-art QCs have only around 100 qubits but still demand large-form-factor room-temperature electronics with many radio-frequency (RF) cables to realize the control and readout of quantum processors. These RF cables routed from room temperature to cryogenic temperature consume a non-negligible power due to the heat load, limiting the scalability and practical implementations of QCs.

We propose a terahertz (THz) wireless link to efficiently deliver the control signals to the cryogenic environment, reducing the heat loss due to the physical

conductive links (Figure 1). We implement a cryogenic THz receiver to send multi-Gb/s control signals modulated on a THz carrier (e.g., 260-GHz). The THz operation allows for a small antenna aperture size, high data rate, and minimal interference with the operation of the qubits, working around a few GHz. For the demodulation of the sub-THz downlink control signal, a THz square-law detector, operating with zero drain bias, is used first to rectify the input to baseband, and then a low-power transimpedance amplifier followed by a post-amplifier are used to boost the baseband signal so that the subsequent digital circuits can operate reliably. Figure 2 shows the chip photo of this prototype. This system opens the door for scalable and practical realization of cryogenic quantum systems.



▲ Figure 1: Block diagram of the proposed THz cryo-CMOS link system.



◀ Figure 2: Die photo of the RX part of the proposed THz cryo-CMOS link.

FURTHER READING

- J. C. Bardin, E. Jeffrey, E. Lucero, T. Huang, S. Das, D. T. Sank, O. Naaman, A. E. Megrant *et al.*, "Design and Characterization of a 28-nm Bulk-CMOS Cryogenic Quantum Controller Dissipating Less Than 2 mW at 3 K," *IEEE J. Solid-State Circuits*, vol. 54, no. 11, pp. 3043–3060, 2019.
- R. Barends, J. Kelly, A. Megrant, A. Veitia, D. Sank, E. Jeffrey, T. C. White, J. Mutus *et al.*, "Superconducting Quantum Circuits at the Surface Code Threshold for Fault Tolerance," *Nature*, vol. 508, no. 7497, pp. 500–503, 2014.

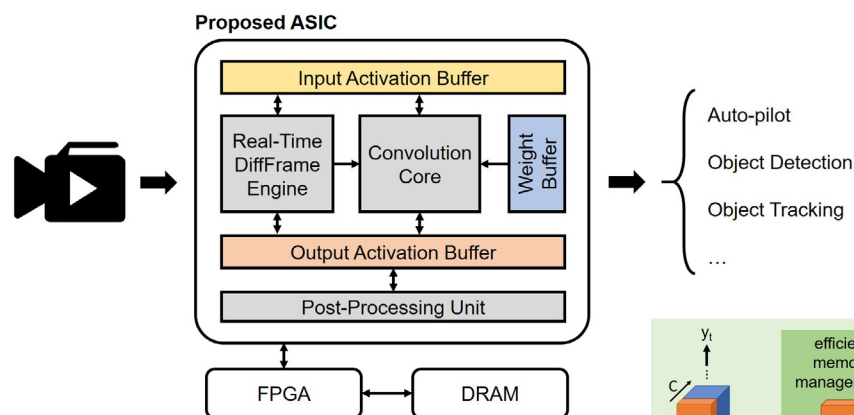
Energy-Efficient System Design for Video Understanding on the Edge

M. Wang, Z. Zhang, J. Lin, Y. Lin, S. Han, A. P. Chandrakasan
Sponsorship: Qualcomm Technologies, Inc.

With the rise of various applications including autonomous driving, object tracking for unmanned aerial vehicles, etc., the need increases for accurate and energy-efficient video understanding on the edge. Although plenty of deep learning chips designed for images exist, little work has been done for videos. Video understanding on the edge has three major challenges. First, video understanding requires temporal modeling. For example, it identifies the difference between opening and closing a box, which is distinguishable only with temporal information. Second, many applications are delay-critical, such as self-driving cars. Third, high energy efficiency matters for edge devices with a tight power budget. Due to temporal continuity, consecutive frames might share much information, providing a potential to improve processing efficiency. However, an image-based processing system, which processes frames individually, cannot utilize that.

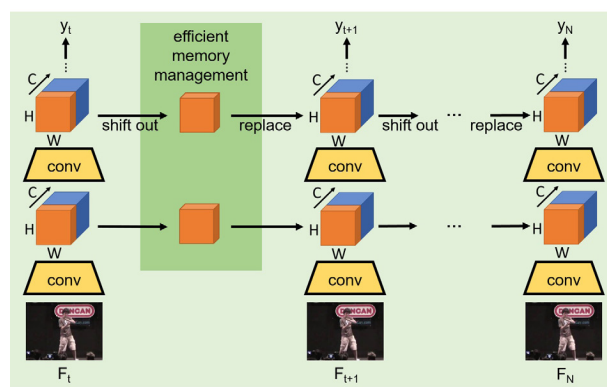
In this project, we co-designed algorithms and hardware for energy-efficient video processing on

delay-critical applications (Figure 1). We applied temporal shift module (TSM) on the backbone built on 2D convolutional neural network (Figure 2). To the best of our knowledge, our work is the first chip with temporal modeling support. Moreover, we propose a Real-Time DiffFrame method to reduce on-chip energy and DRAM traffic. It is based on the linearity of convolution, which has $\text{Conv}(f_t) = \text{Conv}(f_t - f_{t-1}) + \text{Conv}(f_{t-1})$, where f_t and f_{t-1} are the successive frames. Due to temporal continuity, $f_t - f_{t-1}$ is usually sparse. Instead of the ordinary sparsity-aware convolution in previous work, our method utilizes SparseConv, which does not dilate the input pattern and further improves energy efficiency. The load and store of $\text{Conv}(f_{t-1})$ are the overhead of the DiffFrame method. We propose a scheme to reduce memory traffic for real-time processing. The preliminary results show that our method achieves 1.6x reduction in DRAM traffic over previous work and 1.8x estimated reduction in computation and memory access over the baseline.



► Figure 2: TSM delivers state-of-the-art temporal modeling without any increase in computation, and a proposed TSM-aware mapping scheme efficiently handles the data movement.

◀ Figure 1: The proposed system supports temporal modeling and utilizes temporal redundancy in videos with a Real-Time DiffFrame Engine to improve processing efficiency for real-time applications.



FURTHER READING

- J. Lin, C. Gan, and S. Han, "TSM: Temporal Shift Module for Efficient Video Understanding," *Proc. IEEE International Conference on Computer Vision (ICCV)*, pp. 7083–7093, 2019.
- M. Riera, J.-M. Arnau, and A. González, "Computation Reuse in DNNs by Exploiting Input Similarity," *ACM/IEEE 45th Annual International Symposium on Computer Architecture (ISCA)*, pp. 57–68, 2018.
- C. Choy, J. Y. Gwak, and S. Savarese, "4D Spatio-temporal Convnets: Minkowski Convolutional Neural Networks," *Proc. IEEE Conference on Computer Vision and Pattern Recognition (CVPR)*, pp. 3075–3084, 2019.

Sparseloop: An Analytical, Energy-Focused Design Space Exploration Methodology for Sparse Tensor Accelerators

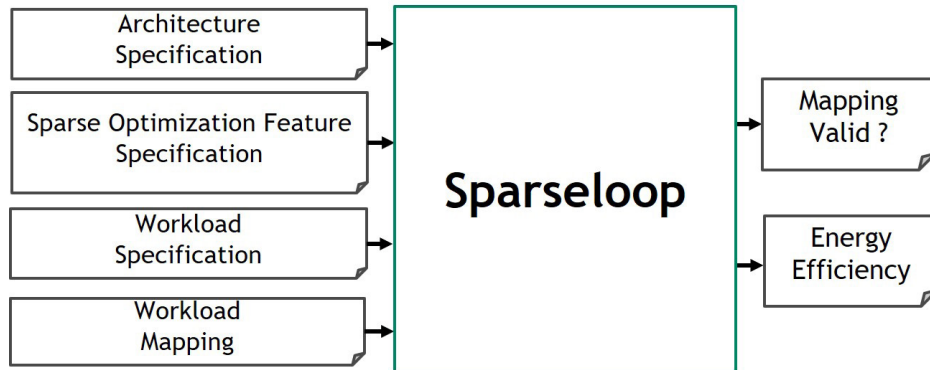
Y. N. Wu, P.-A. Tsai, A. Parashar, V. Sze, J. S. Emer
Sponsorship: DARPA

Many popular applications (e.g., deep neural networks) involve tensor computations (e.g., cross products) whose operand and result tensors can have high sparsity. Due to the nature of multiplication, zero multipliers always result in zero products. Such computations (which are called ineffectual) can be exploited by hardware sparse optimization features to improve energy efficiency and throughput. We classify these sparse optimization features into three categories: zero-gating, zero-skipping, and zero-compression. Zero-gating improves energy efficiency by keeping the associated hardware components idle for ineffectual computations. Zero-skipping further improves throughput by skipping cycles where ineffectual computations would have taken place. Zero-compression reduces required storage by storing only nonzero values.

In recent years, a variety of sparse tensor accelerators have been proposed. Based on the designer's intuitions, each design applies variations of the aforementioned sparse optimization features differently to the storage and compute levels of the

architecture. However, these specific designs are just points in a large and diverse space of sparse tensor accelerators. A fast, flexible, and accurate modeling framework would enable architects to perform early design space exploration in the complete space instead of picking specific points based on intuition.

Existing tensor accelerator models are either very detailed and design-specific, leading to slow and limited design space exploration, or fast and flexible but unable to systematically evaluate the impact of sparse optimization features, resulting in inaccurate modeling. In this work, we propose Sparseloop, an analytical modeling infrastructure for performing fast design space exploration of sparse accelerators that vary in both (1) properties associated with sparsity (e.g., compression formats, ineffectual operations' gating/skipping, and workload attributes) and (2) architecture properties (e.g., organization of the storage hierarchy). To the authors' knowledge, Sparseloop is the first analytical model that allows systematic evaluation of sparse tensor accelerators.



▲ Figure 1: Sparseloop high-level framework. Workload mapping describes the data movement and compute scheduling in space and time of the workload running on the specified architecture.

FURTHER READING

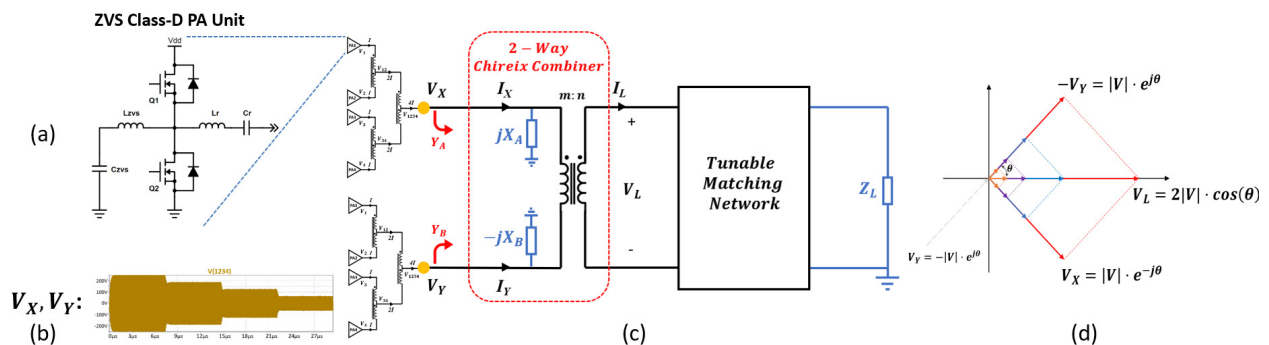
- Y. N. Wu, P.-A. Tsai, A. Parashar, V. Sze, and J. S. Emer, "Sparseloop: An Analytical, Energy-Focused Design Space Exploration Methodology for Sparse Tensor Accelerators," presented at *2020 IEEE International Symposium on Performance Analysis of Systems and Software (ISPASS)*, [city, country], 2021.
- Y. N. Wu, J. S. Emer, and V. Sze, "Accelerger: An Architecture-Level Energy Estimation Methodology for Accelerator Designs," presented at *2019 International Conference on Computer Aided Design (ICCAD)*, 2019.
- A. Parashar et al., "Timeloop: A Systematic Approach to DNN Accelerator Evaluation," presented at *2019 IEEE International Symposium on Performance Analysis of Systems and Software (ISPASS)*, Mar. 2019.

Multi-Inverter Discrete-Backoff: A High-Efficiency, Very-Wide-Range RF Power Generation Architecture

H. Zhang, A. Al Bastami, A. S. Jurkov, A. Radomski, D. J. Perreault
Sponsorship: MKS Instruments, Inc.

Radio-frequency (RF) power amplifiers (PAs) for industrial applications, e.g., plasma generation for semiconductor processing equipment, operate into variable load impedances at high frequency (e.g., tens of MHz) and power levels (e.g., peak power in kW), and often with wide overall power ranges and high peak-to-average-power ratios. To meet the evolving needs for semiconductor processing, goals for RF PAs in these applications include (1) operation over a wide load impedance (as determined by the plasma load); (2) operation across a very wide range of output power (e.g., 100:1 or 20 dB); (3) very fast dynamic response to output commands (e.g., at μs scale); and (4) high peak and average efficiency (to reduce cooling requirements and electricity costs). Unfortunately, meeting all these goals has not been possible to date, and efficiency is often sacrificed in order to meet the other performance metrics.

This work introduces a scalable power amplifier architecture and control approach suitable for such applications. The architecture consists of modular PAs organized in groups and employs (1) a technique which we call Multi-Inverter Discrete Backoff (MIDB), which losslessly combines the outputs of parallel-grouped switched-mode PAs and modulates the number of active PAs within the same group to provide discrete steps in RF output voltage, and (2) outphasing among the voltage outputs of PA-groups, for fast-response and continuous output power control over a wide range. To further expand the high-efficiency output power range of the system, discrete drain modulation may be optionally employed. In doing so, the MIDB-based architecture can maintain high efficiency and fast RF power control across a very wide range of power backoff.



▲ Figure 1: Example MIDB system implementation: (a) PA unit, (b) Achievable voltage magnitudes ($|V|$) with 4 PA units per PA-group, (c) PA system with differential Chireix combiner enabling outphasing between PA group voltage outputs V_X & V_Y and shunt compensation, and (d) Output power control vector diagram.

FUTHER READING

- H. Zhang, A. Al Bastami, A. S. Jurkov, A. Radomski, and D. J. Perreault, "Multi-Inverter Discrete Backoff: A High-Efficiency, Wide-Range RF Power Generation Architecture," 2020 IEEE 21st Workshop on Control and Modeling for Power Electronics (COMPEL), Aalborg, Denmark, 2020. doi: 10.1109/COMPEL49091.2020.9265702.
- A. Al Bastami, H. Zhang, A. Jurkov, A. Radomski, and D. Perreault, "Comparison of Radio-Frequency Power Architectures for Plasma Generation," 2020 IEEE 21st Workshop on Control and Modeling for Power Electronics (COMPEL), Aalborg, Denmark, 2020. doi: 10.1109/COMPEL49091.2020.9265700.

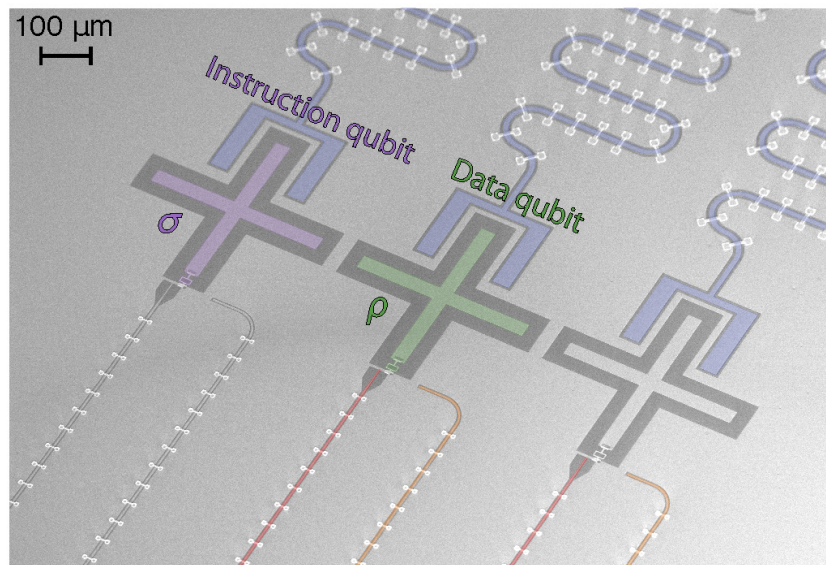
Programming a Quantum Computer with Quantum Instructions

M. Kjaergaard, M. E. Schwartz, A. Greene, G. O. Samach, A. Bengtsson, M. O’Keeffe, C. M. McNally, J. Braumüller, D. K. Kim, P. Krantz, M. Marvian, A. Melville, B. M. Niedzielski, Y. Sung, R. Winik, J. L. Yoder, D. Rosenberg, K. Obenland, S. Lloyd, T. P. Orlando, I. Marvian, S. Gustavsson, W. D. Oliver

Sponsorship: MK acknowledges support from the Carlsberg Foundation during part of this work. AG acknowledges funding from the 2019 Google US/Canada PhD Fellowship in Quantum Computing. IM acknowledges funding from NSF grant FET-1910859. This research was funded in part by the U.S. Army Research Office Grant W911NF-18-1-0411 and the Assistant Secretary of Defense for Research & Engineering under Air Force Contract No. FA8721-05-C-0002.

The use of quantum bits to construct quantum computers opens the door to dramatic computational speedups for certain problems. The maturity of modern quantum computers has moved the field from being predominantly a quantum-device-focused research area to also include practical quantum-computing-application-focused research. Our research explores a new experimental result on a foundational aspect of how to program quantum computers. A central principle of classical computer programming is the equivalence between data and instructions about what to do with that data. In quantum computers, this equiv-

alence is broken: classical hardware is used to generate the sequence of operations to be executed on the quantum data stored in the quantum computer. Our experiment shows for the first time how the instruction-data symmetry can be restored to quantum computers. We use superconducting qubits as a platform to implement high-fidelity quantum operations enabling the so-called density matrix exponentiation algorithm to generate these quantum instructions. This algorithm provides large quantum speedups for a family of other quantum algorithms.



▲ Figure 1: Scanning electron microscope image of three superconducting qubits (the ‘+’ shapes), identical to the qubits used in our experiment.

FURTHER READING

- M. Kjaergaard, et al., "Programming a Quantum Computer with Quantum Instructions," *arXiv:2001.08838*, 2020.
- A. Greene, M. Kjaergaard, et al., "Error Mitigation via Stabilizer Measurement Emulation," *arXiv:2102.05767*, 2021.
- M. Kjaergaard, et al., "Superconducting Qubits: Current State of Play," *Annual Reviews of Condensed Matter Physics* 11, 369-395, 2020.

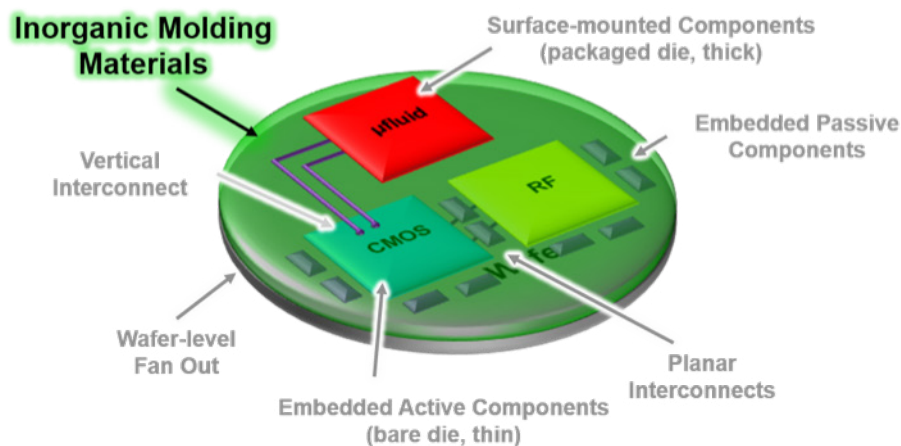
Silicate-Based Composite as Heterogeneous Integration Packaging Material for Extreme Environments

J. C. McRae, M. A. Smith, B. P. Duncan, E. Holihan, V. Liberman, C. Rock, D. Beck, L. M. Racz
Sponsorship: Office of the Under Secretary of Defense for Research and Engineering

Electronic microsystems are foundational to today's computational, sensing, communication, and information processing capabilities, therefore impacting industries such as microelectronics, aerospace, healthcare, and many more. Cell phones are an example of what is possible when a variety of systems can be tightly integrated into a highly portable and capable system. However, as we aim to improve our ability to interact and operate (e.g., sense, communicate, record, compute, move, etc.) in extreme environments (such as outer space or the human body), new methods and materials must be developed to manufacture such integrated systems that will endure post-processing, environmental, and operational challenges.

Typical organic-based packaging materials (e.g., polymer adhesives, coatings, and molding materials) often suffer from outgassing and leaching that can

lead to system contamination, as well as coefficient of thermal expansion (CTE) mismatches that can lead to warpage and breakage with fluctuations in system temperature during operation. This work demonstrates an alternative, by using a silicate-based inorganic glass composite as an electronics packaging material for stability in extreme environments. Combining liquid alkali sodium silicate (water glass) and nanoparticle fillers, composites can be synthesized and cured at low temperatures into chemically, mechanically, and thermally (up to 400°C) stable structures using high-throughput processing methods such as spin and spray coating. Further, this material can be processed into thick layers (10s to 100s of microns), fill high aspect ratio gaps (13:1), withstand common microfabrication processes, and have its CTE tailored to match various subs



DISTRIBUTION STATEMENT A: APPROVED FOR PUBLIC RELEASE. DISTRIBUTION IS UNLIMITED

▲ Figure 1. Common packaging and heterogenous integration technologies

FUTHER READING

- J. C. McRae, M. A. Smith, B. P. Duncan, E. Holihan, V. Liberman, C. Rock, D. Beck, L. M. Racz, "Sodium Metasilicate-Based Inorganic Composite for Heterogeneous Integration of Microsystems," in *IEEE Transactions on Components, Packaging and Manufacturing Technology*, vol. 11, no. 1, pp. 144-152, Jan. 2021

Electronic, Magnetic, Superconducting, and Neuromorphic Devices

100-nm Channel Length E-mode GaN p-Channel Field Effect Transistor (p-FET) on Si Substrate.....	43
GaN CMOS Gate Driver for GaN Power Transistor.....	44
Self-Aligned p-FET with $I_{ON} \sim 100$ mA/mm.....	45
Reliability of AlGaN/GaN-on-Si High-Electron-Mobility Transistors.....	46
CMOS-Compatible Vanadium Pentaoxide-Based Programmable Protonic Resistor for Analog Deep Learning.....	47
Waveguide Quantum Electrodynamics with Superconducting Artificial Giant Atoms.....	48
Dynamics of $\text{Hf}_{0.5}\text{Zr}_{0.5}\text{O}_2$ Ferroelectric Structures: Experiments and Models.....	49
Fault Detection for Semiconductor Processes Using One-Class Parzen Window Classifiers.....	50
Bias Temperature Instability under Forward Bias Stress of Normally-Off GaN High-Electron-Mobility Transistors ...	51
Morphological Stability of Nanometer-Scale Single-Crystal Metallic Interconnects.....	52
Switching Reliability of GaN Power High-Electron-Mobility Transistors.....	53
Automated Design of Superconducting Circuits and Its Application to 4-Local Couplers.....	54
CMOS-Compatible Protonic Programmable Resistor Based on Phosphosilicate Glass Electrolyte for Analog Deep Learning.....	55
III-V Broken-Band Vertical Nanowire Esaki Diodes.....	56
Mysterious Layer on a Hydrogen-Terminated Diamond Surface.....	57
Impact of Ionizing Radiation on Superconducting Qubit Coherence.....	58
NbN-Gated GaN Transistor Technology for Applications in Quantum Computing Systems.....	59
Metal Alloy Enables Reliable Silicon Memristor Synapses.....	60
Highly Tunable Junctions in Magic Angle Twisted Bilayer Graphene Tunneling Devices.....	61
Electronic Cells: Autonomous Micromachines from 2D Materials.....	62
Decoding Complexities in Relaxor Ferroelectrics Using Electron Microscopy.....	63

100-nm Channel Length E-mode GaN p-Channel Field Effect Transistor (p-FET) on Si Substrate

N. Chowdhury, Q. Xie, M. Yuan, T. Palacios
Sponsorship: Intel Corporation

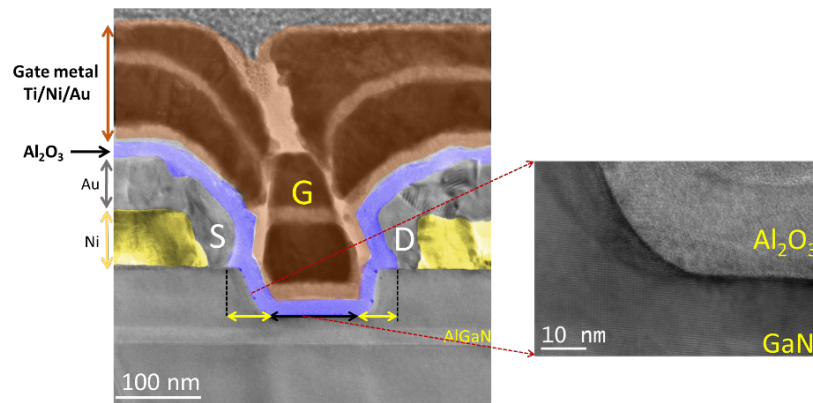
GaN-complementary circuit technology could be instrumental towards realizing high-power-density, high-speed, low-form-factor, and highly efficient power electronic circuits, which has sparked many efforts to develop a high performance GaN p-channel field-effect transistor (p-FET). However, most of these demonstrations show normally-ON operation with ON-resistance over 1 k Ω ·mm. The GaN/AlInGaN heterostructure-based p-FET shows low ON-resistance because of higher 2-DHG density and hole mobility but with D-mode operation. A GaN/AlN heterostructure-based p-FET shows enhanced-mode (E-mode) operation with R_{ON} of 640 Ω ·mm. However, n-FET integration with this p-FET requires regrowth.

In this work, we demonstrate a self-aligned p-FET with a GaN/Al_{0.2}Ga_{0.8}N (20 nm)/GaN heterostructure grown by metal-organic-chemical vapor deposition (MOCVD) on Si substrate. The utilization of a GaN-on-Si platform offers lower cost, availability of 200-mm-diameter substrates, and potential to integrate with high performance logic and analog functionality.

While most of the GaN p-FET demonstrations

so far in the literature focus mainly on recessed gate metal-insulator-semiconductor FET (MISFET) structure, we choose to develop a self-aligned structure (see Figure 1 for the device structure) as it offers the following advantages over a recessed gate MIS p-FET: (1) the shortest possible source to the drain distance, cutting down the access region; (2) low ON-resistance because of negligible access resistance; and (3) easier gate alignment.

Our 100-nm-channel-length self-aligned device with recess depth of 70 nm exhibits a record ON-resistance of 400 Ω ·mm and ON-current over 5 mA/mm with ON-OFF ratio of 6 \times 10⁵ when compared with other p-FET demonstrations based on a GaN/AlGaIn heterostructure (see Figure 2 for benchmarking of our device with other p-FETs demonstrated in the literature). The device shows E-mode operation with a threshold voltage of -1 V, making it a promising candidate for a GaN-based complementary circuit that can be integrated on a Si platform. A monolithically integrated n-channel transistor with p-GaN gate is also demonstrated.



▲ Figure 1: Transmission electron microscopy (TEM) image of the fabricated self-aligned p-FET with 100-nm channel length. TEM image showing the smooth interface between the GaN and gate dielectric attesting to the high quality of gate recess process with low surface roughness.

FURTHER READING

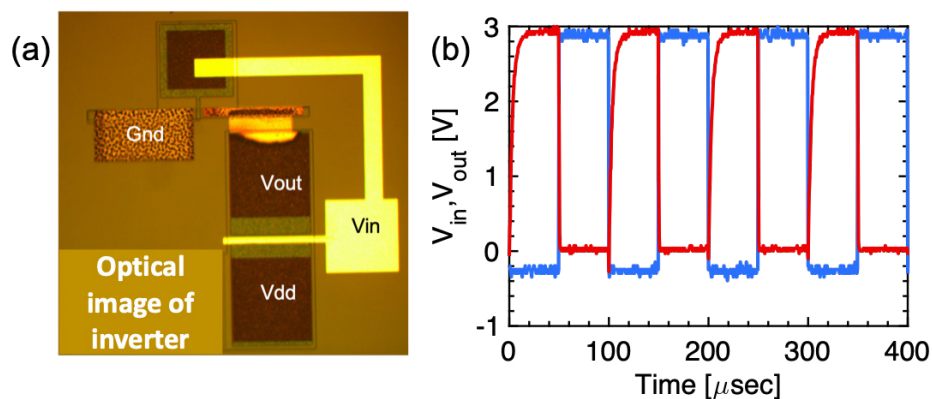
- N. Chowdhury, J. Lemettinen, Q. Xie, NS. Rajput, Y. Zhang, P. Xiang, K. Cheng, HW. Then, et al., "p-Channel GaN Transistor Based on p-GaN/AlGaIn/GaN on Si," *IEEE Electron Device Lett.*, vol. 40, no. 7, pp. 1036-1039, Jul. 2019, DOI: 10.1109/LED.2019.2916253.
- N. Chowdhury, Q. Xie, M. Yuan, K. Cheng, HW. Then and T. Palacios, "Regrowth-free GaN-based Complementary Logic on a Si Substrate," *IEEE Electron Device Letters*, vol. 41, no. 6, pp. 820-823, June 2020, DOI: 10.1109/LED.2020.2987003.
- N. Chowdhury, Q. Xie, M. Yuan, NS Rajput, P. Xiang, K. Cheng, HW. Then and T. Palacios, "First Demonstration of a Self-Aligned GaN p-FET," *Proc. IEEE International Electron Devices Meeting (IEDM)*, vol. 4, no. 6, pp. 1-4, Dec. 2019. DOI: 10.1109/IEDM19573.2019.8993569.

GaN CMOS Gate Driver for GaN Power Transistor

N. Chowdhury, Q. Xie, M. Yuan, T. Palacios
Sponsorship: Intel Corporation

In combination with its excellent transport properties, the high critical electric field of GaN, allows for GaN power transistors with much shorter drift regions and narrower gate widths than their Si or SiC counterparts. This allows for significantly lower gate capacitances and faster switching frequencies than traditional power switches at the same operating voltages. To take full advantage of the reduced gate capacitance and high switching speed of GaN power transistors, it is necessary to minimize parasitic inductances between the power switches/transistors and the gate driver circuit. For this, the GaN community has traditionally leveraged enhancement-mode/depletion-mode logic also known as direct coupled logic (DCL) to integrate relatively simple gate-driver circuits on the same chip as the GaN power devices; however, this technology suffers from significant power consumption and limited

circuit design flexibility. To overcome these issues, recently there has been much research on a new all-GaN complementary technology that allows integration of high-performance n-channel and p-channel GaN enhancement-mode transistors on the same chip without the need for epitaxial regrowth. The epitaxial structure used for the demonstration of the all-GaN complementary technology consists of a GaN/AlGaIn/GaN double heterostructure. This structure was grown by the company Enkris Semiconductor on 6" silicon wafers. Enhancement-mode p-type transistors were fabricated by contacting the two-dimensional hole gas at the top GaN/AlGaIn interface while n-type devices are obtained by recessing the structure to allow direct ohmic contact connection to the two-dimensional electron gas at the bottom AlGaIn/GaN interface. A simple gate driver with a 350-pF load is switched at 100-kHz frequency.



▲ Figure 1: (a) Optical micrograph of an all-GaN complementary gate driver. (b) Input and output voltages for a 35-pF load.

FURTHER READING

- N. Chowdhury, J. Lemettinen, Q. Xie, NS. Rajput, Y. Zhang, P. Xiang, K. Cheng, HW. Then, et al., "p-Channel GaN Transistor Based on p-GaN/AlGaIn/GaN on Si," *IEEE Electron Device Lett.*, vol. 40, no. 7, pp. 1036-1039, Jul. 2019, DOI: 10.1109/LED.2019.2916253.
- N. Chowdhury, Q. Xie, M. Yuan, K. Cheng, HW. Then and T. Palacios, "Regrowth-free GaN-based Complementary Logic on a Si Substrate," *IEEE Electron Device Letters*, vol. 41, no. 6, pp. 820-823, June 2020, DOI: 10.1109/LED.2020.2987003.
- N. Chowdhury, Q. Xie, M. Yuan, NS Rajput, P. Xiang, K. Cheng, HW. Then and T. Palacios, "First Demonstration of a Self-Aligned GaN p-FET," *Proc. IEEE International Electron Devices Meeting (IEDM)*, vol. 4, no. 6, pp. 1-4, Dec. 2019. DOI: 10.1109/IEDM19573.2019.8993569.

Self-Aligned p-FET with $I_{ON} \sim 100$ mA/mm

N. Chowdhury, Q. Xie, M. Yuan, T. Palacios
Sponsorship: Intel Corporation

GaN-complementary circuit technology could be instrumental towards realizing high-power-density, high-speed, low-form-factor, and highly efficient power electronic circuits, which has sparked many efforts to develop a high performance GaN p-channel field-effect transistor (p-FET). However, most of these demonstrations show normally-ON operation with ON-resistance over $1 \text{ k}\Omega\cdot\text{m}$. In this work, we demonstrate a self-aligned p-FET with a GaN/ $\text{Al}_{0.2}\text{Ga}_{0.8}\text{N}$ (20 nm)/GaN heterostructure grown by metal-organic-chemical vapor deposition on Si substrate. The utilization of a GaN-on-Si platform offers lower cost, availability of 200-mm-diameter substrates, and potential to integrate with high performance logic and analog functionality. While most of the GaN p-FET demonstrations so far in the literature focus mainly on a recessed gate metal-insulator-semi-

conductor FET (MISFET) structure, we choose to develop a self-aligned structure as it offers the following advantages over a recessed gate MIS p-FET: (1) the shortest possible source to the drain distance, cutting down the access region; (2) low ON-resistance because of negligible access resistance; and (3) easier gate alignment. The device with $L_{SD}=200$ nm shows a record combination of $I_{ON} \sim 50$ mA/mm and ON-OFF ratio of 10^4 when compared with other p-channel transistor demonstrations. The device also exhibits enhancement mode operation with threshold voltage of -0.5 V. The best device shows a record current density of 100 mA/mm but at the expense of a lower ON-OFF ratio of 10^2 . A monolithically integrated n-channel transistor with p-GaN gate is also demonstrated.

FURTHER READING

- N. Chowdhury, J. Lemettinen, Q. Xie, NS. Rajput, Y. Zhang, P. Xiang, K. Cheng, HW. Then, et al., "p-Channel GaN Transistor Based on p-GaN/AlGaIn/GaN on Si," *IEEE Electron Device Lett.*, vol. 40, no. 7, pp. 1036-1039, Jul. 2019, DOI: 10.1109/LED.2019.2916253.
- N. Chowdhury, Q. Xie, M. Yuan, K. Cheng, HW. Then and T. Palacios, "Regrowth-free GaN-based Complementary Logic on a Si Substrate," *IEEE Electron Device Letters*, vol. 41, no. 6, pp. 820-823, June 2020, DOI: 10.1109/LED.2020.2987003.
- N. Chowdhury, Q. Xie, M. Yuan, NS Rajput, P. Xiang, K. Cheng, HW. Then and T. Palacios, "First Demonstration of a Self-Aligned GaN p-FET," *Proc. IEEE International Electron Devices Meeting (IEDM)*, vol. 4, no. 6, pp. 1-4, Dec. 2019. DOI: 10.1109/IEDM19573.2019.8993569.

Reliability of AlGaIn/GaN-on-Si High-Electron-Mobility Transistors

Y. Gao, W. A. Sasangka, C. L. Gan, C. V. Thompson
Sponsorship: Singapore-MIT Alliance for Research and Technology Center

AlGaIn/GaN high-electron-mobility transistors (HEMTs) are of interest for high-frequency and high-power applications such as in 5G networks and autonomous vehicles. Fabrication of GaN-based devices on silicon substrates can lead to reduced costs as well as enable monolithic integration of Si-complementary metal-oxide-semiconductor devices with GaN HEMTs. However, due to the large mismatches in lattice constant and coefficient thermal expansion between GaN and Si, GaN-on-Si HEMTs face challenges in terms of long-term reliability.

Our previous work has focused on degradation of the maximum drain current observed after off-state and on-state stressing in reverse or zero gate bias conditions. Decreases in the drain current, I_D , and increases in the gate leakage current, I_G , were found to be associated with electrochemical oxidation and pit formation at the gate edges. This degradation can be suppressed by using high-density passivation layers, reducing the threading dislocation density and reducing oxygen impurities at the GaN-cap/passivation layer interface.

Given that HEMTs also operate in forward gate bias, we have more recently focused on forward-bias stressing of research-grade HEMTs by setting the gate bias $V_{G-stress}$ at 2, 2.5, 3, or 4 V with $V_D = V_S = 0$ V. I_D vs. V_G measurements were made at time increments during testing. As shown in Figure 1(a), the drain saturation current and threshold voltage do not change significantly over time while the leakage current increases dramatically. Moreover, increasing the stressing voltage highly accelerates this degradation (Figure 1(b)). This increase in the leakage current was accompanied by a decrease of the Schottky barrier height and an increase in the ideality factor, suggesting the degradation likely occurred at the Schottky gate contact.

Further analysis using photon emission microscopy (PEM), transmission electron microscopy (TEM), and electron energy loss spectroscopy (EELS) revealed that carbon impurities in the gate metal layer (nickel) were responsible for this degradation (Figure 2(a) and 2(b)). The carbon impurities likely originated from photoresist residues from the gate lift-off process.

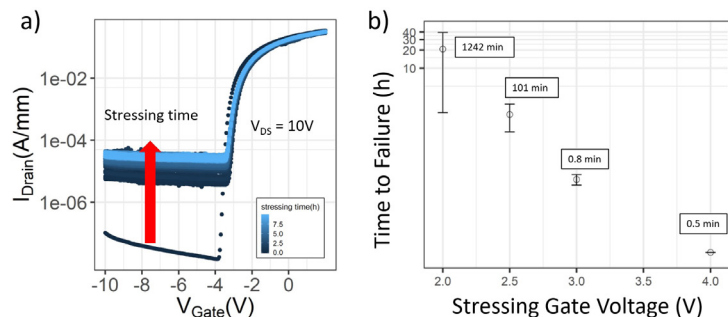
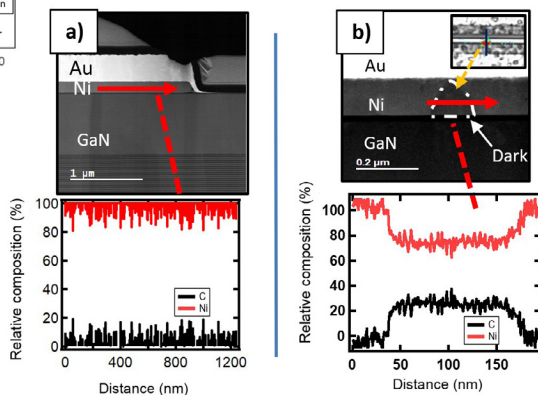


Figure 1: (a) Typical I_D - V_G characteristics over time for a device stressed at $V_{G-stress} = 3$ V. (b) The average device failure times at four different stressing voltages (Failure criterion: I_{Drain} at -8.5 V = $12.5 \mu A/mm$).

Figure 2. EELS line scans for (a) a fresh sample and (b) a stressed sample (failed) at a hotspot region.



FURTHER READING

- Y. Gao, W. A. Sasangka, C. V. Thompson, and C. L. Gan, "Effects of Forward Gate Bias Stressing on the Leakage Current of AlGaIn/GaN High Electron Mobility Transistors," *Microelectronics Reliability*, vols. 100-101, p. 113432, 2019.
- W. A. Sasangka, Y. Gao, C. L. Gan, and C. V. Thompson, "Impact of Carbon Impurities on the Initial Leakage Current of AlGaIn/GaN High Electron Mobility Transistors," *Microelectronics Reliability*, vols. 88-90: pp. 393-396, 2018.
- Gan, C. L., W. A. Sasangka, and C. V. Thompson. "Electrochemical Oxidation in AlGaIn/GaN-on-Si High Electron Mobility Transistors." In *2019 Electron Devices Technology and Manufacturing Conference (EDTM)*, pp. 71-73, 2019.

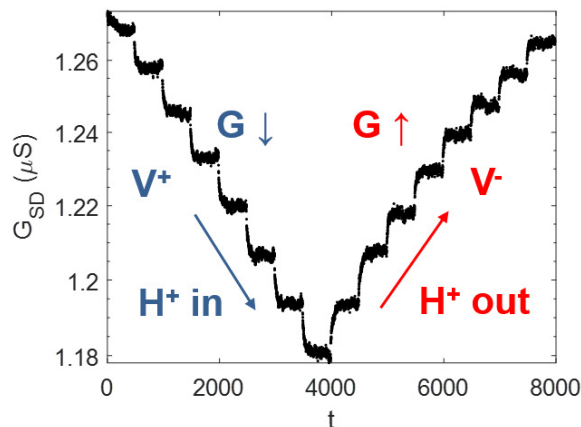
CMOS-Compatible Vanadium Pentoxide-Based Programmable Protonic Resistor for Analog Deep Learning

N. Emond, M. Onen, J. Li, J. A. del Alamo, B. Yildiz
Sponsorship: MIT-IBM Watson AI Lab

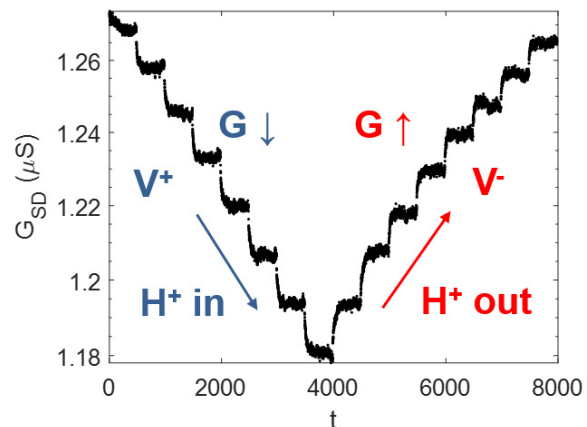
Deep learning proficiency in classification and clustering of data representations has fundamentally changed how information is processed. However, state-of-the-art digital processing units based on complementary metal-oxide-semiconductor (CMOS) circuits require large memory space and high power consumption to train deep neural networks. Improvements in computing performance therefore require designing novel scalable, fast, and energy-efficient hardware structures with both processing and storage capabilities using analog crossbar arrays.

The building block of these arrays is a programmable, non-volatile resistor, which should display multiple conductance states that are modulated reversibly, symmetrically, and reproducibly. Several device technologies, based mainly on filamentary conduction and phase-change mechanisms, have been proposed for analog deep learning; none of these however yet meets all device performance requirements. A recent concept, ion intercalation in transition-metal oxides, can potentially circumvent issues faced by other mechanisms.

We are therefore investigating a CMOS-compatible proton intercalation resistor that relies on a deterministic charge-controlled mechanism. The use of protons, the smallest cations, as the doping ion presents several advantages including high operation speed, good compatibility with current patterning processes, and long lifetime. Our initial design, shown in Figure 1, with a PdH_x solid hydrogen reservoir and a WO_3 active channel, demonstrated promising device characteristics but needs to be improved as: 1) it relied on Nafion, a non-CMOS-compatible electrolyte that strongly reacts with some other promising channel materials, and 2) the conductance of WO_3 and device energy consumption (conductance reading) increases through protonation. Herein, we present our progress towards device integrability using an inert CMOS-compatible electrolyte and on the reduction of the device energy consumption using a vanadium pentoxide (V_2O_5) channel, which conductance decreases through protonation and can be modulated in a non-volatile, symmetric, reversible, and reproducible way, as shown in Figure 2.



▲ Figure 1: Side-view schematic of the V_2O_5 -based protonic programmable resistor.



▲ Figure 2: Modulation characteristics of the V_2O_5 -based protonic programmable resistor.

FURTHER READING

- X. Yao, K. Klyukin, W. Lu, M. Onen, S. Ryu, D. Kim, N. Emond, I. Waluyo, et al., "Protonic Solid-State Electrochemical Synapse for Physical Neural Networks", *Nature Communications*, vol. 11, no. 1-10, 2020.

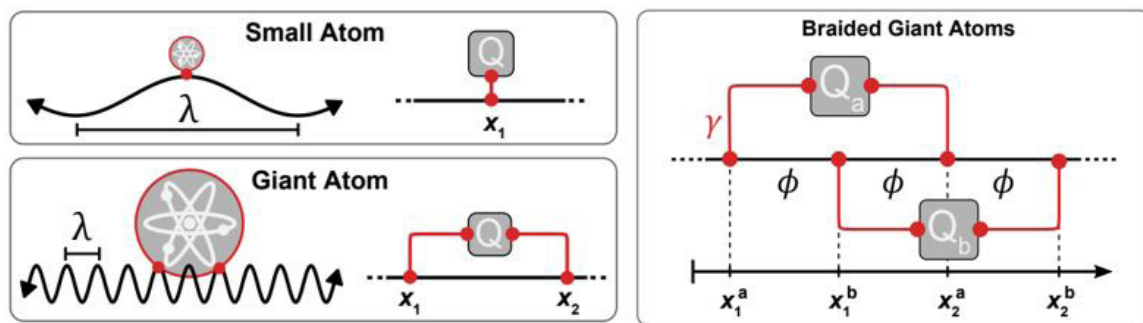
Waveguide Quantum Electrodynamics with Superconducting Artificial Giant Atoms

B. Kannan, M. Ruckriegel, D. L. Campbell, A. F. Kockum, J. Braumüller, D. K. Kim, M. Kjaergaard, P. Krantz, A. Melville, B. M. Niedzielski, A. Vepsäläinen, R. Winik, J. Yoder, F. Nori, T. P. Orlando, S. Gustavsson, W. D. Oliver
 Sponsorship: DoE, Office of Science, Basic Energy Sciences, Materials Sciences and Engineering

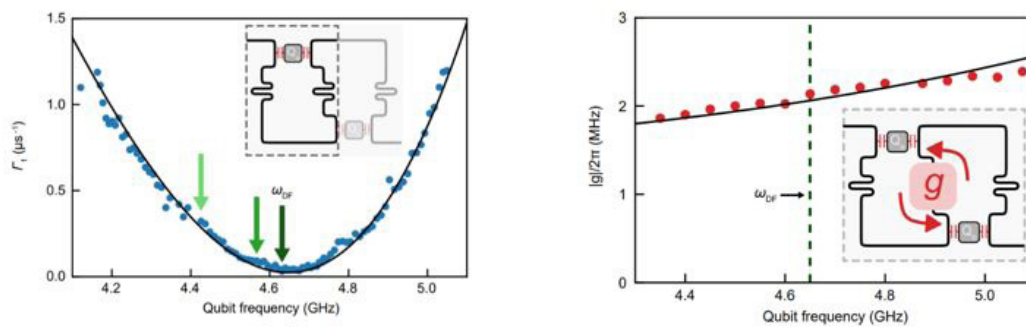
Models of light-matter interactions typically invoke the dipole approximation, within which atoms are treated as point-like objects when compared to the wavelength of the electromagnetic modes that they interact with. However, when the ratio between the size of the atom and the mode wavelength is increased, the dipole approximation no longer holds, and the atom is referred to as a “giant atom.” Thus far, experimental studies with solid-state devices in the giant-atom regime have been limited to superconducting qubits that couple to short-wavelength surface acoustic waves, probing the properties of the atom at only a single frequency.

Figure 1 shows an alternative architecture that realizes a giant atom by coupling small atoms to a waveguide at multiple, but well separated, discrete locations. We also show how multiple giant atoms

can be coupled to the same waveguide in a braided fashion to enable interactions between the qubits that are mediated by the waveguide. Figure 2 shows how our realization of giant atoms enables tunable atom-waveguide couplings with large on-off ratios and a coupling spectrum that can be engineered by device design. We also demonstrate decoherence-free interactions between multiple giant atoms that are mediated by the quasi-continuous spectrum of modes in the waveguide— an effect that is not possible to achieve with small atoms. These features allow qubits in this architecture to switch between protected and emissive configurations in situ while retaining qubit-qubit interactions, opening new possibilities for high-fidelity quantum simulations and non-classical itinerant photon generation.



▲ Figure 1: Schematic representation of small and giant atoms that are discretely coupled to a waveguide.



▲ Figure 2: Tunable atom-waveguide couplings (left) and waveguide-mediated interactions (right).

FURTHER READING

- B. Kannan, M. Ruckriegel, D. L. Campbell, A. F. Kockum, J. Braumüller, D. K. Kim, M. Kjaergaard, P. Krantz, et al., “Waveguide Quantum Electrodynamics with Superconducting Artificial Giant Atoms,” *Nature* 583, 775-779, Jul. 2020.

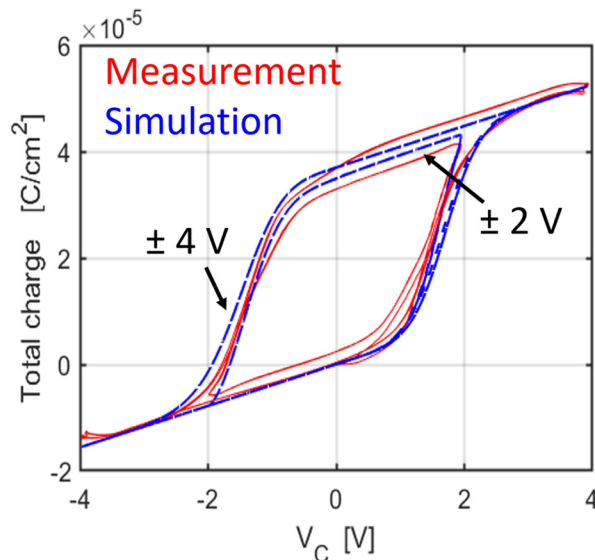
Dynamics of $\text{Hf}_{0.5}\text{Zr}_{0.5}\text{O}_2$ Ferroelectric Structures: Experiments and Models

T. Kim, D. A. Antoniadis, J. A. del Alamo

Sponsorship: Semiconductor Research Corporation, Samsung Electronics

Due to its complementary metal-oxide-semiconductor compatibility, ferroelectric HfZrO_2 (FE-HZO) has attracted enormous interest in various semiconductor device areas, such as analog computing, logic, and memory. Despite intense research, controversy remains about the ferroelectric switching dynamics and the existence of negative capacitance (NC). To develop fundamental understanding, we have carried out detailed experimental studies of the FE-HZO switching dynamics of metal-ferroelectric-metal (MFM) and metal-ferroelectric-insulator-metal (MFIM) structures.

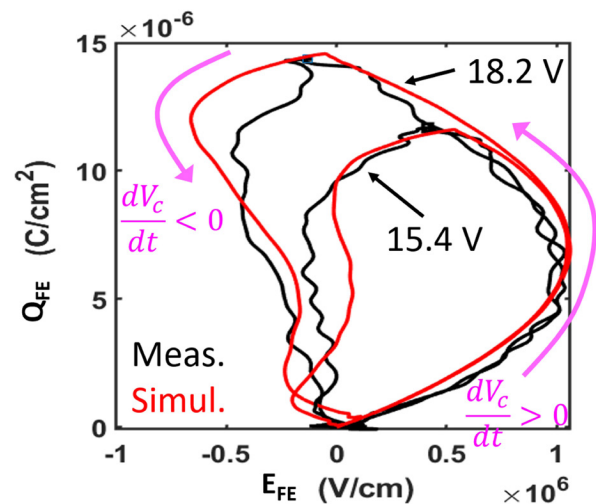
To extract the intrinsic dynamic response of the structures, our experimental methodology has paid close attention to minimizing and calibrating all circuit and sample parasitics. Based on the measured MFM dynamics, we have proposed a new nucleation-limited switching (NLS) model that captures the incubation and growth of polarization domain nuclei within each grain of a polycrystalline ferroelectric film, as described by a Weibull distribution. Figure 1 shows that the model describes well all observed behavior



▲ Figure 1: Extracted major and minor QFE vs. VC loops from trapezoidal bipolar pulse measurement (red) and simulation (blue) for 400- μm^2 MFM capacitor.

including major and minor charge-voltage loops under a broad range of conditions. Further, our work reveals that in R-MFM circuit configurations with an external resistor, the MFM dynamics show no evidence of NC-like behavior in contrast with other reports. Our study suggests that erroneous consideration of parasitic capacitance could explain earlier claims of NC effects in the MFM dynamics.

We observed clear NC behavior in MFIM structures. We confirm the transient quasi-static S-like FE behavior described in the literature and observe a dynamic response that displays hysteretic behavior in the NC region. A model based on the Landau-Khalatnikov equation that incorporates FE dynamics via a phenomenological frictional resistance adequately describes the observed results when that resistance is made dependent on the direction of the voltage drive vs. time, as in Figure 2. Mitigation of this hysteretic NC behavior will be crucial to harness NC in practical metal-oxide-semiconductor field-effect transistors.



▲ Figure 2: Dynamic response of FE-HZO in MFIM structure. Extracted QFE vs. EFE from 15.4-V and 18.2-V unipolar pulses measurement (black) and simulation (red) for 2500 μm^2 capacitor. Purple lines show direction of voltage drive vs. time.

FURTHER READING

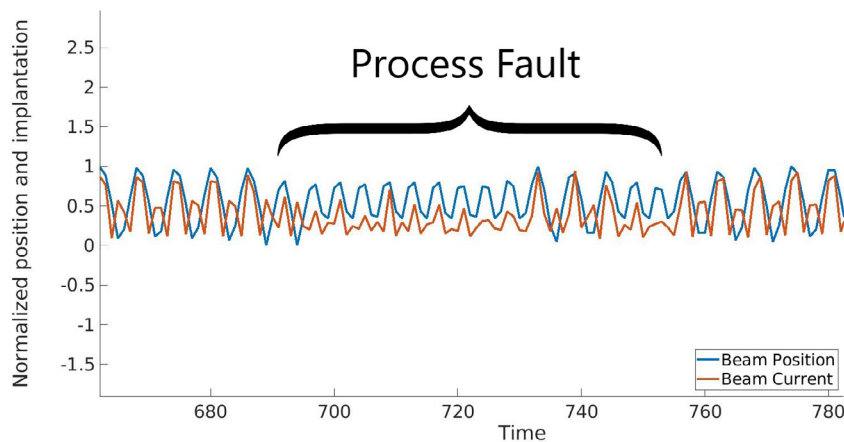
- J. Müller, T. S. Böscke, U. Schröder, S. Mueller, D. Bräuhäus, U. Böttger, L. Frey, and T. Mikolajick, "Ferroelectricity in Simple Binary ZrO_2 and HfO_2 ," *Nano Letters*, vol. 12, pp. 4318-1323, 2012.
- C. Alessandri, P. Pandey, A. Abusleme, and A. Seabaugh, "Monte Carlo Simulation of Switching Dynamics in Polycrystalline Ferroelectric Capacitors," *IEEE Transactions on Electron Devices*, vol. 66, no. 8, 2019.
- M. Hoffmann, F. P. G. Fengler, M. Herzig, T. Mittmann, M. Max, U. Schröder, R. Negrea, P. Lucian, et al., "Unveiling the Double-well Energy Landscape in a Ferroelectric Layer," *Nature*, vol. 565, pp. 464-467, 2019.

Fault Detection for Semiconductor Processes Using One-Class Parzen Window Classifiers

C. Lang, D. S. Boning
Sponsorship: Analog Devices, Inc.

Faults in fabrication processes are extremely costly. When undetected and unaddressed, they will continue to ruin wafer lots until the underlying problem is corrected, leading to massive yield losses. Our work uses one-class Parzen window classifiers to raise alerts when faults are suspected by monitoring process sensor information, reducing future yield loss. These models are kernel-based density estimation methods that determine the similarity of incoming data to known good process data. The method uses only nominal pro-

cess data, which is desirable as faults are often unique, and examples will not be available before they occur. Using historical examples of a wide variety of faults in plasma etching and ion implantation (Figure 1), our fault-detection methodology captures more than 90% of faults, with a false positive rate of less than 0.5%. This method can be applied to a wide variety of processes without significant adjustment, making it ideal for generalized fault detection.



▲ Figure 1: Example fault in the ion implantation process causing yield losses. Within the faulty segment, beam current is lower than expected and does not follow the nominal pattern seen outside this range.

Bias Temperature Instability under Forward Bias Stress of Normally-Off GaN High-Electron-Mobility Transistors

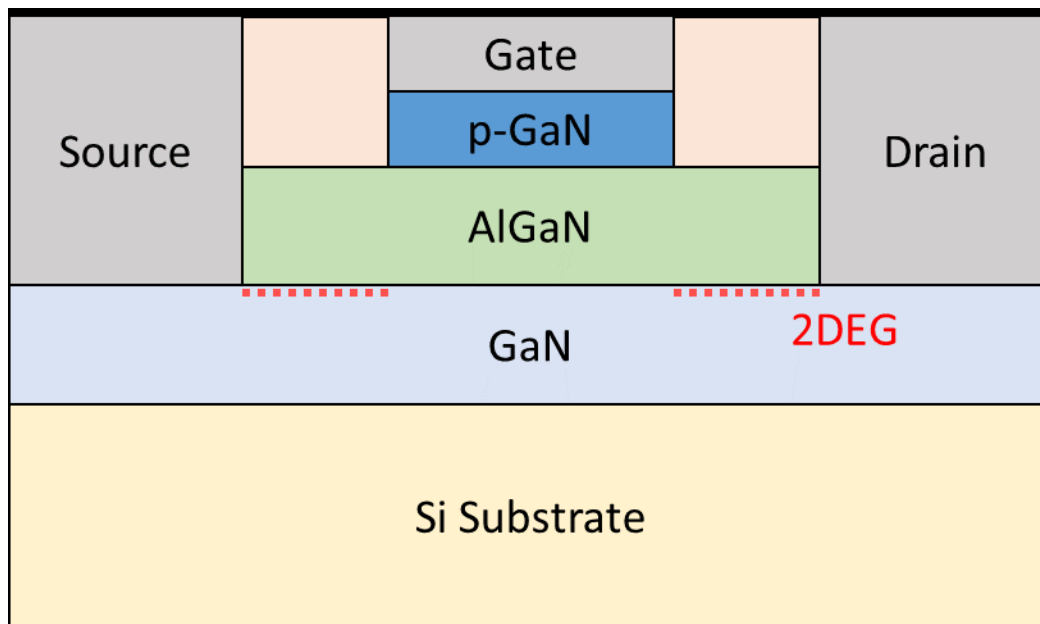
E. S. Lee, J. A. del Alamo
Sponsorship: Texas Instruments

Energy-efficient electronics have been gaining much attention as a necessary path to meet the growing demand for electrical energy and sustainability. GaN field-effect transistors (FETs) show great promise as high-voltage power switches due to their ability to withstand a large voltage and carry high current. For best circuit reliability, safety, and performance, a normally-off transistor is highly desirable. An attractive design is the p-doped GaN-gate high-electron-mobility transistor (p-GaN HEMT).

Our research aims to better understand the reliability issues impeding widespread adoption of p-GaN power HEMTs. One key issue is device degradation under prolonged operation, where key

device performance metrics such as threshold voltage and gate leakage current change with electrical stress.

We show that device degradation under forward-bias electrical stress, i.e., when the transistor is turned on, shows multiple regimes that are voltage and time dependent. Due to the complex gate stack that includes a p-doped GaN layer, the device exhibits bias temperature instability degradation with signature characteristics of electron and hole trapping. Furthermore, we show that some of the degradation is recoverable. Altogether, our research reveals the presence of rich and dynamic degradation physics for the p-GaN HEMTs that must be well understood before the commercial success of this technology.



▲ Figure 1: Simplified cross section of the p-GaN gate HEMT. AlGaN /GaN interface naturally induces a 2-dimensional electron gas (2DEG) that allows for conduction. However, the addition of the p-GaN layer leads to a natural depletion of the 2DEG and enhancement-mode operation.

FURTHER READING

- J. A. del Alamo and E. S. Lee, "Stability and Reliability of Lateral GaN Power Field-Effect Transistors," *IEEE Transactions on Electron Devices*, vol. 66, issue. 11, pp. 4578–4590, Nov. 2019.

Morphological Stability of Nanometer-Scale Single-Crystal Metallic Interconnects

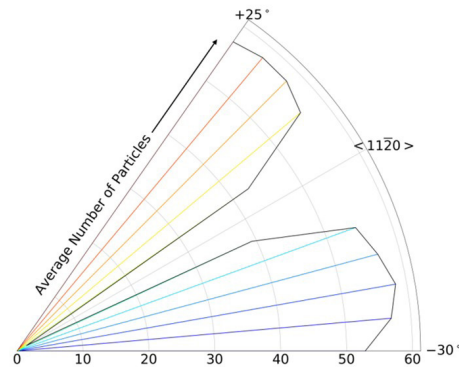
M. A. L'Etoile, Y. A. Shin, B. Wang, Q. Cumston, A. Warren, K. Barmak, K. R. Coffey, C. V. Thompson
Sponsorship: SRC, NSF

Continued integrated-circuit scaling requires interconnects with cross-sectional dimensions in the <10-nm range. At these dimensions, the resistance of interconnects increases dramatically due to surface and grain boundary electron scattering. The reliability of interconnects with nanoscale dimensions is also expected to be compromised by reduced morphological stability. As a part of a collaborative program focused on ballistic conduction and stability of single-crystal nanometer-scale interconnects, we are investigating the crystallographic dependence of the morphological stability of Ru wires.

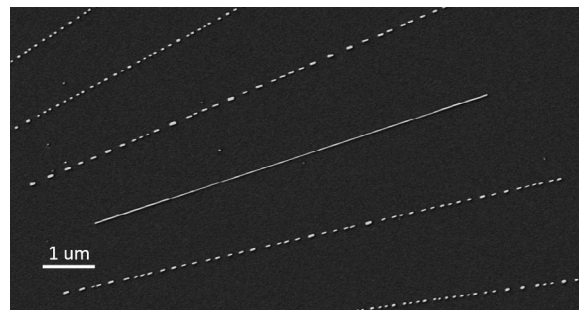
Thin single-crystal films agglomerate into small particles via capillary-driven surface diffusion in a process known as solid-state “dewetting.” With decreasing film thickness, the temperature at which dewetting occurs is well below the constituent material’s melting temperature. However, previous work on single-crystal Ni films has demonstrated that crystalline anisotropy gives rise to special crystallographic orientations along which single-crystal wires exhibit greatly enhanced morphological stability. Ru is a candidate material for future interconnects, and we have studied the morphological stability of arrays of Ru nanowires lithographically patterned from single-crystal (0001) films, such that the individual wires have axes lying in different crystallographic directions. After annealing, we find nanowires oriented along directions that are particularly stable; see Figures 1 and 2. Interconnects composed of such wires should have decreased vulnerability to morphological instabilities during processing and circuit operation. These wires also have strongly faceted surfaces, with facets parallel to the wire axis (Figure 3), which are predicted to reduce electron scattering and decrease interconnect resistance. This high degree of morphological stability and faceting also suggests that wires with these orientations will be particularly resistant to electromigration. Combining new data from this material system with results from past work on Ni, which has weaker surface energy anisotropy, will provide insights that will enable optimization of interconnect structural and crystallographic factors for design of morphologically stable nanowires with cross-sectional dimensions significantly below 10 nm.

FURTHER READING

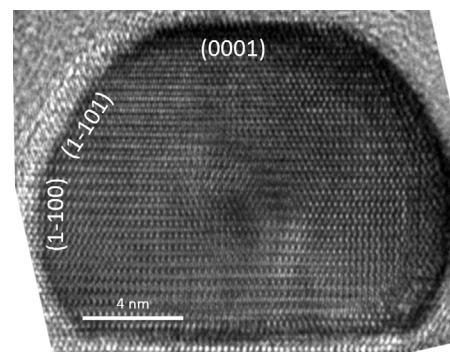
- G. H. Kim and C. V. Thompson, “Effect of Surface Energy Anisotropy on Rayleigh-like Solid-state Dewetting and Nanowire Stability,” *Acta Materialia*, vol. 84, pp. 290-201, Feb. 2015.



▲ Figure 1: A stable, unbroken wire, surrounded by its 5°-offset neighbors, which have decomposed to form particles after annealing at 915 °C for 3 hours. Wires oriented along directions remained intact.



▲ Figure 2: Most nanowires broke into many particles after annealing.



▲ Figure 3: Cross-sectional TEM image of a stable wire confirms that stable wires are strongly faceted.

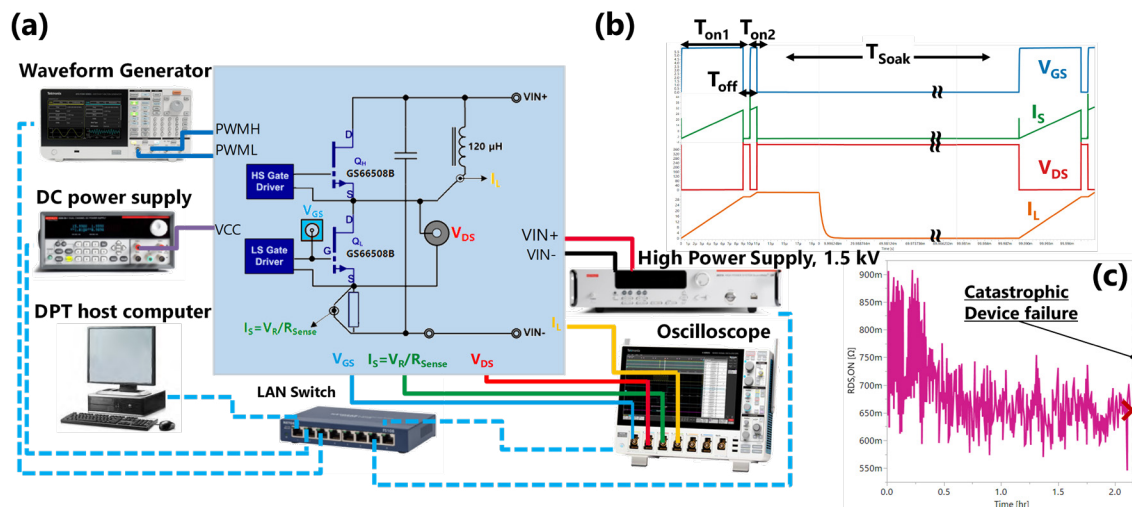
Switching Reliability of GaN Power High-Electron-Mobility Transistors

A. Massuda, J. A. del Alamo
Sponsorship: Analog Devices, Inc.

GaN electronics constitutes a new technology with superior power-handling capabilities compared to those of Si and other semiconductors in many applications. Power management applications typically involve operating the GaN transistors under rapid switching conditions between a high-voltage off-state and a high-current on-state. Depending on the system topology and specifications, two switching modes apply to power applications: soft switching and hard switching. The reliability and robustness of GaN transistors under repeated switching is a concern, particularly when they operate under hard-switching conditions.

The Double-Pulse Test is the most effective test for emulating high-power switching close to the mode of operation of the devices in electrical power management applications. In our work we

have constructed a unique experimental setup to implement the Double-Pulse Testing technique. Figure 1a illustrates a physical implementation of the experimental setup. The system can conduct testing under severe stress conditions and monitor the induced degradation of device parameters up to the point of catastrophic device failure. Figure 1b shows a typical waveform of the Double-Pulse Test. The system allows users to repeat the test multiple times and measure device parameters at fixed intervals. Figure 1c shows an example of catastrophic degradation of dynamic $R_{DS,ON}$ when the transistor is subjected to hours of repeated switching operation. Degradation and hard-fail data will be used to verify failure modes and develop life-time models in order to project device survivability under various conditions.



▲ Figure 1: (a) Schematic diagram of experimental setup for switching reliability of GaN transistors; (b) typical waveform of Double-Pulse Test; (c) $R_{DS,ON}$ degradation vs. time for multiple Double-Pulse Tests.

FURTHER READING

- "Stability and Reliability of Lateral GaN Power Field-Effect Transistors," *IEEE Transactions on Electron Devices*, vol. 66, no. 11, pp. 4578-4590, 2019, doi: 10.1109/TED.2019.2931718.
- S. R. Bahl, J. Joh, L. Fu, A. Sasikumar, T. Chatterjee, and S. Pendharkar, "Application Reliability Validation of GaN Power Devices," in *2016 IEEE International Electron Devices Meeting (IEDM)*, 3-7 Dec. 2016 2016, pp. 20.5.1-20.5.4, doi: 10.1109/IEDM.2016.7838461.
- S. R. Bahl, D. Ruiz, and D. S. Lee, "Product-level Reliability of GaN Devices," in *2016 IEEE International Reliability Physics Symposium (IRPS)*, 17-21 April 2016 2016, pp. 4A-3-1-4A-3-6, doi: 10.1109/IRPS.2016.7574528.

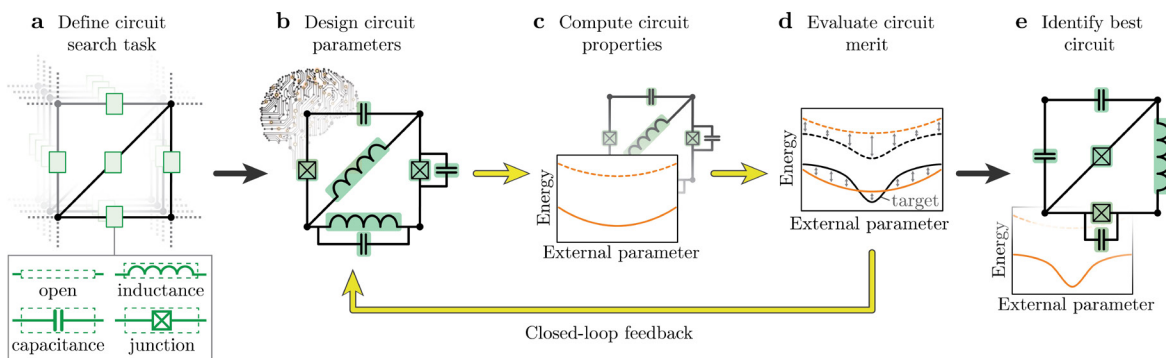
Automated Design of Superconducting Circuits and Its Application to 4-Local Couplers

T. Menke, F. Häse, S. Gustavsson, A. J. Kerman, W. D. Oliver, A. Aspuru-Guzik
Sponsorship: ODNI, IARPA, ARO, DoD via MIT Lincoln Laboratory

Quantum processors are well-controlled quantum systems capable of performing complex computational tasks. They have been shown to hold promise for the simulation of fundamental physical effects, as well as for solving computationally expensive yet practical problems. Superconducting circuits have emerged as a promising platform to build such quantum processors. These are microscale electrical circuit structures that are fabricated on an on-chip device. In a cryogenic environment, the chip behaves quantum mechanically and can be controlled using microwave pulses.

The challenge of designing a circuit is to compromise between realizing a set of performance metrics and reducing circuit complexity and noise sensitivity. At the same time, one needs to explore a large design space, and computational approaches often yield long simulation times. Here, we automate the circuit

design task using **superconducting circuit closed-loop automated design (SCILLA)**. The software SCILLA performs a parallelized, closed-loop optimization to design superconducting circuit diagrams that match predefined properties, such as spectral features and noise sensitivities. We employ SCILLA to design 4-local couplers for superconducting flux qubits and identify a circuit that outperforms an existing proposal with a similar circuit structure in terms of coupling strength and noise resilience for experimentally accessible parameters. Our results are important for the future development of quantum processors in two ways. First, the coupler circuit that we have found is expected to boost the capabilities of quantum processors. Second, our method demonstrates how automated design can facilitate the development of complex circuit architectures for quantum information processing.



▲ Figure 1: Implementation of SCILLA, enabling automated circuit design. (a) Definition of the circuit design task, with details about general circuit architecture, parameter bounds, and design targets. (b) Based on the general architecture, the design module evokes parameter-generating algorithms to place components and choose component parameters in the circuit. (c) Calculation of circuit properties such as spectra or noise sensitivity. (d) Estimation of the agreement between computed properties and target properties. (e) Circuits close to the design target are identified. A database system facilitates asynchronous execution and parallelization of the workflow and refinement of design choices (closed-loop feedback) based on merit evaluations of previously proposed circuits.

FURTHER READING

- T. Menke, F. Häse, S. Gustavsson, A. J. Kerman, W. D. Oliver, and A. Aspuru-Guzik, "Automated Discovery of Superconducting Circuits and its Application to 4-local Coupler Design," *npj Quantum Information*, vol. 7, no. 1, p. 1, 2021.

CMOS-Compatible Protonic Programmable Resistor Based on Phosphosilicate Glass Electrolyte for Analog Deep Learning

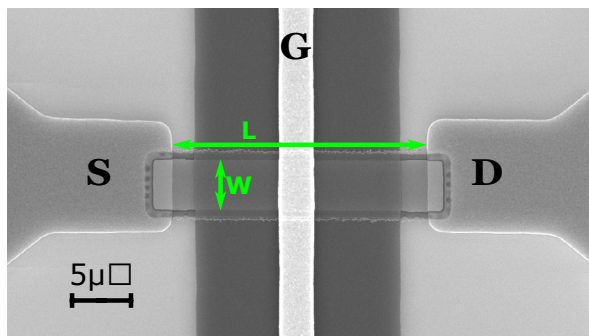
M. Onen, N. Emond, B. Yildiz, J. Li, J. A. del Alamo
Sponsorship: MIT-IBM Watson AI Lab

The success of deep learning in classifying and clustering representations of data at multiple levels of abstraction has fundamentally changed how information is processed. However, conventional digital architectures face increasing difficulties in supporting the heavy computational workloads required to train state-of-the-art deep neural networks. The pressing need for faster and more energy-efficient deep learning processors has therefore led to an intensive investigation of in-memory computation schemes using analog crossbar arrays.

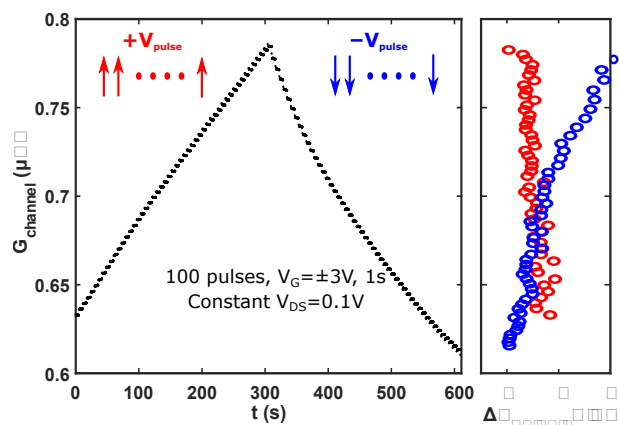
The building block of analog crossbar arrays is the crosspoint element, which can be described as a programmable, non-volatile resistor. Ion intercalation-based programmable resistors have emerged as a potential next-generation technology for analog deep learning applications. Protons, being the smallest ions, are the most promising candidate to enable devices with high modulation speed, low energy consumption, and enhanced endurance. The main bottleneck with developing protonic programmable resistors has been the absence of a suitable solid-state electrolyte that conducts protons but blocks electrons. All designs

so far have relied on approaches that either cannot be integrated and scaled down, such as using organic materials; use chemically and thermally sensitive polymers; or suffer from energy inefficiency such as high electric field-induced water hydrolysis.

In this work, we report on the first back-end complementary metal-oxide-semiconductor (CMOS) compatible protonic programmable resistor enabled by the integration of phosphosilicate glass (PSG) as the proton electrolyte layer. PSG is an outstanding electrolyte material that displays both excellent protonic conduction and electronic insulation characteristics. Moreover, it is a well-known material within conventional Si fabrication that enables high deposition control and scalability. Our scaled three-terminal devices show desirable modulation characteristics in terms of symmetry, retention, endurance, and energy efficiency. Protonic programmable resistors based on PSG, therefore, represent promising candidates to realize nanoscale analog crossbar processors with monolithic CMOS-integration.



▲ Figure 1: Top view scanning electron microscope image of a protonic programmable device.



▲ Figure 2: Basic modulation characteristics of protonic programmable resistor.

FURTHER READING

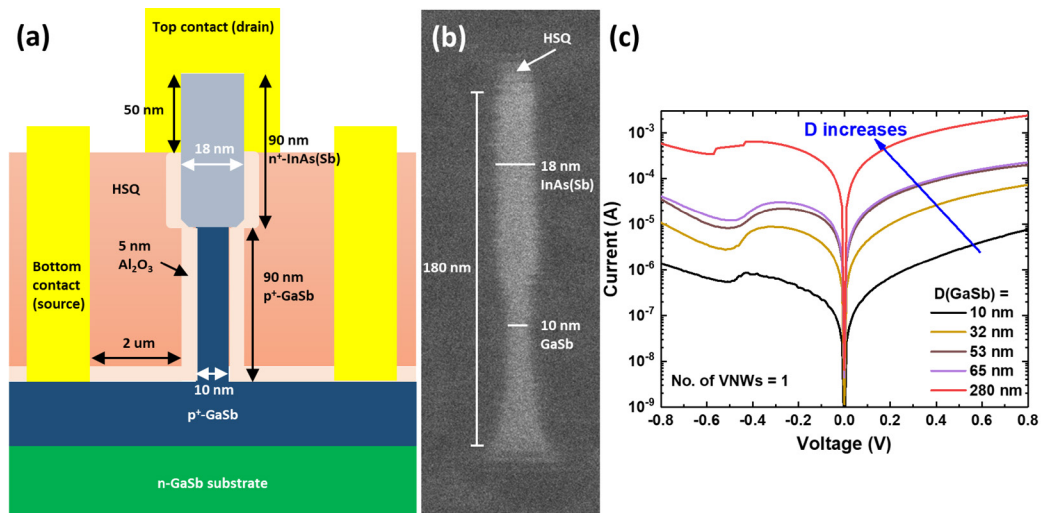
- X. Yao, K. Klyukin, W. Lu, M. Onen, S. Ryu, D. Kim, N. Emond, I. Waluyo, A. Hunt, J. A. del Alamo, J. Li, and B. Yildiz, "Protonic Solid-State Electrochemical Synapse for Physical Neural Networks," *Nature Communications*, vol. 11, 3134 2020.

III-V Broken-Band Vertical Nanowire Esaki Diodes

Y. Shao, J. A. del Alamo
Sponsorship: Intel

Further reducing transistor power consumption of metal-oxide-semiconductor field-effect transistors (MOSFETs) in logic applications requires transport mechanisms other than thermionic emission over an energy barrier. Among all possible mechanisms, quantum tunneling emerges as one of the most promising. Therefore, the design and demonstration of tunnel field-effect transistors (TFETs) have received much attention recently. In spite of intense research, the results to date have been disappointing.

In our research, we aim to utilize the unique broken-band alignment and the superior carrier transport properties in the GaSb/InAs material system to obtain high drive current with tunneling. In order to quantitatively evaluate the quality of the tunneling junction, GaSb/InAs(Sb) vertical nanowire (VNW) Esaki diodes have been fabricated and electrically characterized.



▲ Figure 1: (a) Cross-sectional schematics of a VNW Esaki diode. (b) SEM image of a fabricated 10-nm-diameter VNW. (c) Electrical characteristics of VNW Esaki diodes with different diameters.

FURTHER READING

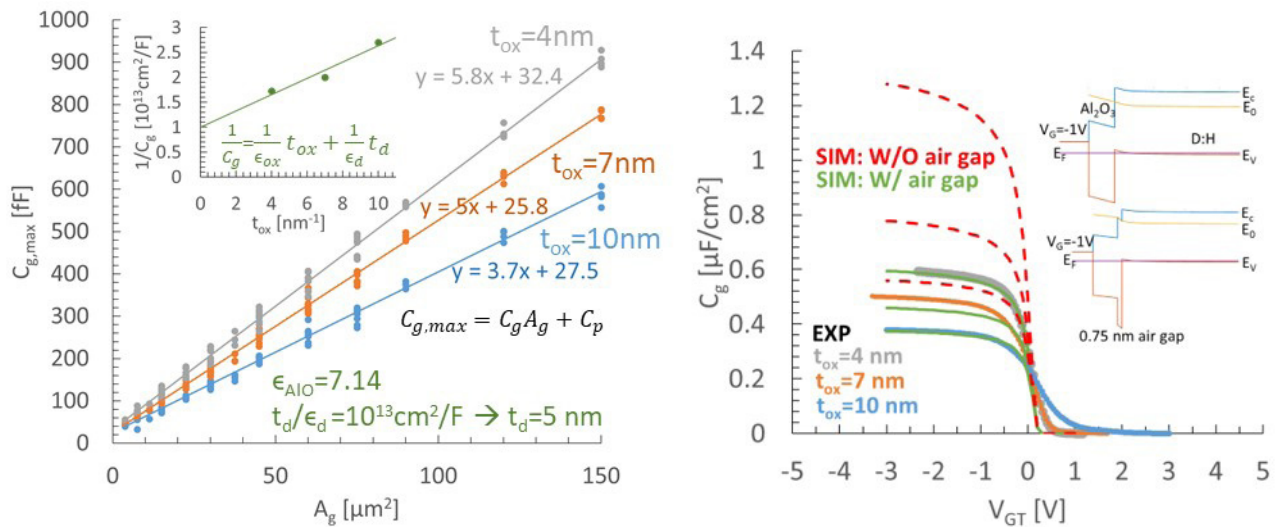
- X. Zhao, A. Vardi, and J. A. del Alamo, "InGaAs/InAs Heterojunction Vertical Nanowire Tunnel FETs Fabricated by a Top-down Approach," *IEDM Tech. Dig.*, pp. 590-593, 2014.
- X. Zhao, A. Vardi, and J. A. del Alamo, "Sub-thermal Subthreshold Characteristics in Top-Down InGaAs/InAs Heterojunction Vertical Nanowire Tunnel FETs," *IEEE Electron Device Letts.*, vol. 38, no. 7, pp. 855-858, Jul. 2017.
- X. Zhao, C. Heidelberger, E. A. Fitzgerald, W. Lu, A. Vardi, and J. A. del Alamo, "Sub-10-nm InGaAs Vertical Nanowire MOSFETs," *IEDM Tech. Dig.*, pp. 807-810, 2017.

Mysterious Layer on a Hydrogen-Terminated Diamond Surface

A. Vardi, M. Tordjman, R. Kalish, J. A. del Alamo
 Sponsorship: U.S Israel Binational Science Foundation, Bose, DARPA

The surface conductivity of H-terminated diamond (D:H) is usually explained by the transfer doping model. The model assumes a surface dopant layer is formed on the D:H surface that generates a two-dimensional hole gas (2DHG) in the diamond. The dopant layer is typically assumed to be of atomic dimensions. However, since the D:H surface is almost perfectly passivated, there are no chemical bonds out of the surface, and the dopants are weakly held by van der Waals forces. Consequently, analysis of the capacitance of MOSFETs

built on D:H show it to be much smaller than expected. To study the nature of this interfacial layer, we have analyzed the scaling properties of the gate capacitance of Al/Al₂O₃/D:H MOS structures. A comparison of the obtained results against Poisson-Schrodinger simulations suggests the existence of an “air gap” of 0.5-1 nm in thickness at the Al₂O₃/D:H interface. If confirmed, this gap will have important implications for the current drivability of diamond MOSFETs.



▲ Figure 1: (Left) Scaling of gate capacitance with gate area for MOS capacitors with different Al₂O₃ thickness. From the slope of the lines, the intrinsic gate capacitance per unit area, C_g , is extracted. Inset: $1/C_g$ vs. Al₂O₃ thickness. From the slope, the Al₂O₃ dielectric constant is extracted (7.1); the intercept is the semiconductor density of states capacitance found to be unrealistically small. Comparison (right) of experimental CV data and P-S simulations with a 0.75-nm “air gap” provides a good explanation for our findings.

FURTHER READING

- A. Vardi, M. Tordjman, J. A. del Alamo, and R. Kalish, “Refractory W-Ohmic Contacts to H-terminated Diamond,” *IEEE Transaction on Electrical Devices*, vol. 67, no. 9, pp. 3516-3521, Sep. 2020.
- Z. Yin, M. Tordjman, A. Vardi, R. Kalish, and J. A. del Alamo, “A Diamond:H/WO₃ Metal-Oxide-Semiconductor Field-Effect Transistor,” *IEEE Electron Device Letters*, vol. 39, no. 4, pp. 540-543, April 2018.
- A. Vardi, M. Tordjman, J. A. del Alamo, and R. Kalish, “A Diamond:H/MoO₃ MOSFET,” *IEEE Electron Device Letters*, vol. 35, no. 12, pp. 1320-1322, Dec. 2014.

Impact of Ionizing Radiation on Superconducting Qubit Coherence

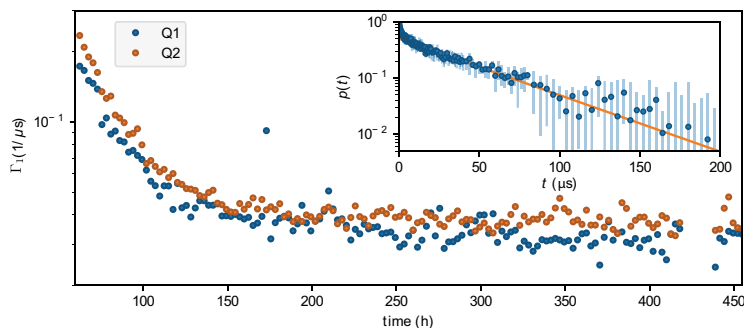
A. Vepsäläinen, A. Karamlou, J. Orrell, A. Dogra, B. Loer, F. Vasconcelos, D. Kim, A. Melville, B. Niedzielski, J. Yoder, S. Gustavsson, J. Formaggio, B. VanDevender, W. D. Oliver
Sponsorship: LPS, ARO

The practical viability of technologies that rely on qubits requires long coherence times and high-fidelity operations. Superconducting qubits are a promising platform for achieving these objectives. However, their coherence is affected by broken Cooper pairs, referred to as quasiparticles. The experimentally observed density of quasi-particles is orders of magnitude higher than the value predicted at equilibrium by the Bardeen-Cooper-Schrieffer theory of superconductivity. Our results suggest that ionizing radiation from cosmic rays and from environmental radioactive materials contribute to the observed difference.

In this work, we use a radioactive ^{64}Cu source to measure the impact of ionizing radiation on superconducting qubits under controlled levels of radiation. While the activity of the source decayed over time, we observed an increase in the coherence of

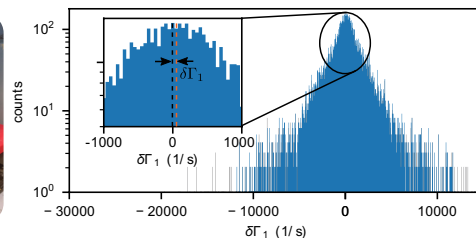
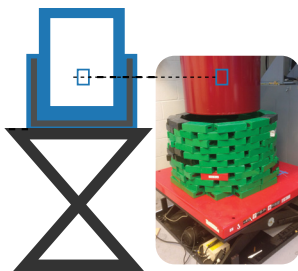
the qubits, see Figure 1. From independently measured level of naturally occurring background radiation, we can extrapolate the impact of ionizing radiation on quasi-particle generation and the qubit coherence. We predict that the ionizing radiation would limit the coherence times of superconducting qubits of the type we measured to the millisecond regime.

Next, we demonstrate that shielding the qubits with lead can mitigate the impact of radiation on the qubits, see Figure 2. We continuously raised and lowered the shield and measured the corresponding change in the qubit energy-relaxation rate. Albeit a small effect in today's qubits, the change in the relaxation time positively correlated with the increased shielding, confirming our hypothesis that naturally occurring ionizing radiation affects the qubit coherence.



◀ Figure 1: Energy-relaxation rate (Γ_1) of the qubits as a function of time from the installation of the radioactive source. The inset shows an example of the measurement used to extract the energy-relaxation rate.

▶ Figure 2: The lead shield used to mitigate the impact of ionizing radiation (left). The histogram of the measured differences in the energy relaxation rates of the qubits when the shield was in up or down positions (right).



FURTHER READING

- A. P. Vepsäläinen, A. H. Karamlou, J. L. Orrell, A. S. Dogra, B. Loer, F. Vasconcelos, D. K. Kim, A. J. Melville, et al., "Impact of Ionizing Radiation on Superconducting Qubit Coherence," *Nature*, vol. 584, pp. 551–556, Aug. 2020.

NbN-Gated GaN Transistor Technology for Applications in Quantum Computing Systems

Q. Xie, N. Chowdhury, A. Zubair, M. Sánchez Lozano, J. Lemettinen, M. Colangelo, O. Medeiros, I. Charaev, K. K. Berggren, T. Palacios
Sponsorship: IBM

High-performance and scalable cryogenic electronics is an essential component of future quantum information systems, which typically operate below 4K. Superconducting qubits need advanced radio-frequency (RF) and pulse-shaping electronics, which typically occupies large instrumentation racks operating at room temperature. This approach is not scalable to the millions of qubits needed in future quantum systems.

This work explores the use of wide band gap heterostructure electronics, specifically the AlGaIn/GaN high electron mobility transistor (HEMT), for cryogenic low-noise applications. These structures take advantage of the polarization-induced two-dimensional electron gas to create a high mobility channel, hence eliminating the heavy doping needed in the other semiconductor technologies. Epitaxially-grown GaN-on-Silicon wafers have been demonstrated in large (12 inch / 300 mm) substrates, therefore making the technology an excellent candidate for scalable RF electronics in quantum computing systems.

Furthermore, the use of electrodes of

superconducting materials is proposed to significantly reduce the parasitic components and therefore push the RF performance of cryogenic devices. Short-channel transistors with NbN gates of length 250 nm have been demonstrated with promising performance.

The next step will study the effect of the superconducting gate on RF characteristics of the transistors, with the eventual goal of pushing the frequency performance of these transistors to new limits. These transistors will be integrated into low-noise amplifier circuits for applications in readout and control electronics at cryogenic temperature. Furthermore, the demonstrated NbN-gated GaN transistor paves the way for the application of high-frequency GaN technology in cryogenic electronics, notably in scalable quantum computing systems. When combined with other highlights in GaN electronics, e.g., a GaN complementary metal-oxide-semiconductor (CMOS) platform, the reported technology brings us one step closer to an all-nitride integrated electronics-quantum device platform.

FURTHER READING

- Q. Xie, N. Chowdhury, A. Zubair, M. Sánchez Lozano, J. Lemettinen, M. Colangelo, O. Medeiros, I. Charaev, K. K. Berggren, P. Gumann, D. Pfeiffer, and T. Palacios, "NbN-Gated GaN Transistor Technology for Applications in Quantum Computing Systems," *2021 Symposium of VLSI Technology*, Jun. 2021.
- N. Chowdhury, Q. Xie, M. Yuan, K. Cheng, H. W. Then, and T. Palacios, "Regrowth-free GaN-based Complementary Logic on a Si Substrate," *IEEE Electron Device Lett.*, vol. 41, no. 6, pp. 820-823, Jun. 2020. DOI: 10.1109/LED.2020.2987003.
- N. Chowdhury, Q. Xie, J. Niroula, N. S. Rajput, K. Cheng, H. W. Then, and T. Palacios, "Field-Induced Acceptor Ionization in GaN p-MOSFETs," *Proc. Int. Electron Device Meeting (IEDM) 2020*, pp. 5.5.1-5.5.4, Dec. 2020. DOI: 10.1109/IEDM13553.2020.9371963.

Metal Alloy Enables Reliable Silicon Memristor Synapses

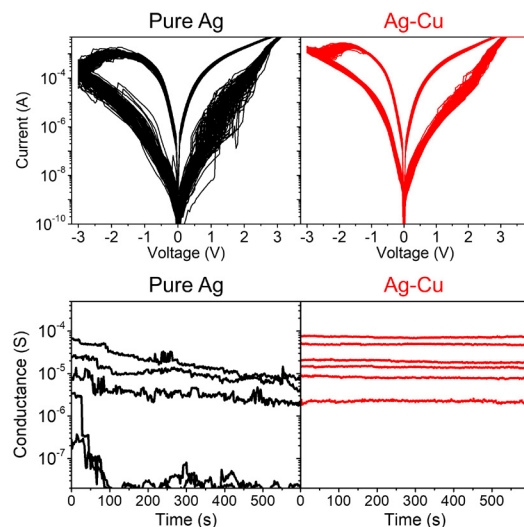
H. Yeun, P. Lin, C. Choi, J. Kim

Sponsorship: Samsung Global Research Laboratory, MIT-IBM Watson AI Lab, NSF-SRC-E2CDA

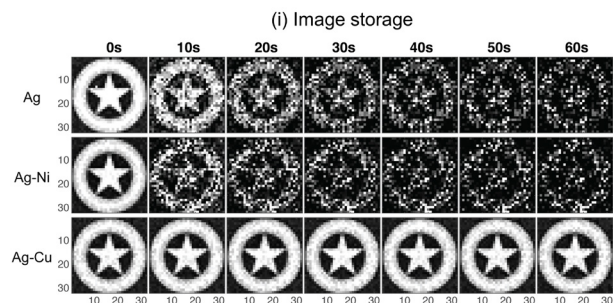
In the age of artificial intelligence (AI), memristors have emerged as an artificial synapse for neuromorphic computing, overcoming the limitations of conventional silicon (Si)-based digital synapses. Interestingly, Si has also been utilized to develop memristor synapses via combination with a silver (Ag) electrode. An electrical conductance of Si medium is reversibly modulated by Ag injection, corresponding to the synaptic weight changes. Owing to the thermodynamic instability of Ag in Si medium (Ag is immiscible in Si), injected Ag exhibits high mobility, resulting in a high-weight modulation ratio and high switching endurance. Unfortunately, large switching variations and poor weight stability occur at the devices and are also induced by the thermodynamic instability. Thus, to mitigate such dilemmas in performance, the regulation of thermodynamic stability of Ag in Si medium would be the fundamental strategy.

Here we have developed Ag alloy for precision tuning of thermodynamic interactions of Ag and Si, thereby achieving highly balanced synaptic performance. We selected copper (Cu) as an alloying element due to its (1) high diffusivity into Si and (2) favorable thermodynamic interactions with both Ag and Si. Our hypothesis was that Cu would migrate into Si simultaneously with Ag and enhance thermodynamic stability of Ag in Si (i.e., be a stabilizer). The device's performance results clearly confirm our metallurgical strategy that switching uniformity and weight retention are significantly enhanced by a Ag-Cu alloyed electrode (Figure 1). It should be noted that other alloying elements such as Ni cannot improve the synaptic performance due to their repulsive interactions with Ag.

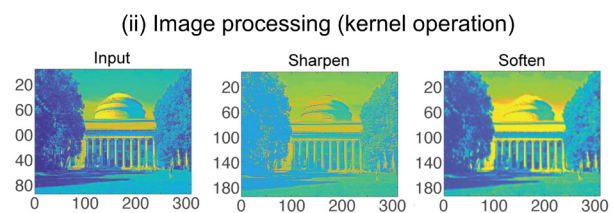
With promising device performance test results, we have demonstrated 32×32 Si memristor array and successfully performed image storage (Figure 2) and image processing (Figure 3), which are only enabled by Ag-Cu active electrode (Figure 3). We believe our alloying strategy can be expanded to other memristive synapses to resolve performance issues in neuromorphic computing applications.



▲ Figure 1: Switching performance of Si memristors. Switching uniformity during 100 cycles (top) and weight retention properties with multi-conductance levels (bottom).



▲ Figure 2: Image storage in 32×32 silicon memristor array with respect to active electrodes: Ag, Ag-Cu, and Ag-Ni.



▲ Figure 3: Image processing (convolutional kernel processing) in Si memristor array with Ag-Cu alloy.

FURTHER READING

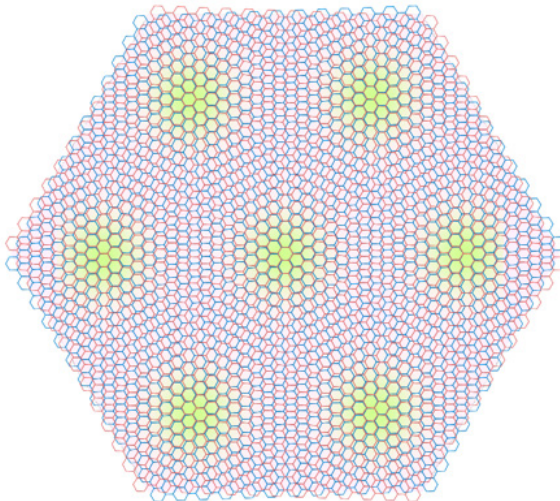
- H. Yeon, P. Lin, C. Choi, S. Tan, Y. Park, D. Lee, J. Lee, F. Xu, et al., "Alloying Conducting Channels for Reliable Neuromorphic Computing," *Nature Nanotechnology*, vol. 15, pp. 574-579, 2020.

Highly Tunable Junctions in Magic Angle Twisted Bilayer Graphene Tunneling Devices

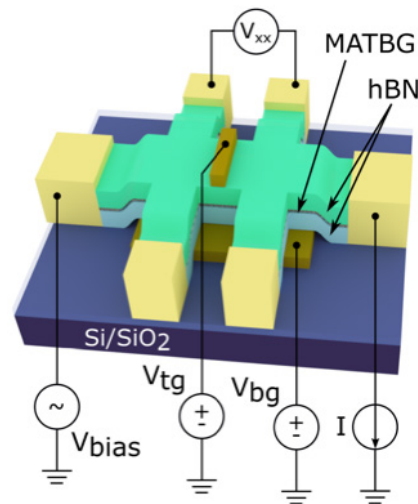
D. Rodan-Legrain, Y. Cao, J. M. Park, S. C. de la Barrera, M. T. Randeria, K. Watanabe, T. Taniguchi, P. Jarillo-Herrero
Sponsorship: NSF, CIQM, DOE, BES, US Army Research Office, Fundación Bancaria 'la Caixa', Gordon and Betty Moore Foundation, Fundación Ramón Areces, MEXT.

The recent observation of superconductivity and correlated insulating states in “magic-angle” twisted bilayer graphene (MATBG) featuring nearly flat bands at twist angles close to 1.1 degrees presents a highly tunable two-dimensional material platform capable of behaving as a metal, an insulator, or a superconductor. Local electrostatic control over these phases may enable the creation of versatile quantum devices that were previously not achievable in other single material platforms. Our research shows how we can exploit the electrical tunability of MATBG to engineer Josephson junctions and tunneling transistors all within one material, defined solely by electrostatic gates. Our multi-gated device geometry offers complete control over the Josephson junction, with the ability to inde-

pendently tune the weak link, barriers, and tunneling electrodes. Utilizing the intrinsic bandgaps of MATBG, we also demonstrate monolithic edge tunneling spectroscopy within the same MATBG devices and measure the energy spectrum of MATBG in the superconducting phase. Furthermore, inducing a double barrier geometry permits the devices to be operated as a single-electron transistor, exhibiting a Coulomb blockade. These MATBG tunneling devices, with versatile functionality encompassed within a single material, may find applications in graphene-based tunable superconducting qubits, on-chip superconducting circuits, and electromagnetic sensing in next-generation quantum nanoelectronics



▲ Figure 1: Illustration of the moiré pattern in twisted bilayer graphene near the magic angle.



▲ Figure 2: Schematic illustration of the device structure.

FURTHER READING

- D. Rodan-Legrain, et al. "Highly Tunable Junctions and Non-local Josephson Effect in Magic-angle Graphene Tunnelling Devices," *Nat. Nanotechnol.* (2021). <https://doi.org/10.1038/s41565-021-00894-4>.

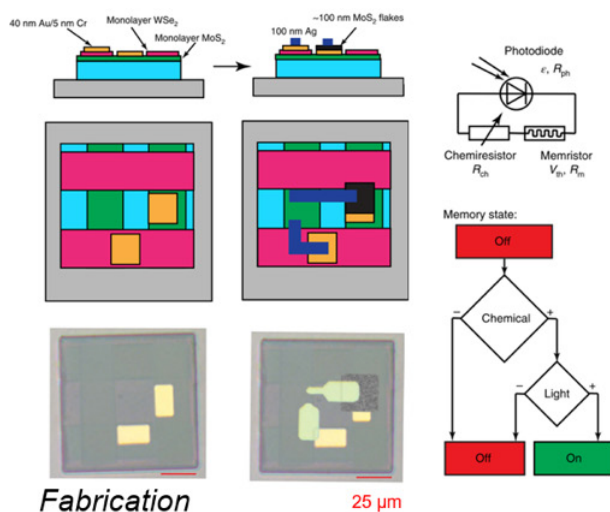
Electronic Cells: Autonomous Micromachines from 2D Materials

V. B. Koman, P. Liu, D. Kozawa, A. T. Liu, A. L. Cottrill, M. S. Strano

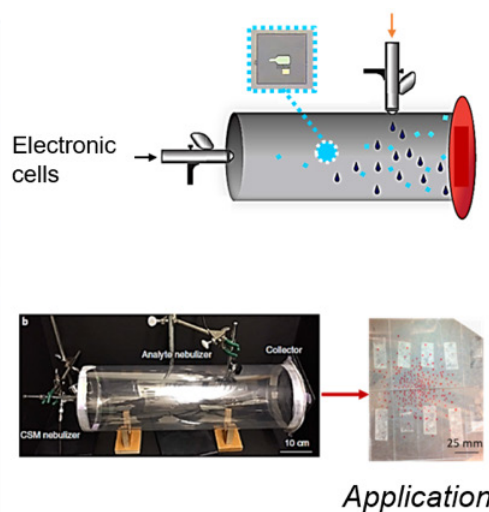
Sponsorship: 2015 US Office of Naval Research Multi University Research Initiative (MURI) grant on Foldable and Adaptive Two-Dimensional Electronics (FATE) at MIT, Harvard and University of Southern California

Electronic cells are micromachines encompassing autonomous on-board functions such as sensing, computation, communication, locomotion, and power management. Akin to their biological counterparts, electronic cells bring specialized capabilities to previously inaccessible locations. Here, we present the design and fabrication of the first-of-its-kind electronic cell composed of the nanoelectronic circuit on top of an SU-8 particle. Powered by a 2D material-based photodiode, the on-board circuit connects a chemiresistor

element and a memristor element, enabling on-board detection and storage capabilities. We demonstrate how our cells sense and record information about the presence of ammonia and dispersed soot when aerosolized in the enclosed tubes, dispersed in a hydrodynamic flow of pipelines, or sprayed over large surfaces. Electronic cells may find widespread application as probes in confined environments, such as the human digestive tract, oil and gas conduits, chemical and biosynthetic reactors, and autonomous environmental sensors.



▲ Figure 1: (left) Summary of electronic cell fabrication steps as well as its electrical circuit diagram.



▲ Figure 2: (right) Aerosolizable electronics as an application of electronic cells. Schematic and its experimental implementation.

FURTHER READING

- V. B. Koman, P. Liu, D. Kozawa, A. T. Liu, A. L. Cottrill, Y. Son, J. A. Lebron, M. S. Strano, "Colloidal Nanoelectronic State Machines Based on 2D Materials for Aerosolizable Electronics", *Nature Nanotechnology*, vol. 13, pp. 9:819-827, Sep. 2018.

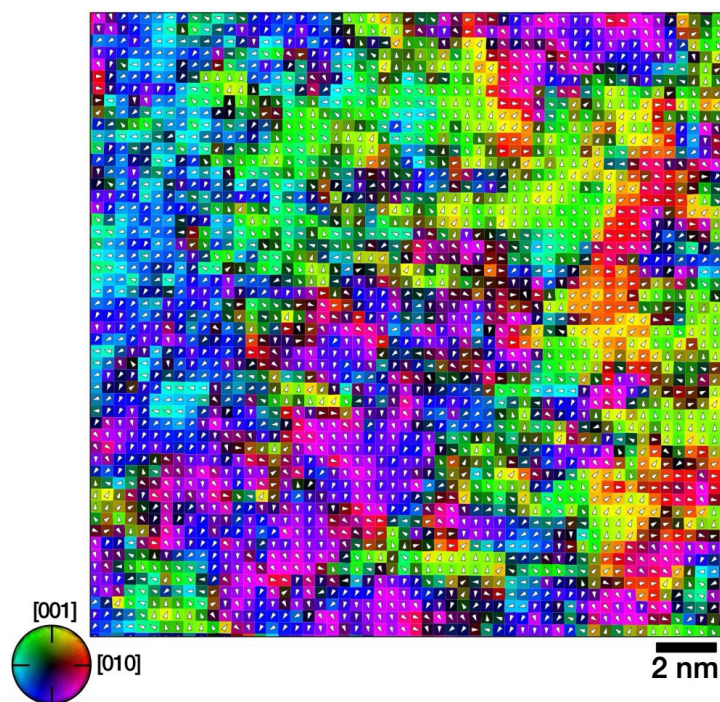
Decoding Complexities in Relaxor Ferroelectrics Using Electron Microscopy

A. Kumar, J. Kim, J. Baker, M. Cabral, P. Bowes, L. Martin, S. Zhang, D. Irving, E. Dickey, J. LeBeau

Sponsorship: Center of Dielectrics and Piezoelectrics (CDP) and Collaborative Hierarchical and Agile Responsive Materials (CHARM)

Relaxor ferroelectrics show slim hysteresis loops, low remanent polarization, high saturation polarization, and exceptional electromechanical coupling, finding applications in ultrasound imaging and energy storage devices. Developing a structure-property relationship in relaxors has been a seemingly intractable problem due to the presence of nanoscale chemical and structural heterogeneities. We have employed aberration-corrected scanning transmission electron microscopy (STEM) to quantify the various contributions of nanoscale heterogeneity to relaxor ferroelectric prop-

erties in a PMN-PT system. Specifically, we found three main contributions-- chemical ordering, oxygen octahedral tilting and oxygen octahedral distortion--that are difficult to otherwise differentiate. STEM reveals the elusive connection between chemical and structural heterogeneity and local polarization variation. Further, the effects of strain and thickness on PMN-PT thin films has been examined. These measurements elucidate the design principles for next-generation relaxor material.



▲ Figure 1: Projected polarization map calculated in relaxor ferroelectric, PMN-PT thin film, showing nanoscale domain structure.

FURTHER READING

- A. Kumar, J. N. Baker, P. C. Bowes, M. J. Cabral, S. Zhang, E. C. Dickey, D. L. Irving, J. M. LeBeau, "Atomic-resolution Electron Microscopy of Nanoscale Local Structure in Lead-based Relaxor Ferroelectrics," *Nature Materials*, vol. 20, pp. 62–67, 2021.

Machine Learning, Neural Networks, AI

- TinyTL: Reduce Memory, Not Parameters for Efficient On-Device Learning..... 65
- Data-Driven Sustainable Design Using Axiomatic Design and Bayesian Network Models..... 66
- Building MEMS Process Knowledge Base 67
- Randomized Probe Imaging through Deep K-Learning..... 68
- Natural Language Processing Accelerator for Transformer Models 69
- MCUNet: Tiny Deep Learning on IoT Devices..... 70
- Neural Accelerator Architecture Search..... 71
- Searching Efficient 3D Architectures with Sparse Point-Voxel Convolution 72
- Embedded Neural Network Models and Inputs through Simple Power and Timing Side-Channels 73
- Realization of High-fidelity CZ and ZZ-free iSWAP Gates with a Tunable Coupler 74

TinyTL: Reduce Memory, Not Parameters for Efficient On-Device Learning

H. Cai, C. Gan, L. Zhu, S. Han
Sponsorship: MIT-IBM Watson AI Lab, NSF Award

On-device learning enables edge devices to continually adapt artificial intelligence (AI) models to new data, which requires a small memory footprint to fit the tight memory constraint of edge devices. Existing work solves this problem by reducing the number of trainable parameters. However, this parameter number reduction does not directly translate to memory saving since the major bottleneck is the activations, not parameters.

In this work, we present Tiny-Transfer-Learning (TinyTL) for memory-efficient on-device learning. TinyTL freezes the weights while it learns only the bias modules; thus no need exists to store the intermediate activations. To maintain the adaptation capacity, we

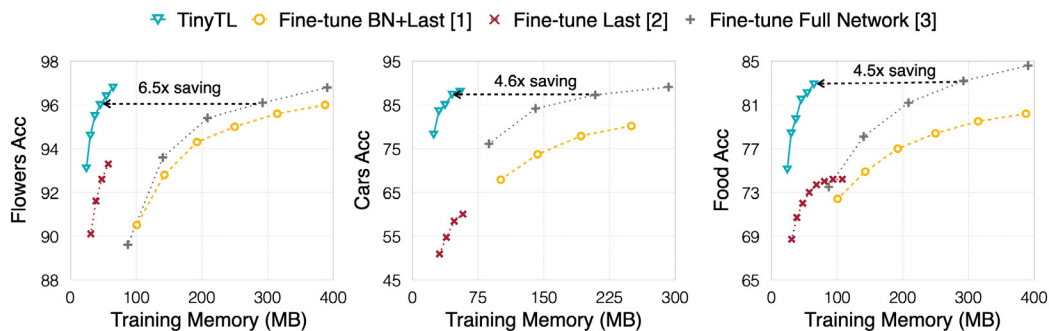
introduce a new memory-efficient bias module, the lite residual module, to refine the feature extractor by learning small residual feature maps adding only a 3.8% memory overhead.

Extensive experiments show that TinyTL significantly saves memory (up to 6.5x) with little accuracy loss compared to fine-tuning the full network. Compared to fine-tuning the last layer, TinyTL provides significant accuracy improvements (up to 34.1%) with little memory overhead. Furthermore, combined with feature extractor adaptation, TinyTL provides 7.3-12.9x memory saving over fine-tuning the full Inception-V3 without sacrificing accuracy.



- Customization: AI systems need to continually adapt to new data collected from the sensors.
- Security: Data cannot leave devices because of security and regularization.

▲ Figure 1: TinyTL enables efficient on-device training.



▲ Figure 2: TinyTL achieves up to 6.5x memory saving without sacrificing accuracy compared to conventional methods.

FURTHER READING

- H. Cai, C. Gan, L. Zhu, S. Han, "TinyTL: Reduce Memory, Not Parameters for Efficient On-Device Learning," *Advances in Neural Information Processing Systems*, vol. 33, pp. 11285-11297, 2020.
- P. K. Mudrakarta, M. Sandler, A. Zhmoginov, A. Howard, "K For The Price Of 1: Parameter Efficient Multi-task And Transfer Learning," *ICLR*, 2019.
- H. Cai, C. Gan, T. Wang, Z. Zhang, S. Han, "Once-for-All: Train One Network and Specialize it for Efficient Deployment," *ICLR*, 2020.

Data-Driven Sustainable Design Using Axiomatic Design and Bayesian Network Models

G. Fardelas, S.-G. Kim

Nowadays, the environmental crisis, economic prosperity, and social well-being push for designs that promote sustainability. Even though this sustainability-centric approach represents a critical driver for innovation, it also increases the design complexity, adding requirements for new functions with better performance, robustness, and flexibility.

Meanwhile, the digitalization of industry, big data technologies, and AI evolution creates a unique opportunity in human history to benefit from technological advances that can foster sustainable design, from concept to decommissioning. Therefore, a design approach that establishes a scientific basis for the design of complex systems and can integrate AI techniques could promote sustainable design.

Axiomatic design (AD), as a design methodology that systematizes the thought process in the interplay between functional requirements and design parameters, and Bayesian networks (BNs), as probabilistic data-based graphical models, share a similar hierarchical parent-child structure and the concept of exploring system entities' couplings that drive complexity. The design hierarchies, matrix

equations, and system architecture diagrams that support the AD methodology, highlighting the interconnections and interfaces between system elements, can be used as tools to manage complexity. At the same time, the process of forming and mapping the hierarchical structures and the relevant diagrams can be used as the roadmap to build a BN. Then, through sensitivity analysis, the trained network can provide data-based feedback for the system architecture; use of the conditional probability tables can calculate the probability of achieving sustainability-related functional requirements. Further, BNs built using the information garnered from the AD process can predict the effect or consequences given some causes or design decisions (causal reasoning) and determine the causes given an observation of the effects (evidential reasoning).

Therefore, AD and Bayesian machine learning technique can be synergistically combined to promote innovative solutions that would enable sustainable design of complex systems.

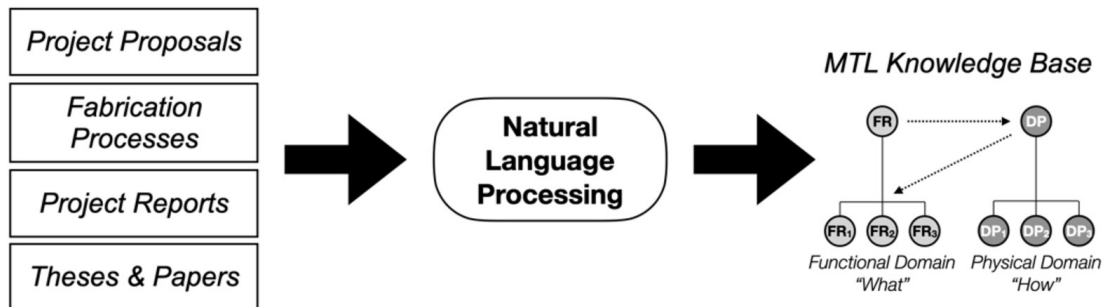
Building MEMS Process Knowledge Base

J. Gammack, H. Akay, S. G. Kim

Sponsorship: NSF, MIT/SenseTime Alliance on Artificial Intelligence

The design and fabrication of microsystems is a complex process with many requirements to satisfy, which often results in long lead times and high costs of fabrication. Decades of microsystems research at MIT have resulted in a rich history of documented device and process designs. However, MTL has not accumulated a centralized data and knowledge base that new incoming students or faculty members can access, search, and retrieve useful knowledge to begin with their new device and process designs. Recently, methods in machine learning and specifically natural language processing (NLP) have demonstrated competency in extractive design tasks that can be leveraged to automatically build a centralized and functionally annotated process database from widely distributed and unstructured data and information.

This design reading framework is being applied to Microsystems Technology Laboratories (MTL) process review documents created by MIT students and faculty. NLP methods are being applied to extract functional requirements, design parameters, and process variables from the fabrication processes, linked student theses, project reports, and published papers. Then the system identifies and connects relevant documents that may be useful to designers. The use of NLP to construct such an evolving Process Knowledge Base will help disseminate microsystems design innovations made at MTL.



▲ Figure 1: Design and fabrication artifacts from MTL research may be processed to construct a microsystems database to facilitate current and future design innovation.

FURTHER READING

- S. G. Kim, S. M. Yoon, M. Yang, J. Choi, H. Akay, and E. Burnell, "AI for Design: Virtual Design Assistant," *CIRP Annals*, vol. 68, no. 1, pp. 141-144, 2019.
- H. Akay and S. G. Kim, "Design Transcription: Deep Learning-based Design Feature Representation," *CIRP Annals*, vol. 69, no. 1, pp. 141-144, 2020.
- H. Akay and S. G. Kim, "Reading Functional Requirements Using Machine Learning-Based Language Processing," *CIRP Annals*, vol. 70, no. 1, 2021.

Randomized Probe Imaging through Deep K-Learning

Z. Guo, A. Levitan, G. Barbastathis, R. Comin
Sponsorship: Intelligence Advanced Research Projects Agency

Single-frame randomized probe imaging (RPI) is a diffractive imaging method that uses randomized light, rather than a finite support constraint, to generate a unique solution to the phase retrieval problem. The combination of randomized illumination and a band-limited object provides enough information in the single-frame diffraction intensity to solve the phase retrieval problem, producing high-fidelity reconstructions using gradient descent-based nonlinear inverse optimization.

Recently, deep learning has led to significant progress in nonlinear inverse problems. For phase retrieval, a deep neural network (DNN) can be trained in supervised mode with examples of complex-valued objects and their corresponding far-field diffraction intensities. After training, the feed-forward model will directly learn the transformation from the far-field domain to the object domain. Compared to conventional iterative optimization, deep learning

algorithms can produce reconstructions with moderate quality while having low data redundancy, low latency, and high computational efficiency. However, preliminary DNN algorithms rely on convolutional feature extraction without considering the properties in k -space imaging. This omission may lead to models with limited reconstruction quality.

In this work, we propose deep k -learning, a deep learning framework that is specifically designed for far-field imaging with attention to frequency in the context of RPI. Deep k -learning adopts frequency attention and frequency self-attention modules to the existing convolutional based frameworks, and it further improves the quality of reconstruction via conditional generative adversarial training. Our approach is capable of generating quality reconstructions in a single-frame and single deterministic step. This method may further enable the application of DNN to far-field diffractive imaging.

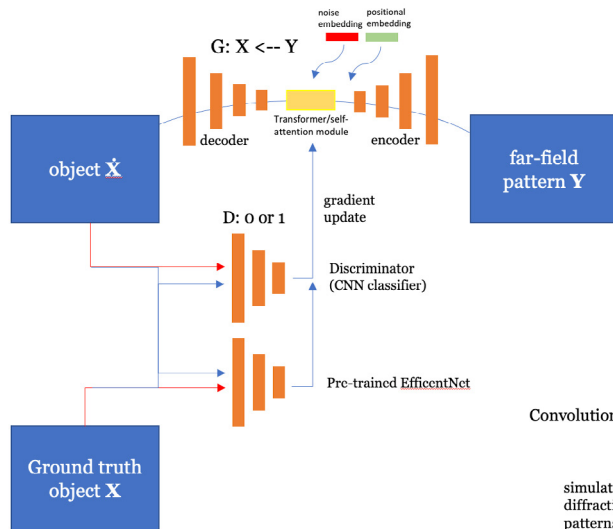
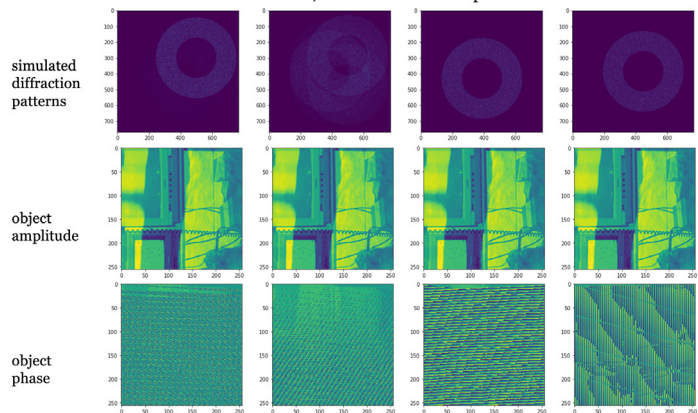


Figure 1: Deep k -learning framework, with encoder/decoder, transformer-based self-frequency attention, and discriminator for generative adversarial training. The patch embedding is to encode the spatial information of feature patches; the noise embedding is to generate artificial features that are not captured by convolutional encoders. The pre-trained EfficientNet produces representation loss in latent space.

Figure 2: Simulated diffraction patterns and their corresponding ground truth objects. For a complex object with added phase ramps, the resulting diffraction patterns will have identical geometric features that shift in real space. If a pure convolutional kernel is adopted in the DNN model, the reconstructed object will be identical regardless of the model size and training strategy.

Convolutional kernel is translational invariant, while our diffraction patterns are not



FURTHER READING

- A. L. Levitan, K. Keskinbora, U. T. Sanli, M. Weigand, and R. Comin, "Single-frame Far-field Diffractive Imaging with Randomized Illumination," *Optics Express*, vol. 28, no. 25, pp. 37103-37117, 2020.

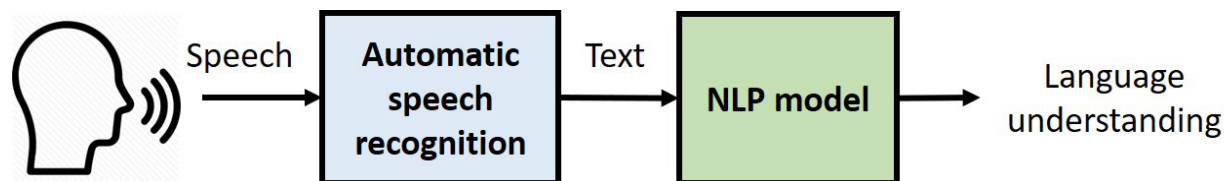
Natural Language Processing Accelerator for Transformer Models

A. Ji, H. Wang, S. Han, A. P. Chandrakasan
Sponsorship: TSMC

Natural language processing (NLP) models based on transformers and the attention mechanism have become widely used for recommendation systems, language modeling, question-answering tasks, sentiment analysis, and machine translation. In recent years, much focus has been placed on accelerating convolutional neural networks (CNNs) for image processing applications. There have been several works that accelerate recurrent neural networks (RNNs), but transformer models and the attention mechanism have remained largely neglected until recently. Many applications using NLP models on mobile devices—especially recommendation systems for advertising, music, and video—require potentially sensitive user data and preferences to be sent to the cloud for processing. To ensure user privacy, these tasks need to be performed directly on the edge device. As more devices rely on voice commands (see Figure 1), it becomes more critical to develop efficient processors for language processing directly on the edge device to ensure privacy, low latency, and extended battery life.

The attention mechanism is a key building block in the transformer model that can account for a significant fraction of the latency. Recently proposed architectures for NLP models have focused on optimizing this component. These works provide insight into the benefits that can be obtained by domain-specific optimizations, though much remains to be explored. The other main component of transformer models is the feed-forward network (i.e., fully connected layers). It is important to integrate these two parts to fully take advantage of optimizations in computation and data movement across layers.

Our goal is to accelerate both the attention mechanism and feedforward network to reduce data movement across layers. In the first test chip, we will exploit domain-specific properties of NLP models using techniques such as token pruning, piecewise linear quantization, and low-precision softmax to reduce memory and computation requirements and enable high-performance NLP models to be deployed on edge devices.



▲ Figure 1: Typical pipeline for processing language from speech input. Our processor will focus on accelerating the NLP model.

FURTHER READING

- H. Wang, Z. Zhang, and S. Han, "SpAtten: Efficient Sparse Architecture with Cascade Token Pruning and Head Pruning," *HPCA*, 2021.
- T. J. Ham, S. J. Jung, S. Kim, Y. H. Oh, Y. Park, Y. Song, J.-H. Park, S. Lee, K. Park, J. W. Lee, and D.-K. Jeong, "A³: Accelerating Attention Mechanisms in Neural Networks with Approximation," *HPCA*, 2020.

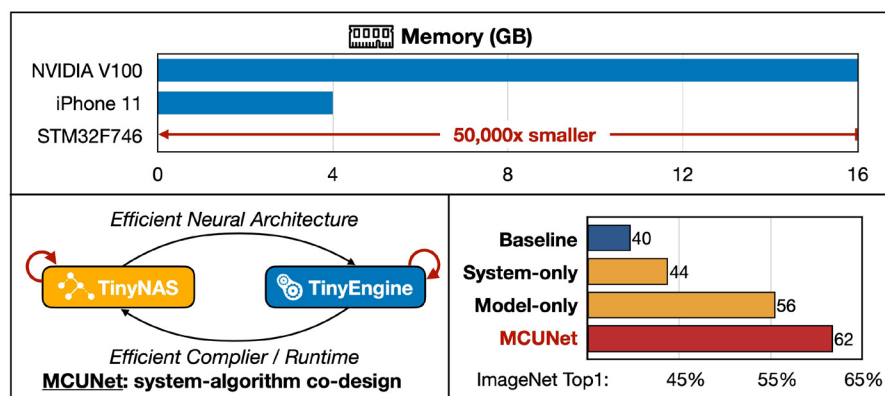
MCUNet: Tiny Deep Learning on IoT Devices

J. Lin, W.-M. Chen, Y. Lin, J. Cohn, C. Gan, S. Han

Sponsorship: MIT Satori, MIT-IBM Watson AI Lab, Qualcomm, NSF CAREER, NSF RAPID Award

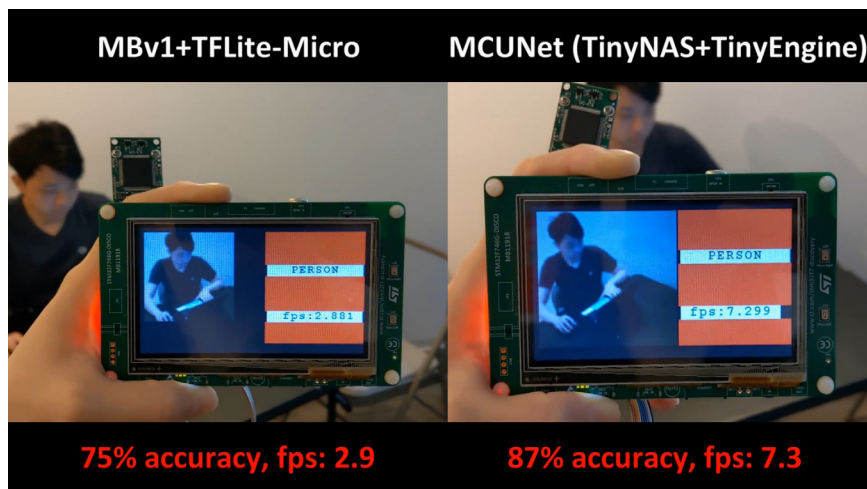
Machine learning on tiny microcontroller units (MCU) is appealing due to its low-cost and low-power nature. But the memory of MCU is 2-3 orders of magnitude smaller even than mobile phones. We propose MCUNet, a framework that jointly designs the efficient neural architecture (TinyNAS) and the light-weight inference engine (TinyEngine), enabling ImageNet-scale inference on MCUs. TinyNAS adopts a two-stage neural architecture search approach that first optimizes the search space to fit the resource constraints and then specializes the network architecture in the opti-

mized space. TinyNAS is co-designed with TinyEngine, a memory-efficient inference library to expand the search space and fit a larger model. MCUNet is the first to achieve >70% ImageNet top1 accuracy on a commercial MCU. On wake word datasets, MCUNet achieves state-of-the-art accuracy and runs 2.4-3.4× faster with 3.7-4.1× smaller peak SRAM. Our study suggests that the era of tiny machine learning on Internet of Things devices has arrived.



◀ Figure 1: (1) TinyML on MCUs is difficult due to limited memory; (2) MCUNet co-designs the efficient neural architecture (TinyNAS) and efficient compiler/runtime (TinyEngine) to significantly improve the deep learning performance on tiny MCUs.

▶ Figure 2: MCUNet demo on real hardware. Our solution achieves higher accuracy at a 2.5x-faster inference speed.



FURTHER READING

- H. Cai, C. Gan, T. Wang, H. Z. Zhang, and S. Han, "Once-for-All: Train One Network and Specialize it for Efficient Deployment," In *ICLR 2020*.
- M. Sandler, A. Howard, M. Zhu, A. Zhmoginov, and L. C. Chen, "MobileNetV2: Inverted Residuals and Linear Bottlenecks," *CVPR 2018*, pp. 4510-4520.
- Y. He, J. Lin, Z. Liu, H. Wang, L. J. Li, and S. Han, "Amc: Automl For Model Compression and Acceleration on Mobile Devices," *ECCV 2018*, pp. 784-800.

Searching Efficient 3D Architectures with Sparse Point-Voxel Convolution

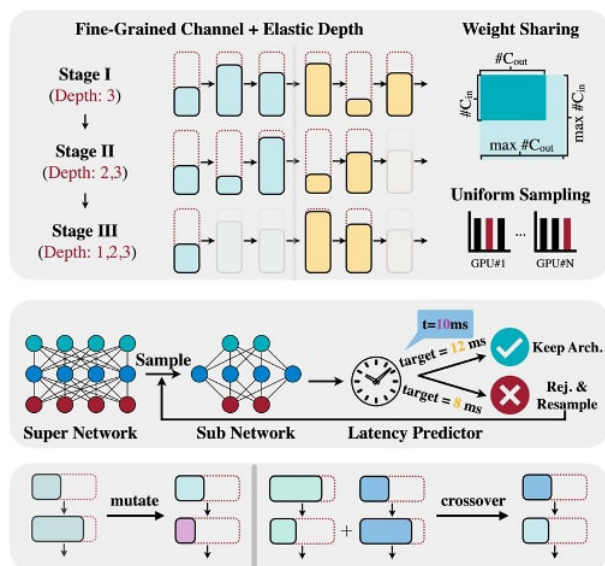
H. Tang, Z. Liu, S. Zhao, Y. Lin, J. Lin, H. Wang, S. Han

Sponsorship: MIT Quest for Intelligence, MIT-IBM Watson AI Lab, Samsung, SONY

3D deep learning has received increased attention thanks to its wide applications: e.g., it has been used in LiDAR perception that serves as the eyes of autonomous driving systems to understand the semantics of outdoor scenes. As the safety of the passenger is the top priority of the self-driving cars, 3D perception models must achieve high accuracy and low latency at the same time. However, the hardware resources on the self-driving cars are tightly constrained by the form factor (since we do not want a whole trunk of workstations) and heat dissipation. Therefore, it is crucial to design efficient and effective 3D neural network models with limited computation resources (e.g., memory).

To this end, we propose Sparse Point-Voxel Convolution (SPVConv), which introduces a low-cost high-resolution point-based branch to the vanilla

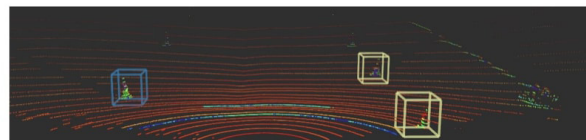
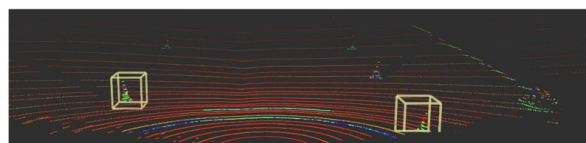
sparse convolution in order to better capture the fine details of the large outdoor scenes. On top of SPVConv, we further present 3D Neural Architecture Search (3D-NAS) to automatically find the best 3D model under a given resource constraint. We incorporate fine-grained channel numbers into the design space to increase diversity and introduce progressive depth shrinking to accelerate the training. The resulting SPVNAS model is fast and accurate: it outperforms MinkowskiNet by 3.3% in mIoU with lower latency. It also achieves 8x computation reduction and 3x measured speedup over MinkowskiNet while still providing higher accuracy. We further transfer our method to KITTI for 3D object detection, and it achieves consistent improvements over the previous one-stage detection baseline.



▲ Figure 1: Overview of 3D-NAS. We train a super network that is composed of multiple SPVConv's and supports fine-grained channel numbers and elastic network depths. Then, we perform an evolutionary architecture search to obtain the best model under a given latency constraint.



MIT Driverless (71 FPS, 95%)



SPVNAS (114 FPS, 99.9%)

▲ Figure 2: SPVNAS has been deployed on the autonomous racing vehicle of MIT Driverless, improving the detection range from 8 meters to 12 meters, reducing the latency from 14 milliseconds to 8 milliseconds, and boosting the accuracy from 95% to nearly 100%.

Embedded Neural Network Models and Inputs through Simple Power and Timing Side-Channels

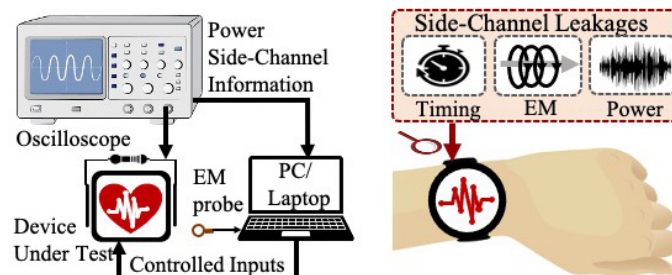
S. Maji, U. Banerjee, A. P. Chandrakasan
Sponsorship: Analog Devices Inc.

Rapid progress in machine learning theory has led to the deployment of energy-efficient neural networks (NNs) on edge devices. Embedded NN implementations, e.g., in health-care electronics, use locally stored models that have been trained using private data and are considered intellectual property of the organizations training them. Machine learning models have been found to leak sensitive information about the individual data records over which the model was trained. Recent years have witnessed new techniques of adversarial attacks on NN models. These adversarial attacks can sometimes be easier to mount if the underlying NN model is known (known as white-box attacks). The user input data needs to be protected for obvious privacy concerns. These concerns strongly motivate the need to protect the NN model as well as the user input from external adversaries.

Side-channel attacks (SCAs) are a major concern in embedded systems where physical access to the device can allow attackers to recover secret data by exploiting information leakage through power consumption, timing, and electro-magnetic emanations. SCAs have traditionally been applied to recover the secret cryptographic keys from the side-channel information. However, SCAs on micro-controller-based NN implementations are also gaining popularity. In this work, we focused on exploiting the side-channel vulnerabilities of embedded NN implementations

to recover their model parameters and inputs with simple power / timing analysis (Figure 1 shows the attack scenario for the example of a health monitoring watch).

We have demonstrated the recovery of model parameters for common NN implementations with different precisions (such as floating point, fixed point, and binary networks) on common embedded micro-controller platforms using only timing and simple power analysis SCAs. Timing side-channel leakage from the multiplication and non-linear activation function computations was utilized to recover model parameters of floating point NNs. For fixed point and binary NNs, zero-crossover input information obtained from the timing side-channel of the non-linear activation function was used with strategically crafted inputs for model recovery. The inputs of floating point NNs were recovered using timing side-channel information from integer-to-float conversion and multiplication operations. Input recovery for fixed point NNs with input normalization was performed using simple power analysis attack on the division operation. The feasibility and simplicity of our attacks, with minimal storage and computation requirements, emphasize the side-channel security concerns of embedded NN implementations and the need for defending against them.



▲ Figure 1: Attack setup for power / timing SCA over embedded NN implementations (exemplified using a health monitoring watch): (left) model parameter recovery and (right) input data recovery.

FURTHER READING

- Q. Xu, T. Arafain, and G. Qu, "Security of Neural Networks from Hardware Perspective: A Survey and Beyond," *Proc. 26th Asia and South Pacific Design Automation Conference*, ACM, Jan. 2021.
- S. Maji, U. Banerjee, and A. P. Chandrakasan, "Leaky Nets: Recovering Embedded Neural Network Models and Inputs through Simple Power and Timing Side-Channels – Attacks and Defenses," *IEEE Internet of Things Journal*, 2021.

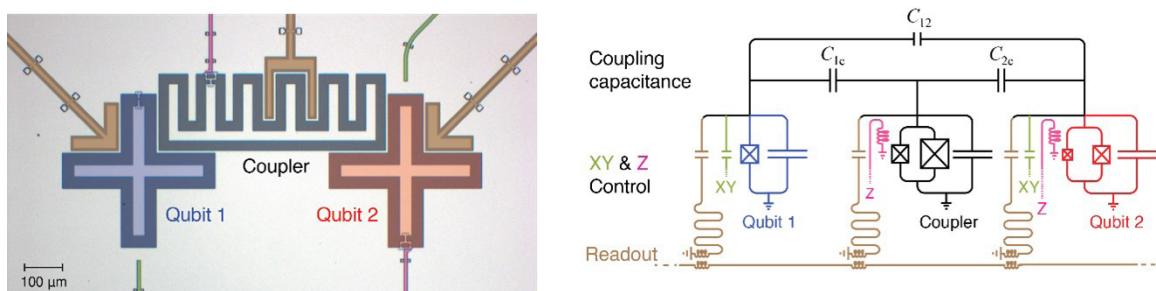
Realization of High-fidelity CZ and ZZ-free iSWAP Gates with a Tunable Coupler

Y. Sung, L. Ding, J. Braumüller, A. Vepsäläinen, B. Kannan, M. Kjaergaard, A. Greene, G. O. Samach, C. McNally, D. Kim, A. Melville, B. M. Niedzielski, M. E. Schwartz, J. L. Yoder, T. P. Orlando, S. Gustavsson, W. D. Oliver
 Sponsorship: ARO, the Assistant Secretary of Defense for Research & Engineering

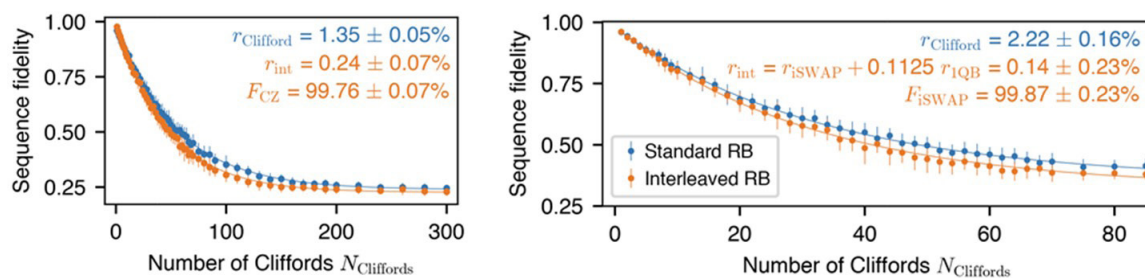
High-fidelity two-qubit gates at scale are a key requirement to realize the full promise of quantum computation and simulation. The advent and use of coupler elements to tunably control two-qubit interactions has improved operational fidelity in many-qubit systems by reducing parasitic coupling and frequency crowding issues. Nonetheless, two-qubit gate errors still limit the capability of near-term quantum applications. The reason, in part, is the existing framework for tunable couplers based on the dispersive approximation does not fully incorporate three-body multi-level dynamics, which is essential for addressing coherent leakage to the coupler and parasitic longitudinal (ZZ) interactions during two-qubit gates. Here, we present a systematic approach that goes beyond the dispersive approximation to exploit the engineered level structure of the coupler and optimize its control. Using this approach, we experimentally demonstrate CZ and ZZ-free iSWAP gates with two-qubit interaction fidelities of $99.76 \pm 0.07\%$ and $99.87 \pm 0.23\%$, respectively, which are close to their T_1 limits.

Figure 1 shows an optical micrograph of the device and the corresponding circuit schematic. We realize a pairwise interacting three-body system in a circuit quantum electrodynamics setup using three capacitively coupled transmons. The transmon coupler at the center mediates interaction between the two distant transmon qubits. The coupler-mediated two-qubit gates are implemented by dynamically modulating the external magnetic flux threading the SQUID loops of the coupler and qubit 2.

In Figure 2, we measure the two-qubit interaction fidelities F_{CZ} and F_{iSWAP} of CZ and iSWAP gates, respectively, by performing interleaved randomized benchmarking. By using an optimized pulse shape, we suppress coherent leakage into the coupler and achieve a 70% error reduction, compared to a simple square-shaped pulse. We also harness the second-excited state of the coupler to eliminate unwanted ZZ interactions that introduce errors during iSWAP, thereby achieving high two-qubit interaction fidelity.



▲ Figure 1: An optical micrograph of the device (left) and the corresponding circuit schematic (right).



▲ Figure 2: Two-qubit interleaved randomized benchmarking results for CZ (left) and iSWAP (right) gates.

FURTHER READING

- Y. Sung, L. Ding, J. Braumüller, A. Vepsäläinen, B. Kannan, M. Kjaergaard, A. Greene, G. O. Samach, C. McNally, D. Kim, A. Melville, B. M. Niedzielski, M. E. Schwartz, J. L. Yoder, T. P. Orlando, S. Gustavsson, W. D. Oliver, "Realization of High-fidelity CZ and ZZ-free iSWAP Gates with a Tunable Coupler," arXiv:2011.01261, 2020.
- F. Yan, P. Krantz, Y. Sung, M. Kjaergaard, D. Campbell, J. I.J. Wang, T.P. Orlando, S. Gustavsson, W.D. Oliver, "Tunable Coupling Scheme for Implementing High-Fidelity Two-Qubit Gates," *Physical Review Applied* 10, 054062, 2018.

MEMS, Field-Emitter, Thermal, and Fluidic Devices

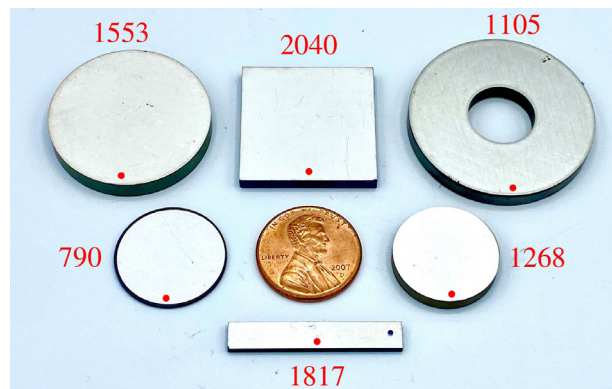
Comparing Piezoelectric Materials and Vibration Modes for Power Conversion	76
Acoustically Active Surface for Automobile Interiors Based on Piezoelectric Dome Arrays.....	77
Advanced Microfluidic Heat Exchangers via 3D Printing and Genetic Algorithms	78
3D-Printed Miniature Vacuum Pumps	79
3D-Printed, Miniaturized Retarding Potential Analyzers for Cubesat Ionospheric Studies	80
Multi-Dimensional Double Spiral Device for Fully Automated Sample Preparation.....	81
Internally Fed, Additively Manufactured Electrospray Thruster.....	82
Planar Field-Emission Electron Sources via Direct Ink Writing	83
Micro Rocket Engine Using Steam Injector and Electric Fuel Pump	84
Nonvolatile Electrically Reconfigurable Photonic Circuits Based on Low-Loss Phase-Change Materials	85
Extremely Dense Arrays of Si Emitters with Self-Aligned Extractor and Focusing Gates.....	86
Gated Silicon Field-Ionization Arrays for Compact Neutron Sources.....	87
Field Emission from a Single Nanotip in Controlled Poor Vacuum.....	88
GaN Vertical Nanostructures Sharpened by A New Digital Etching Process for Field Emission Applications	89
Integrating Object Form and Electronic Function in Rapid Prototyping and Personal Fabrication	90
MEMS Energy Harvesting and AI-based Design Processing.....	91

Comparing Piezoelectric Materials and Vibration Modes for Power Conversion

J. D. Boles, J. E. Bonavia, P. L. Acosta, Y. K. Ramadass, J. H. Lang, D. J. Perreault
Sponsorship: Texas Instruments, NSF GRFP, Enphase Energy, Masdar Institute

Major industries such as transportation, energy systems, manufacturing, healthcare, consumer electronics, and information technology vitally depend on power electronics for processing electrical energy. Power electronics are often the bulkiest components in the systems they serve, and smaller converter designs are typically limited by magnetic energy storage components (i.e., inductors and transformers). The power density and efficiency capabilities of magnetics fundamentally decrease at low volumes, which motivates exploration of other energy storage mechanisms that are more conducive to miniaturization.

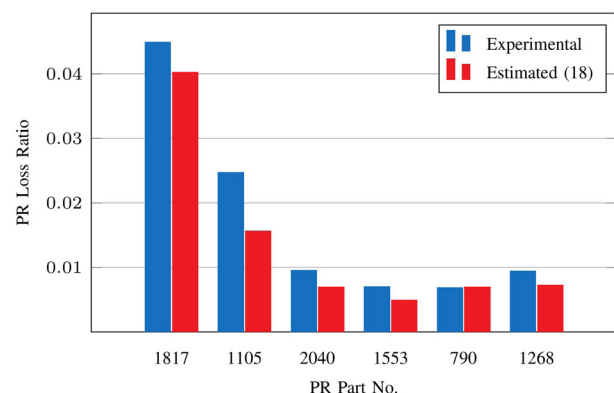
One promising alternative is piezoelectric energy storage; piezoelectrics store energy in the mechanical compliance and inertia of a piezoelectric material, and they offer several potential advantages to power conversion. In previous work, we have demonstrated a converter implementation capable of >99% peak efficiency using a commercially available piezoelectric resonator (PR). However, criteria for selecting piezoelectric materials and/or designing PRs themselves remain murky in the context of power conversion.



▲ Figure 1: PRs tested for experimental validation of efficiency FOMs, with APC International part numbers shown in red. These PRs represent four different PZT materials and span four vibration modes.

In this work, we derive figures of merit (FOMs) for piezoelectric materials and vibration modes specifically for use in power electronics. In particular, we focus on maximum efficiency and maximum power density FOMs for PRs in realistic converter switching sequences. These FOMs are shown to depend on only material properties for each of seven vibration modes, and they correspond to specific PR geometry conditions for realizing both maximum efficiency and maximum power density in PR designs.

We validate these FOMs and their geometry conditions using a numerical solver for converter operation as well as experimental results for six commercially available PRs (shown in Figures 1-2). The proposed FOMs are demonstrated to be highly representative metrics for PR efficiency and power density capabilities, and these properties are likewise shown to scale favorably for converter miniaturization. Thus, by enabling smaller-volume converters, piezoelectrics are positioned to both reduce system costs and open new application spaces for power conversion.



▲ Figure 2: Experimental minimum loss ratio of the PRs in Figure 1 compared to the estimate provided by the efficiency FOMs.

FURTHER READING

- J. D. Boles, J. J. Piel, and D. J. Perreault, "Enumeration and Analysis of DC-DC Converter Implementations Based on Piezoelectric Resonators," *IEEE Transactions on Power Electronics*, vol. 36, no. 1, pp. 129-145, 2021.
- J. D. Boles, J. E. Bonavia, P. Acosta, Y. K. Ramadass, J. H. Lang, and D. J. Perreault, "Evaluating Piezoelectric Materials and Vibration Modes for Power Conversion" (submitted).
- J. D. Boles, P. Acosta, Y. K. Ramadass, J. H. Lang, and D. J. Perreault, "Evaluating Piezoelectric Materials for Power Conversion," *IEEE Workshop on Control and Modeling for Power Electronics (COMPEL)*, Aalborg, Denmark, Nov. 2020.

Acoustically Active Surface for Automobile Interiors Based on Piezoelectric Dome Arrays

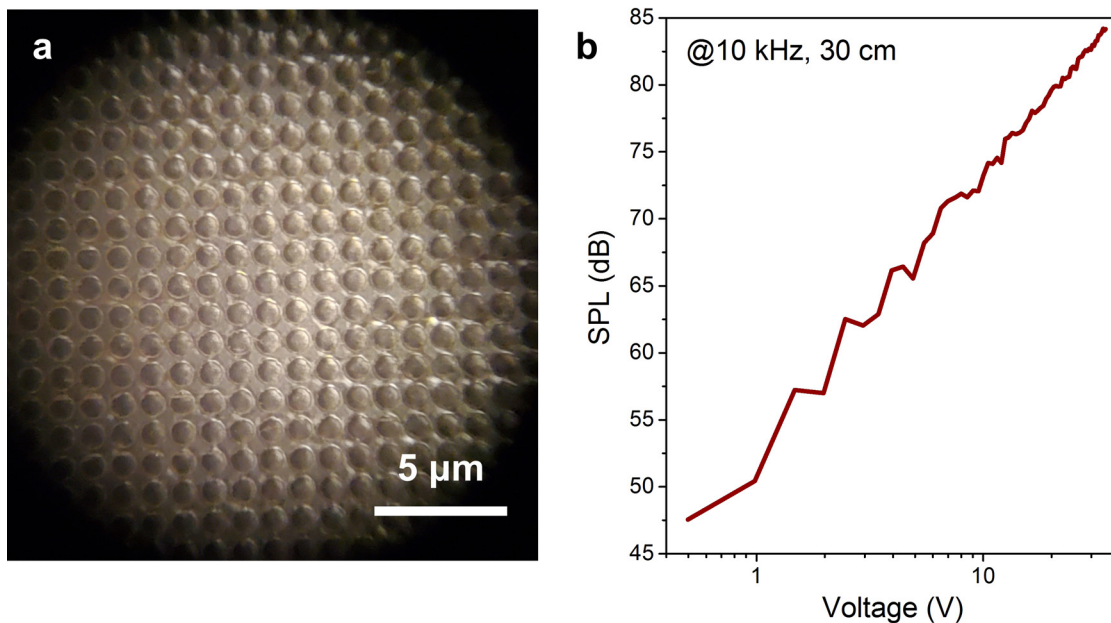
J. Han, J. Lang, V. Bulović

Sponsor: Ford Motor Company

The surfaces of automobile interiors can be rendered acoustically active by mounting on them flexible, wide-area thin-films with arrays of small acoustic transducers. Each small, individually addressable transducer functions as a speaker, a microphone, or an ultrasonic transceiver. Engineering the structures and dimensions of individual transducers on the acoustic surface offers widely tunable performance. Coordinating the phased transducer array based on adaptive control could enable unique functionalities of the acoustic surface such as directional sound generation and detection. As a result, the acoustically active surface can work either in the audio frequency range for noise cancellation, personal entertainment, and communication with the vehicle or in the ultrasound frequency range for gesture detection, alertness monitoring, etc., which collectively improve the comfort and safety of the automobile.

This project seeks to develop and demonstrate a wide-area, paper-thin, robust, and even transparent

acoustic surface based on an array of dome-shaped piezoelectric transducers. Dependencies of the acoustic performance on the design variables of the piezoelectric domes are studied through theoretical modeling, simulation, and experimental characterization of dome vibration and sound radiation by the acoustic surface. A 12- μm -thick, $10\times 10\text{ cm}^2$ acoustic surface consisting of an array of polyvinylidene difluoride (PVDF) can be further enhanced by scaling up the area, utilizing superior piezoelectric materials, enlarging the dome size, and/or reducing the film thickness. A scalable micro-embossing process has been developed to fabricate the small domes with high precision and at low cost. $10\times 10\text{ cm}^2$ samples (Figure 1) were prepared with different dome dimensions and tested in an anechoic chamber. The results confirm outstanding performance of the acoustic surface, owing to the existence of active microstructures in an array, and thereby show great promise for broad application scenarios.



▲ Figure 1: (a) Microscopic image of a $10\times 10\text{ cm}^2$ sample of the acoustic surface based on embossed PVDF domes. (b) Free-field sound generation of the acoustic surface under 10 kHz at 30 cm away.

Advanced Microfluidic Heat Exchangers via 3D Printing and Genetic Algorithms

J. Izquierdo-Reyes, L.F. Velásquez-García

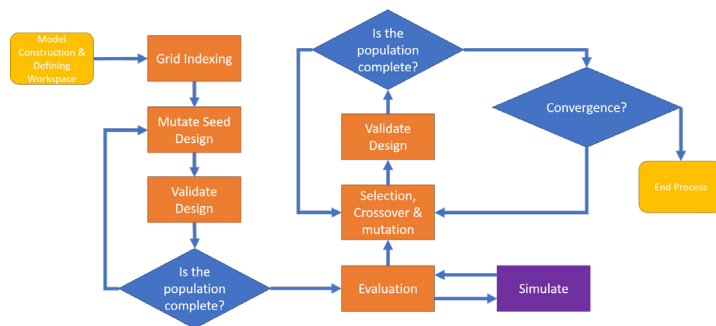
Sponsorship: MIT-Tecnologico de Monterrey Nanotechnology Program

Power electronics are fundamental in many high-tech applications, e.g., electric cars. Adequate heat dissipation of these electronic components is essential for them to operate properly and attain long lifespans. Cooling high-power electronics typically employs heat exchangers that put a liquid in contact with hot surfaces to extract heat. Using microfluidics can greatly increase the surface-to-volume ratio of the liquid, boosting heat transfer. However, classically designed heat exchangers do not properly address the non-uniformity of the heat field, e.g., localized hot spots. In addition, better power microelectromechanical system microfluidics can be created via additive manufacturing, involving better materials and implementing more effective geometries than in mainstream cleanroom microfabrication. In particular, metal 3D printing can monolithically create complex microfluidic devices while greatly simplifying the manufacturing process and requiring significantly less time than subtractive manufacturing.

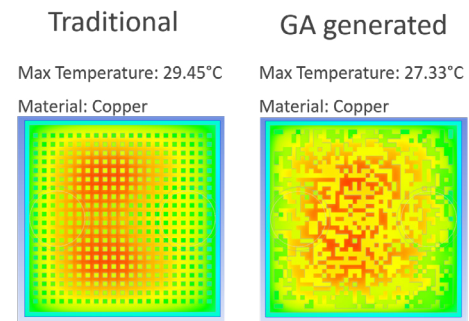
Genetic algorithms (GAs) can be used to implement an iterative design process inspired in natural selection that can potentially create better engineering solutions by generating unexpected

implementations. In a nutshell, GAs are used to create multiple generations of randomized mutations of the parent designs (called subjects), looking to optimize the solution's performance by minimizing/maximizing a particular fitness function.

In this project, we are exploring metal 3D printing and GAs to implement better microfluidic heat exchangers. The fitness function employed ponders trade-offs between temperature and pressure drop in the cold plate to minimize the maximum temperature. We use a finite element solver with a computational fluid dynamics module to obtain solutions of the flow and temperature fields of each subject of each generation and then we used software to compare their performance across each generation and down-select the best designs. The software creates and analyzes new generations until it attains a certain threshold value in the fitness function (Figure 1). The resultant devices are complex, often counter-intuitive, and unlikely to be synthesized by a human using first principles (Figure 2), surpassing the performance of traditional designs.



▲ Figure 1: Block diagram of the algorithm employed to design advanced microfluidic heat exchangers.



▲ Figure 2: Classically designed (left) and GA-designed (right) finned cold plate for a CPU chip. A reduction of 2.12 °C in the maximum device temperature was attained.

FURTHER READING

- E. Segura-Cárdenas and L. F. Velásquez-García, "Additively Manufactured Robust Microfluidics via Silver Clay Extrusion," *J. Microelectromech. Syst.*, vol. 29, no. 3, pp. 427-437, Jun. 2020.
- Z. Sun and L. F. Velásquez-García, "Monolithic FFF Printed, Biodegradable, Biocompatible, Dielectric-Conductive Microsystems," *J. Microelectromech. Syst.*, vol. 26, no. 6, pp. 1356-1370, Dec. 2017.
- A. L. Beckwith, J. T. Borenstein, and L. F. Velásquez-García, "Monolithic, 3D-printed Microfluidic Platform for Recapitulation of Dynamic Tumor Microenvironments," *J. Microelectromech. Syst.*, vol. 27, pp. 1009-1022, Oct. 2018.

3D-Printed Miniature Vacuum Pumps

A. P. Taylor, J. Izquierdo-Reyes, L.F. Velásquez-García
Sponsorship: Edwards Vacuum, MIT-Tecnologico de Monterrey Nanotechnology Program

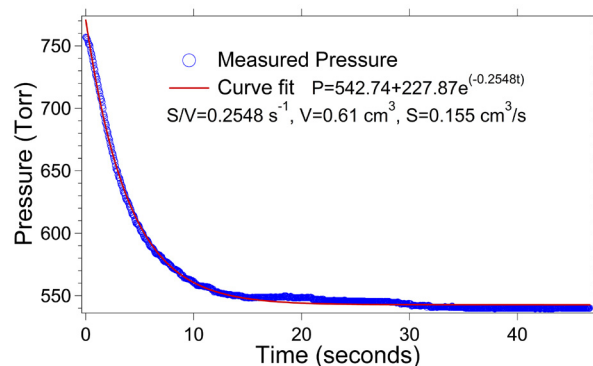
Compact pumps that create and sustain vacuum environments while supplying precise gas flow rates are essential to implement a variety of microsystems. Positive displacement vacuum pumps, e.g., diaphragm pumps, create and maintain vacuum by cycling pockets of gas that are compressed from rarified conditions to atmospheric pressure. Miniaturized positive displacement vacuum pumps typically have dead volumes very similar to the maximum displacement of their compression chambers, resulting in the creation of modest vacuums.

Magnetic, long-stroke actuators could be used to implement pump chambers with large compression ratios; an exciting possibility to implement such actuators at a low cost is additive manufacturing. In this project, we demonstrated the first miniaturized, additively manufactured, magnetic diaphragm pumps for liquids in the literature where all constitutive parts, including the magnets, are monolithically 3D-printed. The devices were created in nylon-based feedstock via fused filament fabrication, in which thermoplastic

filament was extruded from a hot nozzle to create a solid object layer by layer. The miniature pumps use 150- μm - or 225- μm - thick membranes connected to a piston with an embedded magnet, a chamber, two diffusers, and two fluidic connectors (Figure 1). We also experimentally observed that the same pumps for liquids can be used as vacuum pumps if they are first moistened with a small amount of water to enable the pump diffusers to seal during actuation. The miniature 3D-printed pumps can attain an ultimate pressure of 540 Torr at an operating frequency of 230 Hz, i.e., the pumps achieve a pressure of 220 Torr below atmospheric pressure (Figure 2). The ultimate pressure achieved by our pumps is close to values reported from commercially available, non-microfabricated, miniature diaphragm pumps with comparable diaphragm diameters. We speculate that changing the design of the pump chamber to increase its compression ratio and printing a more flexible and compliant material could attain lower ultimate pressure.



▲ Figure 1: 3D-printed miniature magnetic pumps next to a US dime; the fluidic ports and the embedded magnet are visible at either end of the pumps.



▲ Figure 2: Pressure versus time characteristic of a 3D-printed magnetic pump (from A. P. Taylor, J et al., *J. Phys. D: Appl. Phys.*, vol. 53, no. 35-5002, Jun. 2020). Data in blue, exponential curve fit in red.

FURTHER READING

- A. P. Taylor, C. Velez Cuervo, D. P. Arnold, and L. F. Velásquez-García, "Fully 3D-printed, Monolithic, Mini Magnetic Actuators for Low-cost, Compact Systems," *J. Microelectromech. Syst.* vol. 28, no. 3, pp. 481-493, Jun. 2019.
- A. P. Taylor and L. F. Velásquez-García, "Miniaturized Diaphragm Vacuum Pump by Multi-Material Additive Manufacturing," *J. Microelectromech. Syst.*, vol. 26, no. 6, pp. 1316 - 1326, Dec. 2017.
- A. P. Taylor, J. Izquierdo-Reyes, and L. F. Velásquez-García, "Compact, Magnetically Actuated, Additively Manufactured Pumps for Liquids and Gases," *J. Phys. D: Appl. Phys.*, vol. 53, no. 35-5002, Jun. 2020.

3D-Printed, Miniaturized Retarding Potential Analyzers for Cubesat Ionospheric Studies

J. Izquierdo-Reyes, L.F. Velásquez-García

Sponsorship: MIT-Portugal, MIT-Tecnologico de Monterrey Nanotechnology Program

The ionosphere is an upper region of the atmosphere that is made of plasma created and sustained by solar UV radiation. Little is known about some of the layers of the ionosphere, e.g., the thermosphere. Comprehending the processes taking place in the thermosphere is essential to understand local and global weather and global warming. There is evidence that global warming is cooling down the thermosphere, causing serious issues, e.g., variation in satellites' drag and less recycling of water. In-situ data would provide more and better information.

Plasma sensors are used to characterize plasmas, measuring one or more properties that can be derived from the position and velocity distributions of the particles that make up the plasma. A retarding potential analyzer (RPA) is a multi-gridded sensor that measures the ion energy distribution of a plasma. In an RPA, the diameter of the apertures of the outermost grid (the floating grid) measures up to two Debye lengths to trap the plasma outside the sensor while the inter-grid spacing measure up to four Debye lengths to avoid space charge effects that would smear the measurements. The Debye length in the ionosphere is about 1 mm.

Sending hardware to space is quite expensive because, among other reasons, of the physics of rocket propulsion, e.g., requiring ejecting propellant many times the mass of the spacecraft. Therefore, technologies that yield smaller, lighter, and cheaper space hardware without sacrificing performance are of great interest. Consequently, there is great interest in developing mission-focused miniaturized satellites, i.e., cubesats (1-10 Kg, a few L in volume).

In this project we are harnessing additive manufacturing to demonstrate better and cheaper cubesat plasma sensors. Our RPA design uses laser-micromachined stainless steel grids integrated to a 3D-printed ceramic housing made via vat polymerization using 60- μm by 60- μm by 100- μm XYZ voxels (Figure 1). Each grid is assembled to the housing using a set of engineered springs that provide active alignment. Experiments show that the per-level assembly precision is better than 100 μm (Figure 2). Inter-grid alignment results in larger current signals. Current work focuses on completing, fabricating, and characterizing the RPA design.



▲ Figure 1: Example of a 3D-printed ceramic resolution matrix. The width of the piece facing the camera is about 60 mm.



▲ Figure 2: Selected views of an assembly misalignment experiment: a) ceramic grid holder with spring interacting features, b) metallic grid before spring actuation, c) metallic grid with actuated and locked-in springs.

FURTHER READING

- E. Heubel and L. F. Velásquez-García, "Microfabricated Retarding Potential Analyzers with Enforced Aperture Alignment for Improved Ion Energy Measurements in Plasmas," *J. Microelectromech. Syst.* vol. 24, no. 5, pp. 1355-1369, 2015.
- Z. Sun, G. Vladimirov, E. Nikolaev, and L. F. Velásquez-García, "Exploration of Metal 3-D Printing Technologies for the Microfabrication of Freeform, Finely Featured, Mesoscaled Structures," *J. Microelectromech. Syst.*, vol. 27, no. 6, pp. 1171 – 1185, Dec. 2018
- C. Yang and L. F. Velásquez-García, "Low-Cost, Additively Manufactured Electron Impact Gas Ionizer with CNT Field Emission Cathode for Compact Mass Spectrometry," *J. Phys. D – Appl. Phys.* vol. 52, no. 7, 075301 (9pp), Feb. 2019.

Multi-Dimensional Double Spiral Device for Fully Automated Sample Preparation

H. Jeon, J. Han

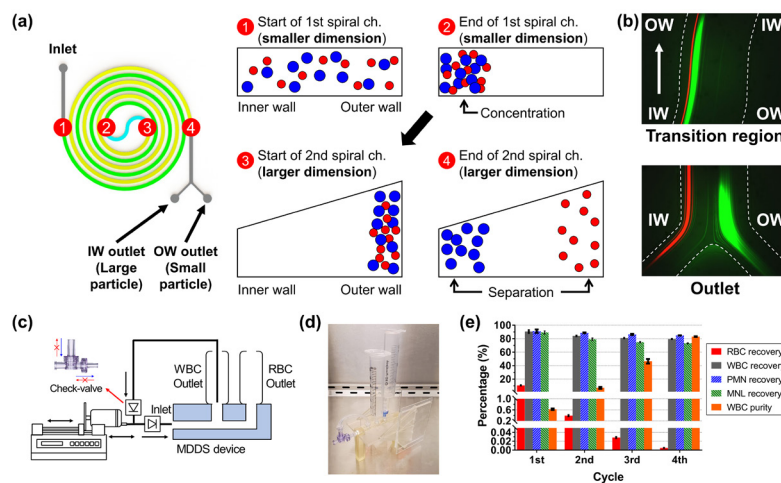
Sponsorship: NIH, Ohana Bioscience

Sample preparation is the process of extracting target analytes from interferents for the sensitive and successful downstream analysis of samples. To overcome the limitations of the current standard (centrifugation), which entails many energy-consuming steps, various microfluidic devices have been developed. Among them, the inertial spiral microfluidic device has been extensively utilized due to its inherent advantages including label-free, high-throughput, and reliable operation without any external force field. However, improvement of separation efficiency and usability is required for field-deployable applications.

In response to this critical need, we developed a new type of spiral device, the multi-dimensional double spiral (MDDS) device. The MDDS device is composed of two sequentially connected spiral channels having different dimensions. Particles can be concentrated through the first, smaller-dimensional spiral channel and subsequently separated through the second, larger-dimensional spiral channel (Figure 1a). The initial focusing in the first spiral channel can significantly de-

crease particle dispersion and effectively extract smaller particles into the outer-wall side of the channel, increasing separation resolution and efficiency (Figure 1b).

To achieve more purified and concentrated output, we also developed a new recirculation platform based on a check-valve which allows only one-way flow. In the platform, an output from the MDDS separation can be extracted back into the input syringe and processed again repeatedly via programmed back-and-forth motions of a syringe pump, resulting in higher purity and concentration (Figure 1c). The developed platform can be operated in a fully automated or even hand-powered manner. Using the platform, we successfully demonstrated the isolation of white blood cells from a diluted blood sample by removing abundant red blood cells (up to 99.99%). We expect that the developed platform could provide an innovative field-deployable sample preparation solution to point-of-care sample analyses (not limited to blood) and diagnostics.



▲ Figure 1: (a) A schematic diagram of the MDDS device and its operation. (b) Trajectories of 6- μm (green) and 10- μm (red) particles. (c) A schematic and (d) an image of the check-valve-based recirculation platform. (e) Recoveries and purity of blood cells from 4 cycles of recirculation.

FURTHER READING

- H. Jeon, B. Jundi, K. Choi, H. Ryu, B. D. Levy, G. Lim, and J. Han, "Fully-automated and Field-deployable Blood Leukocyte Separation Platform Using Multi-dimensional Double Spiral (MDDS) Inertial Microfluidics," *Lab Chip*, vol. 20, pp. 3612–3624, 2020. <https://doi.org/10.1039/DoLCo0675K>

Internally Fed, Additively Manufactured Electro spray Thruster

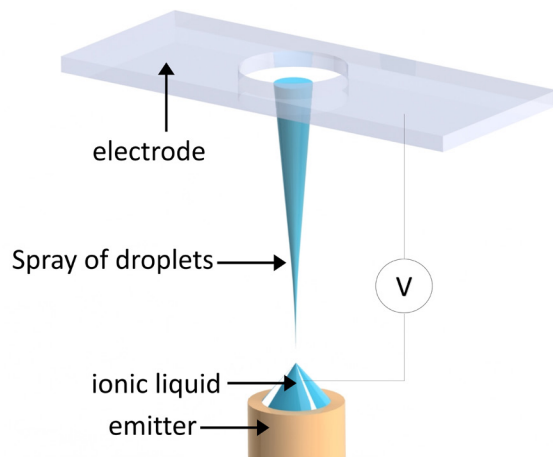
H. Kim, L. F. Velásquez-García
Sponsorship: MIT Portugal

Electrospray engines produce thrust by electrohydrodynamically ejecting high-speed ions or droplets. Electro spray emitters work better if miniaturized because their start-up voltage decreases with the square root of the emitter diameter. A single emitter has very low thrust; multiplexing the emitters, so they uniformly operate in parallel, makes it possible to increase the thrust delivered. Electro spray thrusters are typically created via precision subtractive manufacturing techniques, which is time-consuming and expensive. For New Space, i.e., the development of a commercial space industry, additive manufacturing is an attractive possibility to create complex hardware that is inexpensive and exquisitely iterated and optimized.

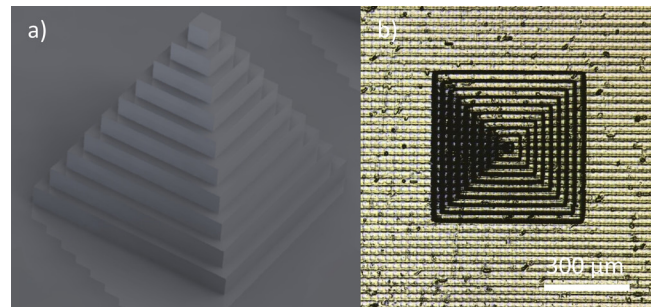
Our group recently demonstrated the first additively manufactured ionic liquid electro spray thrusters in the literature; these devices attain pure ion emission in both polarities, maximizing their specific impulse. However, the propellant flow rate, which has an upper bound for pure ionic emission, limits the thrust per emitter that can be attained for a given bias voltage. An engine that can deliver larger per-emitter

thrust, at the expense of using less efficiently the propellant, is of interest for impulsive maneuvers.

Consequently, we are also interested in developing additively manufactured, low-specific impulse, high per-emitter thrust electro spray engines. Unlike the externally fed, nanoporous fluidic structure used in the ionic thrusters previously described, an internally fed emitter architecture is a better fit to produce droplets (Figure 1), which are heavier than ions, resulting in higher per-emitter thrust. We use the vat polymerization method called digital light processing to make emitters with narrow channels that provide high hydraulic resistance. Using resolution matrices drawn in $\sim 25 \mu\text{m}$ voxels and a resin chemically resistant to an ionic liquid, we verified the high fidelity of the printed parts to the computer-aided design (CAD) models (Figure 2). Current research efforts focus on exploring the resolution limits of the printable feedstock for solid and negative features and developing device designs with hydraulic networks that provide a high and uniform hydraulic impedance to each emitter.



▲ Figure 1: Schematic of a single internally fed electro spray emitter.



▲ Figure 2: a) CAD image and b) confocal microscope image of printed part for one of the test structures used to verify printing fidelity.

FURTHER READING

- F. A. Hill, E. V. Heubel, P. P. de Leon, and L. F. Velásquez-García, "High-Throughput Ionic Liquid Ion Sources Using Arrays of Microfabricated Electro spray Emitters with Integrated Extractor Grid and Carbon Nanotube Flow Control Structures," *J. of Microelectromechanical Systems*, vol. 23, no. 5, pp. 1237-1248, May, 2014.
- D. Olvera-Trejo and L. F. Velásquez-García, "Additively Manufactured MEMS Multiplexed Coaxial Electro spray Sources for High-Throughput, Uniform Generation of Core-Shell Microparticles," *Lab on a Chip*, vol. 16, no. 21, pp. 4121-4132, Oct. 2016.
- D. V. Melo Maximo, and L. F. Velásquez-García, "Additively Manufactured Electro hydrodynamic Ionic Liquid Pure-Ion Sources for Nanosatellite Propulsion," *Additive Manufacturing*, vol. 36, p. 101719, Dec. 2020.

Planar Field-Emission Electron Sources via Direct Ink Writing

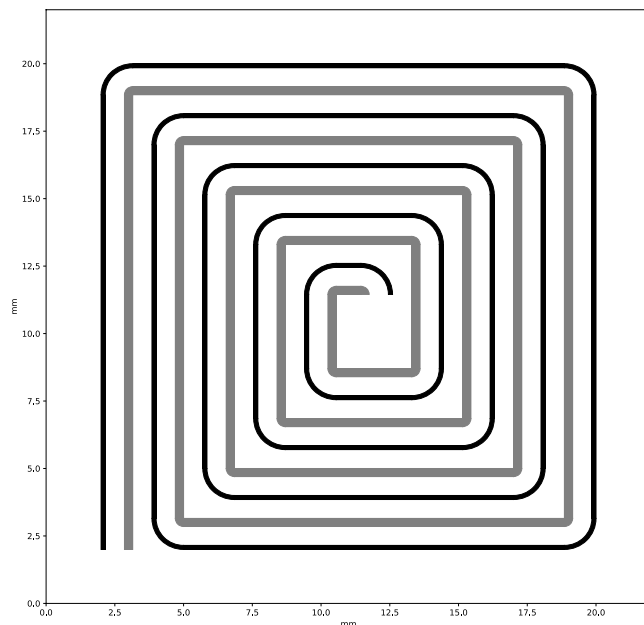
N. Klugman, L. F. Velásquez-García
Sponsorship: MIT Portugal

Vacuum electron sources appear in numerous technologies, from microscopy to displays to mass spectrometry. The two main forms vacuum electron sources can take are thermionic and field emission. Thermionic sources emit electrons by raising the temperature of a conductor so that many of its electrons have an energy greater than the potential barrier trapping them, allowing them to escape. Field-emission sources use an applied electric field to lower the potential barrier, allowing electrons to quantum tunnel out of the conductor. Field-emission sources can therefore operate at lower temperatures, in a poorer vacuum, faster, and using less energy, all of which increase the usability of the electron source.

Field-emission sources' emitting electrodes have been made from many materials, but research has focused on carbon nanotubes (CNTs). CNTs' nanosized tips and high aspect ratio lead to high electric fields at modest voltages, which is useful since the emitted current increases with electric field; in

addition, CNTs have excellent chemical resistance, e.g., resisting oxidation by the trace gases in the vacuum. Manufacturing CNT field-emission sources is often a costly and time-intensive effort, particularly when the CNT growth locations are restricted by desired device geometry.

To affordably implement CNT field emission cathodes, this project explores direct ink writing to create in-plane, gated field-emission sources. A spiral CNT ink trace is printed on an insulating substrate, along with a symmetric, co-planar trace (see Figure 1) of a different conducting (e.g., silver nanoparticle) ink. A voltage applied between the traces induces an electric field, causing electron tunneling from the CNT tips. The planar design reduces manufacturing complexity and increases electron transmission. Current work includes printable feedstock material selection, exploration of geometric modifications to increase device longevity, and increasing imprint density to allow for greater emission current density.



◀ Figure 1: Computer-aided design of 3D-printed field-emission cathode with in-plane gate.

FURTHER READING

- A. Perales and L. F. Velásquez-García, "Fully 3D-Printed Carbon Nanotube Field Emission Electron Sources with In-plane Gate Electrode," *Nanotechnology*, vol. 30, no. 49, p. 495302, Dec. 2019
- C. Yang and L. F. Velásquez-García, "Low-cost, Additively Manufactured Electron Impact Gas Ionizer with CNT Field Emission Cathode for Compact Mass Spectrometry," *Journal of Physics D – Applied Physics*, vol. 52, no. 7, p. 075301, Feb. 2019.
- L. F. Velásquez-García, A. I. Akinwande, and M. Martínez-Sánchez, "Precision Hand Assembly of MEMS Subsystems Using DRIE-patterned Deflection Spring Structures: An Example of an Out-of-Plane Substrate Assembly," *Journal of Microelectromechanical Systems*, vol. 16, no. 3, pp. 598 – 612, Jun. 2007.

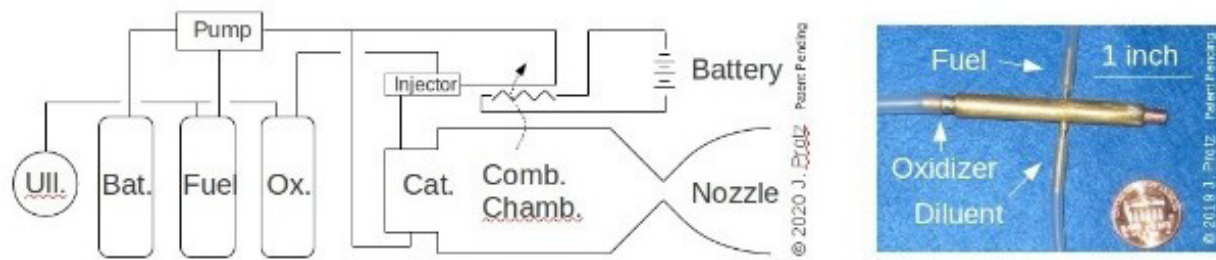
Micro Rocket Engine Using Steam Injector and Electric Fuel Pump

J. Protz

Sponsorship: Protz Lab Group; microEngine, LLC

Micro-fabricated miniature chemical rocket engines have been an active area of research at MIT and elsewhere for two decades; they are a compelling propulsion option for small launch vehicles and spacecraft. At these scales, miniaturized steam injectors like those used in Victorian-era steam locomotives are viable as a pumping mechanism and offer an alternative to pressure feed and high-speed turbo-pumps. Storing propellants at low pressure reduces tank mass, and this improves the vehicle empty-to-gross mass ratio; if one propellant is responsible for most of the propellant mass (e.g., oxidizer), injecting it while leaving the others solid or pressure-fed can still achieve much of the potential gain. Previously, the principal investigator and his group built and tested ultraminiature-machined micro jet injectors that pumped ethanol and explored pressure-fed liquid and hybrid engine designs. Current

work has focused on configurations that use a battery and electric pump to replace the pressure-feed portion of past designs; electric pumps pump fuel and/or coolant while a steam injector motivated by boiled coolant pumps the oxidizer. This replacement allows pressurized tanks to be avoided altogether, greatly simplifying implementation and the sourcing of components while still being compatible with miniaturization via a micro-electromechanical system (MEMS). Current work has focused on designing and implementing an axisymmetric whole-engine mock-up or test article that simultaneously integrates a steam injector, boiler, decomposition chamber, fuel injector, thrust chamber, and electric fuel pump while being practical to build and also retaining compatibility with 2D MEMS fabrication (see Figure 1).



▲ Figure 1: (a) Schematic representation of engine and (b) engineering mock-up in brass of an integrated engine (w/o electric pump).

FURTHER READING

- J. M. Protz, "Steam-Injector and Electric Micro Rocket," presented at *Gas Turbine Laboratory Seminar*, MIT, Cambridge, MA, Nov. 17, 2020.
- J. Protz, "Hybrid and Partially Pressure-Fed Injector-Pumped Micro Rockets," (JANNAF 2019-004BT), presented at the *Joint Army-Navy-NASA-Air Force Joint Meeting of the 13th Modeling and Simulation / 11th Liquid Propulsion / 10th Spacecraft Propulsion Subcommittees and Meeting of the Programmatic and Industrial Base (JANNAF)*, Tampa, FL, Dec. 9-13, 2019.
- J. M. Protz, "Modeling and Analysis of a Giffard-Injector-Pumped Bipropellant Microrocket," invited talk at *Pratt & Whitney Rocketdyne*, Huntsville, AL, Feb. 3, 2010.

Nonvolatile Electrically Reconfigurable Photonic Circuits Based on Low-Loss Phase-Change Materials

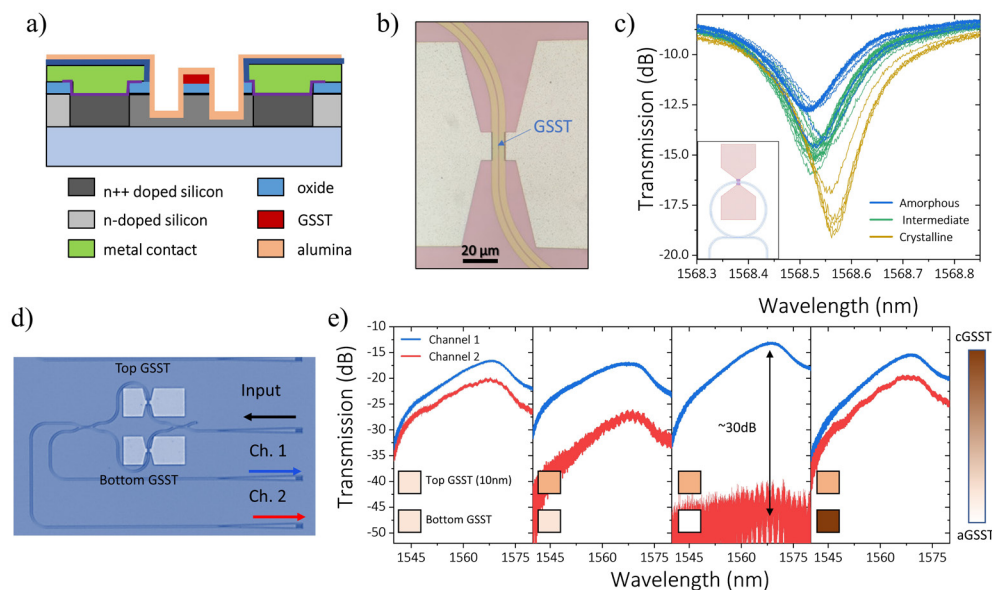
C. Ríos, Q. Du, Y. Zhang, M. Shalaginov, P. Miller, P. Robinson, C. Roberts, T. Gu, S. Vitale, J. Hu
Sponsorship: DARPA

Low-power active components are crucial to achieving programmable photonic integrated circuits (PICs). Reaching this goal drives the development of active components with outstanding performance in the gigahertz-frequency operation required in telecommunication applications but also on slower scales for active reconfiguration of PICs. However, these components are all volatile, which is not ideal for applications where the configurations are performed sporadically or just once. In the latter case, nonvolatile reconfiguration capable of retaining any configuration with zero-power consumption is the desired functionality. To fill this gap, we employ $\text{Ge}_2\text{Sb}_2\text{Se}_4\text{Te}_1$ (GSST), a low-loss broadband optical phase-change material. GSST allows refractive index modulation by using a heat stimulus to switch between the amorphous and the crystalline states, which results in an outstanding modulation of optical properties ($\Delta n \sim 1.7$).

We patterned $\sim 10^{18} \text{ cm}^{-3}$ n-doped silicon microheaters to provide the heat stimuli and electrothermally configure the state of GSST, which was

evanescently coupled to the propagating mode of a half-etched rib waveguide (Figure 1). We evaporated 30 nm of GSST, which theoretically introduced a π phase-shift with a 5- μm -long cell. We demonstrated 50 cycles of reversible and repeatable switching between the amorphous and two partially crystallized states of a 3- μm -long GSST and the subsequent phase shift on a ring resonator (Figure 1c). We used $3.5\text{V} \times 20 \text{ ms}$ and $5\text{V} \times 50 \mu\text{s}$ pulses to crystallize and amorphize, respectively. Our analysis reveals that doped Si contributes only to 0.03 dB/ μm absorption, amorphous GSST shows zero loss, and crystalline GSST shows 0.57 dB/ μm .

Furthermore, we demonstrate GSST-based phase-shifters on a balanced 2×2 MZI switch structure (Figure 1d, Figure 1e). We measured the variations on the two output channels as a function of the state of a 10- μm -long GSST in each arm. Using the same pulse sequence as above, we achieved $\pi/2$ phase-shift upon amorphization followed by full recrystallization with a 30-dB extinction ratio.



▲ Figure 1: a) Sketch of the GSST-based device using n-doped silicon heaters. b) Image of a 10- μm -long microheater with 3- μm -long, 30-nm-thick GSST covering the waveguide. c) Resonance peak for three distinct GSST states on a ring with 120- μm radius; each line represents a switching event. d) Image of a MZI switch with two 80/20-splitting directional couplers and two GSST phase shifters. e) Spectra recorded for both channels under different GSST configurations in a 10- μm -long GSST/20- μm -long microheater.

FURTHER READING

- M. Wuttig, H. Bhaskaran, and T. Taubner, "Phase-change Materials for Non-volatile Photonic Applications," *Nat. Photonics*, vol. 11, pp. 465–476, 2017.
- Y. Zhang, J. B. Chou, J. Li, H. Li, Q. Du, A. Yadav, S. Zhou, M. Y. Shalaginov, Z. Fang, H. Zhong, C. Roberts, P. Robinson, B. Bohlin, C. Rios, H. Lin, M. Kang, T. Gu, J. Warner, V. Liberman, K. Richardson, and J. Hu, "Broadband Transparent Optical Phase Change Materials for High-performance Nonvolatile Photonics," *Nat. Comms.*, vol. 10, p. 4279, 2019.

Extremely Dense Arrays of Si Emitters with Self-Aligned Extractor and Focusing Gates

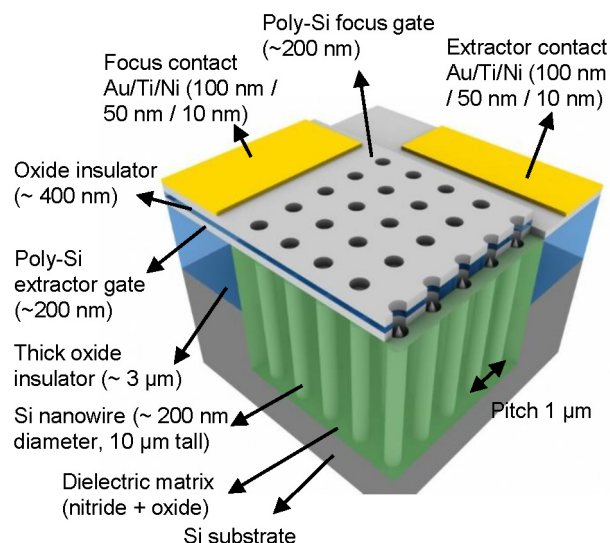
G. Rughoobur, L. Jain, A. I. Akinwande

Sponsorship: Air Force Research Laboratory, Intelligence Advanced Research Projects Activity

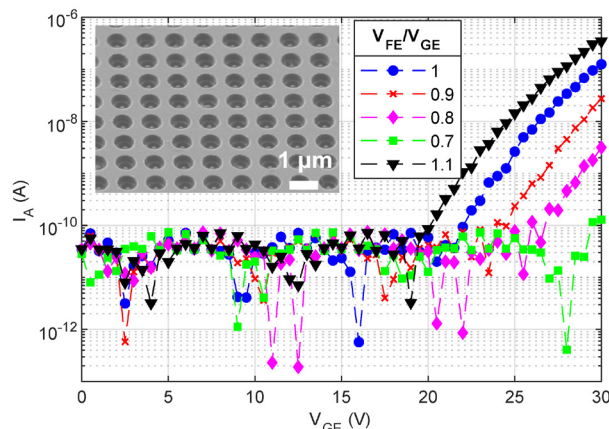
The advent of microfabrication has enabled scalable and high-density Si field-emitter arrays (FEAs). These are advantageous due to compatibility with complementary metal-oxide-semiconductor (CMOS) processes, the maturity of the technology, and the ease in fabricating sharp tips using oxidation. The use of a current limiter is necessary to avoid burn-out of the sharper tips. Active methods using integrated MOS field-effect transistors and passive methods using a nano-pillar (~200-nm wide, 8- μm tall) in conjunction with the tip have been demonstrated. Si FEAs with single gates reported in our previous works have current densities of >100 A/cm² and operate with lifetimes of over 100 hours.

The need for another gate (Figure 1) becomes essential to control the focal spot size of the electron beam as electrons leaving the tip have an emission angle of 12.5°. The focus electrode provides a radial electric field that reduces the lateral velocity of stray electrons

and narrows the cone angle of the beam reaching the anode. Varying the voltage on the focus gate reduces the focal spot size or achieves an electron beam modulator for radio-frequency applications. In this work, we fabricate the densest (1- μm pitch) double-gated Si with an integrated nanowire current limiter (Figure 2). The apertures are ~350 nm and ~550 nm for the extractor and focus gates, respectively, with a 350-nm-thick oxide insulator separating the two gates. Electrical characterization of the fabricated devices shows that the focus-to-gate ratio (V_{FE}/V_{GE}) can be used to control the anode current (Figure 2). When the focus voltage exceeds the gate voltage, the field superposition increases the extracted current, and vice versa. These devices can potentially find applications as high-current focused electron sources in flat panel displays, nano-focused X-ray generation, and microwave tubes.



▲ Figure 1: Si field-emitter array with integrated current limiter, self-aligned extractor, and focus gates for nano-focused cold electron sources.



▲ Figure 2: Electrical characterization of 500 x 500 arrays with different focus/gate voltage ratios; inset shows the fabricated double-gated array.

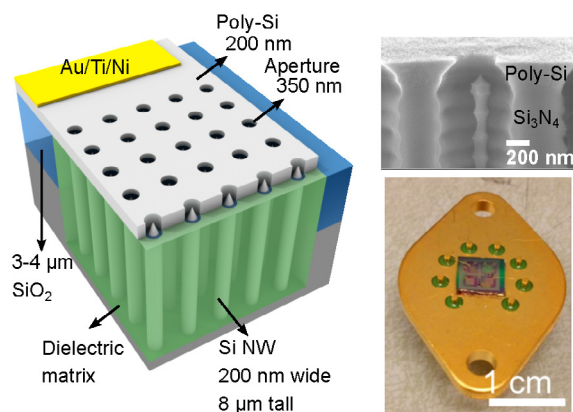
FURTHER READING

- G. Rughoobur, N. Karaulac, L. Jain, O. O. Omotunde, and A. I. Akinwande, "Nanoscale Silicon Field Emitter Arrays with Self-aligned Extractor and Focus Gates," *Nanotechnology*, vol. 31, no. 33, p. 335203, 2020.
- L. Y. Chen and A. I. Akinwande, "Aperture-collimated Double-gated Silicon Field Emitter Arrays," *IEEE Trans. Electron Devices*, vol. 54, no. 3, pp. 601–608, 2007.
- L. Dvorson, I. Kymissis, and A. I. Akinwande, "Double-gated Silicon Field Emitters," *J. Vac. Sci. Technol. B Microelectron. Nanom. Struct.*, vol. 21, no. 1, p. 486, 2003.

Gated Silicon Field-Ionization Arrays for Compact Neutron Sources

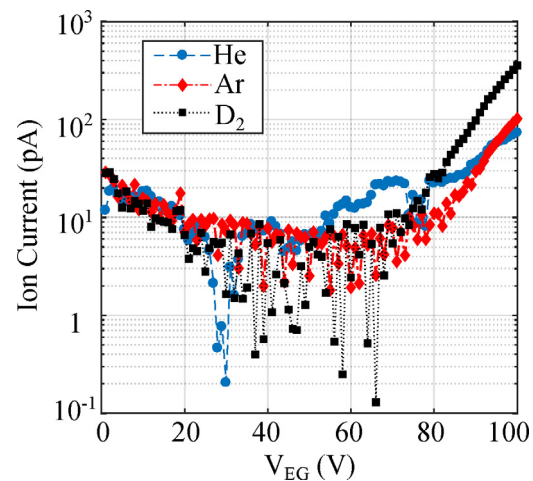
G. Rughoobur, A. I. Akinwande
Sponsorship: DARPA

Neutron radiation is widely used in various applications, ranging from the analysis of the composition and structure of materials and cancer therapy to neutron imaging for security. However, most applications require a large neutron flux, which is often achieved only in large infrastructures such as nuclear reactors and accelerators. Neutrons are generated by ionizing deuterium (D_2) to produce deuterium ions (D^+) that can be accelerated towards a target loaded with either D or tritium (T). The reaction generates neutrons and isotopes of He, with the D-T reaction producing the higher neutron yield. Classic ion sources require extremely high positive electric fields, on the order of 10^8 volts per centimeter (10 V/nm). Such a field is achievable only in the vicinity of sharp electrodes under a large bias; consequently, ion sources for neutron generation are bulky.



▲ Figure 1: Schematic of gated field-ionization array, with SEM cross section of a single field ionizer and photograph of a packaged chip with arrays of different sizes for neutron generation.

This work explores, as an alternative, highly scalable and compact Si field-ionization arrays (FIAs) with a unique device architecture that uses self-aligned gates and a high-aspect-ratio ($\sim 40:1$) Si nanowire current limiter to regulate electron flow to each field emitter tip in the array (Figure 1). The tip radius has a log-normal distribution with a mean of 5 nm and a standard deviation of 1.5 nm, while the gate aperture is ~ 350 nm in diameter and is within 200 nm of the tip. Field factors, β , of $> 1 \times 10^6 \text{ cm}^{-1}$ can be achieved with these Si FIAs, implying that gate-emitter voltages of 250-300 V (if not less) can produce D^+ based on the tip field of 25-30 V/nm. In this work, our devices achieve an ionization current of up to 5 nA at ~ 140 V for D_2 at pressures of 10 mTorr. Gases such as He and Ar can also be ionized at voltages (< 100 V) with these compact Si FIAs (Figure 2).



▲ Figure 2: Ion current measured for different gases (He, Ar, and D_2) at 1 mTorr pressure demonstrating low ionization voltages using 1000 by 1000 Si FIAs.

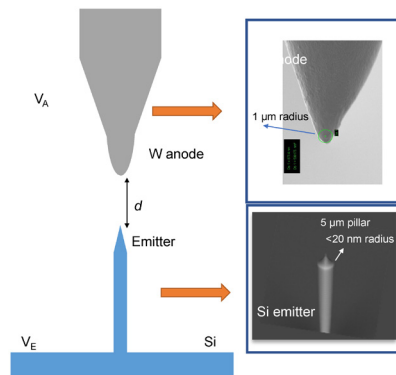
FURTHER READING

- A. Fomani, L. F. Velasquez-Garcia, and A. I. Akinwande, "Low-voltage Field Ionization of Gases up to Torr-level Pressures using Massive Arrays of Self-aligned Gated Nanoscale Tips," *IEEE Trans. Electron Devices*, vol. 61, no. 5, pp. 1520–1528, 2014.
- G. Rughoobur, A. Sahagun, O. O. Ilori, and A. I. Akinwande, "Nanofabricated Low-Voltage Gated Si Field-Ionization Arrays," *IEEE Trans. Electron Devices*, vol. 1, no. c, pp. 1–7, 2020.
- B. Johnson, P. R. Schwoebel, P. J. Resnick, C. E. Holland, K. L. Hertz, and D. L. Chichester, "Field Ionization Characteristics of an Ion Source Array for Neutron Generators," *J. Appl. Phys.*, vol. 114, no. 17, p. 174906, Nov. 2013.

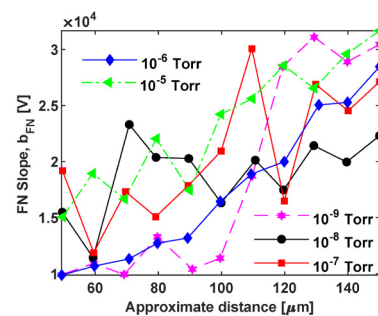
Field Emission from a Single Nanotip in Controlled Poor Vacuum

G. Rughoobur, O. O. Ilori, A. I. Akinwande
Sponsorship: DARPA

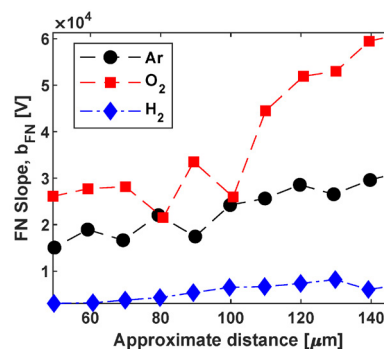
For reliable field emission performance, nano-emitters require ultra-high vacuum, which is bulky and costly. In poor vacuum, the adsorption/desorption of gas molecules on the surface causes work function variations, which results in exponential changes in the emitted current. In this work, we assess the dependence of the Fowler-Nordheim slope, b_{FN} , in different gases using a single un-gated Si emitter. These measurements are enabled by using a scanning anode field emission microscope that has a W tip (radius $<1 \mu\text{m}$) as the anode and with the Si emitter placed on a nano-positioning stage. We first characterized the devices in ultra-high vacuum and in the following gases: Ar, He, N_2 , O_2 , and H_2 . I-V characteristics are recorded by varying the distance, d , between the anode and the emitter (Figure 1). Using the measurement in ultra-high vacuum (UHV, 10^{-9} Torr) as a reference, we extract the geometrical field-factor, β from b_{FN} . In poor-vacuum measurements (10^{-8} Torr – 10^{-5} Torr), we use this β to extract the “modified” work-function of the surface for each gas and each pressure investigated. We find that as pressure increases, the performance in Ar changes very little at the distances scanned (Figure 2). As expected (Figure 3), operation in O_2 resulted in substantial increase in b_{FN} and hence the work-function; however, in H_2 , we measured a decrease in the slope, suggesting a reduction in the work function. This work provides the premise in assessing which gases and pressures are responsible for performance degradation in Si field-emitter arrays, to achieve more stable field-emission current in poor vacuum.



▲ Figure 1: Schematic of measurement of a single Si emitter using a scanning anode field emission microscope using a W anode positioned at a distance d . Scanning electron microscope images of the emitter and the anode.



▲ Figure 2: FN slope extracted for UHV with decreasing d , compared with different pressures of Ar showing only a small increase in b_{FN} .



▲ Figure 3: Comparison of different gases on the FN slope at 10^{-5} Torr demonstrating larger b_{FN} in O_2 , and smaller b_{FN} in H_2 .

FURTHER READING

- G. Rughoobur, J. Zhao, L. Jain, A. Zubair, T. Palacios, J. Kong, and A. I. Akinwande, “Enabling Atmospheric Operation of Nanoscale Vacuum Channel Transistors,” *2020 Device Research Conference (DRC)*, 2020, pp. 1–2.
- L. F. Velásquez-García, S. A. Guerrero, Y. Niu, and A. I. Akinwande, “Uniform High-Current Cathodes Using Massive Arrays of Si Field Emitters Individually Controlled by Vertical Si Ungated FETs-Part 2: Device Fabrication and Characterization,” *IEEE Trans. Electron Devices*, vol. 58, no. 6, pp. 1783–1791, Jun. 2011.
- P. R. Schwoebel and I. Brodie, “Surface-science aspects of vacuum microelectronics,” *J. Vac. Sci. Technol. B Microelectron. Nanom. Struct.*, vol. 13, no. 4, pp. 1391–1410, 1995.

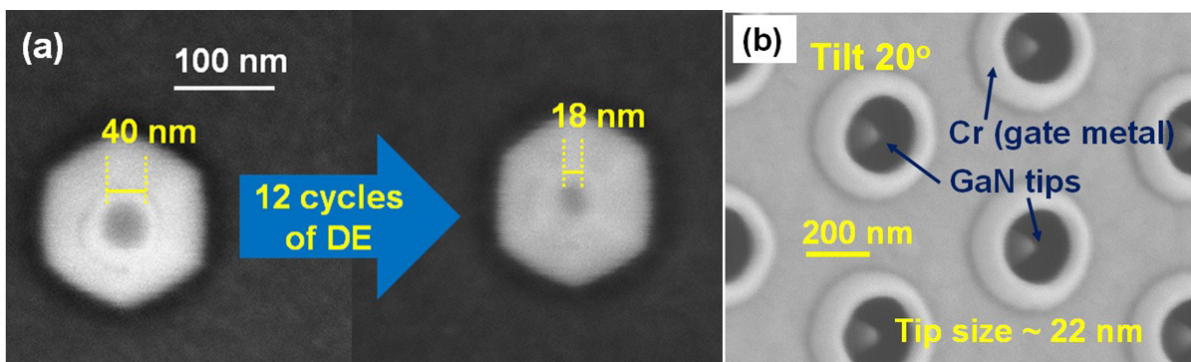
GaN Vertical Nanostructures Sharpened by A New Digital Etching Process for Field Emission Applications

P.-C. Shih, T. Palacios, in collaboration with G. Rughoobur, A. I. Akinwande
Sponsorship: AFOSR

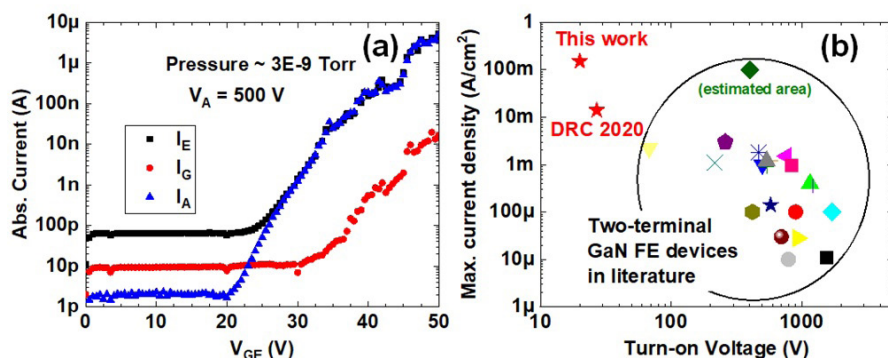
Field emitters (FE), namely vacuum transistors, are promising for harsh-environments and high-frequency electronics. III-nitrides are excellent candidates as FEs due to their tunable electron affinities. However, so far, few works demonstrate sub-100 V turn on in III-nitride field emission devices because of relatively large tip sizes and the lack of self-aligned gate structures.

In this work, we develop a novel wet-based-only digital etching (DE) process for GaN nanopyramid field emission arrays (FEAs). Conventional oxygen-plasma-based DEs on III-nitrides are anisotropic, and they do not sharpen vertical tips. Furthermore, the use of a biased plasma could potentially damage tips. Therefore, a new digital etching process is developed. By using this new technology, tip width can be sharpened from 40 nm down to sub-20 nm with a reasonably controlled etching rate per cycle of DE (Figure 1 (a)).

Combining the sharpened GaN nanopyramids with a self-aligned-gate structure (Figure 1 (b)) we developed before, we demonstrate the world's-best GaN vertical field emission devices with the lowest gate-emitter turn-on voltage (VGE, ON) of 20 V and the highest max current density of 150 mA/cm² at VGE = 50 V (Figure 2). The turn-on voltage and field factor of this device are also already comparable with the-state-of-art Si FEAs. Furthermore, the gate leakage is still only about 0.5 % of the anode current, indicating a space to have future improvement for more drive current. Further performance improvements are expected when applying the developed technologies to N-polar III-nitrides and AlGaN-alloys.



▲ Figure 1: Scanning electron microscope images of (a) a tip before and after DE and (b) finished device.



▲ Figure 2: (a) Transfer characteristics of this gated GaN vertical FEA and (b) benchmark of GaN vertical FEs.

FURTHER READING

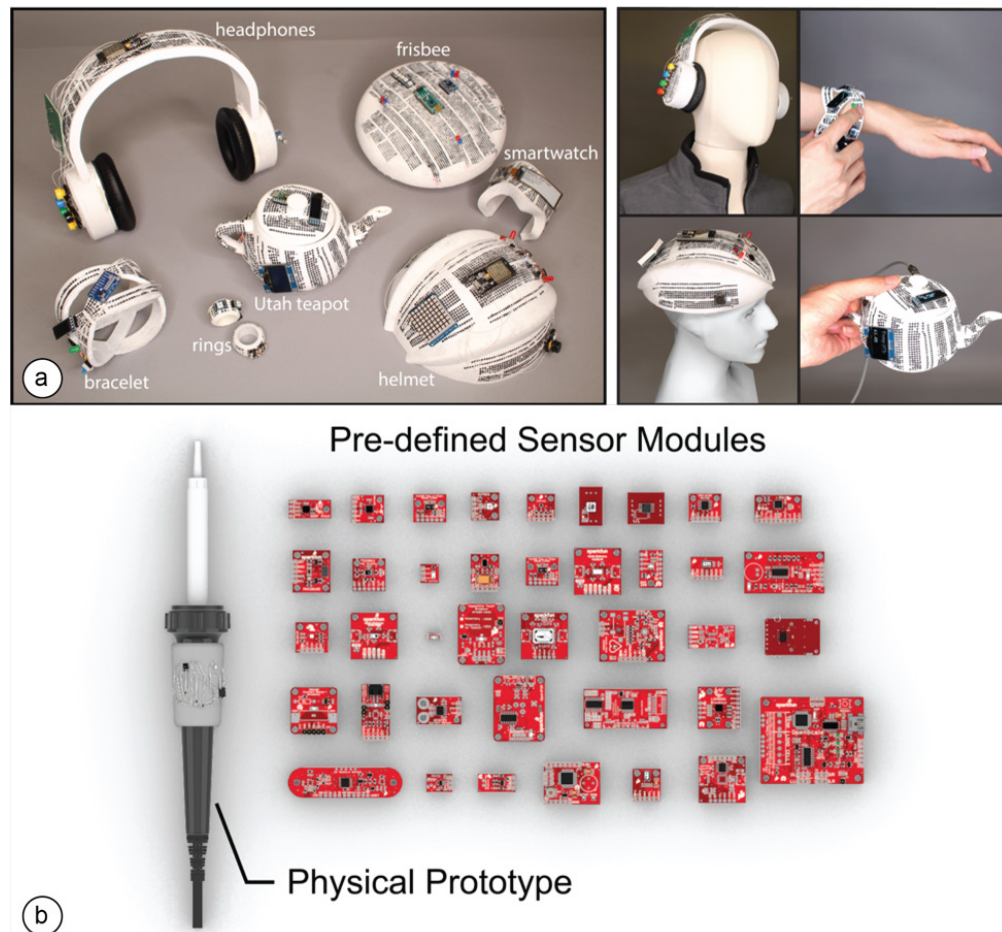
- P.-C. Shih, G. Rughoobur, K. Cheng, A. I. Akinwande, and T. Palacios, "Self-Align-Gated GaN Field Emitter Arrays Sharpened by a Digital Etching Process," *IEEE Electron Device Letters*, vol. 42, no. 3, Mar. 2021, pp. 422-425.
- P.-C. Shih, G. Rughoobur, P. Xiang, K. Liu, K. Cheng, A. I. Akinwande, and T. Palacios, "GaN Nanowire Field Emitters with a Self-Aligned Gate Process," presented at *78th Device Research Conference*, virtual, Jun. 2020.

Integrating Object Form and Electronic Function in Rapid Prototyping and Personal Fabrication

J. Zhu, S. Mueller
Sponsorship: NSF, NCSOFT

Rapid prototyping is a key technique that enables users to quickly realize their digital designs and therefore has been widely used in early-stage prototyping and small-scale customized fabrication. A long-term vision in human-computer interaction is to create interactive objects for which all functions are directly integrated with the form and fabricated at once. So far, rapid prototyping has focused mainly on fabricating passive objects for which the form of an object can be freely

designed; recently we have also moved towards digital specification and fabrication of object functions for interactive design. These advances offer the promise that eventually in rapid function prototyping, the interactive object form and function would be under the same design consideration; therefore, the object form could follow its designated function, and the function could adapt to its physical form.



▲ Figure 1: (a) CurveBoards are 3D breadboards directly integrated into the surface of physical objects. (b) MorphSensor is a 3D electronics design tool for designing electronic function in the context of a prototype's three-dimensional shape.

FUTURE READING

- J. Zhu, L. Blumberg, Y. Zhu, M. Nisser, E. L. Carlson, X. Wen, K. Shum, J. A. Quaye, and S. Mueller, "CurveBoards: Integrating Breadboards into Physical Objects to Prototype Function in the Context of Form," in *Proceedings of the 2020 CHI Conference on Human Factors in Computing Systems (CHI '20)*, ACM, 2020.
- J. Zhu, Y. Zhu, J. Cui, L. Cheng, J. Snowden, M. Chounlakone, M. Wessely and S. Mueller, "MorphSensor: A 3D Electronic Design Tool for Reforming Sensor Modules," in *Proceedings of the 33rd Annual ACM Symposium on User Interface Software and Technology (UIST '20)*, ACM, 2020.

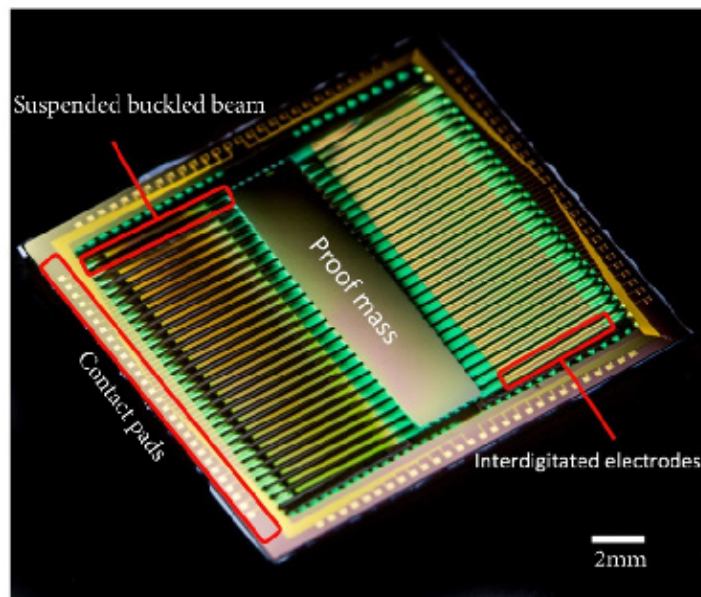
MEMS Energy Harvesting and AI-based Design Processing

H. Akay, S-G. Kim

Sponsorship: MIT-SUTD International Design Center

Vibrational energy-harvesting devices seek to deliver useable electric power in remote or mobile applications by drawing energy from ambient sources of vibration. Due to the spectrum of such ambient vibrations occurring at a very low frequency (below 100Hz), major design challenges must be overcome when developing a piezoelectric energy harvesting device to function in these conditions, namely generating strain at the micro-scale and operating over a wide bandwidth of low input frequencies. The culmination of three generations of this microelectromechanical systems (MEMS) design effort by our research group is a bi-stable buckled beam energy harvester that relies on non-linear oscillations to translate input vibrations to the axial strain of piezoelectric elements to produce sizable electric energy at the MEMS-scale devices.

Various long-term research efforts such as this at MIT produce documentation detailing novel devices and corresponding process designs that could benefit future micro and nano systems designers if the knowledge and design concepts explored for them could be computationally retrievable. To benefit from past designs, their functional requirements must be identified and structured in a searchable and trainable knowledge base which future designers may navigate. Currently, we are developing an AI-based Natural Language Processing (NLP) model which can automate the reading of vast MEMS documentation produced by MTL and MIT.nano. By automatically processing and representing decades of research knowledge at MIT and elsewhere, faster and successful design and innovation in MEMS and Nano-scale systems can be achieved.



▲ Figure: Photograph of fabricated bi-stable buckled beam energy-harvesting device.

FURTHER READING:

- R. Xu, H. Akay & S.G. Kim, "Buckled MEMS Beams for Energy Harvesting from Low Frequency Vibrations," Research, 2019.
- H. Akay, M. Yang & S.G. Kim, "Automating Design Requirement Extraction from Text with Deep Learning," *ASME IDETC/CIE Design Automation Conference*, 2021.
- H. Akay & S.G. Kim, "Reading Functional Requirements Using Machine Learning-based Language Processing," *CIRP Annals 70(1)*, 2021.

Nanotechnology, Nanostructures, Nanomaterials

Lithiation Mechanisms of Si and Ge Thin Film Battery Electrodes.....	93
Gated Nonreciprocal Magnon Transmission from Direction-Dependent Magnetic Damping.....	94
Gigahertz Frequency Antiferromagnetic Resonance and Strong Magnon-Magnon Coupling in Layered Crystal CrCl ₃	95
Nanoparticle-Enhanced Microsputtered Gold Thin Films for Low-Cost, Agile Manufacturing of Interconnects.....	96
Large-Scale 2D Perovskite/Transition Metal Dichalcogenide Heterostructure for Photodetector.....	97
Grayscale Stencil Lithography.....	98
Unraveling the Correlation between Raman and Photoluminescence in Monolayer Molybdenum Disulfide through Machine Learning Models.....	99
Additively Manufactured Electrospray Ion Thrusters for Cubesats.....	100
Low-Temperature Growth of High Quality MoS ₂ by Metal-Organic Chemical Vapor Deposition.....	101
Self-Assembly via Defect-Mediated Metal Nanoisland Nucleation on 2D Materials.....	102
Strain Control of Nanocatalyst Synthesis.....	103
Controlled Cracking to Improve Mechanical Stability of RuO ₂ Thin-Film Li-ion Electrodes.....	104
Seeing Superlattices: Imaging Moiré Periods at the Nanoisland-2D Material Interface Using Scanning Transmission Electron Microscopy.....	105
Small-Molecule Assemblies Inspired by Kevlar: Aramid Amphiphile Nanoribbons.....	106

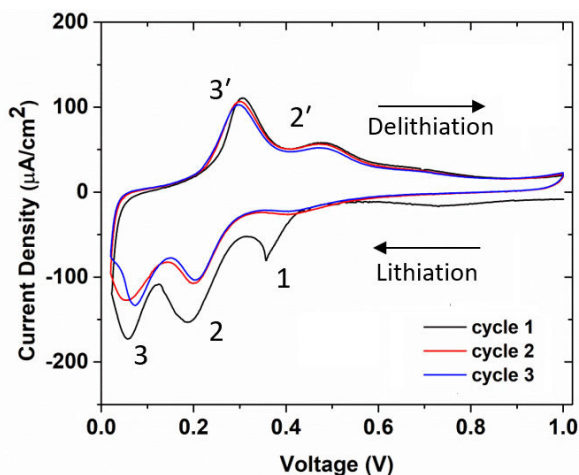
Lithiation Mechanisms of Si and Ge Thin Film Battery Electrodes

J. Miao, B. Wang, C. V. Thompson

Sponsorship: Skolkovo Institute of Science and Technology, SMART

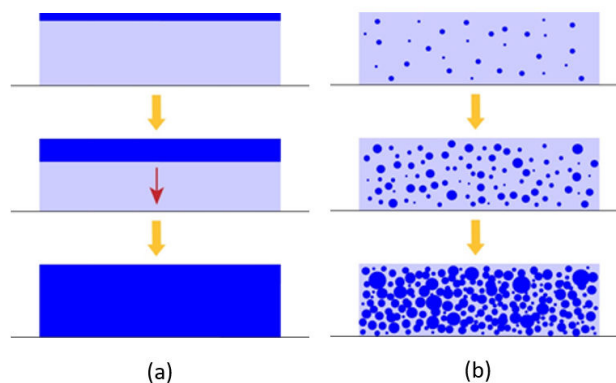
Thin film batteries (TFBs) made using complementary metal-oxide-semiconductor- (CMOS) compatible materials and processes can be integrated with CMOS circuits and energy harvesting and sensing devices to produce low-cost autonomous sensors with small form factors. As part of our research on CMOS-compatible Li-ion TFBs, we are studying Si and Ge films to be used as anode electrodes. While these materials have the highest known charge capacity (8300 mA/cm³ for Si and 7300 mA/cm³ for Ge), they tend to have poor reliability (low cyclability) due to mechanical failures associated with large volume changes. The mechanisms through which lithium is stored in these materials are also poorly understood but are known to be related to poor cyclability. We have carried out mechanistic studies of reversible lithium storage in Si and Ge films using both electrochemical and physical characterization techniques.

Figure 1 shows current-voltage measurements made during the first three lithiation/delithiation cycles of a 315-nm-thick amorphous Si film (a cyclic voltammogram, CV). The current corresponds



▲ Figure 1: CV for the first three cycles of a 315-nm-thick amorphous Si thin film. The current density is related to insertion of Li into Si during lithiation and removal of Li during delithiation. Peaks correspond to phase transitions.

to Li being stored in the electrode (lithiation) or removed (delithiation). Peaks in these curves indicate accelerated charging or discharging associated with phase transitions, all of which are between amorphous phases with different stoichiometries (increasingly Li-rich for lithiation). An irreversible transition is seen in the first cycle (peak 1 in Figure 1), and two reversible transitions are seen in all three and all subsequent cycles (peaks 2-2' and 3-3'). Through new potentiostatic and transmission electron microscopy techniques, we have established that the irreversible transition occurs through propagation of a reaction through the thickness of the film (Figure 2b) and that the reversible transitions occur through an amorphous-to-amorphous nucleation and growth process (Figure 2b), sometimes referred to as a polyamorphous phase transition. In similar experiments on Ge, we have focused on the reversible transition of a Li-rich amorphous phase to a crystalline phase, which also occurs through a nucleation and growth process. These studies have been correlated with the reliability of TFBs.



▲ Figure 2: Schematic illustrations of cross sections of Si films during phase transitions associated with peaks in Figure 1. (a) Irreversible propagation of a sharp interface between two amorphous phases (peak 1). (b) Reversible nucleation and growth transitions between two amorphous phases (peaks 2-2' and 3-3').

FURTHER READING

- J. Miao and C. V. Thompson, "Kinetic Study of the Initial Lithiation of Amorphous Silicon Thin Film Anodes," *J. Electrochem. Soc.*, vol. 165, pp. A650-A656, 2018.
- J. Miao, B. Wang, and C. V. Thompson, "First-order Amorphous-to-Amorphous Phase Transitions During Lithiation of Silicon Thin Films," *Phys. Rev. Materials*, vol. 4, p. 043608, 2020.
- J. Miao, B. Wang, and C. V. Thompson, "Kinetic Study of Lithiation-induced Phase Transitions in Amorphous Germanium Thin Films," *J. Electrochem. Soc.*, vol. 167, p. 090557, 2020.

Gated Nonreciprocal Magnon Transmission from Direction-Dependent Magnetic Damping

J. Han, Y. Fan, B. C. McGoldrick, J. Finley, J. T. Hou, P. Zhang, L. Liu
Sponsorship: NSF, SRC

An important application of magnetic materials in information technology is to provide nonreciprocity, which allows unidirectional signal transmission. A representative device is the two-terminal microwave isolator. A ferromagnet inside naturally breaks the time-reversal symmetry and allows microwave transmission only from port 1 to port 2, while signals from port 2 to port 1 are suppressed. Despite wide applications, these conventional nonreciprocal devices suffer from their bulk volume and the difficulty of being integrated into high-density circuits. Nowadays, new mechanisms that can provide passive and directional isolation of signals are being pursued at sub-micrometer scale. Among various proposals, magnons, the quanta of the collective excitation of magnetic moments, show unique potential due to the tunability and the possibility for on-chip integration. So far, nonreciprocal magnon transmission has been achieved only at resonant conditions with

gigahertz frequency. It is unclear if nonreciprocity can still be observed for magnons with a broad spectrum up to terahertz frequency.

Here we show that using a magnetic gate, one can realize tunable nonreciprocal propagation in spin Hall effect-excited incoherent magnons, whose frequency covers the spectrum from a few gigahertz up to terahertz. We further identify the direction-dependent magnetic damping as the dominant mechanism for the nonreciprocity, which originates from the interlayer dipolar coupling and works both in the ballistic and diffusive regions of magnons. As a natural result of the chiral magnon-magnon coupling, our findings provide a general mechanism for introducing directional magnon transmission and lead to a design of passively gated magnon transistors for applications of information transmission and processing.

Gigahertz Frequency Antiferromagnetic Resonance and Strong Magnon-Magnon Coupling in Layered Crystal CrCl_3

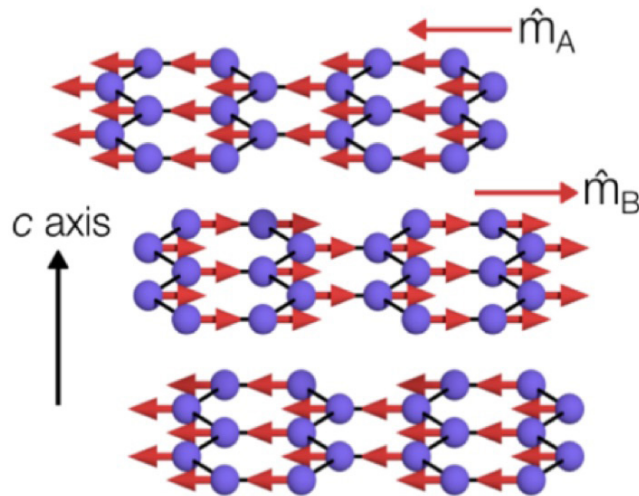
J. T. Hou, D. MacNeill, D. R. Klein, P. Zhang, P. Jarillo-Herrero, L. Liu

Sponsorship: DoE Office of Science, Gordon and Betty Moore Foundation, NSF, NSF GRFP

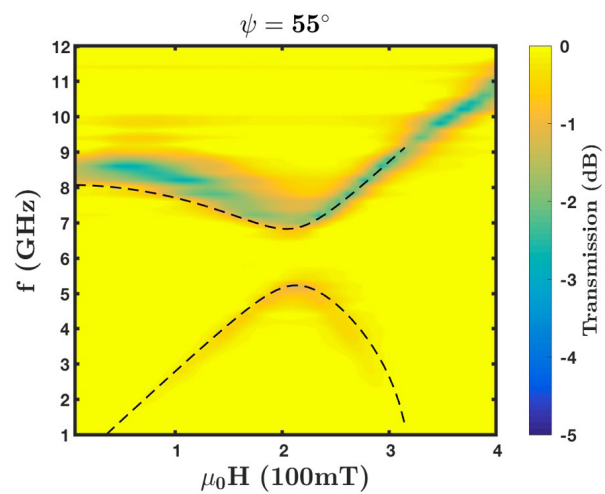
Magnon-magnon hybrid systems have recently been realized between two adjacent magnetic layers, with potential applications to hybrid quantum systems and coherent information processing. Realizing magnon-magnon coupling within a single material requires antiferromagnetic (AFM) or ferrimagnetic materials with magnetic sublattice structures. However, conventional AFM resonance lies in terahertz frequencies, which require specialized techniques to probe.

In this work, we realize strong magnon-magnon coupling within a single material, CrCl_3 . CrCl_3 is a layered van der Waals AFM material, with parallel intralayer alignment and antiparallel interlayer alignment of magnetic moments (Figure 1). Because of weak anisotropy and interlayer magnetic coupling,

we observe both optical and acoustic modes of AFM resonances within the range of typical microwave electronics ($<20\text{GHz}$), in contrast to conventional AFM resonances. By breaking rotational symmetry, we further show that strong magnon-magnon coupling with large tunable gaps can be realized between the two resonant modes (Figure 2). Our results demonstrate strong magnon-magnon coupling within a single material and establish CrCl_3 as a convenient platform for studying AFM dynamics in microwave frequencies. Because CrCl_3 is a van der Waals material that can be cleaved to produce air-stable monolayer thin films, these results open up the possibility to realize magnon-magnon coupling in magnetic van der Waals heterostructures by symmetry engineering.



▲ Figure 1: Magnetic structure of bulk CrCl_3 below the Neel temperature. Blue spheres represent Cr atoms.



▲ Figure 2: Strong magnon-magnon coupling realized with magnetic field applied at a 55° angle with respect to the crystal plane.

FURTHER READING

- D. MacNeill, J. T. Hou, D. R. Klein, P. Zhang, P. Jarillo-Herrero, and L. Liu, *Physical Review Letters*, vol. 123, p. 047204, 2019.

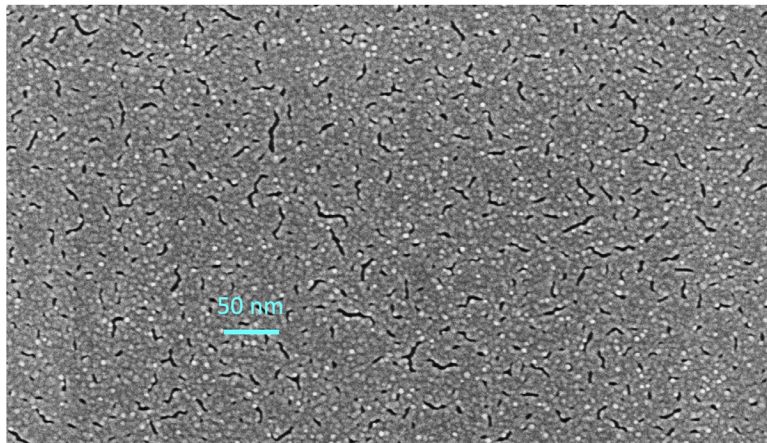
Nanoparticle-Enhanced Microsputtered Gold Thin Films for Low-Cost, Agile Manufacturing of Interconnects

Y. Kornbluth, R. Mathews, L. Paramswaran, L. Racz, L.F. Velásquez-García
Sponsorship: US Air Force

Silicon and gold are ubiquitous in the microelectronics industry—silicon as the cornerstone of semiconductor devices, and gold as a material with unmatched electro-optical properties. However, gold films do not adhere well to silicon or silicon dioxide, necessitating the need for an adhesion layer made of a third material. This need increases complexity and cost. Also, reworking interconnects via traditional (cleanroom) technology poses challenges, e.g., thermal budget, vacuum compatibility.

In this project, we explore microplasma sputtering to implement at low-cost interconnects for agile electronics. We have shown that under proper operational conditions, a microplasma sputterer creates at room temperature and atmospheric pressure dense, highly conductive gold films with a fivefold better adhesion than the state of the art, without using an adhesion layer, annealing, or any other pre/post printing steps. If the gold film is sputtered in an

atmospheric-pressure microsputterer in the presence of a fast-moving jet of air, gold nanoparticles form. The high collisionality of the atmospheric-pressure gas and high energy of the plasma facilitate nanoparticle formation, while the jet carries the nanoparticles to the substrate. The speed of the jet of air determines the size of the nanoparticles. These nanoparticles then act as an adhesion layer to allow a gold film, made of these nanoparticles and individual atoms, to adhere well to a silicon or silicon dioxide substrate. By rastering the printhead over the desired deposition area, we can interweave large nanoparticles and smaller atoms, creating a dense film (Figure 1). This process allows us to optimize adhesion, density, and conductivity simultaneously. Conductivity of the resultant films is also near-bulk (120% of bulk gold—the highest value reported for a room-temperature additive manufacturing method), allowing for their use in microelectronics.



▲ Figure 1: SEM micrograph of microsputtered gold imprint (from Kornbluth et al., *Additive Manufacturing*, vol. 36, p. 101679, Dec. 2020). The film is dense, highly electrically conductive and is made of the agglomeration of nanoparticles created in the plume of a room-temperature, atmospheric pressure microsputterer.

FURTHER READING

- Y. Kornbluth, R. H. Mathews, L. Parameswaran, L. M. Racz, and L. F. Velásquez-García, "Nano-additively Manufactured Gold Thin Films with High Adhesion and Near-bulk Electrical Resistivity via Jet-assisted Nanoparticle-dominated, Room-temperature Microsputtering," *Additive Manufacturing*, vol. 36, p. 101679, Dec. 2020.
- Y. Kornbluth, R. H. Mathews, L. Parameswaran, L. M. Racz, and L. F. Velásquez-García, "Room-temperature, Atmospheric-pressure Microsputtering of Dense, Electrically Conductive, Sub-100 nm Gold Films," *Nanotechnology*, vol. 30, no. 28, p. 285602, Apr. 2019.
- Y. Kornbluth, R. H. Mathews, L. Parameswaran, L. M. Racz, and L. F. Velásquez-García, "Microsputterer with Integrated Ion-drag Focusing for Additive Manufacturing of Thin, Narrow Conductive Lines," *Journal of Physics D – Applied Physics*, vol. 51, no. 16, p. 165603, Apr. 2018.

Large-Scale 2D Perovskite/Transition Metal Dichalcogenide Heterostructure for Photodetector

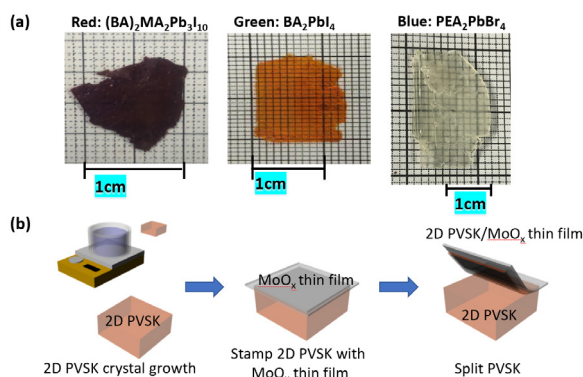
D. Lee, S. Bae, J. Kim
Sponsorship: SUSTECH

Monolayer transition metal dichalcogenides (TMDCs) have been attractive nanomaterials for optoelectronics due to their extremely high quantum efficiency, but their atomically thin thickness prevents them from absorbing sufficient light for optoelectrical applications.

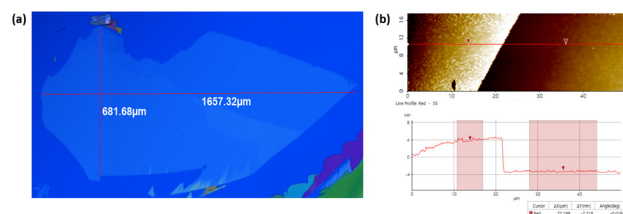
To improve the optoelectrical performance of TMDCs, during the past years, 2D Ruddlesden-Popper perovskites (PVSs)/TMDC heterostructures have been demonstrated. Thanks to their high absorption coefficient, long diffusion length of charge carrier, sharp exciton emission, and high power conversion efficiency, 2D PVSs have been used as an absorption layer for TMDCs. However, 2D PVS/TMDC heterostructures are limited in the micrometer scale,

since 2D PVSs have been fabricated only by the tape-exfoliation method.

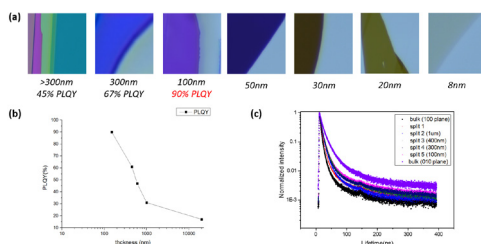
We reported a layer resolved splitting (LRS) technique to isolate multilayer 2D materials into a monolayer in wafer scale in 2018. To improve the scalability of 2D PVSs for large-scale application, in this work, we successfully split micrometer-thick 2D PVSs into nanometer-thick and millimeter-width scale with the LRS technique. We also obtained 90% of photoluminescence quantum yield, which is the world's best record to the best our knowledge. Then we plan to demonstrate large-scale 2D PVS/TMDC heterostructures for photodetectors, which only has been previously demonstrated up to micrometer scale.



▲ Figure 1: (a) Images of as-grown bulk 2D perovskite single crystals (b) schematic of stamping process to split 2D perovskite into atomic layer



▲ Figure 2: (a) Optical image of 8nm-thick and mm-width scale 2D perovskite layers (b) AFM image of split 2D perovskite layer.



▲ Figure 3: (a) Optical images of split 2D perovskite layers with different thickness (b) Photoluminescence quantum yield (PLQY) of 2D perovskite with different thickness (c) Carrier lifetime of 2D perovskite with different thickness.

FURTHER READING

- J. Shim, et al., "Controlled Crack Propagation for Atomic Precision Handling of Wafer-scale Two-dimensional Materials," *Science*, vol. 362.6415 pp. 665-670, 2018.
- U. Erkiş, et al., "Vapor Phase Selective Growth of Two-dimensional Perovskite/WS₂ Heterostructures for Optoelectronic Applications." *ACS Applied Materials & Interfaces*, vol. 11, no. 43, pp. 40503-40511, 2019.
- Q. Wang, et al., "Optoelectronic Properties of a van der Waals WS₂ Monolayer/2D Perovskite Vertical Heterostructure," *ACS Applied Materials & Interfaces*, vol. 12, no. 40, pp. 45235-45242, 2020.

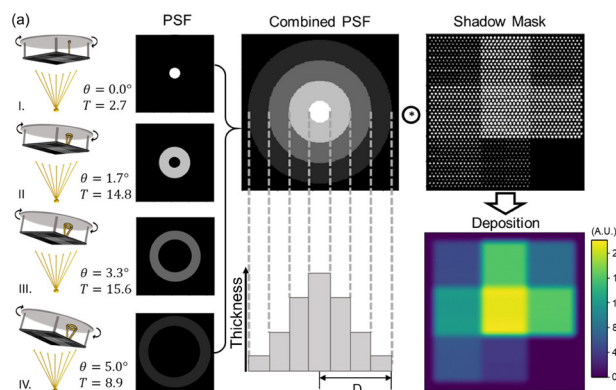
Grayscale Stencil Lithography

X. H. Li, Z. J. Tan, N. Fang
Sponsorship: ExxonMobil

In this work, we demonstrate a new eBeam evaporation method with fixed single stencil shadow mask to generate 2D patterns with spatial thickness variation across wafer-scale substrate. This method outperforms conventional approaches like the iterative photo-lithography-and-lift-off method or grayscale photolithography, due to their limitations of efficiency, material choices, and manufacturing complexity. We applied the method to create a multi-spectral reflective color filter arrays with two layers of variable thickness. It offers a broader design space to achieve a wide color spectrum with simple and efficient fabrication procedures. This method shows potential for scaling up and high-resolution patterning, which could be widely applied in manufacturing for optical imaging, sensing, and computing.

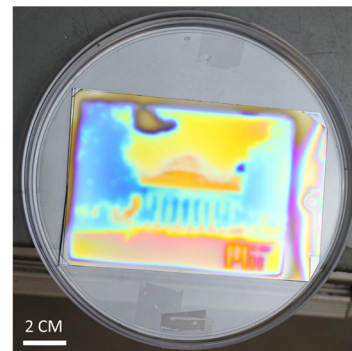
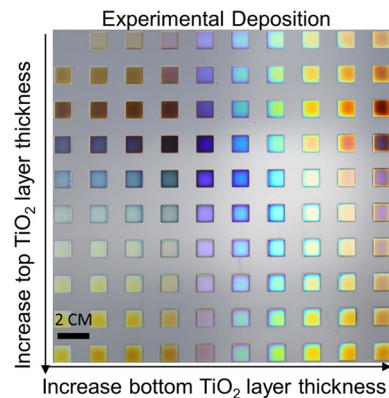
The method takes inspiration from the “pin-hole imaging” in optics to generate the convoluted pattern of the material source and the stencil shadow mask, as shown in Figure 1.

The ejection of materials in the eBeam pockets is analogous to the “light source,” which passes through the pin holes on the shadow masks to finally cast the “image” in terms of deposition thickness. By controlling the deposition dose (T) and the tilting angle (θ) of the substrate, we could create the “point spreading function” (PSF) of the material target passing through the shadow mask, which can create smooth deposition with less than 5-nm surface roughness. As show in Figure 2, we applied this method to create a multi-spectral color filter array and a 2D pattern of the MIT “Dome” to demonstrate the capability of this method for customizable patterning. Higher resolution deposition is also possible by combining the available micro/nano stencil lithography techniques and our grayscale stencil lithography method.



▲ Figure 1: Schematic of PSF control and convoluted deposition of the grayscale stencil lithography method.

► Figure 2: Demonstration of spatially variable thickness deposition for multispectral color filter array and MIT “Dome.”



FURTHER READING

- X. H. Li, Z. J. Tan, and N. Fang, “Grayscale Stencil Lithography for Patterning Multispectral Color Filters,” *Optica*, vol. 7, no. 9, pp. 1154-1161, Sep. 2020.
- K. Du, J. Ding, Y. Liu, I. Wathuthanthri, and C.H. Choi, “Stencil Lithography for Scalable Micro and Nano Manufacturing,” *Micromachines*, vol 8, no. 4, pp. 131-155, Apr. 2017.

Unraveling the Correlation between Raman and Photoluminescence in Monolayer Molybdenum Disulfide through Machine Learning Models

A.-Y. Lu, L. G. Pimenta-Martins, P.-C. Shen, J.-H. Park, Z. Chen, J. Han, J. Kong
Sponsorship: ISN

Two-dimensional (2D) transition metal dichalcogenides (TMDs) with intense and tunable photoluminescence (PL) have opened up new opportunities for optoelectronic and photonic applications such as light-emitting diodes, photodetectors, and single-photon emitters. Among the standard characterization tools for 2D materials, Raman spectroscopy stands out as a fast and non-destructive technique capable of probing materials' crystallinity and perturbations such as doping and strain. However, the correlation between photoluminescence and Raman spectra in monolayer MoS₂ remains elusive due to its highly nonlinear correlation. Here, we systematically explore the correlation between PL signatures and Raman modes through ma-

chine learning models. First, we adopt a convolution neural network, DenseNet, to predict PL by spatial Raman maps with relatively small pixel dimensions but deep channels. Moreover, we apply a gradient boosted trees model (XGBoost) with the Shapley additive explanation (SHAP) to evaluate the impact of individual Raman features in PL behavior, which allows us to further link the strain and doping of monolayer MoS₂ with its PL behavior. Our analytical method unravels the nonlinear correlations of physical or chemical properties for 2D materials and provides the knowledge for tuning and synthesizing 2D semiconductors for high-yield photoluminescence.

FURTHER READING

- Y. Kornbluth, R. H. Mathews, L. Parameswaran, L. M. Racz, and L. F. Velásquez-García, "Room-temperature, Atmospheric-pressure Microsputtering of Dense, Electrically Conductive, Sub-100 nm Gold Films," *Nanotechnology*, vol. 30, no. 28, p. 285602, Apr. 2019.
- Y. Kornbluth, R. H. Mathews, L. Parameswaran, L. M. Racz, and L. F. Velásquez-García, "Microsputterer with Integrated Ion-drag Focusing for Additive Manufacturing of Thin, Narrow Conductive Lines," *Journal of Physics D – Applied Physics*, vol. 51, no. 16, p. 165603, Apr. 2018.

Additively Manufactured Electro spray Ion Thrusters for Cubesats

D. Melo-Máximo, L. F. Velásquez-García

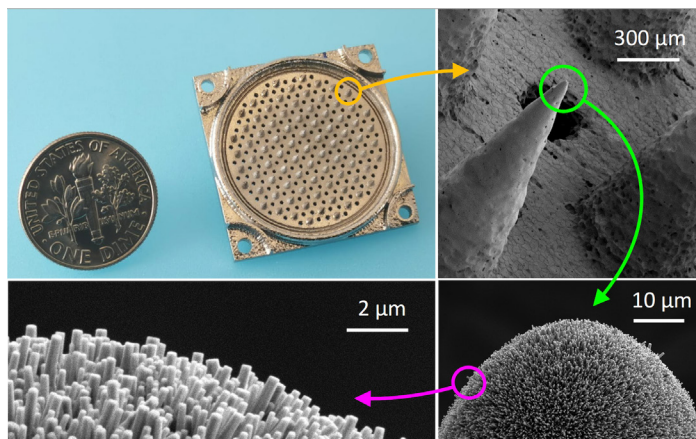
Sponsorship: MIT Portugal, MIT-Tecnológico de Monterrey Nanotechnology Program

Putting satellites in orbit is very expensive: typical rocket launches cost up to hundreds of millions of US dollars, and typical per-kilogram of payload costs are up to tens of thousands of US dollars). Therefore, great interest exists to develop smaller, lighter, and cheaper space satellites with adequate performance. In particular, since the 1990s, research groups across the world have been developing and launching cubesats, i.e., 1-10 Kg, a few L in volume, miniaturized, mission-focused satellites. Multi-material additive manufacturing is of great interest for fabricating cubesats, as it can monolithically create complex, multi-functional objects composed of freeform components made of materials matched to performance.

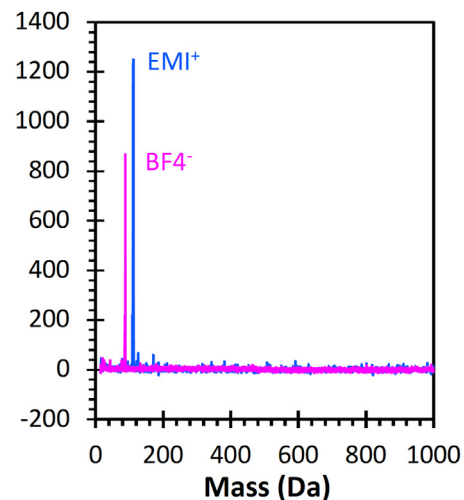
Electrospray engines produce thrust by electrohydrodynamically ejecting charged particles from liquid propellant. Electro spray thrusters are an attractive choice for propelling cubesats because their physics favors miniaturization, e.g., their start-up voltage scales with the square root of the emitter diameter. The thrust of an electro spray emitter is very

low; thus, electro spray engines have large arrays of emitters to greatly boost the thrust they can deliver.

We recently demonstrated the first additively manufactured electro spray engines. Our devices are composed of large arrays of conical emitters coated by a conformal forest of zinc oxide nanowires (ZnONWs) that transport the propellant to the emitter tips (Figure 1). The ZnONWs provide a large hydraulic impedance that regulates and uniformizes the flow across the emitter array, restricting the flow rate per emitter to attain ionic emission. Our devices are also remarkable because, unlike all the other electro spray ionic liquid engines reported in the literature, they emit only ions using the ionic liquid EMI-BF₄ as propellant (Figure 2), which maximizes their specific impulse for a given bias voltage, i.e., they produce more thrust per unit of propellant flow rate. Current work focuses on optimizing device design and fabrication and on developing a multi-electrode stack to control the plume.



▲ Figure 1: From the top left, clockwise: an additively manufactured electro spray array next to a U.S. dime, close-up of emitters, close-up of an emitter tip, close-up of the ZnONW forest.



▲ Figure 2: Mass spectra of emitted plume using EMI-BF₄ as propellant. In both polarities, the plume is composed exclusively of ions.

FURTHER READING

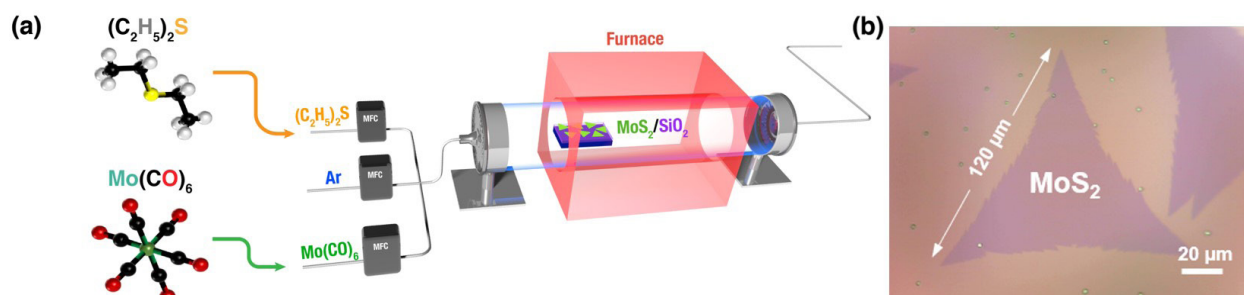
- F. A. Hill, E. V. Heubel, P. P. de Leon, and L. F. Velásquez-García, "High-Throughput Ionic Liquid Ion Sources Using Arrays of Microfabricated Electro spray Emitters with Integrated Extractor Grid and Carbon Nanotube Flow Control Structures," *J. Microelectromech. Syst.*, vol. 23, no. 5, pp. 1237-1248, May 2014.
- D. Olvera-Trejo and L. F. Velásquez-García, "Additively Manufactured MEMS Multiplexed Coaxial Electro spray Sources for High-Throughput, Uniform Generation of Core-Shell Microparticles," *Lab Chip*, vol. 16, no. 21, pp. 4121-4132, Oct. 2016.
- D. V. Melo Máximo and L. F. Velásquez-García, "Additively Manufactured Electrohydrodynamic Ionic Liquid Pure-Ion Sources for Nanosatellite Propulsion," *Additive Manufacturing*, vol. 36, p. 101719, Dec. 2020.

Low-Temperature Growth of High Quality MoS₂ by Metal-Organic Chemical Vapor Deposition

J.-H. Park, A.-Y. Lu, P.-C. Shen, J. Kong
Sponsorship: ARO MURI, NSF

The large-area and high-quality synthesis of molybdenum disulfide (MoS₂) plays an important role in realizing industrial applications of flexible, wearable, and ultimately scaled devices due to its atomically thin thickness, sizable bandgap, and dangling-bond-free interface. However, currently used synthesis of MoS₂ by chemical vapor deposition (CVD) require high temperature and a transfer process, which limits its utilization in device fabrications. In this work, we achieved the direct synthesis of high-quality monolayer MoS₂ by metal-organic chemical vapor deposition (MOCVD) at a low temperature of 320°C by designing the experimental setup for better controlling the flow rate of

the organic precursors. Large single-crystal monolayer MoS₂ with a domain size up to 120 μm can be obtained on SiO₂/Si substrate (Figure 1). Owing to the low substrate temperature, the MOCVD-grown MoS₂ exhibits low impurity doping and nearly unstrained properties on the growth substrate, demonstrating enhanced electronic performance with high electron mobility of 68.3 cm² V⁻¹s⁻¹ at room temperature. In addition, we propose a model to quantitatively analyze the shape change of the MoS₂ flakes grown under different conditions, which provides an insight into the growth mechanism for optimizing growth conditions.



▲ Figure 1: (a) Schematic diagram of the experimental setup of the MOCVD system for MoS₂ growth and (b) Optical image of MoS₂ flake grown on SiO₂/Si substrate at low temperature.

FURTHER READING

- J.-H. Park, A.-Y. Lu, P.-C. Shen, B. G. Shin, H. Wang, N. Mao, R. Xu, S. J. Jung, D. Ham, K. Kern, Y. Han, and J. Kong, "Synthesis of High-Performance Monolayer Molybdenum Disulfide at Low Temperature," *Small Methods*, submitted.
- K. Kang, S. Xie, L. Huang, Y. Han, P. Y. Huang, K. F. Mak, C.-J. Kim, D. Muller, and J. Park, "High-Mobility Three-Atom-Thick Semiconducting Films with Wafer-Scale Homogeneity," *Nature*, vol. 520, pp. 656-660, Apr. 2015.

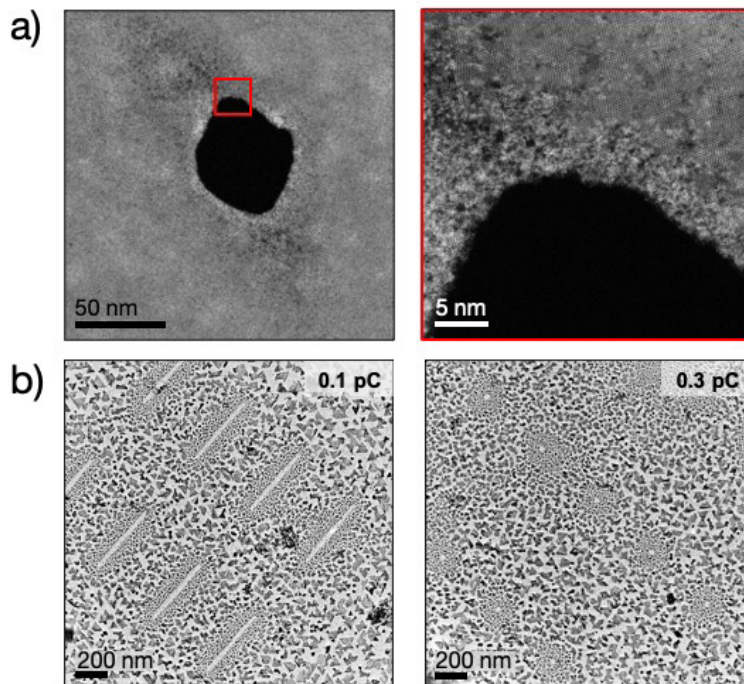
Self-Assembly via Defect-Mediated Metal Nanoisland Nucleation on 2D Materials

K. Reidy, V. Zarubin, Y. Yu, I. Charaev, J. D. Thomsen, F. M. Ross
Sponsors: MIT OGE, Mathworks Engineering, Microscopy Society of America (MSA)

Patterning point defects, nanopores, and nanoribbons can enhance (opto-)electronic properties of two-dimensional (2D) materials. Moreover, metal adatoms and small clusters can nucleate on point defects in 2D materials. This nucleation suggests that defect patterning may be used for templated self-assembly of metal nanoislands on 2D materials, enabling applications in plasmonics and single-photon emission. Focused ion beams (FIBs) are well-suited for patterning 2D materials with nanometer precision and can be used for the controlled creation of point defects and sub-10-nm features. For applications that require control of the locations of metal islands, the optimization of FIB irradiation parameters for metal nucleation is crucial.

In this work, we study the structural changes that arise from FIB patterning of suspended 2D materials and the influence of patterning on metal nucleation and growth. We calibrate the irradiation parameters

to achieve patterning with minimal damage to the 2D material, and the features are characterized by scanning transmission electron microscopy (STEM) (Figure 1a). Using these patterned 2D materials, we study the extent to which the defects, ion species, dose rate, and sample thickness affect the nucleation and growth of metals. Figure 1 shows representative results after the deposition of Au. At high deposition amounts, Au forms small islands around graphene nanopores, indicative of defect-mediated nucleation (Figure 1b). The templating and nucleation control presented here can be generalized to anchor other materials on 2D materials, such as Si and Ge via chemical vapor deposition or other metals via thermal and e-beam evaporation. This strategy opens routes towards the directed self-assembly of semiconducting and metallic nanoislands on 2D materials with optimized charge transfer and strong light-matter interactions.



◀ Figure 1: STEM characterization of defects and deposition on defective 2D materials. a) Defect in monolayer MoS₂ irradiated with He⁺ in the Helium Ion Microscope showing 50-nm hole created by ~600,000 He⁺ ions per spot irradiation. Right panel is a high magnification view of the amorphized region around a hole. b) Nucleation of Au islands on irradiated graphene flakes patterned with lines (left) and points (right), where Au appears as dark areas. Inset shows dose used.

FURTHER READING

- K. Reidy, G. Varnavides, J. D. Thomsen, A. Kumar, T. Pham, A.M. Blackburn, P. Anikeeva, P. Narang, J.M. LeBeau, F.M. Ross, "Direct Imaging and Electronic Structure Modulation of Moiré Superlattices at the 2D/3D Interface," *Nat. Comm.* vol. 12, pp. 1290, 2021, DOI:<https://doi.org/10.1038/s41467-021-21363-5>.
- J. Thomsen, K. Reidy, T. Pham, and F. M. Ross, "Nucleation and Growth of Metal Films and Nanocrystals on Two-dimensional Materials," *Microscopy and Microanalysis*, vol. 26, no. S2, pp. 1094-1096, 2020, DOI:10.1017/S1431927620016931.

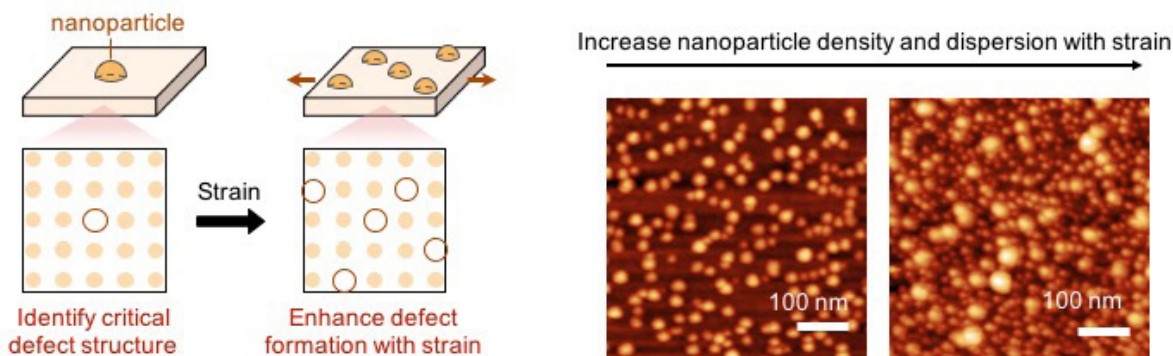
Strain Control of Nanocatalyst Synthesis

J. Wang, B. Yildiz
Sponsorship: Exelon Corporation

A central theme in renewable energy technologies today is designing nanostructured catalysts for desired reactions. Exsolution generates stable and catalytically active metal nanoparticles via phase precipitation out of a host oxide. Unlike traditional nanoparticle infiltration techniques, the nanoparticle catalysts from exsolution are anchored in the parent oxide. This strong metal-oxide interaction makes the exsolved nanoparticles more resistant against particle agglomeration than the infiltrated ones. While exsolution is an exciting and promising pathway for generating stable oxide supported nanoparticles, rational control over the exsolved particles has yet to be achieved. In particular, controlling the size and density of the exsolved nanoparticles remains a big challenge.

In this work, we propose point defect formation in the oxide lattice to be the fundamental knob to control exsolution and demonstrate this approach in epitaxial $\text{La}_{0.6}\text{Sr}_{0.4}\text{FeO}_3$ (LSF) thin films. By combining in-

situ surface characterization and ab-initio defect modeling, we show oxygen vacancy and Schottky defects to be the primary point defects formed upon FeO exsolution. Lattice strain tunes the formation energy, and thus the abundance of these defects, and alters the amount and size of the resulting exsolution particles. As a result, the tensile strained LSF with a facile formation of these critical point defects results in a higher FeO metal concentration, a larger density of nanoparticles, and reduced particle size at its surfaces. These observations highlight the critical role of point defects in controlling the size and density of the exsolved nanoparticles on the perovskite surface. The strain-controlled synthesis of nanocatalysts can benefit a wide range of applications in clean energy conversion and fuels generation such as solid oxide cells (SOCs), chemical looping (CL), and ceramic membrane reactors (CMRs).



▲ Figure 1: Schematics and atomic force microscopy images showing lattice strain can facilitate nanoparticle synthesis by tailoring point defect formation in the host oxide.

FURTHER READING

- J. Wang, B. Yildiz et al., "Tuning Point Defects by Strain Modulates Nanoparticle Exsolution on Perovskite Oxides," under review.

Controlled Cracking to Improve Mechanical Stability of RuO₂ Thin-Film Li-ion Electrodes

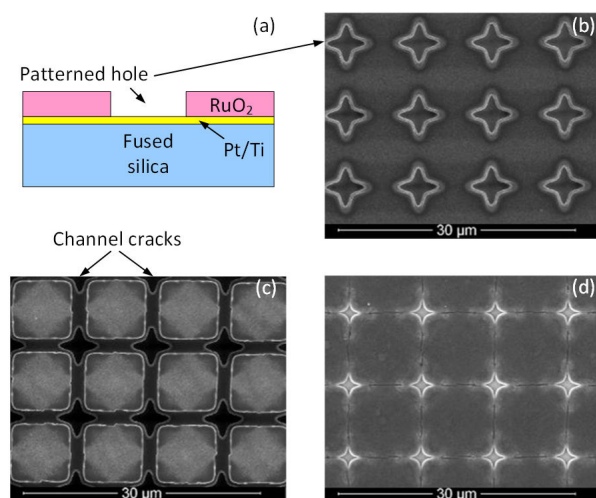
L. Xu, C. V. Thompson
Sponsorship: SMART

Thin film Li-ion batteries are of interest for low-cost autonomous sensors. We have investigated high-performance electrode materials, such as Si and Ge for anodes and RuO₂ for cathodes, that can reversibly store high concentrations of Li. RuO₂ is of particular interest as a cathode material because of its ability to reversibly store high concentrations of Li without requiring high-temperature processing, unlike conventional cathode materials. While high Li capacities are beneficial for high energy density, high Li concentrations lead to large volume changes, which can lead to mechanical degradation during battery cycling. In particular, removal of Li (delithiation) leads to tensile stresses that can cause cracking and delamination of electrodes, which can severely limit the number of times that batteries can be charged and discharged.

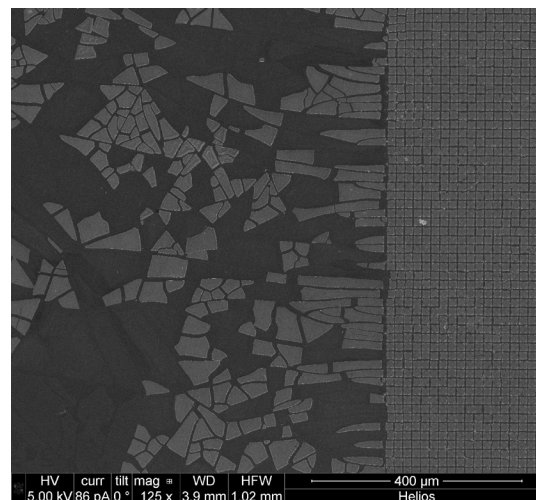
Motivated by the finding that patterned small patches of Si demonstrated higher mechanical stability compared to continuous films, patterned arrays of holes with stress-raising corners were fabricated within sputtered RuO₂ thin films (Figures 1a and b). After

lithiation and delithiation, channel cracks form along the directions defined by the hole array (Figure 1c). We found that this method for controlled crack formation led to increased mechanical stability, as no delamination occurred within the patterned area (Figure 2, right side), while severe delamination occurred in the unpatterned areas (Figure 2, left side). These results may occur because the formation of the controlled crack array dissipates the strain energy that would otherwise drive delamination.

It was further discovered that the formation of cracks was reversible. After re-lithiation, the RuO₂ patches expanded, and the channel cracks closed again (Figure 1d). The sizes of the channel cracks were controlled by the state of charge of the film. In addition to use for mechanical stabilization of thin film electrodes, this process has potential application for creation of channel networks with electrochemically modulated channel sizes, which might be of use in microfluidic devices.



▲ Figure 1: (a) Schematic cross-section and (b) top-view SEM image of a patterned RuO₂ film; (c) channel cracks formed after lithiation and delithiation and (d) channel cracks closed after re-lithiation.



▲ Figure 2: Comparison of unpatterned RuO₂ film (left side) and patterned film (right side) after cycling.

FURTHER READING

- D. Perego, J. S. T. Heng, X. Wang, Y. Shao-Horn, and C. V. Thompson, "High-performance Polycrystalline RuO_x Cathodes for Thin Film Li-ion Batteries," *Electrochim. Acta*, vol. 283, pp. 228–233, 2018.
- L. Xu and C. V. Thompson, "Mechanisms of the Cyclic (de)lithiation of RuO₂," *J. Mater. Chem. A*, vol. 8, pp. 21872–21881, 2020.

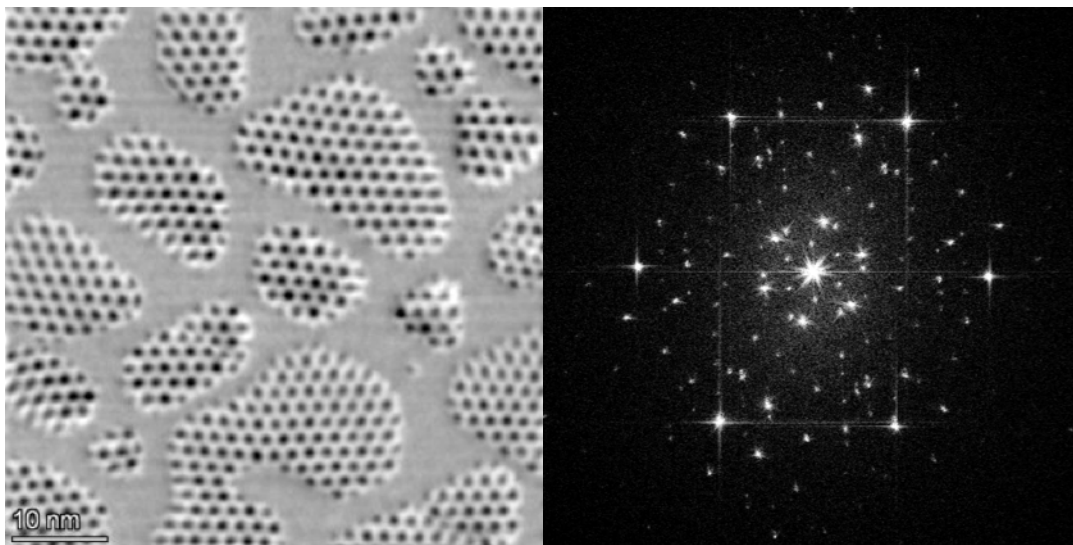
Seeing Superlattices: Imaging Moiré Periods at the Nanoisland-2D Material Interface Using Scanning Transmission Electron Microscopy

K. Reidy, G. Varnavides, J. Dahl Thomsen, A. Kumar, T. Pham, A. M. Blackburn, P. Anikeeva, P. Narang, J.M. LeBeau, F. M. Ross

Sponsorship: MIT MathWorks Engineering, MIT OGE, Office of Naval Research (ONR)

Opportunities are emerging to combine van der Waals (2D) materials with (3D) metals /semiconductors to explore fundamental charge-transport phenomena at their interfaces and exploit them for devices. Recent advances in scanning transmission electron microscopy (STEM) allow detailed analysis of atomic structure, properties, and ordering at these interfaces. We use 4D STEM and integrated differential phase contrast

(iDPC) to directly image moiré periodicities arising from epitaxial growth of nanoislands on 2D materials in ultra-high vacuum. Our research explores the role of emerging microscopy techniques in unveiling the alignment and ordering of moiré superlattices and the implications of moiré periodicities for the properties of 2D/3D junctions.



▲ Figure 1: Characterization of 2D/3D moiré superlattices: a) Integrated differential phase contrast (iDPC) STEM image of Au on MoS2 showcasing the moiré cells. b) Fast Fourier transform (FFT) of atomic resolution high-resolution TEM image of the Au on MoS2 showing $1/3\{422\}$ reflection and visible moiré periodicities around the central spot. Illustrative yellow dots represent frequencies from Au crystal planes, while purple represent frequencies from MoS2 crystal planes. Scale bar, 0.5 \AA^{-1}

FURTHER READING

- K. Reidy, et al., "Direct Imaging and Electronic Structure Modulation of Moiré Superlattices at the 2D/3D Interface," *Nat. Comm.* vol. 12, pp. 1290, 2021, DOI:<https://doi.org/10.1038/s41467-021-21363-5>

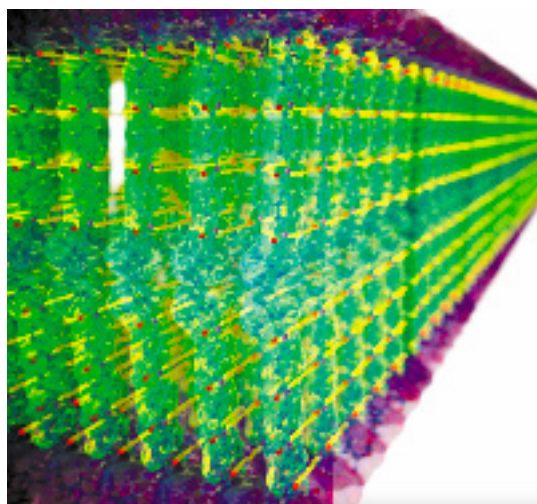
Small-Molecule Assemblies Inspired by Kevlar: Aramid Amphiphile Nanoribbons

T. Christoff-Tempesta, Y. Cho, D.-Y. Kim, J.H. Ortony

Sponsorship: NSF, J-WAFS, Professor Amar G. Bose Research Grant Program

Small-molecule self-assembly offers a powerful bottom-up approach to producing nanostructures with high surface areas, tunable surfaces, and defined internal order. Historically, the dynamic nature of these systems has limited their use to specific cases, especially biomedical applications, in solvated environments. Here, we present a self-assembling small-molecule platform, the aramid amphiphile (AA), which overcomes these dynamic limitations. AAs incorporate a Kevlar-inspired domain within each molecule to produce strong interactions between molecules. We ob-

serve that AAs spontaneously form nanoribbons when added to water with aspect-ratios exceeding 4000:1. Robust internal interactions suppress the ability of AAs to move between assemblies and result in nanoribbons with mechanical properties rivaling silk. We harness this stability to extend small-molecule assemblies to the solid-state for the first time, forming macroscopic threads that are easily handled and support 200 times their weight when dried. The AA platform offers a novel route to use small-molecule self-assembly to achieve aligned nanoscale materials in the solid-state



▲ Figure 1: Illustration of a nanoribbon constructed from the spontaneous self-assembly of aramid amphiphiles in water, with strong hydrogen bonding interactions between molecules shown in yellow.

FURTHER READING

- T. Christoff-Tempesta, Y. Cho, D.-Y. Kim, M. Geri, G. Lamour, A.J. Lew, X. Zuo, W.R. Lindemann, and J.H. Ortony, "Self-assembly of Aramid Amphiphiles into Ultra-stable Nanoribbons and Aligned Nanoribbon Threads," *Nature Nanotechnology*, vol. 16, pp. 447-454, January 2021
- T. Christoff-Tempesta, D.-Y. Kim, G. Lamour, X. Zuo, K.-H. Ryu, and J.H. Ortony, "Morphological Transitions of a Photoswitchable Aramid Amphiphile Nanostructure," *Nano Letters*, vol. 21, pp. 2912-2918, March 2021
- T. Christoff-Tempesta and J.H. Ortony, "Aramid Amphiphile Nanoribbons for the Remediation of Lead from Contaminated Water," *Environmental Science: Nano*, May 2021

Photonics and Optoelectronics

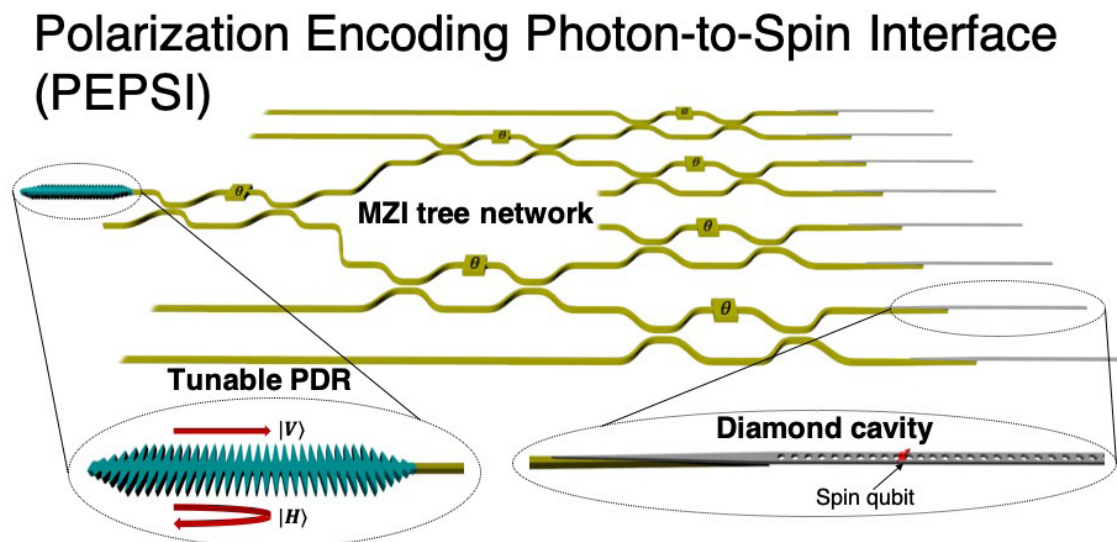
A Polarization Encoded Photon-to-Spin Interface.....	108
Reliability of AlInGaP-on-Si Light Emitting Diodes.....	109
Enhancing SiN Waveguide Optical Nonlinearity via Hybrid Gallium Sulfide Integration.....	110
Waveguide-Integrated Mid-Infrared Photodetection using Graphene on a Scalable Chalco-genide Glass Platform	111
Imaging Transparent Objects through Dynamic scattering Media Using Recurrent Neural Networks	112
Field-Based Design of a Resonant Dielectric Antenna for Coherent Spin-Photon Interfaces	113
Strategies for High-Performance Solid-State Photon Upconversion Based on Triplet Exciton Annihilation.....	114
Magnet Field-switchable Laser via Optical Pumping of Rubrene	115
Multiplexed Raman Sensors using Swept-Source Excitation	116
Hafnia-Filled Photonic Crystal Emitters for Mesoscale Thermophotovoltaic Generators.....	117
High-performance Non-mechanically-tunable Meta-lens.....	118
GaN μ LEDs for Microsystem Optical Communications	119
Large-area Optical Metasurface Fabrication Using Nanostencil Lithography.....	120
The Effect of O:N Ratio in a HfOxNy Interlayer on Triplet Energy Transfer in Singlet-fission-sensitized Silicon.....	121
LION: Learning to Invert 3D Objects by Neural Networks	122
Light Sources and Single Photon Detectors in Bulk CMOS	123
Inference of Process Variations in Silicon Photonics from Characterization Measurements.....	124
Integrated Photonics and Electronics for Chip-Scale Control of Trapped Ions	125

A Polarization-Encoded Photon-to-Spin Interface

K. C. Chen, E. Bersin, D. Englund
Sponsorship: NSF, U.S. Army Research Laboratory

The central goal of quantum communication is to deliver quantum information in a way that is resilient against eavesdropping. One notable approach is the measurement-device-independent quantum key distribution (MDI-QKD) protocol, in which a secret key is shared between two parties connected by quantum and classical channels. Essential to this architecture, however, is the ability to faithfully transfer quantum states between two distant qubits. Here, we propose an integrated photonics device for mapping qubits encoded

in the polarization of a photon onto the spin state of a cavity-coupled artificial atom: a “polarization-encoded photon-to-spin interface” (PEPSI). We perform theoretical analysis of the state fidelity’s dependence on the device’s polarization extinction ratio and atom-cavity cooperativity. Furthermore, we explore the rate-fidelity trade-off through analytical and numerical models. In simulation, we show that our design enables efficient, high-fidelity photon-to-spin mapping.



▲ Figure 1: Polarization encoding photon-to-spin interface (PEPSI) consisted of a polarization-selective photonic crystal mirror, a Mach-Zehnder interferometer (MZI) tree network, and an array of integrated diamond nanophotonic cavities in a photonic integrated circuit (PIC). The system includes active phase shifters that permit arbitrary spatial routing of single photons.

FURTHER READING:

- H.-K. Lo, M. Curty, and B. Qi, “Measurement-Device-Independent Quantum Key Distribution,” *Phys. Rev. Lett.* 108, 130503, 2012.
- S. L. Braunstein and S. Pirandola, “Side-Channel-Free Quantum Key Distribution,” *Phys. Rev. Lett.* 108, 130502, 2012.

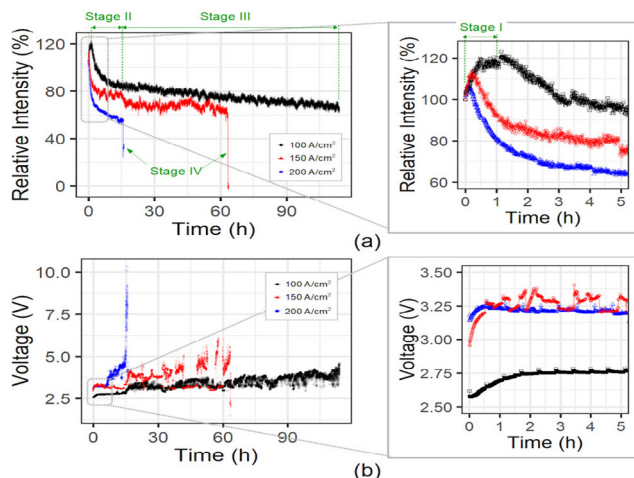
Reliability of AlInGaP-on-Si Light-Emitting Diodes

W. A. Sasangka, Y. Gao, K. H. Lee, B. Wang, C. L. Gan, C. V. Thompson
Sponsorship: SMART

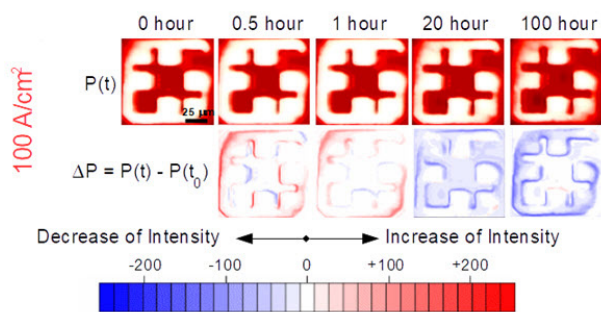
Micro-sized light-emitting diodes (μ LEDs) are emerging candidates for next-generation microdisplays. To achieve high resolution, it is preferable to integrate red, green, and blue self-emissive LEDs with a Si-complementary metal-oxide-semiconductor (CMOS) driver within a single die using a monolithic CMOS-compatible process. Therefore, fabrication of AlInGaP (for red emission) and InGaN (for blue and green emission) LEDs directly on Si substrates is of great interest.

We have reported on the reliability of InGaN on Si LEDs in previous years. Similar to InGaN on Si, the mismatch in lattice constant between AlInGaP and Si is large, so it is very challenging to grow high-quality AlInGaP on Si. AlInGaP layers on germanium-on-insulator (GOI) on Si substrates with a threading dislocation density of $\sim 1.2 \times 10^{-6} \text{ cm}^{-2}$ have recently been made using wafer bonding and layer transfer techniques.

We have conducted constant current stressing of AlInGaP-on-Si LEDs made using this process by measuring the light intensity over time. Four stages of degradation of the light emission were observed (Figure 1(a)), and the degradation was seen to be non-uniform across the devices (Figure 2). The rate and degree of degradation are seen to be strongly dependent on the stressing current. The initial increase of light emission in stage I is due to the carbonization of organic hydrocarbon residues. These carbonized residues enhance current spreading and therefore increase the light emission. The stage II and III degradation is caused by the oxidation of the top C-doped p-GaAs layer by organic residues. No structural degradation is observed in the multiple quantum well layers. Finally, as the oxidation increases the contact resistance, the applied voltage also increases to keep the stressing current constant, leading to the avalanche breakdown of the contact, which is indicated as stage IV in Figure 1.



▲ Figure 1: Optical and electrical properties of LEDs stressed at different current densities: (a) Relative optical intensity vs. time. (b) Applied voltage vs. time.



▲ Figure 2: Spatial distribution of light intensity of LED stressed at 100 A/cm^2 . $P(t)$ is a snap-shot taken at a time t during stressing. ΔP is the difference of snapshot at time t with initial snapshot at $t = 0$.

FURTHER READING

- Y. Wang, B. Wang, W. A. Sasangka, S. Bao, Y. Zhang, H. V. Demir, J. Michel, K. E. K. Lee, et al., "High-performance AlGaInP Light-emitting Diodes Integrated on Silicon through a Superior Quality Germanium-on-insulator," *Photon. Res.*, vol. 6, pp. 290-295, 2018.
- R. I. Made, G. Yu, G. J. Syaranamual, W. A. Sasangka, L. Zhang, X. S. Nguyen, Y. Y. Tay, J. S. Herrin, et al., "Characterization of Defects Generated During Constant Current InGaN-on-Silicon LED Operation," *Microelectronics Reliability*, vol. 76-77, pp. 561, 2017.

Enhancing SiN Waveguide Optical Nonlinearity via Hybrid Gallium Sulfide Integration

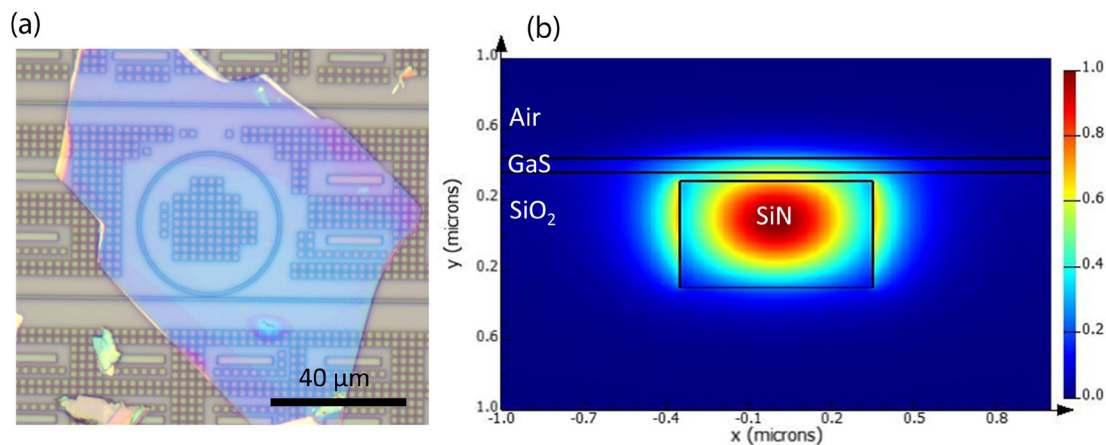
S. Deckoff-Jones, V. Pelgrin, J. Zhang, C. Lafforgue, L. Deniel, S. Guerber, R. Ribeiro-Palau, F. Boeuf, C. Alonso-Ramos, L. Vivien, J. Hu, S. Serna

Sponsorship: NSF Graduate Research Fellowship Program, Chateaubriand Fellowship

Silicon nitride (SiN) has become an increasingly prevalent material platform for integrated photonic circuits. SiN enables low-loss waveguides, and it is transparent in both visible and near-infrared (0.25 – 4.3 μm).

In spite of its small nonlinear index, SiN has been a particularly popular platform for chip-based nonlinear photonic applications, such as supercontinuum generation and frequency combs. However, if SiN's nonlinear index could be increased, the intensity threshold for these useful nonlinear processes could be further reduced. The group-III monochalcogenides (MX, M = Ga, In; X = S, Se, Te) are a class of layered van der Waals materials with strong second- and third-order optical nonlinearities. Gallium sulfide (GaS) in particular has a bulk bandgap of 2.5 eV, large enough to make multiphoton absorption at telecom wavelengths negligible. In this work, we create hybrid waveguides that benefit from the low-loss processing of SiN and the large nonlinear index of the group-III monochalcogenides.

Mechanically exfoliated GaS crystals are transferred onto planarized SiN microring resonators. Figure 1a shows an optical microscope image of a uniform GaS flake fully covering a microring resonator and its coupling region. As the simulated optical TE mode profile in Figure 1b shows, due to the large refractive index (2.6) of GaS, the mode from the SiN core is drawn into GaS. To characterize the nonlinear properties of our hybrid waveguide structures, we measure all-optical cross-wavelength modulation in the microring resonator. We measure enhanced all-optical modulation from the GaS up to 10 MHz (limited by equipment) and measure its nonlinear index to be 10 times larger than that of SiN. This work shows the potential for future incorporation of the group-III monochalcogenides in hybrid waveguides for enhanced optical nonlinearities.



▲ Figure 1: (a) Optical micrograph of SiN microring resonator with mechanically exfoliated GaS flake. (b) Simulated TE mode profile in SiN/GaS hybrid waveguide.

FURTHER READING

- S. Deckoff-Jones, V. Pelgrin, J. Zhang, C. Lafforgue, L. Deniel, S. Guerber, R. Ribeiro-Palau, F. Boeuf, C. Alonso-Ramos, L. Vivien, J. Hu, S. Serna, "Enhancing SiN Waveguide Optical Nonlinearity via Hybrid 2D Material Integration," *J. Opt.* vol. 23, p. 025802, 2021.
- S. Deckoff-Jones, J. Zhang, C. E. Petoukhoff, M. K. L. Man, S. Lei, R. Vajtai, P. M. Ajayan, D. Talbayev, J. Madéo, and K. M. Dani, "Observing the Interplay Between Surface and Bulk Optical Nonlinearities in Thin van der Waals Crystals," *Sci. Rep.* vol. 6, p. 22620, 2016.

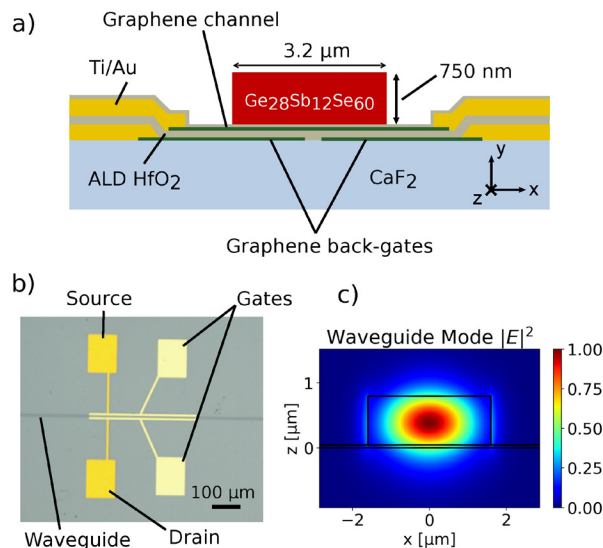
Waveguide-Integrated Mid-Infrared Photodetection Using Graphene on a Scalable Chalcogenide Glass Platform

J. Goldstein, H. Lin, S. Deckoff-Jones, M. Hempel, A.-Y. Lu, J. Kong, J. Hu, D. Englund

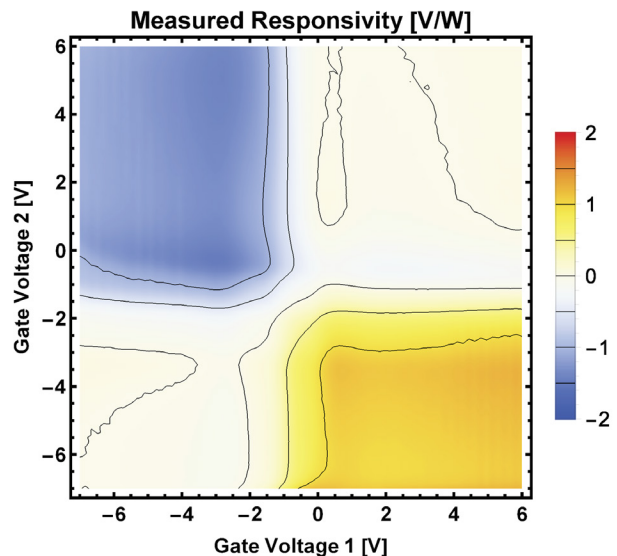
Sponsorship: MIT Institute for Soldier Nanotechnologies Army University-Affiliated Research Center

The development of compact and fieldable mid-infrared (IR) spectroscopy devices represents a critical challenge for distributed sensing with applications from gas leak detection to environmental monitoring. Greenhouse gases in particular represent an opportunity for IR gas sensing technology, as many of them are relatively inert and cannot be detected by chemical means. Recent work has focused on mid-IR photonic integrated circuit (PIC) sensing platforms and waveguide-integrated mid-IR light sources and detectors based on semiconductors such as PbTe, black phosphorus, and tellurene. However, material bandgaps and reliance on SiO₂ substrates limit operation to wavelengths $\lambda < 4 \mu\text{m}$, whereas the main absorption peaks of the most potent

greenhouse gases occur at longer wavelengths. Here we overcome these challenges with a chalcogenide glass-on-CaF₂ PIC architecture incorporating split-gate photothermoelectric graphene photodetectors, shown in Figure 1. Figure 2 plots the photovoltage map of our device, with a maximum responsivity of 1.5 V/W. Our design extends operation to $\lambda = 5.2 \mu\text{m}$ with a Johnson noise-limited noise-equivalent power of 1.1 nW/Hz^{1/2} with no fall-off in photoresponse up to $f_{3\text{dB}} = 1 \text{ MHz}$ and a predicted 3-dB bandwidth of $f_{3\text{dB}} > 1 \text{ GHz}$. This mid-IR PIC platform readily extends to longer wavelengths and opens the door to applications from distributed gas sensing and portable dual comb spectroscopy to weather-resilient free space optical communications.



▲ Figure 1: a) Illustration of the device's cross section perpendicular to the waveguide axis. The optical mode supported by the Ge₂₈Sb₁₂Se₆₀ waveguide evanescently couples to and is absorbed by the graphene channel, which is gated by two graphene back-gates to induce a p-n junction. b) Optical image of the device depicting source, drain, and gate contact pads. c) Depiction of the optical guided mode at $\lambda = 5.2 \mu\text{m}$.



▲ Figure 2: Measured responsivity map of our device as a function of the voltages applied to the two back-gates. The photoresponse pattern indicates a photothermoelectric response mechanism and is qualitatively consistent with the behavior predicted by our device model.

FURTHER READING

- A. Yadav and A. M. Agarwal, "Integrated Photonic Materials for the Mid-Infrared," *International Journal of Applied Glass Science*, vol. 11, pp. 491-510, 2020.

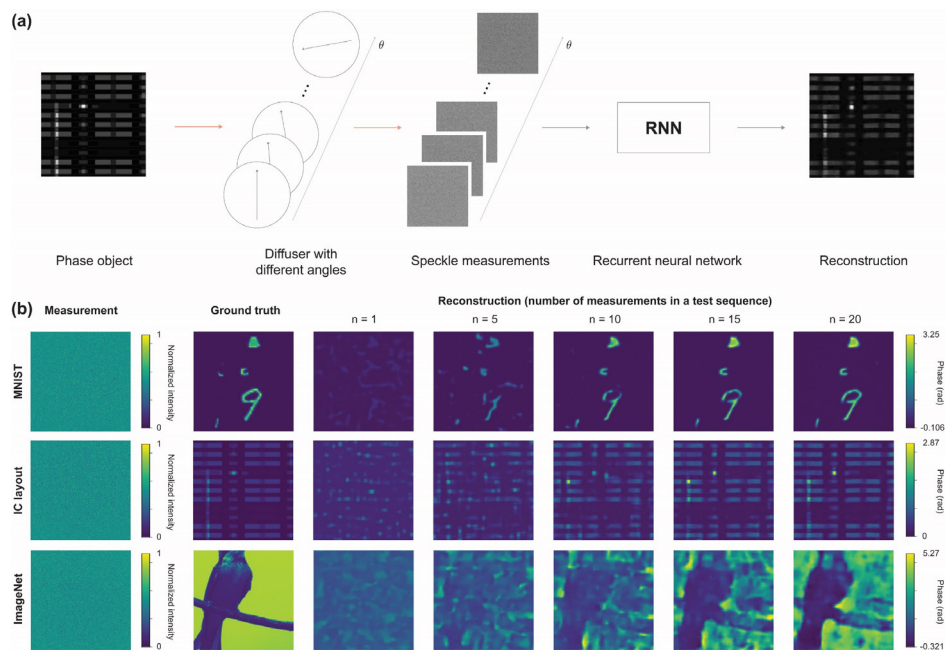
Imaging Transparent Objects through Dynamic Scattering Media Using Recurrent Neural Networks

I. Kang, S. Pang, Q. Zhang, N. Fang, G. Barbastathis

Sponsorship: Intelligence Advanced Research Projects Agency, Korea Foundation for Advanced Studies

Transparent objects in biological imaging and X-ray imaging are imaged by solving inverse problems based on their diffraction intensity patterns. However, the scattering process induced by their complex interiors complicates inverse problems with a severity depending on the statistics of the refractive index gradient and contrast profiles. Recently, static neural networks were used to retrieve original information from the scattering. Here, we propose a novel dynamical machine learning approach to image phase objects through dynamic diffusers. The motivation of this study is to accommodate the input with spatiotemporal dynamics, such as a temporal recording of time-varying scattering profiles. This dynamical machine learning architecture

is adopted to strengthen and exploit the correlation among adjacent scattering patterns during the training and testing processes. To impart dynamics, we propose a simplified dynamical model as follows. We use the on-axis rotation of a diffuser and utilize multiple speckle measurements from different angles to form a sequence of images for training. Our recurrent neural network (RNN) architecture effectively discards any redundancies and enhances/filters out the static pattern, that is, the quantitative phase information of transparent objects. This method is also applicable to other imaging applications that involve any other spatiotemporal dynamics.



▲ Figure 1: (a) Collimated beam illuminates a phase object, and the diffracted optical field is strongly scattered by a diffuser, which is rotated on-axis for several different angles. For each angle of rotation, a camera records speckle measurements; they are processed by our proposed RNN architecture, hence the reconstruction. (b) Seen angles of the rotation with unseen phase objects. Qualitatively shown are the progressions of reconstructions according to the number of measurements in a test sequence (n) for three different priors.

FURTHER READING

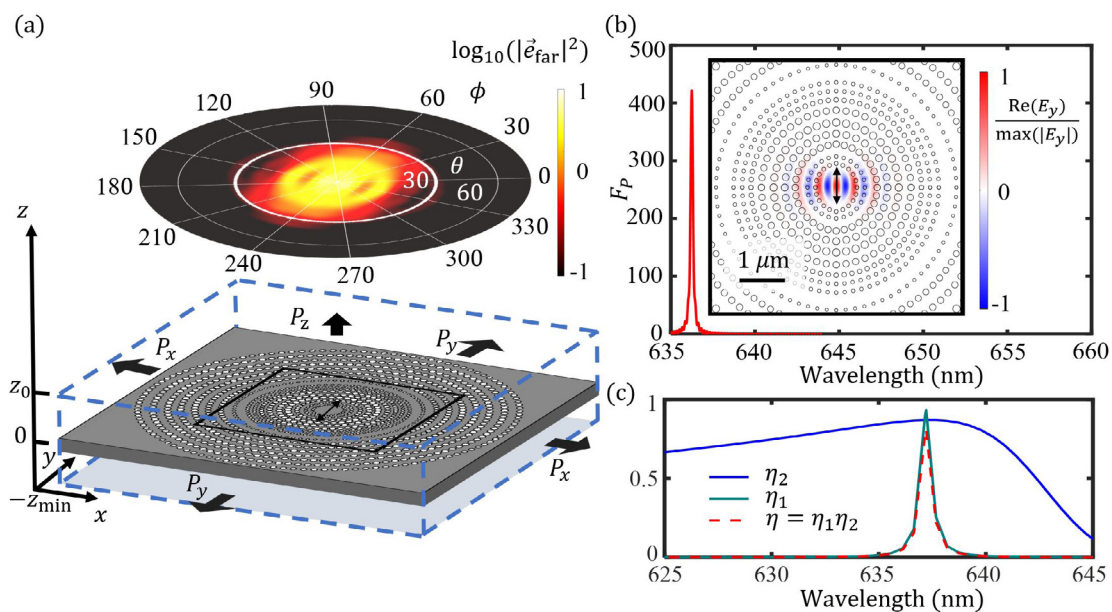
- S. Li, M. Deng, J. Lee, A. Sinha, and G. Barbastathis, "Imaging Through Glass Diffusers Using Densely Connected Convolutional Networks," *Optica*, vol. 5, no. 7, pp. 803-813, 2018.
- Y. Li, Y. Xue, and L. Tian, "Deep Speckle Correlation: a Deep Learning Approach Toward Scalable Imaging Through Scattering Media," *Optica*, vol. 5, no. 10, pp. 1181-1190, 2018.

Field-Based Design of a Resonant Dielectric Antenna for Coherent Spin-Photon Interfaces

L. Li, H. Choi, M. Heuck, D. Englund
Sponsorship: MITRE, NSF

We propose a field-based design for dielectric antennas to interface diamond color centers in dielectric membranes with a Gaussian propagating far field. This antenna design enables an efficient spin-photon interface with a Purcell factor exceeding 400 and a 93% mode overlap to a 0.4 numerical aperture far-field Gaussian mode. The antenna design with the back reflector is ro-

bust to fabrication imperfections, such as variations in the dimensions of the dielectric perturbations and the emitter dipole's location. The field-based dielectric antenna design provides an efficient free-space interface to closely packed arrays of quantum memories for multiplexed quantum repeaters, arrayed quantum sensors, and modular quantum computers.



▲ Figure 1: (a) Illustration of the dielectric antenna structure, along with a far-field distribution plot. (b) Purcell factor spectrum of the antenna structure. The inset is a linear-scale plot of normalized electric field corresponding to the black square region in (a). (c) The spin-photon interface efficiency η , spin-antenna interface efficiency η_1 , and antenna efficiency η_2 as the function of wavelength of the antenna structure in (a).

FURTHER READING:

- L. Li, H. Choi, M. Heuck, and D. Englund, "Field-based Design of a Resonant Dielectric Antenna for Coherent Spin-photon Interfaces," *Opt. Express* 29, 16469 (2021).
- L. Li, H. Choi, M. Heuck, and D. Englund, "Field-based Design of a Resonant Dielectric Antenna for Coherent Spin-photon Interfaces," 2021 *Conference on Lasers and Electro-Optics (CLEO)*, 2021, pp. 1-2.

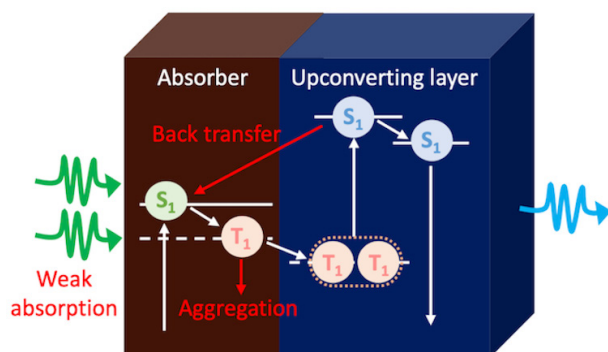
Strategies for High-Performance Solid-State Photon Upconversion Based on Triplet Exciton Annihilation

T.-A. Lin, C. F. Perkinson, M. Wu, J. O. Tjepelt, V. Bulović, M. A. Baldo
Sponsorship: DoE

Photon upconversion, a non-linear optical process to convert low-energy photons into higher energies, has various applications such as photovoltaics, infrared sensing, and bio-imaging. In particular, upconversion based on triplet exciton annihilation is one of the most promising approaches to achieve high efficiency at low excitation intensity for practical applications. However, the reported performance in solid-state is limited due to energy back transfer, materials aggregation, and weak optical absorption, which complicates the integration with solid-state applications (Figure 1).

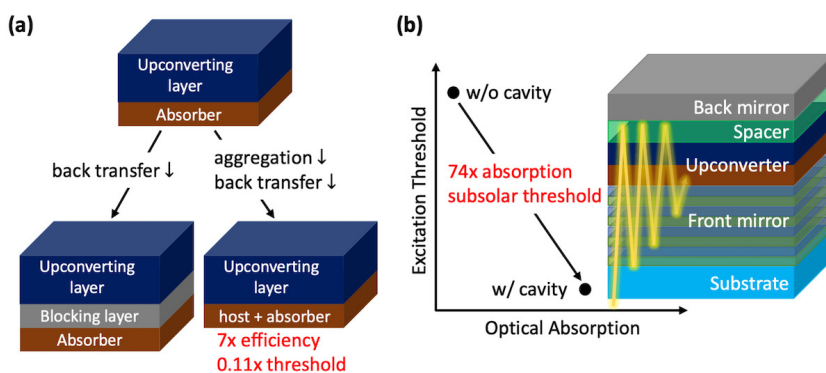
Here, we propose strategies to improve the performance in solid-state via device structure engineering. In a green-to-blue upconverter consisting of a bilayer of an absorbing and an upconverting

material, we reduce energy back transfer by inserting a blocking layer in between and mitigate aggregation by doping the absorber into a host material. The upconversion efficiency had a 7-fold enhancement, with the excitation intensity reduced by 9 times (Figure 2a). To improve optical absorption, we investigate an infrared- to-visible upconverter and integrate the upconverting layers into a Fabry-Pérot microcavity. At the resonant wavelength, infrared absorption increases 74-fold, and the threshold excitation intensity for upconversion is reduced by two orders of magnitude to a sub-solar flux (Figure 2b). Our work demonstrates the importance of device structure engineering to improve the performance of solid-state photon upconversion and offers a path towards practical applications.



◀ Figure 1: Schematic of a solid-state triplet excitonic upconverter out-lining the three major loss pathways.

▼ Figure 2: Device structure designs for (a) mitigating back transfer and aggregation and (b) enhancing optical absorption.



FURTHER READING

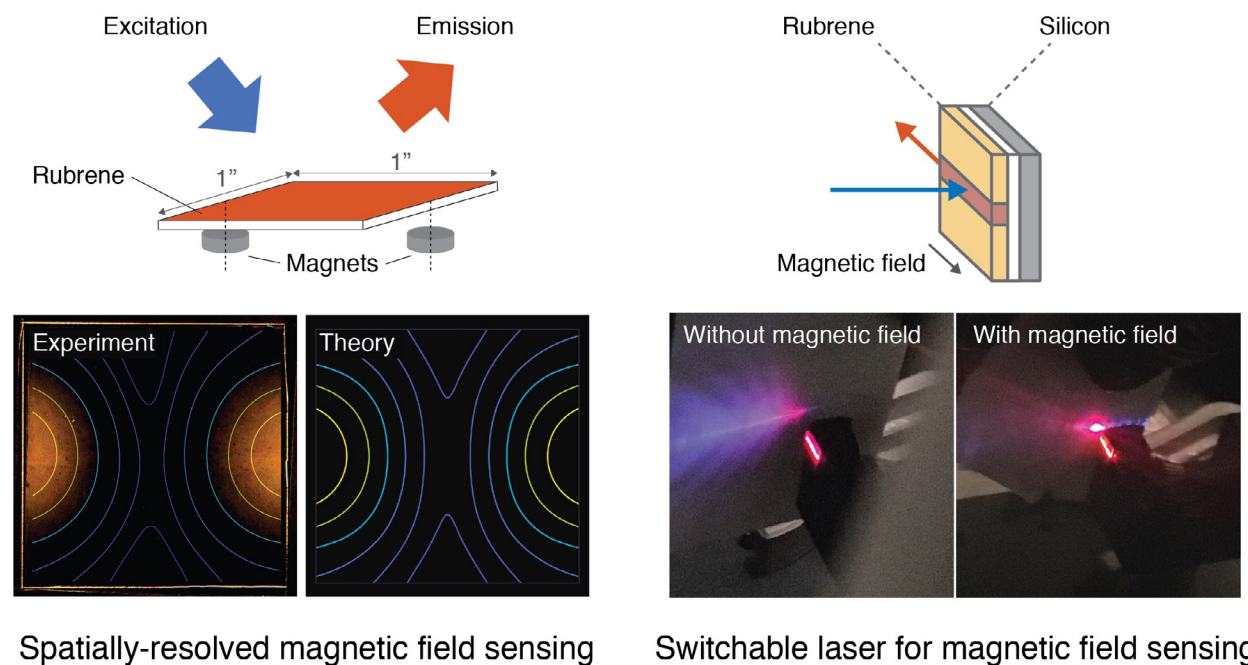
- T.-A. Lin, C. F. Perkinson, and M. A. Baldo, "Strategies for High-Performance Solid-State Triplet-Triplet-Annihilation-Based Photon Upconversion," *Advanced Materials*, vol. 32, no. 26, p. 1908175, 2020.
- M. Wu, T.-A. Lin, J. O. Tjepelt, V. Bulović, and M. A. Baldo, "Nanocrystal-Sensitized Infrared-to-Visible Upconversion in a Microcavity under Subsolar Flux," *Nano Letters*, vol. 21, no. 2, p. 1011, 2021.

Magnet Field-Switchable Laser via Optical Pumping of Rubrene

C. F. Perkinson, M. Einzinger, J. Finley, M. G. Bawendi, M. A. Baldo
Sponsorship: Department of Energy, NSF Graduate Research Fellowship

Optical imaging of magnetic fields is used in spintronics, magnetic resonance imaging, and radiology. Most conventional approaches to magnetic field imaging rely on expensive crystalline materials or garnets, but the cost of these materials makes them poorly suited to high-area imaging. Magnetic sensing applications may benefit from cheaper magnetically active dyes. We demonstrate that the well-studied organic molecule rubrene can be used to spatially resolve magnetic fields. Furthermore, we report a 460% enhancement

in rubrene brightness under a 0.4-T magnetic field in a first-of-its-kind magnetic field-switchable laser. We attribute the high magnetic sensitivity of rubrene to the magnetic field dependence of singlet fission, a process whereby one spin-singlet excitation splits into two spin-triplet excitations. These results suggest that rubrene—and other organic molecules that exhibit singlet fission—are promising candidates for low-cost, high-sensitivity magnetic imaging.



▲ Figure 1: (Left) Spatially resolved magnetic field sensing through modulation of rubrene emission intensity. (Right) Optically pumped waveguide laser, showing magnetic field switching between non-lasing and lasing modes.

Multiplexed Raman Sensors Using Swept-Source Excitation

N. Persits, J. Kim, Z. Li, R. Ram

Sponsorship: Food and Drug Administration (FDA)

Spontaneous Raman spectroscopy is routinely used in pharmaceutical production, chemical analysis, and the semiconductor industry for characterization of structural features, strain, and doping. Standard Raman systems require dispersive spectrometers and often specialized cooled charge-coupled device (CCD) detectors to compensate for the low signals, making them prohibitively expensive and bulky. In this work we introduce and demonstrate a novel Raman system architecture using a swept-source laser excitation, replacing the spectrometer. The laser is delivered through optical fibers to custom-made Raman probes, which are designed to be compatible with either single-mode or telecom-standard multimode optical fibers. Each probe delivers the excitation light onto a sample and

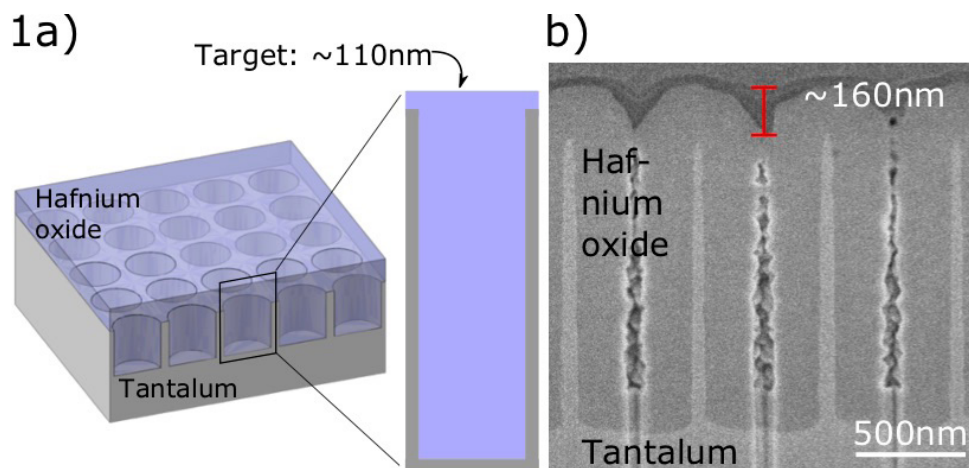
collects the Raman signal, which is then detected using a narrow optical filter in front of a room-temperature high-gain Si photodiode. With a standard telecom optical switch, we can multiplex up to 16 channels and deploy remote probes using an optical fiber network. As an initial proof-of-concept, we present the spectra collected with our probes for both solid polystyrene and liquid urea solutions and further show that the acquired spectra have signal-to-noise ratios comparable to that collected with our lab-built bench top Raman system. We believe this new system, in which a single tunable laser can serve a distributed sensor network, significantly reduces the space and cost of current spectrometer-based Raman systems and promotes the use of Raman for online process control.

Hafnia-Filled Photonic Crystal Emitters for Mesoscale Thermophotovoltaic Generators

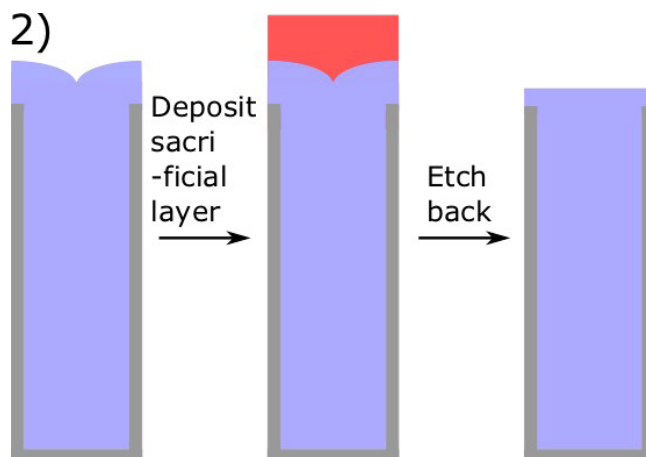
R. Sakakibara, V. Stelmakh, W. R. Chan, R. Geil, M. Ghebrebrhan, J. D. Joannopoulos, M. Soljačić, I. Čelanović
Sponsorship: U.S. ARO, DOE

Thermophotovoltaic (TPV) systems are promising as small-scale, portable generators for power sensors, small robotic platforms, and portable computational and communication equipment. In TPV systems, an emitter at high temperature emits radiation that is then converted to electricity by a low-bandgap photovoltaic cell. One way to increase both TPV power and efficiency is to use two-dimensional, hafnia-filled-and-capped tantalum photonic crystals (PhCs); they enable spectral tailoring of thermal radiation for a wide range

of angles. However, two key features are hard to realize simultaneously: a uniformly filled cavity and a thin capping film. Cavity-filling leads to a capping film that is both thick and uneven, so that trying to thin the film removes hafnia from within the cavity. Here, we present a method to reduce the film roughness and better control the thickness. Improved PhCs can pave the way toward high-performance TPV micro-generators for off-the-grid applications.



▲ Figure 1: a) The ideal filled PhC should have a flat and thin capping layer. b) The fabricated PhC cross section shows a thick and uneven capping film.



◀ Figure 2: A planarization and etch back process is used to reduce both roughness and thickness.

FURTHER READING

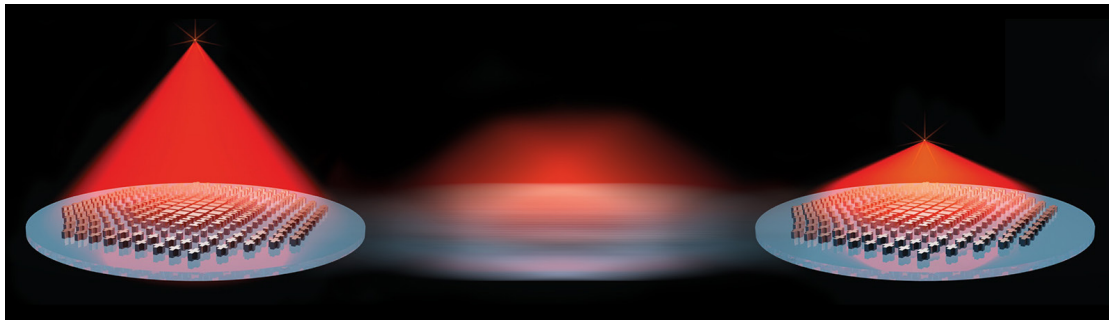
- W. R. Chan, V. Stelmakh, M. Ghebrebrhan, M. Soljačić, J. D. Joannopoulos, and I. Čelanović, "Enabling Efficient Heat-to-electricity Generation at the Mesoscale," *Energy Environ. Sci.*, vol. 10, pp. 1367-1371, 2017.
- Y. X. Yeng, J. Chou, V. Rinnerbauer, Y. Shen, S.-G. Kim, J. D. Joannopoulos, M. Soljačić, and I. Čelanović, "Global Optimization of Omnidirectional Wavelength Selective Emitters/absorbers Based on Dielectric-filled Anti-reflection Coated Two-dimensional Metallic Photonics Crystals," *Opt. Express*, vol. 22, pp. 21711-21718, 2014.

High-Performance Non-Mechanically-Tunable Meta-Lens

M. Y. Shalaginov, S. An, Y. Zhang, F. Yang, P. Su, V. Liberman, J. B. Chou, C. M. Roberts, M. Kang, C. Rios, Q. Du, C. Fowler, A. Agarwal, K. Richardson, C. Rivero-Baleine, H. Zhang, J. Hu, T. Gu
Sponsorship: Defence Advanced Research Projects Agency Extreme Optics and Imaging (EXTREME) Program

Optical metasurfaces, i.e., ultra-thin arrays of sub-wavelength antennae, have enabled a new range of photonic devices with unprecedented functionalities in sculpting wavefronts and a substantially reduced form-factor. Recently special interest has been drawn to a class of so-called “active metasurfaces,” whose optical properties can be modulated post-fabrication by non-mechanical effects. A variety of tuning mechanisms have been harnessed; however, demonstrated meta-optical devices often incur narrow tuning ranges and low op-

tical efficiencies. Here, we implemented an active varifocal meta-lens based on phase-change materials that offers 1) aberration-free performance across arbitrary optical states; 2) extremely low crosstalk of nearly 30 dB; and 3) considerably enhanced focusing efficiency exceeding 20% in both states with a clear pathway for further improvement. This advancement will further unveil a new cohort of exciting applications of active metasurfaces in imaging, sensing, display, and optical ranging.



▲ Figure 1: Illustration of a non-mechanically-actuated varifocal meta-lens made of phase-change material ($\text{Ge}_2\text{Sb}_2\text{Se}_4\text{Te}_1$). Focal plane position is switched between the two states depending on the optical material state (amorphous or crystalline).

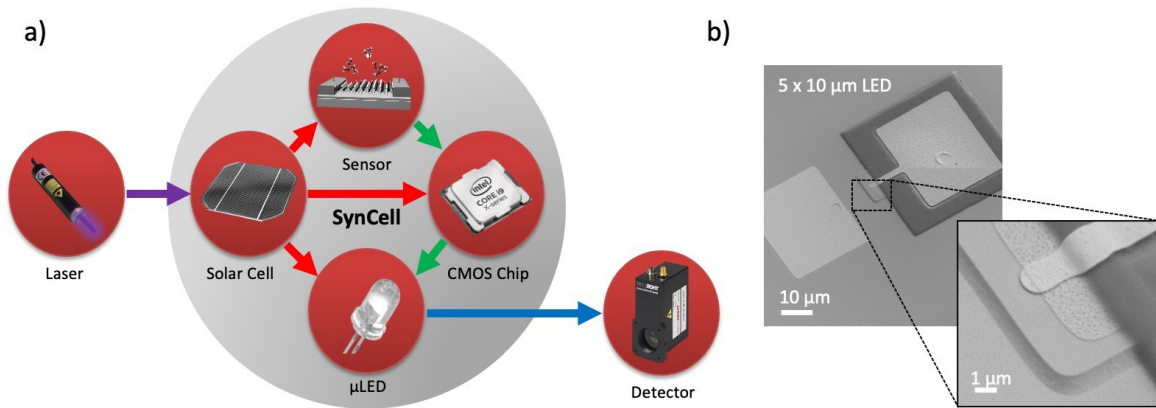
GaN μ LEDs for Microsystem Optical Communications

S. Spector, M. Hempel, T. Palacios

Sponsorship: AFOSR, MIT Experiential Learning Opportunity

Electronic systems smaller than $50\ \mu\text{m}$ are promising for ubiquitous sensing; however, wireless communication with such systems is challenging since radio-frequency communication is inefficient at the micron scale. Small length scales motivate the use of optical communications for micro-devices, which must be low-power due to the size constraint on solar cell surface area. Here we present an analysis of blue GaN microLEDs (μ LEDs) for optical communications with $50 \times 50\ \mu\text{m}^2$ sensor microsystems called SynCells. We

analyzed μ LEDs with sizes from $5 \times 10\ \mu\text{m}^2$ up to $150 \times 150\ \mu\text{m}^2$, developing a test setup that can detect an LED driven by only $1\ \text{nW}$ (Figure 1). We found higher external quantum efficiency (EQE) for larger μ LEDs; also, EQE increased with current density up to a peak value, after which we observed an efficiency droop resulting from Auger recombination. GaN μ LEDs operating at maximally efficient current density will be able to produce detectable optical signals at sufficiently low power for practical use in SynCells.



▲ Figure 1: a) Block diagram of SynCell operation including μ LED and photomultiplier tube detector for optical communication; b) SEM image of a $5 \times 10\ \mu\text{m}^2$ GaN μ LED.

Large-area Optical Metasurface Fabrication using Nanostencil Lithography

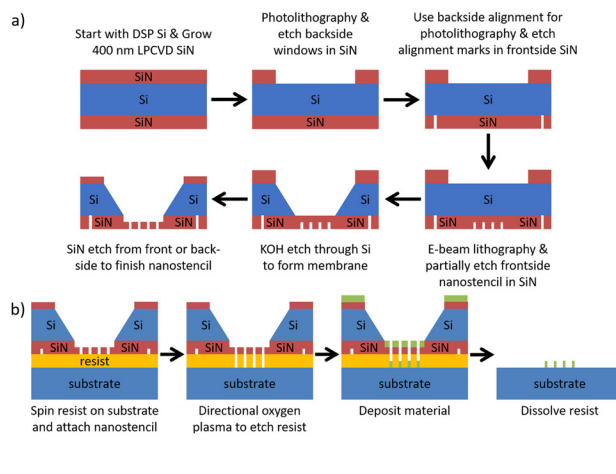
P. Su, M. Shalaginov, T. Gu, S. An, D. Li, L. Li, H. Jiang, S. Joo, L. C. Kimerling, H. Zhang, J. Hu, A. Agarwal
Sponsorship: DARPA

Optical metasurfaces promise optical components with on-demand control of light and reduced size, weight, and power (SWaP) compared to their bulk counterparts. However, fabrication of metasurfaces in the optical spectral range often relies on electron beam lithography due to the high resolution requirements, which makes fabrication scale poorly with the device dimensions. Recently, deep ultraviolet (DUV) lithography has been validated as a scalable manufacturing route for optical metasurfaces. However, DUV lithographic fabrication requires significant capital investment and is also limited to standard materials and processes available in foundries.

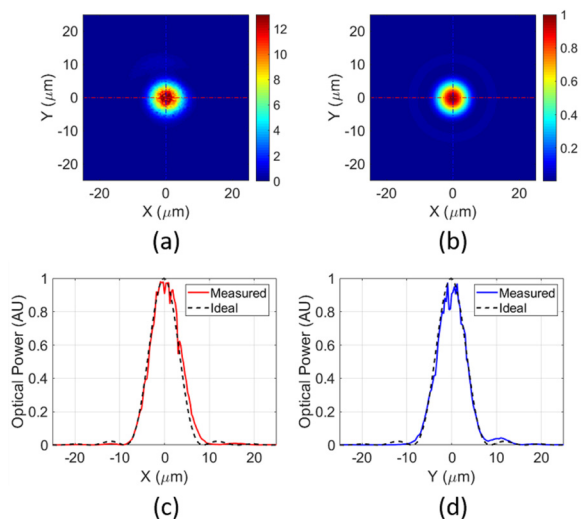
We are developing nanostencil lithography as an alternative technique for scalable, versatile, and rapid prototyping of metasurface devices. Nanostencils are nano-scale shadow masks, which allow repeated fabrication of a pattern via any anisotropic deposition process once the nanostencil is made. Previous research that used nanostencil lithography required only deposition of very thin layers (100 nm or less)

through the nanostencil, while transmissive dielectric metasurfaces require significantly thicker layers, especially as the wavelength of light increases. Previous nanostencils were also limited to 1 mm by 1 mm in size. We improved previous processes for fabricating and using nanostencils, increasing the yield of nanostencil fabrication by not fully etching through the nanostencil membrane before the KOH etch and improving the consistency of metasurface fabrication by developing a resist-based spacer layer. Figure 1 outlines the resulting processes.

To show the effectiveness of nanostencil lithography for large-area optical metasurface fabrication, we used 2 mm by 2 mm nanostencils to fabricate 1.5-mm-diameter PbTe metalenses on CaF_2 . The lenses showed diffraction-limited focusing, with a representative focal spot shown in Figure 2, and focusing efficiencies comparable to efficiencies reported in state-of-the-art large-area dielectric metalenses.



▲ Figure 1: Schematics of (a) the fabrication process for large-area silicon-nitride-based nanostencils and (b) the process for using nanostencils on rigid substrates.



▲ Figure 2: Representative (a) measured and (b) simulated images, along with the (c) x-axis and (d) y-axis cross sections of the focal spot of a metalens fabricated using nanostencils.

FURTHER READING

- P. Su, M. Shalaginov, T. Gu, S. An, D. Li, L. Li, H. Jiang, S. Joo, L. C. Kimerling, H. Zhang, J. Hu, and A. Agarwal, "Large-area Optical Metasurface Fabrication Using Nanostencil Lithography," *Optics Letters*, vol. 46, no. 10, pp. 2324-2327, May 2021.
- P. Su, K. Stoll, M. Shalaginov, T. Gu, S. An, D. Li, L. Li, H. Jiang, S. Joo, L. C. Kimerling, H. Zhang, J. Hu, and A. Agarwal, "Nanostencil Lithography for Scalable Optical Metasurfaces," to be presented at OSA *Optical Design and Fabrication Congress*, online, June 2021.
- P. Su, "Lead Chalcogenide Thin Film Materials and Processing for Infrared Optical Devices," *Ph.D. dissertation*, Massachusetts Institute of Technology, Cambridge, 2020.

The Effect of O:N Ratio in a HfO_xN_y Interlayer on Triplet Energy Transfer In Singlet-Fission-Sensitized Silicon

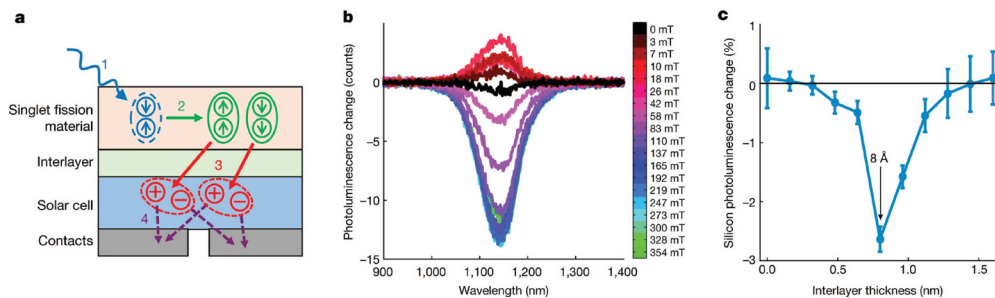
C. F. Perkinson*, N. Wong*, M. A. Baldo

*These authors contributed equally to this work

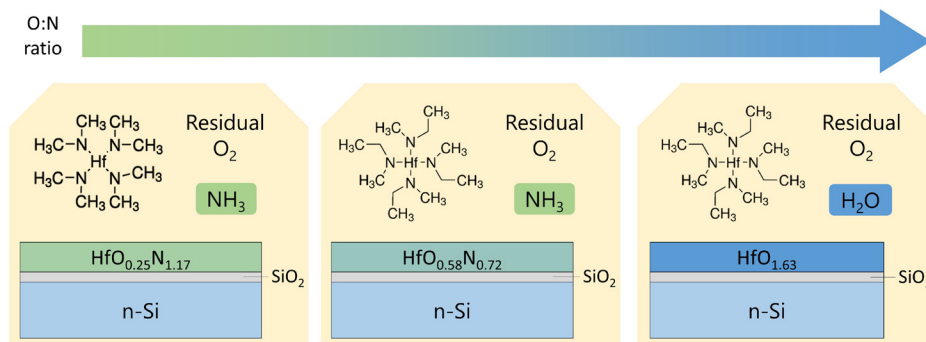
Sponsorship: DOE

With the climate changing, the Sun is a promising source of renewable energy. However, silicon photovoltaics, the current industry standard, are approaching their theoretical efficiency limit. A proposed method to exceed this limit is to sensitize silicon with a material that undergoes singlet exciton fission, a carrier multiplication process with the potential to reduce thermalization losses by creating two excited electrons from a single photon. Successful transfer of these two electrons to silicon could result in increased photocurrent and improved device efficiency. Recently, our group demonstrated the first proof-of-concept solar cell incorporating tetracene as a singlet fission material to produce additional carriers that are transported to silicon via a thin layer of hafnium oxynitride (HfO_xN_y). With the aim of improving singlet-fission-sensitized silicon solar cells, our research focuses on understand-

ing what properties are necessary for the transport layer between singlet fission materials and silicon and the mechanism for the energy transfer process. In this work, the defect density of a HfO_xN_y interlayer is varied by changing the oxygen-to-nitrogen ratio, and different interlayer thicknesses are studied to examine the role of defect states on energy transfer from tetracene to silicon. The transfer efficiency is inferred via magnetic field modulation of the silicon photoluminescence. The results form a preliminary basis for unravelling the exciton transfer mechanism, which will subsequently be studied using time-resolved spectroscopy. Ultimately, knowledge of interlayer material properties and insights into the mechanism of energy transfer to silicon may inform the design of sensitizing layers for silicon and pave the way to commercializing the use of singlet fission to boost silicon photovoltaic efficiencies.



▲ Figure 1: a) Schematic of a singlet-fission-sensitized solar cell, b) applying a magnetic field changes the efficiency of singlet fission, which is observable as a change in silicon photoluminescence, c) singlet fission sensitization is maximized using a HfO_xN_y interlayer thickness of 8 Å.



▲ Figure 2: The choice of precursors used in atomic layer deposition modifies the O:N atomic ratio in a passivating layer of HfO_xN_y.

FURTHER READING

- M. Einzinger, T. Wu, J. F. Kompalla, H. L. Smith, C. F. Perkinson, L. Nienhaus, S. Wiegold, D. N. Congreve, et al., "Sensitization of Silicon by Singlet Exciton Fission in Tetracene," *Nature*, vol. 571, pp. 90-94, 2019. [Online.] Available: <https://www.nature.com/articles/s41586-019-1339-4>.

LION: Learning to Invert 3D Objects by Neural Networks

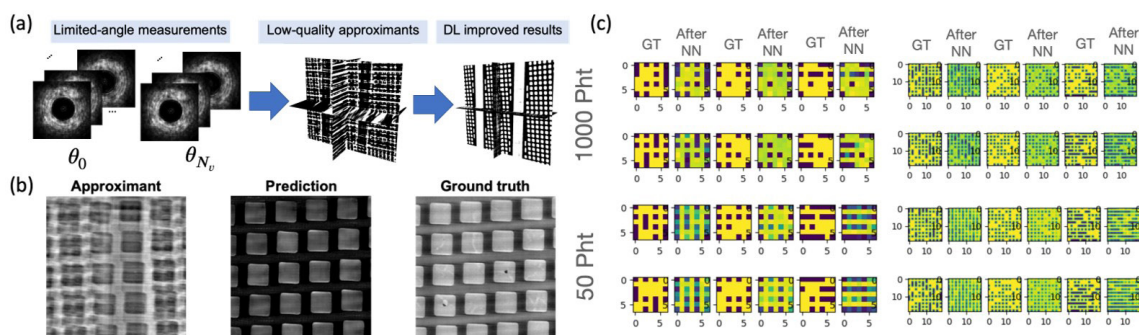
G. Barbastathis, J. Song, Z. Wu, I. K. S. Pang, Z. Guo

Sponsor: IARPA RAVEN (Rapid Analysis of Various Emerging Nanoelectronics)

Non-destructive three-dimensional imaging is important to establish the internal structure of a 3D object non-invasively. In our work, objects of interest are integrated circuits (ICs). This operation requires sufficient measurements for computational reconstruction, such as measurements from different angles or depths. Meanwhile, if the required acquisition time is too long, the operation may become impractical, not to mention the risk of instabilities or even damage to the samples from X-ray radiation. Reducing the number of angular views and the radiation dosage per view can be used to limit beam exposure, but low-dose data acquisition schemes yield noisy measurements that significantly reduce the quality of the reconstructed image.

Our goal in this project is to reduce the acquisition time by a factor of 10-100 through augmenting image reconstruction with machine learning. In the LION

approach, we embed the physics of X-ray propagation and interaction with matter into the learning process. This improves both the fidelity and the efficiency of learning. We study two types of information-starved 3D imaging: limited-angle tomography and low-dose tomography. A limited-angle tomography combined with an advanced ptychography technique, achieves high-resolution (10 nm) reconstruction with the advanced technique of recurrent neural network and generative adversarial network (see Figure 1a, b). On the other hand, low-dose tomography suffers from shot noise as the photon budget reduces (<50 photons per ray). Regardless of 20% reduction in photon budget for 50 photons case, the physics-assisted machine learning still reconstructs ICs with high fidelity (Test PCC: 0.80) (see Figure 1c).



▲ Figure 1: (a) Deep learning-based 3D volume reconstruction framework for limited-angle tomography. (b) Deep learning-based reconstruction results in terms of low-quality approximants, deep learning-based reconstruction results, and ground truth from sufficient measurements. (c) Reconstruction ICs ($7 \times 7 \times 5$, left and $19 \times 19 \times 5$, right) from low-dose tomography with reducing photon counts per ray (from 1000 to 50).

FURTHER READING

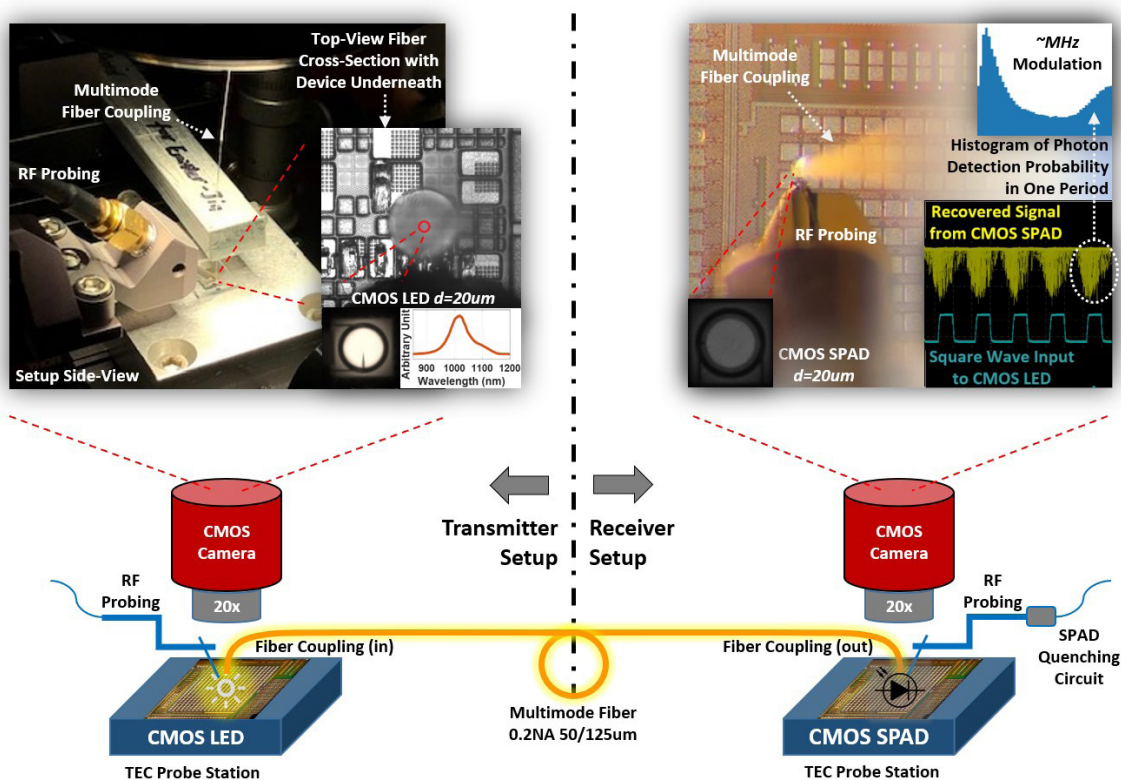
- Kang, I., Goy, A., and Barbastathis, G. (2021). "Dynamical Machine Learning Volumetric Reconstruction of Objects' Interiors from Limited Angular Views," *Light: Science & Applications*, 10(1), 1-21.
- Goy, A., Rughoobur, G., Li, S., Arthur, K., Akinwande, A. I., & Barbastathis, G. (2019). "High-resolution Limited-angle Phase Tomography of Dense Layered Objects Using Deep Neural Networks," *Proceedings of the National Academy of Sciences*, 116(40), 19848-19856.

Light Sources and Single-Photon Detectors in Bulk CMOS

J. Xue, J. Kim, A. Mestre, K. M. Tan, D. Chong, S. Roy, H. Nong, K. Y. Lim, D. Gray, D. Kramnik, A. Atabaki, E. Quek, R. J. Ram
Sponsorship: GlobalFoundries, A*STAR, Kwanjeong Educational Foundation

Silicon photonics realized in complementary metal-oxide semiconductor (CMOS) processes has transformed computing, communications, sensing, and imaging. Here, we demonstrate a chip-to-chip fiber optic link that implements both the light source and detector in bulk CMOS. A high-brightness infrared light emission in forward bias for a silicon p-n junction is implemented in an open-foundry CMOS process – 55 BCDLite. Emission intensity of 50 mW/cm² light at a wavelength of 1020 nm is realized at room temperature by using a deep vertical junction with lightly doped rings.

An infrared-enhanced single photon avalanche diode (SPAD) was designed in the same process and used to collect the 1020-nm light emission. We find that a detector using the p-substrate as part of the p-n junction achieves good detection (6% quantum efficiency for a 20- μm diameter device) even at a wavelength of 1020 nm. This device has a breakdown voltage of -24V and can be operated in Geiger mode to achieve photon detection at low light levels. The capabilities of the two devices combine to demonstrate a complete chip-to-chip optical interconnect utilizing only silicon CMOS devices.



▲ Figure 1: Optical transmission of modulation waveform from CMOS LED to CMOS SPAD over a standard multimode optical fiber.

FURTHER READING

- J. Xue et al., "Low Voltage, High Brightness CMOS LEDs," *2020 IEEE International Electron Devices Meeting (IEDM)*, 2020, pp. 33.5.1-33.5.4, doi: 10.1109/IEDM13553.2020.9371911.

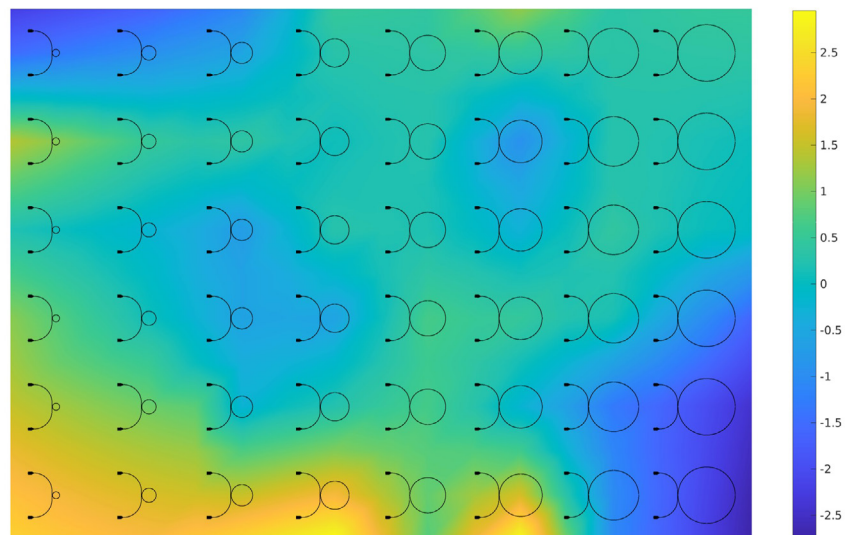
Inference of Process Variations in Silicon Photonics from Characterization Measurements

Z. Zhang, S. I. El-Henawy, C. Ríos, D. S. Boning

Silicon photonics, which manipulates photons instead of electrons, shows promise for higher data rates, lower-energy communication and information processing, biomedical sensing, and novel optically based functionality applications such as wavefront engineering and beam steering of light. In silicon photonics, both electrical and optical components can be integrated on the same chip, using a shared silicon integrated circuit (IC) technology base. However, silicon photonics does not yet have mature process, device, and circuit variation models for the existing IC and photonic process steps; this lack presents a key challenge for design in this emerging industry.

Our goal is to develop key elements of a robust design for manufacturability (DFM) methodology for silicon photonics. One of the key steps for the goal is to find the distribution map of process variation in the actual fabrication, which is usually inferred from well-designed test structure measurements.

In this work, we develop a Bayesian-based method to infer the distribution of systematic geometric variations in silicon photonics that aims to reduce the extraction error caused by measurement noise. We apply this method to characterization data from multiple silicon nitride ring resonators with different design parameters and produce the estimated spatial map of device geometric variations (e.g., waveguide width, Si_3N_4 on SiO_2 thickness, partial etch depth), as shown in Figure 1. Our results show that this characterization scheme can serve as a good test structure for process variation inference. Since characterization measurements are commonly used for device optimization design, our method provides an efficient alternative approach to study process variation in silicon photonics without requiring separate or replicated test structure design and thus facilitates the design of high-yield silicon photonic circuits in the future.



▲ Figure 1: The characterization design layout with our estimation of the Si_3N_4 on SiO_2 thickness variation map inferred from the measurement.

FURTHER READING

- L. Chrostowski and M. Hochberg, "Silicon Photonics Design: from Devices to Systems," Cambridge: Cambridge University Press, 2015.

Integrated Photonics and Electronics for Chip-Scale Control of Trapped Ions

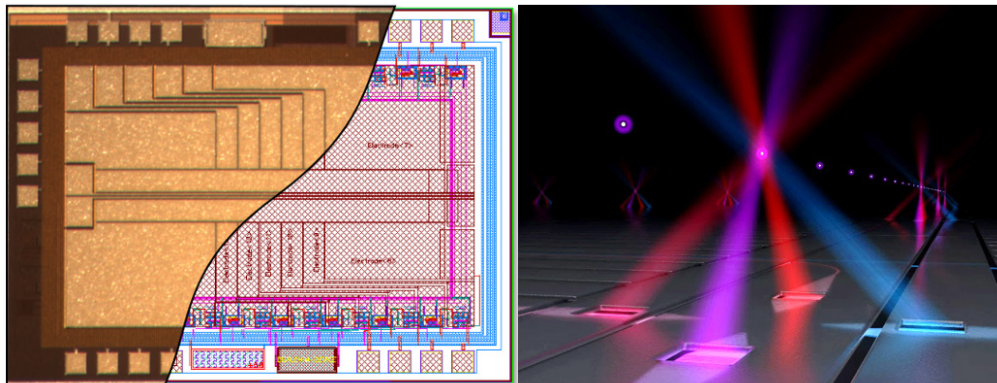
J. Stuart, J. M. Sage, I. L. Chuang, J. Chiaverini

Sponsorship: Under Secretary of Defense for Research and Engineering and Department of Defense, MIT Lincoln Laboratory

Trapped atomic ions are promising candidates for quantum information processing and quantum sensing. Current state-of-the-art trapped-ion systems require many lasers and electronics to achieve precise timing and control over quantum states. Usually, electronic signals are sent into vacuum chambers via wire feedthroughs, and laser light is focused down to a trapped ion's location with external lenses mounted outside viewports on the chamber. These requirements lead to dense and complex setups that may be prone to drift and limit the amount of control that can be achieved. We have made recent progress toward integrating control technology into the substrate of the ion trap itself. By using a planar trap design, which is compatible with lithographic fabrication, we may implement other well-developed processes in order to enhance the function of the ion trap. In one experiment, we demonstrate an ion trap with integrated, complementary met-

al-oxide-semiconductor-based high-voltage sources that can be used to control the motional frequency and position of a trapped ion. In another demonstration, we use photonic waveguides and diffractive grating couplers to route light around a chip and focus it onto ions trapped above the surface.

Integrating controls into ion traps has the potential to increase the density of independently controllable ions on a chip in next-generation systems, but there are also many immediate practical benefits. Reducing the number of required feedthroughs allows chambers to be made more compact, which may be useful for ion-based clocks or sensors. We also show that integrated-photonics platforms help to reduce vibration-induced noise seen when using external optics, which may enable portable systems based on trapped-ion quantum information processing.



▲ Figure 1: Cutaway view of an ion trap with integrated electronics. The micrograph shows the top metal layer of the integrated circuit, with trap electrodes, and the circuit diagram shows the active voltage sources in the interior layers. [Right] Notional depiction of laser light focusing above an ion trap using integrated photonics. Diffractive grating couplers (beneath square holes in the plane) direct light of multiple wavelengths from integrated waveguides towards ions trapped above the surface.

FURTHER READING

- R. J. Niffenegger, J. Stuart, C. Sorace-Agaskar, D. Kharas, S. Bramhavar, C. D. Bruzewicz, W. Loh, R. T. Maxson, R. McConnell, D. Reens, G. N. West, J.M. Sage, and J. Chiaverini, "Integrated Multi-wavelength Control of an Ion Qubit", *Nature* 586, 538-542 (2020).
- J. Stuart, R. Panock, C. D. Bruzewicz, J.A. Sedlacek, R. McConnell, I. L. Chuang, J. M. Sage, and J. Chiaverini, "Chip-integrated Voltage Sources for Control of Trapped Ions", *Physical Review Applied* 11, 024010 (2019).

Nano Explorations Videos

A Student & Postdoc Webinar Series from MIT.nano

[Fluorescent Janus Droplet and its Application in Biosensing of Listeria Monocytogenes](#)

Jie Li | Abstract on page 17

[Dance-inspired Investigation of Human Movement](#)

Praneeth Namburi | Abstract on page 18

[Nanoscale Insights into the Mechanisms of Cellular Growth and Proliferation](#)

Kacper Rogala | Abstract on page 19

[Programming a Quantum Computer with Quantum Instructions](#)

Morten Kjaergaard | Abstract on page 40

[Silicate-Based Composite as Heterogeneous Integration Packaging Material for Extreme Environments](#)

James McRaen | Abstract on page 41

[Highly Tunable Junctions in Magic Angle Twisted Bilayer Graphene Tunneling Devices](#)

Daniel Rodan-Legrain | Abstract on page 61

[Electronic Cells: Autonomous Micromachines from 2D Materials](#)

Volodymyr Koman | Abstract on page 62

[Decoding Complexities in Relaxor Ferroelectrics Using Electron Microscopy](#)

Abinash Kumar | Abstract on page 63

[Integrating Object Form and Electronic Function in Rapid Prototyping and Personal Fabrication](#)

Junyi Zhu | Abstract on page 90

[Seeing Superlattices: Imaging Hidden Moiré Periods at the Nanoisland-2D Material Interface Using 4D Scanning Transmission Electron Microscopy](#)

Kate Reidy | Abstract on page 105

[Small Molecule Assemblies with a Bulletproof Design: The Aramid Amphiphile](#)

Ty Christoff-Tempesta | Abstract on page 106

[Integrated Photonics and Electronics for Chip-scale Quantum Control of Trapped Ions](#)

Jules Stuart | Abstract on page 124

Research Centers

Center for Integrated Circuits and Systems 129
MIT/MTL Center for Graphene Devices and 2-D Systems..... 130
The MIT Medical Electronic Device Realization Center 131

Center for Integrated Circuits and Systems

Professor Hae-Seung Lee, Director

The Center for Integrated Circuits and Systems (CICS) at MIT, established in 1998, is an industrial consortium created to promote new research initiatives in circuits and systems design, as well as to promote a tighter technical relationship between MIT's research and relevant industry. Nine faculty members participate in the CICS: Director Hae-Seung (Harry) Lee, Anantha Chandrakasan, Ruonan Han, Song Han, David Perreault, Negar Reiskarimian, Max Shulaker, Charles Sodini, and Vivienne Sze.

CICS investigates a wide range of circuits and systems, including wireless and wireline communication, high-speed, THz, and RF circuits, microsensor/actuator systems, imagers, digital and analog signal processing circuits, biomedical circuits, deep learning systems, emerging technologies, and power conversion circuits, among others.

We strongly believe in the synergistic relationship between industry and academia, especially in practical research areas of integrated circuits and systems. CICS is designed to be the conduit for such synergy.

CICS's research portfolio includes all research projects that the eight participating faculty members conduct, regardless of source(s) of funding, with a few exceptions.

Technical interaction between industry and MIT researchers occurs on both a broad and individual level. Since its inception, CICS recognized the importance of holding technical meetings to facilitate communication among MIT faculty, students, and industry. We hold two informal technical meetings per year open to CICS faculty, students, and representatives from participating companies. Throughout each full-day meeting, faculty and students present their research, often presenting early concepts, designs, and results that have not been published yet. The participants then offer valuable technical feedback, as well as suggestions for future research. More intimate interaction between MIT researchers and industry takes place during work on projects of particular interest to participating companies. Companies may invite students to give on-site presentations, or they may offer students summer employment. Additionally, companies may send visiting scholars to MIT or enter into a separate research contract for more focused research for their particular interest. The result is truly synergistic, and it will have a lasting impact on the field of integrated circuits and systems.

MIT/MTL Center for Graphene Devices and 2-D Systems

Professor Tomás Palacios, Director

The MIT/MTL Center for Graphene Devices and 2-D Systems (MIT-CG) brings together MIT researchers and industrial partners to advance the science and engineering of graphene and other two-dimensional (2-D) materials.

Two-dimensional materials are revolutionizing electronics, mechanical and chemical engineering, physics and many other disciplines thanks to their extreme properties. These materials are the lightest, thinnest, strongest materials we know of. At the same time that they have extremely rich electronic and chemical properties. MIT has been leading research on the science and engineering of 2-D materials for more than 40 years. Since 2011, the MIT/MTL Center for Graphene Devices and 2-D Systems (MIT-CG) has played a key role in coordinating most of the work going on at MIT on these new materials, and in bringing together MIT faculty and students, with leading companies and government agencies interested in taking these materials from a science wonder to an engineering reality.

Specifically, the Center explores advanced

technologies and strategies that enable 2-D materials, devices, and systems to provide discriminating or breakthrough capabilities for a variety of system applications ranging from energy generation/storage and smart fabrics and materials to optoelectronics, RF communications, and sensing. In all these applications, the MIT-CG supports the development of the science, technology, tools, and analysis for the creation of a vision for the future of new systems enabled by 2-D materials.

Some of the many benefits of the Center's membership include complimentary attendance to meetings, industry focus days, and live webcasting of seminars related to the main research directions of the Center. Our industrial members also gain access to a resume book that connects students with potential employers, as well as access to timely white papers on key issues regarding the challenges and opportunities of these new technologies. There are also numerous opportunities to collaborate with leading researchers on projects that address some of today's challenges for these materials, devices, and systems.

The MIT Medical Electronic Device Realization Center

Professor Charles Sodini, Director

The vision of the MIT Medical Electronic Device Realization Center (MEDRC) is to revolutionize medical diagnostics and treatments by bringing health care directly to the individual and to create enabling technology for the future information-driven healthcare system. This vision will, in turn, transform the medical electronic device industry. Specific areas that show promise are wearable or minimally invasive monitoring devices, medical imaging, portable laboratory instrumentation, and the data communication from these devices and instruments to healthcare providers and caregivers.

Rapid innovation in miniaturization, mobility, and connectivity will revolutionize medical diagnostics and treatments, bringing health care directly to the individual. Continuous monitoring of physiological markers will place capability for the early detection and prevention of disease in the hands of the consumer, shifting to a paradigm of maintaining wellness rather than treating sickness. Just as the personal computer revolution has brought computation to the individual, this revolution in personalized medicine will bring the hospital lab and the physician to the home, to emerging countries, and to emergency situations. From at-home cholesterol monitors that can adjust treatment plans, to cell phone-enabled blood labs, these system solutions containing state-of-the-art sensors, electronics, and computation will radically change our approach to health care. This new generation of medical systems holds the promise of delivering better quality health care while reducing medical costs.

The revolution in personalized medicine is rooted in fundamental research in microelectronics from materials to sensors, to circuit and system design. This knowledge has already fueled the semiconductor industry to transform society over the last four decades. It provided the key technologies to continuously increase performance while constantly lowering cost for computation, communication, and consumer electronics. The processing power of current smart phones, for example, allows for sophisticated signal processing to extract information from this sensor data. Data analytics can combine this information with other patient data and medical records to produce actionable information customized to the patient's needs. The aging population, soaring healthcare costs, and the need for improved healthcare in developing nations are the driving force for the next semiconductor industry's societal transformation, Medical Electronic Devices.

The successful realization of such a vision also demands innovations in the usability and productivity of medical devices, and new technologies and approaches to manufacturing devices. Information technology is a critical component of the intelligence that will enhance the usability of devices; real-time image and signal processing combined with intelligent computer systems will enhance the practitioners' diagnostic intuition. Our research is at the intersection of Design, Healthcare, and Information Technology innovation. We perform fundamental and applied research in the design, manufacture, and use of medical electronic devices and create enabling technology for the future information-driven healthcare system.

The MEDRC has established a partnership between microelectronics companies, medical device companies, medical professionals, and MIT to collaboratively achieve needed radical changes in medical device architectures, enabling continuous monitoring of physiological parameters such as cardiac vital signs, intracranial pressure, and cerebral blood flow velocity. MEDRC has 4 sponsoring companies, 8 faculty members, 12 active projects, and approximately 15 students. A visiting scientist from a project's sponsoring company is present at MIT. Ultimately this individual is the champion that helps translate the technology back to the company for commercialization and provide the industrial viewpoint in the realization of the technology. MEDRC projects have the advantage of insight from the technology arena, the medical arena, and the business arena, thus significantly increasing the chances that the devices will fulfill a real and broad healthcare need as well as be profitable for companies supplying the solutions. With a new trend toward increased healthcare quality, disease prevention, and cost-effectiveness, such a comprehensive perspective is crucial.

In addition to the strong relationship with MTL, MEDRC is associated with MIT's Institute for Medical Engineering and Science (IMES) that has been charged to serve as a focal point for researchers with medical interest across MIT. MEDRC has been able to create strong connections with the medical device and microelectronics industry, venture-funded startups, and the Boston medical community. With the support of MTL and IMES, MEDRC will serve as the catalyst for the deployment of medical devices that will reduce the cost of healthcare in both the developed and developing world.

Faculty Profiles

Anuradha M. Agarwal.....	135
Akintunde I. (Tayo) Akinwande.....	136
Polina Anikeeva.....	137
George Barbastathis.....	138
Duane S. Boning.....	139
Edward S. Boyden.....	140
Vladimir Bulović.....	141
Jacopo Buongiorno.....	142
Anantha Chandrakasan.....	143
Yufeng (Kevin) Chen.....	144
Luca Daniel.....	145
Jesús A. del Alamo.....	146
Dirk R. Englund.....	147
Jongyoon Han.....	148
Ruonan Han.....	149
Song Han.....	150
Juejun (JJ) Hu.....	151
Qing Hu.....	152
Jeehwan Kim.....	153
Sang-Gook Kim.....	154
Jing Kong.....	155
Jeffrey H. Lang.....	156
James M. LeBeau.....	157
Hae-Seung Lee.....	158
Luqiao Liu.....	159
Scott R. Manalis.....	160
Farnaz Niroui.....	161
Jelena Notaros.....	162
William D. Oliver.....	163
Tomás Palacios.....	164
Negar Reiskarimian.....	165
Jennifer L. M. Rupp.....	166
Charles G. Sodini.....	167
Vivienne Sze.....	168
Carl V. Thompson.....	169
Luis Fernando Velásquez-García.....	170
Joel Voldman.....	171
Evelyn N. Wang.....	172

Anuradha M. Agarwal

Principal Research Scientist, Materials Research Laboratory
Leader, Lab for Education and Application Prototypes (LEAP),
AIM Photonics Academy

Planar, integrated, Si-CMOS-compatible microphotonic platform for on-chip MIR hyperspectral imaging and chem-bio sensing applications; radiation effects on silicon microphotonic; non-linear materials and devices; chalcogenide glasses; aerosol detection; lead chalcogenide detectors, optoelectronic packaging.

Rm. 13-4126 | 617-253-5302 | anu@mit.edu

VISITING/SUMMER STUDENTS

Francesco Zanetto, Progetto Rocca Scholar

GRADUATE STUDENTS

Eveline Postelnicu, DMSE

Katherine Stoll, DMSE

Drew Weninger, DMSE

SELECTED PUBLICATIONS

R. Singh, Y. Nie, M. Gao, A. M. Agarwal, and B. W. Anthony, "Inverse Design of Photonic Meta-structure for Beam Collimation in On-chip Sensing," *Scientific Reports*, 11 (1), 1-11, 2021.

M. Y. Shalaginov, S. An, Y. Zhang, F. Yang, P. Su, V. Liberman, J. B. Chou, C. M. Roberts, M. Kang, C. Rios, Q. Du, C. Fowler, A. M. Agarwal, K. A. Richardson, C. Rivero-Baleine, H. Zhang, J. Hu, and T. Gu, "Reconfigurable All-dielectric Metalens with Diffraction-limited Performance," *Nature Communications*, 12 (1), 1-8, 2021.

R. Singh, A. M. Agarwal, and B. W. Anthony, "Design of Optical Meta-structures with Applications to Beam Engineering Using Deep Learning," *Scientific Reports* 10 (1), 1-10, 2020.

M. Y. Shalaginov, S. An, F. Yang, P. Su, D. Lyzwa, A. M. Agarwal, H. Zhang, J. Hu, and T. Gu, "Single-Element Diffraction-Limited Fisheye Metalens," *Nano Letts.*, 20 (10), 7429-7437, 2020.

R. Singh, A. M. Agarwal, and B. W. Anthony, "Mapping the Design Space of Photonic Topological States via Deep Learning," *Optics Express*, 28 (19), 27893-27902, 2020.

A. Yadav, and A. M. Agarwal, "Integrated Photonic Materials for the Mid-infrared," *International Journal of Applied Glass Science (IJAGS)*, Special Issue Article; DOI: 10.1111/ijag.15252, Feb. 2020.

P. Xing, D. Ma, L. C. Kimerling, A. M. Agarwal, and D. T. H. Tan, "High Efficiency Four-wave Mixing and Optical Bistability in Amorphous Silicon Carbide Ring Resonators" *APL Photonics* 5, 076110: <https://doi.org/10.1063/5.0009692>, 2020.

S. Savagatrup, D. Ma, H. Zhong, K. S. Harvey, L. C. Kimerling, A. M. Agarwal, and T. M. Swager, "Dynamic Complex Emulsions as Amplifiers for On-Chip Photonic Cavity-Enhanced Resonators," *ACS Sensors*, 2020.

P. Su, R. Pujari, V. Boodhoo, S. Aggarwal, P. Bhattacharya, O. Maksimov, K. Wada, S. Merlo, H. B. Bhandari, L. C. Kimerling, and A. M. Agarwal, "Ternary Lead Chalcogenide Alloys for Mid-Infrared Detectors," *Journal of Electronic Materials (JEM)*, Vol. 49, No. 8, pp. 4577-4580, 2020.

R. Singh, A. B. G. Frydman, L. Kimerling, A. M. Agarwal, and B. W. Anthony, "Integrated Optofluidic Sensor for Coagulation Risk Monitoring in COVID-19 Patients at Point-of-Care," *arXiv preprint arXiv:2010.02081*, 2020.

Akintunde I. (Tayo) Akinwande

Professor of Electrical Engineering
Department of Electrical Engineering & Computer Science

Empty space electronics. Nano vacuum channel transistors. Chip scale scale electron, ion, neutron and x-ray sources for imaging and sensing. Micro and nano structures for charged particle beams.

Rm. 39-553 | 617-258-7974 | akinwand@mtl.mit.edu

POSTDOCTORAL ASSOCIATES

Girish Rugubor, MTL
Winston Chern, MTL
Olusoji Ilori, MTL

GRADUATE STUDENTS

Nedeljko Karaulac, EECS
Álvaro Sahagún EECS

UNDERGRADUATE STUDENTS

Lay Jain, Physics
Jack Bouhanna, EECS
Olutimilehin O. Omotunde, EECS

SUPPORT STAFF

Steven O'Hearn, Administrative Assistant

SELECTED PUBLICATIONS

N. Karaulac, G. Rughoobur, and A. I. Akinwande, "Highly uniform silicon field emitter arrays fabricated using a trilevel resist process," *J. Vac. Sci. Technol. B*, vol. 38, no. 2, p. 023201, 2020.

G. Rughoobur, N. Karaulac, L. Jain, O. O. Omotunde, and A. I. Akinwande, "Nanoscale silicon field emitter arrays with self-aligned extractor and focus gates," *Nanotechnology*, vol. 31, p. 335203, Jun. 2020.

G. Rughoobur, J. Zhao, L. Jain, A. Zubair, T. Palacios, J. Kong and A. I. Akinwande, "Enabling Atmospheric Pressure Operation of Nanoscale Vacuum Channel Transistors," in *2020 78th Device Research Conference (DRC)*, 2020.

P-C Shih, G. Rughoobur, P. Xiang, K. Cheng, A. I. Akinwande and T. Palacios, "GaN Nanowire Field Emitters with a Self-Aligned Gate Process," in *2020 78th Device Research Conference (DRC)*, 2020.

Y. Mo, Z. Lu, G. Rughoobur, P. Patil, N. Gershenfeld, A. I. Akinwande, S. L. Buchwald, and K. F. Jensen, "Microfluidic electrochemistry for single electron transfer redox-neutral reactions," *Science*, vol. 368, pp. 1352–1357, Jun. 2020.

G. Rughoobur, L. Jain and A. I. Akinwande, "Low energy electron transmission through suspended graphene layers," in *2020 33rd International Vacuum Nanoelectronics Conference (IVNC)*, 2020.

G. Rughoobur, N. Karaulac and A. I. Akinwande, "Nanoscale Vacuum Channel Electron Sources," in *2020 33rd International Vacuum Nanoelectronics Conference (IVNC)*, 2020.

G. Rughoobur, A. Sahagun, O. O. Ilori, and A. I. Akinwande, "Nanofabricated low-voltage gated si field-ionization arrays," *IEEE Transactions on Electron Devices*, pp. 1–7, 2020.

W. Chern, N. Karaulac, G. Rughoobur, and A. I. Akinwande, "Space Charge Limited Transport in Si Field Emitter Arrays," in *33rd International Vacuum Nanoelectronics Conference (IVNC)*, IEEE, Jul. 2020.

W. Chern, G. Rughoobur, A. Zubair, N. Karaulac, A. Cramer, R. Gupta, T. Palacios, and A. Akinwande "Demonstration of a 40 kV Si Vacuum Transistor as a Practical High Frequency and Power Device," in *2020 IEEE International Electron Devices Meeting (IEDM)*, San Francisco, CA, USA, 2020, pp. 5.2.1-5.2.4.

P-C Shih, G. Rughoobur, K. Cheng, A. I. Akinwande and T. Palacios, "Self-Align-Gated GaN Field emitter Arrays Sharpened by A Digital Etching Process," *IEEE Electron Device Letters*, vol. 42, no. 3, pp. 422–425, Mar. 2021.

G. Rughoobur, L. Jain, and A. I. Akinwande, "Electron transmission through suspended graphene membranes measured with a low-voltage gated Si field emitter array," *Nanotechnology*, vol. 32, no. 28, p. 285201, Jul. 2021.

R. Bhattacharya, N. Karaulac, W. Chern, A. I. Akinwande, and J. Browning, "Temperature effects on gated silicon field emission array performance", *Journal of Vacuum Science & Technology B* 39, 023201 (2021).

R. Bhattacharya, N. Karaulac, G. Rughoobur, W. Chern, A. I. Akinwande, and J. Browning, "Ultraviolet light stimulated water desorption effect on emission performance of gated field emitter array," *Journal of Vacuum Science & Technology B*, vol. 39, p. 033201, May 2021.

Ranajoy Bhattacharya, Nedeljko Karaulac, Winston Chern, Akintunde I. Akinwande and Jim Browning, "Gated Silicon Field Emitter Array Characterization", *2020 IEEE International Vacuum Electronics Conference*, 19-22 Oct. 2020

Polina Anikeeva

Professor

Department of Materials Science and Engineering

Department of Brain and Cognitive Sciences

Neuroprosthetic materials and devices: chemistry, device physics, fabrication, and testing in biological systems. Minimally invasive neural stimulation.

Rm. 36-849 | 617-253-3301 | anikeeva@mit.edu

RESEARCH SCIENTIST

Dekel Rosenfeld, RLE

POSTDOCTORAL ASSOCIATE

Marie Manthey, RLE

GRADUATE STUDENTS

Harrison Allen, EECS

Marc-Joseph Antonini, HST, Friends of McGovern Fellow

Indie Garwood, HST, NSF Fellow

Hannah Field, EECS

Florian Koehler, EECS

Ye Ji Kim, DMSE

Youngbin Lee, DMSE, Kwangjeong Fellow

Keisuke Nagao, DMSE

Karen Pang, BCS

Jimin Park, DMSE, Kwangjeong Fellow

Atharva Sahasrabudhe, Chemistry, Lore McGovern Fellow

Anthony Tabet, ChemE, NSF Fellow, Soros Fellow

Georgios Varnavides, DMSE

D. Rosenfeld, A. W. Senko, J. Moon, I. Yick, G. Varnavides, G., D. Gregurec, F. Koehler, P. Chiang, M. G. Christiansen, L. Y. Maeng, A. S. Widge, and P. Anikeeva, "Remote Magnetothermal Control of Adrenal Hormones," *Science Advances* 6: p. eaaz3734, 2020.

M. Kanik, S. Orguc, G. Varnavides, J. Kim, T. Benavides, D. Gonzalez, T. Akintilo, C. C. Tasan, A. P. Chandrakasan, Y. Fink, and P. Anikeeva, "Strain-Programmable Fiber-Based Artificial Muscle," *Science* 365: p. 145-150, 2019.

D. Shahriari, Z. J. G. Loke, I. Tafel, S. Park, P. Chiang, Y. Fink, P. Anikeeva, "Scalable Fabrication of Porous Microchannel Nerve Guidance Scaffolds with Complex Geometries," *Advanced Materials* 31: p. 1902021, 2019.

J. A. Frank, M.-J. Antonini, and P. Anikeeva, "Next-generation Interfaces for Studying Neural Function," Invited Review, *Nature Biotechnology*, 37: p. 1013-1023, 2019.

S. Rao, R. Chen, A. A. LaRocca, M. G. Christiansen, A. W. Senko, C. H. Shi, P. Chiang, G. Varnavides, J. Xue, Y. Zhou, S. Park, R. Ding, J. Moon, G. Feng, and P. Anikeeva, "Chemomagnetic Modulation of Targeted Neural Circuits," *Nature Nanotechnology* 4: p. 967-973, 2019.

S. Park, Y. Guo, X. Jia, H. K. Choe, B. Grena, J. Park, C. Lu, A. Canales, R. Chen, Y. S. Yim, G. B. Choi, Y. Fink, and P. Anikeeva, "One-step Optogenetics with Multifunctional Flexible Polymer Fibers," *Nature Neuroscience*, 20, 612-619, 2017.

C. Lu, S. Park, T. Richner, A. Derry, I. Brown, J. Kang, C. Hou, Y. Fink, C. T. Moritz, and P. Anikeeva, "Flexible and Stretchable Fibers for Optoelectronic Probing of Spinal Cord Circuits," *Science Advances*, 3, e1600955, 2017.

G. Romero, M. G. Christiansen, L. Stocche Barbosa, F. Garcia, and P. Anikeeva, "Localized Excitation of Neural Activity via Rapid Magnetothermal Drug Release," *Advanced Functional Materials*, 26: p. 6471-6478, 2016.

S. Schuerle, J. S. Dudani, M. G. Christiansen, P. Anikeeva, and S. N. Bhatia, "Magnetically Actuated Protease Sensors for in Vivo Tumor Profiling," *Nano Letts.*, 16: p. 6303-6310, 2016.

UNDERGRADUATE STUDENTS

Flor Garza Romero, DMSE

Melissa Hummel, DMSE

Katherine Kutina, AeroAstro

Katherine Lei, DMSE

Gabi Ogata, DMSE

Melissa Stok, DMSE

Veronica Will, DMSE

Alicia Yang, DMSE

SUPPORT STAFF

Cindy Higgins, Administrative Assistant

SELECTED PUBLICATIONS

J. Park, K. Jin, A. Sahasrabudhe, P. Chiang, J. H. Maalouf, F. Koehler, D. Rosenfeld, S. Rao, T. Tanaka, T. Khudiyev, Z. J. Schiffer, Y. Fink, O. Yizhar, K. Manthiram, P. Anikeeva, "In situ Electrochemical Generation of Nitric Oxide for Neuronal Modulation," *Nature Nanotechnology* 15: p. 690-697, 2020.

J. Park, A. Tabet, J. Moon, P. Chiang, F. Koehler, A. Sahasrabudhe, P. Anikeeva, "Remotely Controlled Proton Generation for Neuromodulation," *Nano Letts.* 20, p. 6535-6541, 2020.

G. Varnavides, A. Jermyn, P. Anikeeva, C. Felser, P. Narang, "Electron Hydrodynamics in Anisotropic Materials," *Nature Communications* 11, p. 4710, 2020.

George Barbastathis

Professor of Mechanical Engineering
Department of Mechanical Engineering
Singapore-MIT Alliance for Research and Technology

Computational imaging, machine learning, diffractive imaging, phase retrieval
in low photon condition.

Rm. 3-461C | 617-253-1960 | grab@mit.edu

RESEARCH SCIENTISTS AND STAFF

Kwabena K. Arthur
Maciej Baranski
Sharvaj Kubal

A. Goy, K. Arthur, S. Li, and G. Barbastathis, "Low Photon Count Phase Retrieval Using Deep Learning," *Physical Review Letters*, 121 (24), 243902, 2018.

POSTDOCTORAL ASSOCIATE

Mo Deng, Singapore-MIT Alliance for Research and Technology
Jungki Song, MechE
Lakshmi Venkatraman, Singapore-MIT Alliance for Research and Technology
Ziling Wu, MechE
Elizabeth Yin, Singapore-MIT Alliance for Research and Technology

GRADUATE STUDENTS

Van Coykendall, EECS
Zhen Guo, EECS
Iksung Kang, EECS
Subeen Pang, MechE
Qihang Zhang, EECS

SUPPORT STAFF

Irina Gaziyeva, Administrative Assistant

SELECTED PUBLICATIONS

I. Kang, A. Goy, and G. Barbastathis, "Dynamical Machine Learning Volumetric Reconstruction of Objects' Interiors From Limited Angular Views," *Light: Science and Applications*, 10(74), 2021.

S. Pang and G. Barbastathis, "Machine Learning Regularized Solution of The Lippmann-Schwinger Equation," *arXiv:2010.15117*, 2020.

I. Kang, A. Goy, and G. Barbastathis, "Limited-angle Tomographic Reconstruction of Dense Layered Objects by Dynamical Machine Learning," *arXiv:2007.10734*, 2020.

A. Goy, G. Rughoobur, S. Li, K. Arthur, A. I. Akinwande, and G. Barbastathis, "High-resolution Limited-angle Phase Tomography of Dense Layered Objects Using Deep Neural Networks," *Proceedings of the National Academy of Sciences*, 116 (40) 19848-19856, 2019.

S. Li and G. Barbastathis, "Spectral Pre-modulation of Training Examples Enhances the Spatial Resolution of the Phase Extraction Neural Network (PhENN)," *Optics Express*, 26 (22), 29340-29352, 2018.

Duane S. Boning

Clarence J. LeBel Professor of Electrical Engineering
Professor of Electrical Engineering & Computer Science
Department of Electrical Engineering & Computer Science

Design for manufacturability of processes, devices, and circuits. Understanding and reduction of variation in semiconductor, photonics and MEMS manufacturing, emphasizing statistical, machine learning, and physical modeling of spatial and operating variation in circuits, devices, and CMP, electroplating, spin coating, etch, and embossing processes.

Rm. 39-415a | 617-253-0931 | boning@mit.edu

GRADUATE STUDENTS

Hongge Chen, EECS
Felix Dumont, EECS and Sloan
Sally El-Henawy, EECS
Christopher Lang, EECS
Christopher Lui, EECS and Sloan
Damien Martin, EECS
Tareq Saqr, SDM
Tanya Smith, EECS
Fan-Keng Sun, EECS
Aik Jun Tan, EECS and Sloan
Peter Tran, EECS
Zhengxing Zhang, EECS

SUPPORT STAFF

Jami L. Mitchell, Administrative Assistant

SELECTED PUBLICATIONS

Z. Zhang, S. I. El-Henawy, A. Sadun, R. Miller, L. Daniel, J. K. White, and D. S. Boning, "Enabling Wavelength-Dependent Adjoint-Based Methods for Process Variation Sensitivity Analysis in Silicon Photonics," *J. of Lightwave Technology*, vol. 39, no. 6, pp. 1762-1769, Mar. 2021.

K. Yeo, D. Grullon, F.-K. Sun, D. Boning, and J. Kalagnanam, "Variational Inference Formulation for a Model-Free Simulation of a Dynamical System with Unknown Parameters by a Recurrent Neural Network," accepted, *SIAM J. on Scientific Computing*, Feb. 2021

J. H. Lee, G. Traverso, D. Ibarra-Zarate, D. S. Boning, and B. W. Anthony, "Ex Vivo and In Vivo Imaging Study of Ultrasound Capsule Endoscopy," *J. of Medical Devices*, vol. 14, no. 2, p. 021005, June 2020.

H. Zhang, H. Chen, C. Xiao, S. Goyal, R. Stanforth, B. Li, D. S. Boning, and C.-J. Hsieh, "Towards Stable and Efficient Training of Verifiably Robust Neural Networks," *International Conference on Learning Representations (ICLR)*, May 2020.

M. B. Alawieh, D. S. Boning, and D. Z. Pan, "Wafer Map Defect Patterns Classification using Deep Selective Learning," *ACM/IEEE Design Automation Conference (DAC)*, San Francisco, CA, July 2020.

Y. Wang, H. Zhang, H. Chen, D. Boning, and C.-J. Hsieh, "On Lp-norm Robustness of Ensemble Decision Stumps and Trees," *International Conference on Machine Learning (ICML)*, pp. 10104-10114, July 2020.

H. Chen, Y. Wang, H. Zang, C.-J. Hsieh, S. Si, Y. Li, and D. Boning, "Robustness Verifications for Ensemble Stumps and Trees," *3rd Workshop on Formal Methods for ML-Enabled Autonomous Systems (FoMLAS 2020)*, July 2020.

Z. Zhang, S. I. El-Henawy, R. Miller, and D. S. Boning, "Decomposed Representation of S-Parameters for Silicon Photonic Variation Analysis," *SPIE Optics + Photonics*, Proc. Vol. 11484, p. 1148408, Aug. 2020.

H. Chen, S. Si, Y. Li, C. Chelba, S. Kumar, D. Boning, and C.-J. Hsieh, "Multi-Stage Influence Function," *Advances in Neural Information Processing Systems (NeurIPS)*, vol. 33, Dec. 2020.

H. Zhang, H. Chen, C. Xiao, B. Li, M. Liu, D. Boning, and C.-J. Hsieh, "Robust Deep Reinforcement Learning against Adversarial Perturbations on Observations," *Advances in Neural Information Processing Systems (NeurIPS)*, vol. 33, Dec. 2020. (Spotlight presentation.)

H. Zhang, H. Chen, D. S. Boning, and C.-J. Hsieh, "Robust Reinforcement Learning on State Observations with Learned Optimal Adversary," *International Conference on Learning Representations (ICLR)*, May 2021.

D. Boning, S. E. El-Henawy, and Z. Zhang, "Process Variation-Aware Photonic Design," *OFC 2021*, June 2021.

Edward S. Boyden

Y. Eva Tan Professor in Neurotechnology at MIT
Co-Director, Center for Neurobiological Engineering
Departments of Brain and Cognitive Sciences, Media Arts and Sciences, Biological Engineering

Developing tools that enable the mapping of the molecules and wiring of the brain, the recording and control of its neural dynamics, and the repair of its dysfunction. Systematically analyzing and repairing normal and pathological-brain computations.

Rm. 46-2171C | 617-324-3085 | edboyden@mit.edu

RESEARCH SCIENTISTS AND STAFF

Bobae An, McGovern
Yosuke (Bandy) Bando, Visiting Scientist
Yi Cui, McGovern
Burcu Guner-Ataman, McGovern
Kylie Leung, McGovern
Shubhra Pandit, McGovern
Demian Park, McGovern
Matthew Sears, McGovern
Doug Weston, Lab Manager
Aimei Yang, McGovern
Jian-Ping Zhao, McGovern

Tay Won Shin, MAS
Anubhav Sinha, HST
Michael Skuhersky, BCS
Corban Swain, BE
Shiwei Wang, Chem
Zeguan Wang, MAS
Ruihan Zhang, MAS

SUPPORT STAFF

Macey Lavoie, Administrative Assistant
Lisa Lieberman, Senior Administrative Assistant
Fira Zainal, Administrative Assistant

POSTDOCTORAL ASSOCIATES

Shahar Bracha, McGovern
Ruixuan (Rui) Gao, McGovern
Jinyoung Kang, McGovern
Changyang Linghu, McGovern
Yangning Lu, McGovern
Yong Qian, McGovern
Nava Shmoel David, McGovern
Panagiotis (Panos) Symvoulidis, McGovern
Giovanni Talei Franzesi, McGovern
Gaojie Yang, McGovern
Chi Zhang, McGovern

SELECTED PUBLICATIONS

R. Gao, C. J. Yu, L. Gao, K. D. Piatkevich, R. L. Neve, J. B. Munro, S. Upadhyayula, E. S. Boyden, "A Highly Homogeneous Polymer Composed of Tetrahedron-like Monomers for High-isotropy Expansion Microscopy," *Nature Nanotechnology*, doi: 10.1038/s41565-021-00875-7. Online ahead of print, 2021.

S. Alon, D. R. Goodwin, A. Sinha, A. T. Wassie, F. Chen, E. R. Daugharthy, Y. Bando, A. Kajita, A. G. Xue, K. Marrett, R. Prior, Y. Cui, A. C. Payne, C. C. Yao, H. J. Suk, R. Wang, C. J. Yu, P. Tillberg, P. Reginato, N. Pak, S. Liu, S. Punthambaker, E. P. R. Iyer, R. E. Kohman, J. A. Miller, E. S. Lein, A. Lako, N. Cullen, S. Rodig, K. Helvie, D. L. Abravanel, N. Wagle, B. E. Johnson, J. Klughammer, M. Slyper, J. Waldman, J. Jané-Valbuena, O. Rozenblatt-Rosen, A. Regev; IMAXT Consortium, G. M. Church, A. H. Marblestone, and E. S. Boyden, "Expansion Sequencing: Spatially Precise In Situ Transcriptomics in Intact Biological Systems," *Science* 371(6528):eaax2656, 2021.

A. C. Payne, Z. D. Chiang, P. L. Reginato, S. M. Mangiameli, E. M. Murray, C. C. Yao, S. Markoulaki, A. S. Earl, A. S. Labade, R. Jaenisch, G. M. Church, E. S. Boyden, J. D. Buenrostro, F. Chen, "In Situ Genome Sequencing Resolves DNA Sequence and Structure in Intact Biological Samples," *Science*, doi:10.1126/science.aay3446. Online ahead of print, 2020.

C. Linghu, S. L. Johnson, P. A. Valdes, O. A. Shemesh, W. M. Park, D. Park, K. D. Piatkevich, A. T. Wassie, Y. Liu, B. An, S. A. Barnes, O. T. Celiker, C.-C. Yao, C.-C. (Jay) Yu, R. Wang, K. P. Adamala, M. F. Bear, A. E. Keating, and E. S. Boyden, "Spatial Multiplexing of Fluorescent Reporters For Imaging Signaling Network Dynamics," *Cell* 183(6):1682-1698, 2020.

GRADUATE STUDENTS

Jenna Lauren Aronson, BCS
Nick Barry, MAS
Cristina Torres Caban, BE
Orhan Celiker, EECS
Alexi Georges Choueiri, BCS
Danielle Orozco Cosio, BCS
Amauche Emenari, BCS
Daniel Estandian, BCS
Daniel Goodwin, MAS
Kettner Griswold, MAS
Jordan Harrod, HST
Brennan Jackson, HST
Shannon Johnson, MAS
Irena Victoria King, HST
Yixi Liu, EECS
Mitchell Murdock, BCS
Daniel Oran, MAS
Andrew Payne, MAS
Paul Reginato, MAS
Cipriano Romero, EECS
Catherine Marin Della Santina, BE
Margaret Elizabeth Schroeder, BCS
Sarah Sclarsic, MAS

Vladimir Bulović

MIT.nano Director

Fariborz Maseeh (1990) Professor of Emerging Technology
Department of Electrical Engineering and Computer Science

Physical properties of nanostructured materials and composite structures and their use in development of electronic, excitonic, optical, and nano-mechanical devices. Applications of nanostructures in large-scale technologies.

Rm. 13-3138 | 617-253-7012 | bulovic@mit.edu

RESEARCH SCIENTISTS

Jeremiah Mwaura, RLE

Annie Wang, RLE

POSTDOCTORAL ASSOCIATES

Dane deQuilettes, RLE

Benjia Dak Dou, RLE

Apoorva Murarka, RLE

Anurag Panda, RLE

GRADUATE STUDENTS

Roberto Brenes, EECS, NSF Fellow

Matthew Ruiyan Chua, EECS, A*STAR Fellow

Jinchi Han, EECS

Madeliene Laitz, EECS, NSF Fellow

Mayuran Saravanapavanantham, EECS, NSF Fellow

Melany Sponseller, EECS

Richard Swartout, EECS

Ella Wassweiler, EECS, NSF Fellow

Sihan Jonas Xie, DMSE

VISITOR

Emma Belliveau, U. of Waterloo

SUPPORT STAFF

Samantha Farrell, Sr. Administrative Assistant

SELECTED PUBLICATIONS

M.M. Tavakoli, J.H. Park, J. Mwaura, M. Saravanapavanantham, V. Bulović, J. Kong, "Monolayer Hexagonal Boron Nitride: An Efficient Electron Blocking Layer in Organic Photovoltaics," *Advanced Functional Materials*, 2101238 (2021).

F. Niroui, M. Saravanapavanantham, J. Han, J.J. Patil, T.M. Swager, J.H. Lang, V. Bulović, "Hybrid Approach to Fabricate Uniform and Active Molecular Junctions," *Nano Letters* 21, 1606-1612 (2021).

J.J. Yoo, G. Seo, M.R. Chua, T.G. Park, Y. Lu, F. Rotermund, Y.K. Kim, C.S. Moon, N.J. Jeon, J.-P. Correa-Baena, V. Bulović, S.S. Shin, M.G. Bawendi, J. Seo, "Efficient perovskite solar cells via improved carrier management," *Nature* 590 (7847), 587-593 (2021).

T. Sannicolo, W.H. Chae, J. Mwaura, V. Bulović, J.C. Grossman, "Silver Nanowire Back Electrode Stabilized with Graphene Oxide Encapsulation for Inverted Semitransparent Organic Solar Cells with Longer Lifetime," *ACS Applied Energy Materials* 4, 1431-1441 (2021).

M. Wu, T.A. Lin, J.O. Tjepelt, V. Bulović, M.A. Baldo, "Nanocrystal-Sensitized Infrared-to-Visible Upconversion in a Microcavity under Subsolar Flux," *Nano Letters* 21, 1011-1016 (2021).

S.S. Peled, M. Perez, D. Meron, A. Osherov, V. Bulović, E.A. Katz, Y. Golan, "Morphology control of perovskite films: a two-step, all solution process for conversion of lead selenide into methylammonium lead iodide," *Materials Chemistry Frontiers* 5, 1410-1417 (2021).

M. Perez, S.S. Peled, T. Templeman, A. Osherov, V. Bulović, E.A. Katz, Y. Golan, "A Two-Step, All Solution Process for Conversion of Lead Sulfide to Methylammonium Lead Iodide Perovskite Thin Films," *Thin Solid Films* 714, 138367 (2020).

R. Swartwout, R. Patidir, E. Belliveau, B. Dou, D. Beynon, P. Greenwood, N. Moody, M. Bawendi, T.M. Watson, V. Bulović, "Predicting Low Toxicity and Scalable Solvent Systems for High Speed Roll-to-Roll Perovskite Manufacturing," *ChemRxiv* preprint 13221851.v1 (2020).

R. Zimmerman, A. Panda, V. Bulović, "Techno-economic assessment and deployment strategies for vertically-mounted photovoltaic panels," *Applied Energy* 276, 115149 (2020).

S.S. Peled, M. Perez, A. Osherov, V. Bulović, Y. Golan, "Morphology control in chemical solution deposited lead selenide thin films on fluorine-doped tin oxide," *Thin Solid Films* 710, 138256 (2020).

S. Xie, H. Zhu, M. Li, V. Bulović, "Voltage-Controlled Reversible Modulation of Colloidal Quantum Dot Thin Film Photoluminescence," arXiv preprint arXiv:2008.05375 (2020).

M. V. Khenkin, et al, "Consensus statement for stability assessment and reporting for perovskite photovoltaics based on ISOS procedures," *Nature Energy* 5, 35-49, 2020.

N. Moody, S. Sesena, D.W. deQuilettes, B.D. Dou, R. Swartwout, J.T. Buchman, A. Johnson, U. Eze, R. Brenes, M. Johnston, C.L. Haynes, V. Bulović, M.G. Bawendi, "Assessing the regulatory requirements of lead-based perovskite photovoltaics," *Joule* 4, 970-974 (2020).

S. Xie, A. Osherov, V. Bulović, "All-vacuum-deposited inorganic cesium lead halide perovskite light-emitting diodes," *APL Materials* 8 (5), 051113 (2020).

Jacopo Buongiorno

TEPCO Professor, Department of Nuclear Science and Engineering
MacVicar Faculty Fellow
Director, Center for Advanced Nuclear Energy Systems (CANES),
Director of Science and Technology, Nuclear Reactor Laboratory (NRL)

GRADUATE STUDENTS

Isabel Naranjo De Candido, NSE
Edward James Garcia, NSE
Xyniao (Anna) Liang, NSE
Lorenzo Venneri, NSE

UNDERGRADUATE STUDENTS

Leanne S. Galanek, NSE
Lucy M. Nester, NSE
Abdalla Osman, MechE
Katherine Zhao, EECS

SUPPORT STAFF

Carolyn Carrington, Administrative Assistant

SELECTED PUBLICATIONS

P. Eash-Gates, M. M. Klemun, G. Kavlak, J. McNerney, J. Buongiorno, and J. E. Trancik, "Sources of Cost Overrun in Nuclear Power Plant Construction Call for a New Approach to Engineering Design", *Joule*, 4, 2348-2373, Nov. 2020.

K. Dawson, M. Corradini, J. Parsons, and J. Buongiorno, "Deep Decarbonization of the Power Sector: the Need for a Low-Carbon, Dispatchable, Scalable and Widely Available Energy Source", *The Bridge*, 50, 3, Sep. 2020.

A. Kossolapov, F. Chavagnat, R. Nop, N. Dorville, B. Phillips, J. Buongiorno, and M. Bucci, "The Boiling Crisis of Water Under Exponentially Escalating Heat Inputs in Subcooled Flow Boiling at Atmospheric Pressure", *Int. J. Heat Mass Transfer*, 160, 120137, 2020.

J. Conway, N. Todreas, J. Halsema, C. Guryan, A. Birch, T. Isdanavich, J. Florek, J. Buongiorno, and M. Golay, "Physical Security Analysis and Simulation of the Multi-Layer Security System for the Offshore Nuclear Plant (ONP)", *Nuc. Eng. Design*, 352, 2019.

G. Su, F.P. D'Aleo, B. Phillips, R. Streich, E. Al-Safran, J. Buongiorno, and H. M. Prasser, "On the Oscillatory Nature of Heat Transfer in Steady Annular Flow", *International Communications in Heat and Mass Transfer*, 108, 104328, 2019.

J. Buongiorno, M. Corradini, J. Parsons, and D. Petti, "The Future of Nuclear Energy in a Carbon-constrained World," *IEEE Power and Energy Magazine*, Mar. 2019.

Innovations in nuclear technology; boiling heat transfer; nuclear reactor design and safety; offshore floating nuclear power plant; nanofluids for nuclear applications.

Rm. 24-206 | 617-253-7316 | jacopo @ mit . edu

J. Parsons, J. Buongiorno, M. Corradini, and D. Petti, "A Fresh Look at Nuclear Energy," *Science*, vol. 363, issue 6423, p. 105, 11 Jan. 2019.

S. Afkhami, J. Buongiorno, A. Guion, S. Popinet, R. Scardovelli, and S. Zaleski, "Transition in a Numerical Model of Contact Line Dynamics and Forced Dewetting," *J. Computational Physics*, 374, pp. 1061-1093, 2018.

A. Richenderfer, A. Kossolapov, J. H. Seong, G. Saccone, E. Demarly, R. Kommajosyula, E. Baglietto, J. Buongiorno, and M. Bucci, "Investigation of Subcooled Flow Boiling and CHF using High-resolution Diagnostics Experimental Thermal and Fluid Science," *Experimental Thermal and Fluid Science*, 99, pp. 35-58, 2018.

J. L. Moran, A. L. Cottrill, J. D. Benck, P. Liu, Z. Yuan, M. S. Strano, and J. Buongiorno, "Noble-Gas-Infused Neoprene Closed-cell Foams Achieving Ultra-low Thermal Conductivity Fabrics," *RSC Advances*, 8, pp. 21389-21398, 2018.

M. Trojer, R. Azizian, J. Paras, T. McKrell, K. Atkhen, M. Bucci, and J. Buongiorno, "A Margin Missed: the Effect of Surface Oxidation on CHF Enhancement in IVR Accident Scenarios," *Nucl. Eng. Design*, 335, pp. 140-150, 2018.

Y. Zhang, J. Buongiorno, M. Golay, and N. Todreas, "Safety Analysis of a 300 MWe Offshore Floating Nuclear Power Plant in Marine Environment," *Nuclear Technology*, 2018.

E. Lizarraga-Garcia, J. Buongiorno, E. Al-Safran, and D. Lakehal, "A Broadly-applicable Unified Closure Relation for Taylor Bubble Rise Velocity in Pipes with Stagnant Liquid," *Int. J. Multiphase Flow*, 89, pp. 345-358, 2017.

R. Sugrue and J. Buongiorno, "A Modified Force-balance Model for Prediction of Bubble Departure Diameter in Subcooled Flow Boiling," *Nuc. Eng. Design*, pp. 717-722, 2016.

M. Tetreault-Friend, R. Azizian, M. Bucci, T. McKrell, J. Buongiorno, M. Rubner, and R. Cohen, "Critical Heat Flux Maxima Resulting from the Controlled Morphology of Nanoporous Hydrophilic Surface Layers," *Applied Physics Lett.*, 108, 243102, 2016.

Anantha Chandrakasan

Dean of Engineering
Vannevar Bush Professor of Electrical Engineering &
Computer Science
Department of Electrical Engineering and Computer Science

Design of digital integrated circuits and systems. Energy efficient implementation of signal processing, communication and medical systems. Circuit design with emerging technologies.

Rm. 38-107 | 617-258-7619 | anantha@mit.edu

POSTDOCTORAL ASSOCIATE

Yeseul Jeon

GRADUATE STUDENTS

Aya Amer, EECS (co-supervised with M. Shulaker)
Mohamed Radwan Abdelhamid, EECS (co-supervised
with F. Adib)
Maitreyi Ashok, EECS
Utsav Banerjee, EECS
Kaustav Brahma, EECS
Minghan Chao, EECS (co-supervised with M. Shulaker)
Ruicong Chen, EECS
Di-Chia Chueh, EECS (co-supervised with J. Glass)
Gloria (Yu Liang) Fang, EECS
Alex Ji, EECS
Eunseok Lee, EECS (co-supervised with R. Han)
Kyungmi Lee, EECS
Saurav Maji, EECS
Vipasha Mittal, EECS (co-supervised with H-S. Lee)
Rishabh Mittal, EECS (co-supervised with H-S. Lee)
Miaorong Wang, EECS
Jongchan Woo, EECS (co-supervised with Rabia T.
Yazicigil)
Deniz Yildirim, EECS

VISITING SCHOLARS

Chiraag Juvekar
Rabia Tugce Yazicigil, Boston University

SUPPORT STAFF

Margaret Flaherty, Senior Administrative Assistant
Jessie-Leigh Thomas, Administrative Assistant

SELECTED PUBLICATIONS

T. Jeong, A. P. Chandrakasan, and H. S. Lee, "S2ADC: A 12-bit, 1.25MS/s Secure SARADC with Power Side-Channel Attack Resistance," *IEEE Journal of Solid-State Circuits*, vol. 56, no. 3, pp.844-854, Mar. 2021.

M. I. W. Khan, M. I. Ibrahim, C. S. Juvekar, W. Jung, R. T. Yazicigil, A. P. Chandrakasan, and R. Han, "CMOS THz-ID: A 1.6-mm² Package-Less Identification Tag Using Asymmetric Cryptography and 260-GHz Far-Field Backscatter Communication," *IEEE Journal of Solid-State Circuits*, vol. 56, no. 2, pp.340-354, Feb. 2021.

S. Maji, U. Banerjee, and A. P. Chandrakasan, "Leaky Nets: Recovering Embedded Neural Network Models and Inputs through Simple Power and Timing Side-Channels - Attacks and Defenses," *IEEE Internet of Things Journal*, Feb. 2021.

A. J. Wentworth, J. D. Byrne, S. Orguc, J. Sands, S. Maji, C. Tov, S. Babae, H. Huang, H. Boyce, P. R. Chai, S. Min, C. Li, J. N. Chu, A. Som, S. L. Becker, M. Gala, A. P. Chandrakasan, and G. Traverso, "Prospective Evaluation of the Transparent, Elastomeric, Adaptable, Long-Lasting (TEAL) Respirator," *ACS Pharmacology & Translational Science*, vol. 3, no. 6, pp.1076-1082, Nov. 2020.

Z. Ji, W. Jung, J. Woo, K. Sethi, S. Lu, and A. P. Chandrakasan, "CompAcc: Efficient Hardware Realization for Processing Compressed Neural Networks Using Accumulator Arrays," *IEEE Asian Solid-State Circuits Conference (A-SSCC)*, Nov. 2020.

M. R. Abdelhamid, R. Chen, J. Cho, A. P. Chandrakasan, and F. Adib, "Self-Reconfigurable Micro-Implants for Cross-Tissue Wireless and Batteryless Connectivity," *Annual International Conference on Mobile Computing and Networking (MobiCom)*, Sep. 2020.

R. T. Yazicigil, P. M. Nadeau, D. Richman, C. Juvekar, S. Maji, U. Banerjee, S. H. Fuller, M. R. Abdelhamid, N. Desai, M. I. Ibrahim, M. I. W. Khan, W. Jung, R. Han, and A. P. Chandrakasan, "Beyond Crypto: Physical-Layer Security for Internet of Things Devices," *IEEE Solid-State Circuits Magazine*, vol. 12, no. 4, pp.66-78, Fall 2020.

S. Orguc, J. Sands, A. Sahasrabudhe, P. Anikeeva, and A. P. Chandrakasan, "Modular Optoelectronic System for Wireless, Programmable Neuromodulation During Free Behavior," *Annual International Conference of the IEEE Engineering in Medicine and Biology Society (EMBC)*, Jul. 2020.

S. Maji, U. Banerjee, S. H. Fuller, M. R. Abdelhamid, P. M. Nadeau, R. T. Yazicigil, and A. P. Chandrakasan, "A Low-Power Dual-Factor Authentication Unit for Secure Implantable Devices," *IEEE Custom Integrated Circuits Conference (CICC)*, Mar. 2020.

Yufeng (Kevin) Chen

Assistant Professor of Electrical Engineering Department of
Electrical Engineering & Computer Science

Biomimetic Robotics, Insect-scale robots, intermediate Reynolds number fluid dynamics, unsteady aerodynamics, soft artificial muscles, electroactive polymer actuators

Rm. 10-140H | 617-253-7351 | yufengc@mit.edu

GRADUATE STUDENTS

Suhan Kim, EECS

Zhijian Ren, EECS

UNDERGRADUATE STUDENT

Cathleen Arase, MechE

SUPPORT STAFF

Catherine Bourgeois, Administrative Assistant

SELECTED PUBLICATIONS

Y. Chen, S. Xu, Z. Ren, and P. Chirarattananon, "Collision Resilient Insect-Scale Soft-Actuated Aerial Robots with High Agility," *IEEE Transaction on Robotics*. Early Access, 2021.

Y. Chen, N. Doshi, and R. J. Wood, "Inverted and Inclined Climbing Using Capillary Adhesion in a Quadrupedal Insect-Scale Robot," *IEEE Robotics and Automation Letters*. 5(3), 4820-4827, 2020.

K. Becker, Y. Chen, and R. J. Wood, "Mechanically Programmable Dip Molding of High Aspect Ratio Soft Actuator Arrays," *Advanced Functional Materials*. 1908919, 2020.

Y. Chen, H. Zhao, J. Mao, P. Chirarattananon, E. H. Helbling, N.-s.P. Hyun, R. D. Clarke, and R. J. Wood, "Controlled Flight of a Microrobot Powered by Soft Artificial Muscles," *Nature*. 575(7782), 324-329, 2019.

Y. Chen, N. Doshi, N. Goldberg, H. Wang, and R. J. Wood, "Controllable Water Surface to Underwater Transition Through Electrowetting in a Hybrid Terrestrial-aquatic Microrobot," *Nature Communications*. 9(1), pp 2495, 2018.

Y. Chen, H. Wang, E. F. Helbling, N. T. Jafferis, R. Zufferey, A. Ong, K. Ma, N. Gravish, P. Chirarattananon, M. Kovac, and R. J. Wood, "A Biologically Inspired, Flapping-wing, Hybrid Aerial-aquatic Microrobot," *Science Robotics*. 2(11), eaao5619, 2017.

Y. Wang*, X. Yang*, Y. Chen*, D. K. Wainwright, C. P. Kenaley, Z. Gong, Z. Liu, H. Liu, J. Guan, T. Wang, J. C. Weaver, R. J. Wood, and L. Wen, "A Biorobotic Adhesive Disc for Underwater Hitchhiking Inspired by the Remora Suckerfish," *Science Robotics*. 2(10), eaan8072, 2017. (*equal contribution).

P. Chirarattananon, Y. Chen, E. F. Helbling, K. Y. Ma, R. Cheng, and R. J. Wood, "Dynamics and Flight Control of a Flapping-wing Robotic Insect in the Presence of Wind Gusts," *Interface Focus*. 7(1), 20160080, 2017.

Y. Chen, N. Gravish, A. L. Desbiens, R. Malka, and R. J. Wood, "Experimental and Computational Studies of the Aerodynamic Performance of a Flapping and Passively Rotating Insect Wing," *Journal of Fluid Mechanics*. 791, pp.1-33, 2016.

S. Wang, L. Li, Y. Chen, Y. Wang, W. Sun, J. Xiao, D. Wainwright, W. Sun, T. Wang, R. Wood, and L. Wen, "A Bio-robotic Remora Disc with Attachment and Detachment Capabilities for Reversible Underwater Hitchhiking," *IEEE/RSJ International Conference on Intelligent Robots and Systems (ICRA)*. 4653-4659, 2019.

Y. Chen, A. Ong, and R. J. Wood, "An Efficient Method for the Design and Fabrication of 2D Laminate Robotic Structures," *IEEE International Conference on Real-time Computing and Robotics (RCAR)*, 2018.

Y. Chen, K. Ma, and R. J. Wood, "Influence of Wing Morphological and Inertial Parameters on Flapping Flight Performance," *IEEE/RSJ International Conference on Intelligent Robots and Systems (IROS)*. 2329-2336, 2016.

Y. Chen, E. F. Helbling, N. Gravish, K. Ma, and R. J. Wood, "Hybrid Aerial and Aquatic Locomotion in an At-scale Robotic Insect," *IEEE/RSJ International Conference on Intelligent Robots and Systems (IROS)*. 331-338, 2015.

N. Gravish, Y. Chen, S. A. Combes, and R. J. Wood, "High-throughput Study of Flapping Wing Aerodynamics for Biological and Robotic Applications," *IEEE/RSJ International Conference on Intelligent Robots and Systems (IROS)*. 3397-3403, 2014. (*equal contribution)

R. Malka, A. L. Desbiens, Y. Chen, and R. J. Wood, "Principles of Microscale Flexure Hinge Design for Enhanced Endurance," *IEEE/RSJ International Conference on Intelligent Robots and Systems (IROS)*. 2879-2885, Sep. 2014.

Luca Daniel

Professor

Department of Electrical Engineering & Computer Science

Development of numerical techniques: parameterized model order reduction, uncertainty quantification, inverse problems and robust optimization for high dimension parameter spaces. Current applications: magnetic resonance imaging; electrical power distribution networks; robustness of deep neural networks.
Rm. 36-849 | 617-253-2631 | luca@mit.edu

POSTDOCTORAL ASSOCIATES

Ian Butterworth, EECS (co-advisor Martha Gray)
Praneeth Namburi, EECS
Yujia Yang, EECS (co-advisor Karl Berggren)

T. Bradde, S. Chevalier, M. De Stefano, S. Grivet-Talocia, L. Daniel, "Handling Initial Conditions in Vector Fitting for Real Time Modeling of Power System Dynamics," in *Energies Journal*, accepted 2021.

GRADUATE STUDENTS

Adina Bechhofer, EECS (co-advisor Karl Berggren)
Samuel Chevalier, MechE
Durgesh Das, LGO
Ismail Degani, EECS (co-advisor Hakho Lee)
Quang P. Kieu, EECS (co-advisor Martha Gray)
Ching-Yun (Irene) Ko, EECS
Jeet Mohapatra, EECS
Oliver Regele, LGO
Jose E. C. Serralles, EECS
Lydia Sherwood, LGO
Marco Turchetti, EECS (co-advisor Karl Berggren)
Tsui-Wei (Lily) Weng, EECS
Wang Zhang, MechE

I. Giannakopoulos, J. E. C. Serralles, L. Daniel, D. K. Sodickson, A. G. Polimeridis, J. K. White, and R. Lattanzi, "Magnetic-resonance-based Electrical Property Mapping Using Global Maxwell Tomography with an 8-channel Head Coil at 7 Tesla: a Simulation Study," in *IEEE Transactions on Biomedical Engineering*, vol. 68, no. 1, pp. 236-246, Jan. 2021.

J. Mohapatra, C.-Y. Ko, T.-W. Weng, S. Liu, P.-Y. Chen, L. Daniel, "Hidden Cost of Randomized Smoothing," *AISTATS*, 2021.

J. Mohapatra, C.-Y. Ko, T.-W. Weng, P.-Y. Chen, S. Liu, and L. Daniel, "Higher-Order Certification For Randomized Smoothing," *NeurIPS*, Dec. 2020.

UNDERGRADUATE STUDENTS

Pawan Goyal, EECS
Alexander Gu, EECS
Melissa Hummel, BioE
Wonjune Kang, EECS
Tuomas Oikarinen, EECS
Victor Rong, EECS
Marina Zhang, EECS

Z. Zhang, S. I. El-Henawy, A. Sadun, R. Miller, L. Daniel, J. K. White, and D. Boning, "Enabling Wavelength-Dependent Adjoint-Based Methods for Process Variation Sensitivity Analysis in Silicon Photonics," *IEEE Journal of Lightwave Technology*. Nov. 2020.

S. Genovesi, I. R. Butterworth, J. E. C. Serralles, and L. Daniel, "Metasurface Matching Layers for Enhanced Electric Field Penetration into the Human Body," *IEEE Access* 8: 197745-197756, Oct. 2020.

VISITORS

Roberta Bardini, Politecnico di Torino
Tommaso Bradde, Politecnico di Torino
Marco De Stefano, Politecnico di Torino
David Esseni, Univ. di Udine
Stefano Grivet, Politecnico di Torino
Giambattista Gruosso, Politecnico di Milano
Luca Schenato, Univ. di Padova
Tommaso Rollo, Univ. di Udine
Valentin De La Rubia, Universidad Politecnica de Madrid

T. Bradde, S. Grivet-Talocia, G. C. Calafiore, A. V. Proskurnikov, Z. Mahmood, L. Daniel, "On Dissipativity Conditions for Linearized Models of Locally Active Circuit Blocks," *IEEE 29th Conference on Electrical Performance of Electronic Packaging and Systems (EPEPS)*, Oct. 2020.

T. P. Oikarinen, T.-W. Weng, and L. Daniel, "Robust Deep Reinforcement Learning through Adversarial Loss," *International Conference on Machine Learning, Uncertainty & Robustness in Deep Learning Workshop*. Jul. 2020.

SUPPORT STAFF

Chadwick Collins, Administrative Assistant

SELECTED PUBLICATIONS

M. Turchetti, Y. Yang, M. R. Bionta, A. Nardi, L. Daniel, K. K. Berggren, and P. D. Keathley, "Emission Behavior of Planar Nano-Vacuum Field Emitters," in *34th Intern. Vacuum Nanoelectronics Conf. (IVNC)*, Jul. 2021.

Jesús A. del Alamo

Donner Professor
Professor of Electrical Engineering
Department of Electrical Engineering & Computer Science

Nanometer-scale III-V compound semiconductor transistors for future digital, power, RF, microwave and millimeter wave applications. Reliability of compound semiconductor transistors. Diamond transistors. Ionic non-volatile programmable synapses.

Rm. 38-246 | 617-253-4764 | alamo@mit.edu

RESEARCH SCIENTIST

Alon Vardi, MTL

GRADUATE STUDENTS

Ebrahim Al Johani, EECS
Taekyong Kim, EECS
Ethan Lee, EECS
Aviram Massuda, EECS
Murat Onen, EECS
Yanjie Shao, EECS

VISITOR

Jin Soak Kim, Samsung Electronics

SUPPORT STAFF

Elizabeth Kubicki, Administrative Assistant

X. Yao, K. Klyukin, W. Lu, M. Onen, S. Ryu, D. Kim, N. Emond, I. Waluyo, A. Hunt, J. A. del Alamo, J. Li, and B. Yildiz, "Protonic Solid-State Electrochemical Synapse for Physical Neural Networks," *Nature Communications*, 11:3134, DOI: 10.1038/s41467-020-16866-6. 2020.

J. A. del Alamo, "Nanoscale III-V Electronics," *2020 SEMI Advanced Semiconductor Manufacturing Conference (ASMC 2020)*, Invited Keynote, Online, Aug. 24-26, 2020.

J. A. del Alamo, "Nanoscale III-V Electronics: InGaAs FinFETs and Nanowire MOSFETs," *Latin America Electron Devices Conference*, San Jose, Costa Rica, Invited Keynote. Feb. 25-28, 2020.

SELECTED PUBLICATIONS

X. Cai, A. Vardi, J. Grajal, and J. A. del Alamo, "Ballistic Mobility and Injection Velocity in Nanoscale InGaAs FinFETs," *2020 IEEE International Electron Devices Meeting*, Online, pp. 172-175. Dec. 12-18, 2020,

T. Kim, J. A. del Alamo, and D. A. Antoniadis, "Dynamics of HfZrO₂ Ferroelectric Structures: Experiments and Models," *2020 IEEE International Electron Devices Meeting*, Online, pp. 441-444. Dec. 12-18, 2020

M. Emond, X. Yao, M. Onen, S. Ryu, J. A. del Alamo, J. Li, and B. Yildiz, "Proton Intercalation in Solid-State Electrochemical Synapse for Energy-Efficient Neuromorphic Computing," *Materials Research Society Fall Meeting & Exhibit*, Boston, MA, Nov. 27-Dec. 4, 2020.

A. Vardi, M. Tordjman, R. Kalish, and J. A. del Alamo, "Refractory W Ohmic Contacts to H-Terminated Diamond," *IEEE Transactions on Electron Devices*, Vol. 67, No. 9, pp. 3516-3521, DOI: 10.1109/TED.2020.3009174. Sep. 2020.

X. Cai, A. Vardi, J. Grajal, and J. A. del Alamo, "A New Technique for Mobility Extraction in MOSFETs in the Presence of Prominent Gate Oxide Trapping: Application to InGaAs MOSFETs," *IEEE Transactions on Electron Devices*, Vol. 67, No. 8, pp. 3075-3081, DOI: 10.1109/TED.2020.3003844. Aug. 2020.

Dirk R. Englund

Associate Professor

Department of Electrical Engineering & Computer Science

Quantum Communications, Quantum Computing, and Quantum Sensing:
Devices and systems.

Rm. 36-351 | 617-324-7014 | englund@mit.edu

RESEARCH SCIENTISTS

Ryan Hamerly, RLE
Matthew Trusheim, ISN

POSTDOCTORAL ASSOCIATES

Jacques Carolan, Marie Curie Fellow
Lorenzo De Santis, RLE
Chitraleema Chakraborty, RLE
Carlos Errando Herranz, RLE
Laura Kim, IC Postdoctoral Fellow
Stefan Krastanov, RLE
Adrian Menssen, Humboldt Fellow
Matt Trusheim, ARL Postdoctoral Fellow

GRADUATE STUDENTS

Saamil Bandyopadhyay, NSF Fellow
Eric Bersin, NTSRF fellow
Darius Bunandar, Physics
Uttara Chakraborty, NDSEG Fellow
Kevin Chen, NSF Fellow
Hyeonrak (Chuck) Choi
Ian Christen, NDSEG Fellow
Ronald Davis, RLE
Erik Eisenach, NSF Fellow
Christopher Foy, NSF fellow
Jordan Goldstein, NSF fellow
Zhen Guo, EECS
Isaac Harris, EECS
Hugo Larocque, NSERC Postgraduate Scholarship
Tsung-Ju Lu, NDSEG Fellow
Hyowon Moon, EECS
Christopher Panuski, Hertz Fellow
Cheng Peng, EECS
Mihika Prabhu, NSF Fellow
Liane Sarah Bel Bernstein, NSERC Postgraduate
Scholarship
Alex Sludds, NSF Fellow
Madison Sutula
Michael Walsh, EECS
Noel Wan, EECS
Reggie Wilcox, EECS

UNDERGRADUATE STUDENT

Yuan Lee, EECS & Physics

SUPPORT STAFF

Janice Balzer, Administrative Assistant

SELECTED PUBLICATIONS

C. J. Ciccarino, J. Flick, I. B. Harris, M. E. Trusheim, D. Englund, P. Narang, "Strong Spin-Orbit Quenching via the Product Jahn-Teller Effect in Neutral Group IV Artificial Atom Qubits in Diamond," *NPJ Quantum Information* 75: 2020.

E. D. Walsh, W. Jung, G.-H. Lee, D. K. Efetov, B.-I. Wu, K.-F. Huang, T. A. Ohki, T. Taniguchi, K. Watanabe, P. Kim, D. Englund, K. C. Fong, "Josephson-junction infrared single-photon detector," to appear in *Science*, 2021.

M. K. Bhaskar, R. Riedinger, B. Machielse, D. S. Levonian, C. T. Nguyen, E. N. Knall, H. Park, D. Englund, M. Lončar, D. D. Sukachev, and M. D. Lukin, "Experimental demonstration of memory-enhanced quantum communication," *Nature* 580, pages 60–64: 2020.

C. Roques-Carmes, Y. Shen, C. Zanoci, M. Prabhu, F. Atieh, L. Jing, T. Dubcek, V. Ceperic, J. D. Joannopoulos, D. Englund, and M. Soljacic, "Photonic Recurrent Ising Sampler," *Nature Communications* 11, Article number: 249; 2020.

L. Bernstein, A. Sludds, R. Hamerly, V. Sze, J. Emer, D. Englund, "Freely scalable and reconfigurable optical hardware for deep learning," *Scientific Reports*, 2021.

S. Castilla, I. Vangelidis, V.-V. Pusapati, J. Goldstein, M. Autore, T. Slipchenko, K. Rajendran, S. Kim, K. Watanabe, T. Taniguchi, L. Martin-Moreno, D. Englund, K.-J. Tielrooij, R. Hillenbrand, E. Lidorikis, and F. H. L. Koppens, "Plasmonic antenna coupling to hyperbolic phonon-polaritons for sensitive and fast mid-infrared photodetection with graphene," *Nature Communications* 11, Article number: 4872; 2020.

J. Carolan, M. Mohseni, J. P. Olson, M. Prabhu, C. Chen, D. Bunandar, M. Y. Niu, N. C. Harris, F. N. C. Wong, M. Hochberg, S. Lloyd, and D. Englund, "Variational Quantum Unsampling on a Quantum Photonic Processor," *Nature Physics*, 2020.

D. Bunandar, L. C. G. Govia, H. Krovi, and D. Englund, "Numerical finite-key analysis of quantum key distribution," *NPJ Quantum Information* 6, Article number: 104; 2020.

Jongyoon Han

Professor

Department of Electrical Engineering & Computer Science

Department of Biological Engineering

Nanofluidic / Microfluidic technologies for advanced biomolecule analysis and sample preparation: cell and molecular sorting, novel nanofluidic phenomena, biomolecule separation and pre-concentration, seawater desalination and water purification.

Rm. 36-841 | 617-253-2290 | jyhan@mit.edu

POSTDOCTORAL ASSOCIATES

Hyungkook Jeon, RLE

Kerwin Keck, SMART Center

Hyukjin Kwon, RLE

Taehong Kwon, RLE

Yaoping Liu, SMART Center

Ishita Shrivastava, RLE

Smitha Thamarath Surendran, SMART Center

Dahou Yang, SMART Center

Junghyo Yoon, RLE

Cong Wang, SMART Center

M. Shang, S. B. Lim, K. Jiang, Y.-S. Yap, B. L. Khoo, J. Han, and C. T. Lim, "Microfluidic Studies of Hydrostatic Pressure-enhanced Doxorubicin Resistance in Human Breast Cancer Cells," *Lab on a Chip*, 21, 746-754, 2021.

M. Shang, T. Kwon, J.-F. P. Hamel, C. T. Lim, B. L. Khoo, and J. Han, "Investigating the Influence of Physiologically Relevant Hydrostatic Pressure on CHO Cell Batch Culture," *Scientific Reports*, 11, 162, 2021.

W. K. Peng, L. Chen, B. Boehm, J. Han, and T. P. Loh, "Molecular Phenotyping of Oxidative Stress in Diabetes Mellitus with Point-of-care NMR system," *Aging and Mechanisms of Disease*, 6, 11, 2020.

H. Jeon, B. Jundi, K. Choi, H. Ryu, B. D. Levy, G. Lim, and J. Han, "Fully-automated and Field-deployable Blood Leukocytes Separation Platform Using Multi-dimensional Double Spiral (MDDS) Inertial Microfluidics," *Lab on a Chip*, 20, 3612-3624, 2020.

A. Xiong, P. Prakash, X. Gao, M. Chew, I. J. J. Tay, C. J. Woodrow, B. P. Engelward, J. Han, and P. R. Preiser, "K13-Mediated Reduced Susceptibility to Artemisinin in Plasmodium falciparum is Overlaid on a Trait of Enhanced DNA Damage Repair," *Cell Reports*, Cell Reports, 32, 107996, 2020.

S. Y. Ng, K. X. Ong, S. T. Surendran, A. Sinha, J. J. H. Jia, J. Chen, J. Liang, L. K. S. Tay, L. Cui, H. L. Loo, P. Ho, J. Han, and W. Moreira, "Hydrogen Sulfide Sensitizes Acinetobacter Baumannii to Killing by Antibiotics," *Frontiers in Microbiology*, 11, 1875, 2020.

K. K. Zeming, Y. Sato, L. Yin, N.-J. Huang, L. H. Wong, H. L. Loo, Y. B. Lim, C. T. Lim, J. Chen, P. R. Preiser, and J. Han, "Microfluidic Label-free Bioprocessing of Human Reticulocytes from Erythroid Culture," *Lab on a Chip*, 20, 3445-3460, 2020.

B. Al-Anzi, S. Al-Hammadi, J. Yoon, and J. Han, "Techno-economic Analysis of Multi-stage ion Concentration Polarization with Recirculation for Treatment of Oil Produced Water," *J. of Environmental Management*, 269, 110788, 2020.

W. Ouyang, and J. Han, "One-Step Nucleic Acid Purification and Noise-Resistant Polymerase Chain Reaction by Electrokinetic Concentration for Ultralow-Abundance Nucleic Acid Detection," *Angewandte Chemie International Edition*, 59, 27, 10981-10988, 2020.

GRADUATE STUDENTS

Kyungyong Choi, EECS

Matthew Flavin, EECS

Menglin Shang, SMART Center, NUS

Zhumei Sun, ME

Ching Ann Tee, SMART Center, NUS

Eric Wynne, EECS

Itay Fayer, BE

VISITORS

Eric Brack, Army Natick Research Center

Dongho Kim, Hanyang University, Korea

Tingyu Li, Peking University, China

SUPPORT STAFF

Cindy Higgins, Administrative Assistant

SELECTED PUBLICATIONS

K. K. Zeming, R. Vernekar, M. T. Chua, K. Y. Quek, G. Sutton, T. Kruger, W. S. Kuan, and J. Han, "Label-Free Biophysical Markers from Whole Blood Microfluidic Immune Profiling Reveal Severe Immune Response Signatures," *Small* 2021, 17, 2006123.

M. T. Flavin, M. A. Paul, A. S. Lim, S. Abdulhamed, C. A. Lissandrello, R. Ajemian, S. J. Lin, and J. Han, "Rapid and Low Cost Manufacturing of Cuff Electrodes," *Frontiers in Neuroscience*, 15, 121, 2021

L. Yin, W. Y. Au, C. C. Yu, T. Kwon, Z. Lai, M. Shang, M. E. Warkiani, R. Rosche, C. T. Lim, and J. Han, "Miniature Auto-perfusion Bioreactor System with Spiral Microfluidic Cell Retention Device," *Biotechnology and Bioengineering*, 118, 1951-1961, 2021.

Ruonan Han

Associate Professor

Department of Electrical Engineering & Computer Science

Integrated circuits and systems operating from RF to THz frequencies for sensing and communication applications. Electromagnetism, Chip-scale wave-matter interactions for miniature spectroscopy and frequency metrology.

Rm. 39-527A | 617-324-5281 | ruonan@mit.edu

POSTDOCTORAL ASSOCIATE

Xiang Yi, MTL

GRADUATE STUDENTS

Xibi Chen, EECS

Mohamed Elsheikh, EECS

Jack Holloway, EECS

Mohamed I. Ibrahim, EECS

Muhammad I. Khan, EECS

Mina Kim, EECS (Co-supervised with Hae-Seung Lee)

Eunseok Lee (Co-supervised with Anantha Chandrakasan)

Nathan Monroe, EECS

Yukimi Morimoto, EECS

Jinchen Wang, EECS

Alec Yen, EECS

Xingyu Zou, EECS

UNDERGRADUATE STUDENTS

Reed Foster, EECS

Jose Guajardo, EECS

VISITORS

Xingcun Li, Tsinghua University

Rui Ma, Mitsubishi Electric Research Labs

SUPPORT STAFF

Kathleen Brody, Administrative Assistant

SELECTED PUBLICATIONS

M. I. W. Khan, J. Woo, X. Yi, M. Ibrahim, R. Yazicigil, A. Chandrakasan, and R. Han, "A 0.31THz CMOS Uniform Circular Antenna Array Enabling Generation/Detection of Waves with Orbital-Angular Momentum," *IEEE Radio-Frequency Integrated Circuit Symp. (RFIC)*, Atlanta, GA, Jun. 2021.

J. W. Holloway, G. C. Dogiamis, and R. Han, "A 105Gbps Dielectric-Waveguide Link in 130nm BiCMOS Using Channelized 220-330GHz Signal and Integrated Waveguide Coupler," *IEEE Intl. Solid-State Circuit Conf. (ISSCC)*, San Francisco, CA, Feb. 2021.

X. Yi, J. Wang, M. Colangelo, C. Wang, K. E. Kolodziej, and R. Han, "Realization of In-Band Full-Duplex Operation at 300 K and 4.2 K Using Bilateral Single-Sideband Frequency Conversion," *IEEE Journal of Solid-State Circuits (JSSC), RFIC Special Issue*, 2021 (Invited)

M. I. Ibrahim*, C. Foy*, D. R. Englund†, and R. Han†, "High-Scalability CMOS Quantum Magnetometer with Spin-State Excitation and Detection of Diamond Color Centers," *IEEE Journal of Solid-State Circuits (JSSC)*, vol. 56, no. 3, Mar. 2021. (*†: equal contribution)

M. I. Wasif Khan, M. I. Ibrahim, C. Juvekar, W. Jung, R. T. Yazicigil, A. P. Chandrakasan, and R. Han, "CMOS THz-ID: A 1.6-mm² Package-Less Identification Tag Using Asymmetric Cryptography and 260-GHz Far-Field Backscatter Communication," *IEEE Journal of Solid-State Circuits (JSSC)*, vol. 56, no. 2, Feb. 2021.

X. Yi, C. Wang, J. Grajal, and R. Han, "A 220-to-320GHz FMCW Radar Frontend in 65-nm CMOS Using a Frequency-Comb Architecture," *IEEE Journal of Solid-State Circuits (JSSC)*, vol. 56, no. 2, Feb. 2021.

C. Wang, X. Yi, M. Kim, Q. Yang, and R. Han, "A Terahertz Molecular Clock on CMOS Using High-Harmonic-Order Interrogation of Rotational Transition for Medium/Long-Term Stability Enhancement," *IEEE Journal of Solid-State Circuits (JSSC)*, vol. 56, no. 2, Feb. 2021.

A. Aleksov, G. Dogiamis, T. Kamgaing, A. Elsherbini, J. Swan, J. Holloway, and R. Han, "Organic Package Substrates Using Lithographic Via Technology for RF to THz Applications," *IEEE Intl. Electron Device Meetings (IEDM)*, Dec. 2020.

Q. Yu, S. Rami, V. Neeli, J. Garret, J. Koo, M. Marulanda, S. Ravikumar, S. Moraka, Y. Ma, J. Waldemer, G. Liu, S. Joglekar, M. Armstrong, D. Ali, N. Monroe, R. Han, B. Sell, and E. Karl, "mmWave and Sub-THz Technology Development in Intel 22nm Low-Power FinFET Process," *IEEE Intl. Electron Device Meetings (IEDM)*, Dec. 2020.

R. Tugce Yazicigil, P. Nadeau, D. Richman, C. Juvekar, S. Maji, U. Banerjee, S. Fuller, M. Abdelhamid, N. Desai, M. Ibrahim, M. Khan, W. Jung, R. Han, and A. Chandrakasan, "Beyond Crypto: Physical-Layer Security for Internet of Things Devices," *IEEE Solid-State Circuits Magazine*, vol. 12, no. 4, pp. 66-78, Fall 2020. (Invited)

X. Yi, J. Wang, C. Wang, K. E. Kolodziej, and R. Han, "A 3.4-4.6-GHz In-Band Full-Duplex Front-End in CMOS Using A Bi-Directional Frequency Converter," *IEEE Radio-Frequency Integrated Circuit Symposium (RFIC)*, Los Angeles, CA, Jun. 2020.

Song Han

Assistant Professor

Department of Electrical Engineering & Computer Science

Machine learning, artificial intelligence, model compression, hardware accelerator, domain-specific architecture.

Rm. 38-344 | 707-797-7288 | songhan@mit.edu

GRADUATE STUDENTS

Han Cai, EECS

Katharina Gschwind, EECS

Ji Lin, EECS

Yujun Lin, EECS

Zhijian Liu, EECS

Haotian Tang, EECS

Hanrui Wang, EECS

Zhekai Zhang, EECS

Ligeng Zhu, EECS

Z. Liu, H. Tang, Y. Lin, and S. Han, "Point Voxel CNN for Efficient 3D Deep Learning," *Neural Information Processing System (NeurIPS)*, Spotlight presentation, 2019.

L. Zhu, Z. Liu, and S. Han, "Deep Leakage from Gradients," *Neural Information Processing System (NeurIPS)*, 2019.

J. Lin, C. Gan, and S. Han, "TSM: Temporal Shift Module for Efficient Video Understanding," *International Conference on Computer Vision (ICCV)*, 2019.

H. Cai, L. Zhu, S. Han, "ProxylessNAS: Direct Neural Architecture Search on Target Task and Hardware," *International Conference on Learning Representations (ICLR)*, 2019.

J. Lin, C. Gan, and S. Han, "Defensive Quantization: When Efficiency Meets Robustness," *International Conference on Learning Representations (ICLR)*, 2019.

K. Wang, Z. Liu, Y. Lin, J. Lin, and S. Han, "HAQ: Hardware-Aware Automated Quantization with Mixed Precision," *IEEE Conference on Computer Vision and Pattern Recognition (CVPR)*, Oral presentation, 2019.

Y. He, J. Lin, Z. Liu, H. Wang, L.-J. Li, and S. Han, "AMC: AutoML for Model Compression and Acceleration on Mobile Devices," *European Conference on Computer Vision (ECCV)*, 2018.

UNDERGRADUATE STUDENT

Kevin Shao, EECS

SELECTED PUBLICATIONS

J. Lin, W.-M. Chen, Y. Lin, J. Cohn, C. Gan, and S. Han, "MCUNet: Tiny Deep Learning on IoT Devices," *Neural Information Processing System (NeurIPS)*, Spotlight presentation, 2020.

H. Cai, C. Gan, L. Zhu, and S. Han, "Tiny Transfer Learning: Reduce Memory, not Parameters for Efficient On-Device Learning," *Neural Information Processing System (NeurIPS)*, 2020.

S. Zhao, Z. Liu, J. Lin, J. Zhu, and S. Han, "Differentiable Augmentation for Data-Efficient GAN Training," *Neural Information Processing System (NeurIPS)*, 2020.

M. Li, J. Lin, Y. Ding, Z. Liu, J. Zhu, and S. Han, "GAN Compression: Learning Efficient Architectures for Conditional GANs," *IEEE Conference on Computer Vision and Pattern Recognition (CVPR)*, 2020.

H. Cai, C. Gan, T. Wang, Z. Zhang, and S. Han, "Once For All: Train One Network and Specialize It for Efficient Deployment," *International Conference on Learning Representations (ICLR)*, 2020.

H. Wang, K. Wang, J. Yang, L. Shen, N. Sun, H.-S. Lee, and S. Han, "Transferable Transistor Sizing with Graph Neural Networks and Reinforcement Learning," *Design Automation Conference (DAC)*, 2020.

Z. Zhang, H. Wang, S. Han, and B. Dally, "SpArch: Efficient Architecture for Sparse Matrix Multiplication," *International Symposium on High-Performance Computer Architecture (HPCA)*, 2020.

Juejun (JJ) Hu

Associate Professor

Department of Materials Science & Engineering

Integrated photonics, optical thin films, glass and amorphous materials, silicon photonics, light management in photovoltaics, magneto-optical isolation, integration on unconventional substrates (polymers, optical crystals, 2-D materials, etc.), infrared imaging, spectroscopy, metasurface.

Rm. 13-4054 | 302-766-3083 | hujuejun@mit.edu

RESEARCH SCIENTIST

Tian Gu, MRL

POSTDOCTORAL ASSOCIATES

Qingyang Du, DMSE

Carlos A. Ríos Ocampo, DMSE

Mikhail Shalaginov, DMSE

Shaoliang Yu, DMSE

GRADUATE STUDENTS

Cosmin Constantin Popescu, DMSE

Skylar Deckoff-Jones, DMSE

Tushar Karnik, DMSE

Gillian Micale, DMSE

Luigi Ranno, DMSE

Fan Yang, DMSE

Yifei Zhang, DMSE

UNDERGRADUATE STUDENT

Marilyn Meyers, DMSE

VISITOR

Samuel Serna, Bridgewater State University

SUPPORT STAFF

Sandra Crawford, Administrative Assistant

SELECTED PUBLICATIONS

M. Shalaginov, S. An, Y. Zhang, F. Yang, P. Su, V. Liberman, J. Chou, C. Roberts, M. Kang, C. Rios, Q. Du, C. Fowler, A. Agarwal, K. Richardson, C. Rivero-Baleine, H. Zhang, J. Hu, and T. Gu, "Reconfigurable all-dielectric metalens with diffraction limited performance," *Nat. Commun.*, vol. 12, pp. 1225, 2021.

M. Shalaginov, S. An, F. Yang, P. Su, D. Lyzwa, A. Agarwal, H. Zhang, J. Hu, and T. Gu, "Single-Element Diffraction-Limited Fisheye Metalens," *Nano Lett.*, vol. 20, pp. 7429-7437, 2020.

Y. Zhang, J. Chou, J. Li, H. Li, Q. Du, A. Yadav, S. Zhou, M. Shalaginov, Z. Fang, H. Zhong, C. Roberts, P. Robinson, B. Bohlin, C. Rios, H. Lin, M. Kang, T. Gu, J. Warner, V. Liberman, K. Richardson, and J. Hu, "Broadband Transparent Optical Phase Change Materials for High-Performance Nonvolatile Photonics," *Nat. Commun.*, Vol. 10, pp. 4279, 2019.

Y. Zhang, Q. Du, C. Wang, T. Fakhru, S. Liu, L. Deng, D. Huang, P. Pintus, J. Bowers, C. A. Ross, J. Hu, and L. Bi, "Monolithic Integration of Broadband Optical Isolators for Polarization-diverse Silicon Photonics," *Optica*, vol. 6, pp. 473-478, 2019.

Q. Du, C. Wang, Y. Zhang, Y. Zhang, T. Fakhru, W. Zhang, C. Gonçalves, C. Blanco, K. Richardson, L. Deng, C. A. Ross, L. Bi, and J. Hu, "Monolithic On-chip Magneto-optical Isolator with 3 dB Insertion Loss and 40 dB Isolation Ratio," *ACS Photonics*, vol. 5, pp. 5010-5016, 2018.

D. Kita, B. Miranda, D. Favela, D. Bono, J. Michon, H. Lin, T. Gu, and J. Hu, "High-performance and Scalable On-chip Digital Fourier Transform Spectroscopy," *Nat. Commun.*, vol. 9, pp. 4405, 2018.

D. Kita, J. Michon, S. G. Johnson, and J. Hu, "Are Slot and Sub-wavelength Grating Waveguides Better than Strip Waveguides for Sensing?" *Optica*, vol. 5, pp. 1046-1054, 2018.

L. Zhang, J. Ding, H. Zheng, S. An, H. Lin, B. Zheng, Q. Du, G. Yin, J. Michon, Y. Zhang, Z. Fang, M. Shalaginov, L. Deng, T. Gu, H. Zhang, and J. Hu, "Ultra-thin, High-efficiency mid-Infrared Transmissive Huygens Meta-optics," *Nat. Commun.*, vol. 9, pp. 1481, 2018.

L. Li, H. Lin, Y. Huang, R. Shiue, A. Yadav, J. Li, J. Michon, D. Englund, K. Richardson, T. Gu, and J. Hu, "High-performance Flexible Waveguide-integrated Photodetectors," *Optica*, vol. 5, pp. 44-51, 2018.

L. Li, H. Lin, S. Qiao, Y. Huang, J. Li, J. Michon, T. Gu, C. Ramos, L. Vivien, A. Yadav, K. Richardson, N. Lu, and J. Hu, "Monolithically Integrated Stretchable Photonics," *Light Sci. Appl.*, vol. 7, e17138, 2018.

H. Lin, Y. Song, Y. Huang, D. Kita, S. Deckoff-Jones, K. Wang, L. Li, J. Li, H. Zheng, Z. Luo, H. Wang, S. Novak, A. Yadav, C. Huang, R. Shiue, D. Englund, T. Gu, D. Hewak, K. Richardson, J. Kong, and J. Hu, "Chalcogenide Glass-on-Graphene Photonics," *Nat. Photonics*, vol. 11, pp. 798-805, 2017.

L. Li, H. Lin, S. Qiao, Y. Zou, S. Danto, K. Richardson, J. D. Musgraves, N. Lu, and J. Hu, "Integrated Flexible Chalcogenide Glass Photonic Devices," *Nature Photonics*, vol. 8, pp. 643-649, 2014.

Qing Hu

Professor

Department of Electrical Engineering & Computer Science

Physics and applications of millimeter-wave, terahertz, and infrared devices.

Rm. 36-465 | 617-253-1573 | qhu@mit.edu

COLLABORATORS

Jianrong Gao, Delft University

John L. Reno, Sandia National Lab.

Zbig Wasilewski, University of Waterloo

Gerard Wysocki, Princeton University

A. Khalatpour, A. K. Paulsen, C. Deimert, Z. R. Wasilewski, and Qing Hu, "High power portable terahertz laser systems," *Nat. Phot.* 15, 16-20, 2021.

GRADUATE STUDENTS

Ali Khalatpour, EECS

Theodore Letsou, EECS

Andrew Paulsen, EECS

Elise Uyehara, EECS

Tianyi Zeng, EECS

SUPPORT STAFF

Shayne Fernandes, Administrative Assistant

SELECTED PUBLICATIONS

L. A. Sterczewski, J. Westberg, Y. Yang, D. Burghoff, J. Reno, Q. Hu, and G. Wysocki, "Terahertz multi-species sensing with dual chip-scale combs," *ACS Phot.* 7, 1082, 2020.

Y. Gan, B. Mirzaei, S. van der Poel, J. R. G. Silva, M. Finkel, M. Eggens, M. Ridder, A. Khalatpour, Q. Hu, F. van der Tak, and J.-R. Gao, "3.9 THz Spatial Filter Based on Back-to-back Si-lens System," *Opt. Ex.* 28, 32693, 2020.

Y. Gan, B. Mirzaei, J. R. G. Silva, A. Khalatpour, Q. Hu, C. Groppi, J. V. Siles, F. F. S. van der Tak, and J. R. Gao, "Multi-beam Local Oscillator for a 100-pixel Heterodyne Array Receiver at FIR," *SPIE Photonics West*, San Francisco, Feb. 1-6, 2020.

Y. Gan, B. Mirzaei, S. van der Poel, J. Silva, M. Finkel, M. Eggens, M. Ridder, A. Khalatpour, Q. Hu, F. van der Tak, and J. R. Gao, "4 THz beam filter based on a Back-to-back Si-lens System," *31st IEEE International Symposium on Space Terahertz Technology (ISSTT 2020)*, Tempe, AZ, March 8-11, 2020.

B. Mirzaei, M. Finkel, J. R. Silva, W. Laauwen, C. Groppi, A. Khalatpour, Q. Hu, A. Young, C. Walker, and J. R. Gao, "1 to 8 Beam Distributor at 4.7 THz for GUSTO," *31st IEEE International Symposium on Space Terahertz Technology (ISSTT 2020)* Tempe, AZ, March 8-11, 2020.

Q. Hu, "THz quantum cascade lasers," *International Quantum Cascade Laser School & Workshop (IQCLSW2020)*, Virtual, Sep. 7, 2020. (Invited tutorial)

Jeehwan Kim

Associate Professor

Department of Mechanical Engineering

Department of Materials Science and Engineering

Research Laboratory of Electronics

Two-dimensional material based layer transfer, brain-inspired neuromorphic computing, single-crystalline graphene electronics, advanced photovoltaics.

Rm. 38-276 | 617-324-1948 | jeehwan@mit.edu

POSTDOCTORAL ASSOCIATES

Sanghoon Bae, MechE

Celesta Chang, MechE

Jihoon Kang, MechE

Hyunseok Kim, MechE

Yeongin Kim, MechE

Hyunseong Kum, MechE

Ki Seok Kim, MechE

Jiho Shin, MechE

Hanwool Yeun, MechE

GRADUATE STUDENTS

Chanyeol Choi, EECS

Kuangye Lu, MechE

Yunpeng Liu, MechE

Sangho Lee, MechE

Doyoon Lee, MechE

Kuan Qiao, MechE

Xinyuan Zhang, DMSE

SUPPORT STAFF

Emilie Heilig, Administrative Assistant

SELECTED PUBLICATIONS

H. Yeon, P. Lin, C. Choi, S. Tan, Y. Park, D. Lee, J. Lee, F. Xu, B. Gao, H. Wu, H. Qian, Y. Nie, S. Kim, and J. Kim, "Alloying Conducting Channels for Reliable Neuromorphic Computing," *Nature Nanotechnology*, vol. 15, pp. 574-579, 2020.

S.-H. Bae, K. Lu, Y. Han, S. Kim, K. Qiao, C. Choi, Y. Nie, H. Kim, H. S. Kum, P. Chen, W. Kong, B.-S. Kang, C. Kim, J. Lee, Y. Baek, J. Shim, J. Park, M. Joo, D. A. Muller, K. Lee, and J. Kim, "Graphene-assisted Spontaneous Relaxation Towards Dislocation-free Heteroepitaxy," *Nature Nanotechnology*, vol. 15, pp. 272-276, 2020.

H. S. Kum, H. Lee, S. Kim, S. Lindemann, W. Kong, K. Qiao, P. Chen, J. Irwin, J. H. Lee, S. Xie, S. Subramanian, J. Shim, S.-H. Bae, C. Choi, L. Ranno, S. Seo, S. Lee, J. Bauer, H. Li, K. Lee, J. A. Robinson, C. A. Ross, D. G. Schlom, M. S. Rzechowski, C.-B. Eom, and J. Kim, "Heterogeneous Integration of Singlecrystalline Complex-oxide Membranes," *Nature*, vol. 578, pp. 75-81, 2020.

H. Kum, D. Lee, W. Kong, H. Kim, Y. Park, Y. Kim, Y. Baek, S.-H. Bae, K. Lee, and J. Kim, "Epitaxial Growth And Layer-Transfer Techniques for Heterogeneous Integration of Materials for Electronic and Photonic Devices," *Nature Electronics*, vol. 2, pp. 439-450, 2019.

W. Kong, H. Kum, S.-H. Bae, J. Shim, H. Kim, L. Kong, Y. Meng, K. Wang, C. Kim, and J. Kim, "Path Towards Graphene Commercialization from Lab to Market," *Nature Nanotechnology* vol. 14, pp. 927-938, 2019.

S.-H. Bae, H. Kum, W. Kong, Y. Kim, C. Choi, B. Lee, P. Lin, and J. Kim, "Integration of Bulk Materials with Two-dimensional Materials for Physical Couplings," *Nature Materials*, vol. 18, pp. 550-560, 2019.

J. Shim, S.-H. Bae, W. Kong, D. Lee, K. Qiao, D. Nezhich, Y. Ju Park, R. Zhao, S. Sundaram, X. Li, H. Yeon, C. Choi, H. Kum, R. Yue, G. Zhou, Y. Ou, K. Lee, J. Moodera, X. Zhao, J.-H. Ahn, C. Hinkle, A. Ougazzaden, and J. Kim, "Controlled Crack Propagation for Atomic Precision Handling of Wafer-scale Two-dimensional Materials," *Science*, vol. 362, pp. 665-670, 2018.

W. Kong, H. Li, K. Qiao, Y. Kim, K. Lee, Y. Nie, D. Lee, T. Osadchy, R. J. Molnar, D. K. Gaskill, R. L. Myers-Ward, K. M. Daniels, Y. Zhang, S. Sundram, Y. Yu, S.-H. Bae, S. Rajan, Y. Shao-Horn, K. Cho, A. Ougazzaden, J. C. Grossman, and J. Kim, "Polarity Governs Atomic Interaction through Two-dimensional Materials," *Nature Materials*, vol. 17, pp. 999-1004, 2018.

S. Choi, S. H. Tan, Z. Li, Y. Kim, C. Choi, P.-Y. Chen, H. Yeun, S. Yu, and J. Kim, "SiGe Epitaxial Memory for Neuromorphic Computing with Reproducible High Performance Based on Engineered Dislocations," *Nature Materials*, vol. 17, pp. 335-340, 2018.

Y. Kim, S. S. Cruz, K. Lee, B. O. Alawode, C. Choi, Y. Song, J. M. Johnson, C. Heidelberger, W. Kong, S. Choi, K. Qiao, I. Almansouri, E. A. Fitzgerald, J. Kong, A. M. Kolpak, J. Hwang, and J. Kim, "Remote Epitaxy through Graphene for Two-dimensional Material Based Layer Transfer," *Nature*, vol. 544, pp. 340-343, 2017.

S. Bae, X. Zhou, S. Kim, Y. S. Lee, S. Cruz, Y. Kim, J. B. Hannon, Y. Yang, D. K. Sadana, F. M. Ross, H. Park, and J. Kim, "Unveiling the Carrier Transport Mechanism in Epitaxial Graphene for Forming Wafer-scale, Single-domain Graphene," *PNAS*, vol. 114, pp. 4082-4086, 2017.

Sang-Gook Kim

Professor

Department of Mechanical Engineering

AI for Design and Manufacturing, MEMS Knowledge Representation.

1-306 | 617-452-2472 | sangkim@mit.edu

VISITING RESEARCH STAFF

Sergio A Navarro Tuch, Tecnologico de Monterrey

GRADUATE STUDENTS

Haluk Akay, DME

Georgios Fardelas, DME, Sloan

Jack Gammack, DME

SUPPORT STAFF

Tony Pulsone, Administrative Assistant

SELECTED PUBLICATIONS

H. Akay, and S.-G. Kim, "Measuring Functional Independence in Design With Deep-Learning Language Representation Models," *26th CIRP Design Conference, Procedia CIRP Volume 50*, 2020.

H. Akay, and S.-G. Kim, "Design Transcription: Deep Learning Based Design Feature Representation," *CIRP Annals - Manufacturing Technology*, v69.1, 2020.

W. Kim, S. M. Howell, and S.-G. Kim, "Artifact-user Affordances Versus Artifact-Artifact Affordances Applied to Graft Placements During Knee Reconstruction," *J. Rheumatol Res.*, 2(3): 133-139, 2020.

H. Akay, S.G. Kim, "Measuring Functional Independence in Design With Deep-Learning Language Representation Models," *26th CIRP Design Conference, Procedia CIRP Volume 50*, 2020.

W. Kim, D. Araujo, S. Kohles, S.-G. Kim, and H. Alvarez Sanchez, "Affordance-Based Surgical Design Methods Considering Biomechanical Artifacts," *Ecological Psychology*, V. 33.1, 2021.

H. Akay, S.-G. Kim, "Extracting Functional Requirements from Design Documentation using Machine Learning," *27th CIRP Design Conference, Procedia CIRP Volume 50*, 2021.

H. Akay, S.-G. Kim, "Reading Functional Requirements Using Machine Learning-Based Language Processing," *CIRP Annals - Manufacturing Technology*, v70.1, 2021.

Jing Kong

MTL Associate Director
Professor of Electrical Engineering
Department of Electrical Engineering & Computer Science

Synthesis, characterization and applications of low-dimensional materials, including carbon nanotube, graphene and other two dimensional materials.

Rm. 13-3065 | 617-324-4068 | jingkong@mit.edu

RESEARCH SCIENTISTS

Xiang Ji, RLE
Mohammad Mahdi Tavakoli, RLE

POSTDOCTORAL ASSOCIATES

Minghui (Hill) Chiu, RLE
Yunfan Guo, RLE
Qingqing Ji, RLE
Nannan Mao, RLE
JiHoon Park, RLE
Jiangtao Wang, RLE

GRADUATE STUDENTS

Zhantao Chen, MechE
Luiz Gustavo Pimenta Martins, Physics
Angyu Lu, EECS
Pin-Chun Shen, EECS
Haozhe Wang, EECS
Zhien Wang, DMSE

SUPPORT STAFF

Arlene Wint, Administrative Assistant

SELECTED PUBLICATIONS

M. M. Tavakoli, R. Po, G. Bianchi, C. Carbonera, and J. Kong, "Efficient and Stable Mesoscopic Perovskite Solar Cells Using a Dopant-Free D-A Copolymer Hole-Transporting Layer," *Solar RRL*, 5 (4), 2000801, 2021.

L. G. P. Martins, D. L. Silva, J. S. Smith, A.-Y. Lu, C. Su, M. Hempel, C. Occhialini, X. Ji, R. Pablo, R. S. Alencar, A. CR Souza, A. A. Pinto, A. B. de Oliveira, R. JC Batista, T. Palacios, M. SC Mazzoni, M. JS Matos, R. Comin, J. Kong, and L. G. Cançado, "Hard, Transparent, sp³-containing 2D Phase Formed from Few-layer Graphene Under Compression," *Carbon*, 173, 744-757, 2021.

H. Xu, H. Wang, J. Zhou, Y. Guo, J. Kong, and J. Li, "Colossal Switchable Photocurrents in Topological Janus Transition Metal Dichalcogenides", npj *Computational Materials*, 7 (1), 1-9, 2021.

N. Wang, N. Mao, Z. Wang, X. Yang, X. Zhou, H. Liu, S. Qiao, X. Lei, J. Wang, H. Xu, X. Ling, Q. Zhang, Q. Feng, and J. Kong, "Electrochemical Delamination of Ultralarge Few-Layer Black Phosphorus with a Hydrogen-Free Intercalation Mechanism," *Advanced Materials*, 33 (1), 2005815, 2021.

M. M. Tavakoli, H. Si, and J. Kong, "Suppression of Photovoltaic Losses in Efficient Tandem Organic Solar Cells (15.2%) with Efficient Transporting Layers and Light Management Approach," *Energy Technology*, 9 (1), 2000751, 2021.

K. Zhang, Y. Guo, Q. Ji, A.-Y. Lu, C. Su, H. Wang, A. A Puretzky, D. B Geohegan, X. Qian, S. Fang, E. Kaxiras, J. Kong, and S. Huang, "Fluidic Flow Assisted Deterministic Folding of Van der Waals Materials Enhancement of van der Waals interlayer coupling through polar Janus MoSSe," *Journal of the American Chemical Society*, 142 (42), 17499-17507, 2020.

Q. Qian, R. Zu, Q. Ji, G. S. Jung, K. Zhang, Y. Zhang, M. J Buehler, J. Kong, V. Gopalan, and S. Huang, "Chirality-Dependent Second Harmonic Generation of MoS₂ Nanoscroll with Enhanced Efficiency," *ACS Nano* 14 (10), 13333-13342, 2020.

Y. Han, X. Fan, H. Wang, F. Zhao, C. G. Tully, J. Kong, N. Yao, and N. Yan, "Monolayer Graphene-covered Grids Enable 2.6-Å Single-particle Cryo-EM Reconstruction of 52-kDa Streptavidin," *Microscopy and Microanalysis* 26 (S2), 1030-1031, 2020.

M. M. Tavakoli, M. H. Gharahcheshmeh, N. Moody, M.G Bawendi, K. K Gleason, and J. Kong, "Efficient, Flexible, and Ultra-Lightweight Inverted PbS Quantum Dots Solar Cells on All-CVD-Growth of Parylene/Graphene/oCVD PEDOT Substrate with High Power-per-Weight", *Advanced Materials Interfaces* 7 (16), 2000498, 2020.

M. M. Tavakoli, G. Azzellino, M. Hempel, A.-Y. Lu, F. J Martin-Martinez, J. Zhao, J. Yeo, T. Palacios, M. J Buehler, and J. Kong, "Synergistic Roll-to-Roll Transfer and Doping of CVD-Graphene Using Parylene for Ambient-Stable and Ultra-Lightweight Photovoltaics," *Advanced Functional Materials* 30 (31), 2001924, 2020.

R. Pablo-Pedro, M. A. Magana-Fuentes, M. Videia, J. Kong, M. Li, J. L Mendoza-Cortes, and T. Van Voorhis, "Understanding disorder in 2D materials: the case of carbon doping of Silicene," *Nano Letters* 20 (9), 6336-6343, 2020.

P. Valencia-Acuna, P. Zereshki, M. M. Tavakoli, J.-H. Park, J. Kong, and H. Zhao, "Transient Absorption Of Transition Metal Dichalcogenide Monolayers Studied By A Photodope-pump-probe Technique," *Physical Review B*, vol. 102, pp. 035414, 2020.

Jeffrey H. Lang

Vitesse Professor of Electrical Engineering
Department of Electrical Engineering & Computer Science

Analysis, design, and control of electro-mechanical systems with application to traditional rotating machinery and variable-speed drives, micro/nano-scale (MEMS/NEMS) sensors and actuators, flexible structures, and the dual use of actuators as force and motion sensors.

Rm. 10-176 | 617-253-4687 | lang@mit.edu

POSTDOCTORAL ASSOCIATE

Apoorva Murarka, RLE

GRADUATE STUDENTS

Benjamin Cary, EECS

Jinchi Han, EECS

Damien Martin, EECS

Sajjad Mohammadiyangijeh, EECS

Phoebe Piercy, EECS

Tareq Saqr, LGO

Daniel Sheen, EECS

John Zhang, Meche

UNDERGRADUATE STUDENT

Aaron Yeiser, EECS

SUPPORT STAFF

Donna Gale, Administrative Assistant

Arlene Wint, Administrative Assistant

SELECTED PUBLICATIONS

F. Niroui, M. Saravanapavanantham, J. Han, J. J. Patil, T. M. Swager, J. H. Lang, and V. Bulovic, "A Hybrid Approach To Fabricate Uniform and Active Molecular Junctions"; *Nano Letters*, Feb. 3, 2021. Accepted.

S. Zhao, U. Radhakrishna, and J. H. Lang; "Power-Bandwidth-Voltage Interaction in Piezoelectric Vibration Energy Harvesters with Constrained Load Voltage"; *Smart Materials and Structures*, 30, 025037, Jan. 2021.

P. Garcha, V. Schaffer, S. Ramaswamy, B. Haroun, J. Wieser, J. H. Lang, and A. P. Chandrakasan; "A 770 kS/s integrated-fluxgate magnetometer with duty cycling for contactless current sensing"; Proceedings: *International Solid-State Circuits Conference*, San Francisco, CA, Feb. 14-18, 2021. Accepted.

N. X. Wang, H. W. Wang, J. Mei, S. Mohammadi, J. Moon, J. H. Lang and J. L. Kirtley; "Robust wireless power transfer system based on rotating fields for multi-user charging"; *IEEE Transactions on Energy Conversion*. Also doi.org/10.1109/TEC.2020.3034794. Accepted.

Y. Yang, U. Radhakrishna, J. F. Hunter, T. W. Eagar, and J. H. Lang; "An electromagnetic translational vibration energy harvester fabricated in MP35N Alloy"; *IEEE Journal of Microelectromechanical Systems*, 29, 1518-1522, Dec. 2020.

J. D. Boles, P. L. Acosta, Y. Ramadass, J. H. Lang, and D. J. Perreault, "Evaluating piezoelectric materials for power conversion"; Proceedings: *21st IEEE Workshop on Control and Modeling for Power Electronics (COMPEL)*, 1-8, Aalborg, Denmark, Nov. 9-12, 2020.

J. D. Boles, E. Ng, J. H. Lang, and D. J. Perreault; "High-efficiency operating modes for isolated piezoelectric-transformer-based DC-DC converters"; Proceedings: *21st IEEE Workshop on Control and Modeling for Power Electronics (COMPEL)*, 1-8, Aalborg, Denmark, November 9-12, 2020.

F. Niroui, M. Saravanapavanantham, J. Han, J. J. Patil, T. M. Swager, J. H. Lang and, V. Bulovic, "Precise fabrication of uniform molecular gaps for active nanoscale devices"; arXiv:2006.14992, June 26, 2020.

N. Klugman, J. Vedral, and J. H. Lang, "Field-based Model of Flux Compression Generators," Proceedings: *2020 International Applied Computational Electromagnetics Society Symposium*, Monterey, CA, March 22-26, 2020. Postponed to July 27-31.

N. Klugman, J. Vedral and J. H. Lang, "Self-inductance of an Extrusion of a Planar Curve," Proceedings: *2020 International Applied Computational Electromagnetics Society Symposium*, Monterey, CA, March 22-26, 2020. Postponed to July 27-31.

V. Bulovic, J. H. Lang, T. S. Mahony, and F. Niroui, "Electrically Driven Light-emitting Tunnel Junctions," US Patent 10,566,492, Feb. 18, 2020.

V. Bulovic, J. H. Lang, F. Niroui, E. Sletten, and T. M. Swager, "Tunneling Nanomechanical Switches and Tunable Plasmonic Nanogaps," US Patent 10,475,601, Nov. 12, 2019.

S. J. Choi, S. Savagatrup, Y. Kim, J. H. Lang and T. Swager, "Precision pH Sensor Based on WO₃ Nanofiber-polymer Composites and Differential Amplification," *ACS Sensors*, 4, 10, 2593-2598, Oct. 2019, also doi: 10.1021/acssensors.9b01579.

J. Y. Yoon, J. H. Lang and D. L. Trumper, "Double-sided Linear Iron-core Fine-tooth Motor for Low Acoustic Noise and High Acceleration," *IEEE/ASME Transactions on Mechatronics*, 24, 2161-2170, Oct. 2019, also doi: 10.1109/TMECH.2019.2929236.

James M. LeBeau

Associate Professor

John Chipman Professor of Materials Science and Engineering

Department of Materials Science and Engineering (DMSE)

Aberration correction electron microscopy, understanding material properties from atomic structure, interfaces between dissimilar materials, quantitative atomic resolution microscopy imaging and diffraction, automation and machine learning applied to microscopy, image processing and analysis techniques.

Rm. 13-5034 | 617-253-6889 | lebeau@mit.edu

POSTDOCTORAL ASSOCIATES

Dennis Kim, DMSE

Jung Hwa Kim, DMSE

GRADUATE STUDENTS

Xi Chen, DMSE

Colin Gilgenbach, DMSE

Abinash Kumar, DMSE

Aubrey Penn, NC State University

Michael Xu, DMSE

SUPPORT STAFF

Julia Hollingsworth, Administrative Assistant

SELECTED PUBLICATIONS

A. N. Penn, S. Koohfar, D. P. Kumah, and J. M. LeBeau, "On the Redistribution of Charge in $\text{La}_{0.7}\text{Sr}_{0.3}\text{CrO}_3/\text{La}_{0.7}\text{Sr}_{0.3}\text{MnO}_3$ Multilayer Thin Films," *AIP Advances*, vol. 10, iss. 4, pp. 045113, Apr. 2020.

T. B. Eldred, M. Abdelhamid, J. G. Reynolds, N. A. El-Masry, J. M. LeBeau, and S. M. Bedair, "Observing relaxation in device quality InGaN templates by TEM techniques," *Applied Physics Letters*, vol. 116, iss. 10, pp. 102104, Mar. 2020.

Z. H. Lim, M. Chrysler, A. Kumar, J. P. Mauthe, D. P. Kumah, C. Richardson, J. M. LeBeau, and J. H. Ngai, "Suspended single-crystalline oxide structures on silicon through wet-etch techniques: Effects of oxygen vacancies and dislocation on etch rates," *Journal of Vacuum Science & Technology A*, vol. 38, iss. 1, pp. 013406, Jan. 2020.

S. S. Jo, Y. Li, A. Singh, A. Kumar, S. Frisone, J. M. LeBeau, and R. Jaramillo, "Formation of large-area MoS_2 thin films by oxygen-catalyzed sulfurization of Mo thin films," *Journal of Vacuum Science & Technology A*, vol. 38, iss. 1, pp. 013405, Jan. 2020.

A. Nozariasbmarz, F. Suarez, J. H. Dycus, M. J. Cabral, J. M. LeBeau, M. C. Ozturk, and D. Vashaee, "Thermoelectric generators for wearable body heat harvesting: Material and Device concurrent optimization," *Nano Energy*, vol. 67, pp. 104265, Jan. 2020.

A. Kumar, J. N. Baker, P. C. Bowes, M. J. Cabral, S. Zhang, E. C. Dickey, D. L. Irving, and J. M. LeBeau, "Atomic-Resolution Electron Microscopy Of Nanoscale Local Structure In Lead-Based Relaxor Ferroelectrics," *Nature Materials*, 20(1):62–67. 2021.

R. Trappen, A. J. Grutter, C. Y. Huang, A. N. Penn, N. Mottaghi, S. Yousefi, A. Haertter, S. Kumari, J. M. LeBeau, B. J. Kirby, and M. B. Holcomb, "Effect of oxygen stoichiometry on the magnetization profiles and negative magnetization in LSMO thin films," *Journal of Applied Physics*, vol. 126, iss. 10, p. 105301, Sep. 2019.

Z. H. Lim, N. F. Quackenbush, A. N. Penn, M. Chrysler, M. Bowden, Z. Zhu, J. M. Ablett, T. -L. Lee, J. M. LeBeau, J. C. Woicik, P. V. Sushko, S. A. Chambers, and J. H. Ngai, "Charge Transfer and Built-in Electric Fields between a Crystalline Oxide and Silicon," *Phys. rev. lett.*, vol. 123, iss. 2, pp. 26805, Jul. 2019.

Hae-Seung Lee

Director of Microsystems Technology Laboratories
Director of Center for Integrated Circuits and Systems
ATSC Professor of Electrical Engineering & Computer Science
Department of Electrical Engineering & Computer Science

Analog and Mixed-signal Integrated Circuits, with a Particular Emphasis in Data Conversion Circuits in scaled CMOS.

Rm. 39-521 | 617-253-5174 | hslee@mit.edu

POSTDOCTORAL ASSOCIATE

Anand Chandrasekhar, EECS

GRADUATE STUDENTS

Ruicong Chen, EECS

Rebecca Ho, EECS

Tae-hoon Jeong, EECS

Mina Kim, EECS

Jaehwan Kim, EECS

Harneet Singh Khurana, EECS

Rishabh Mittal, EECS

Vipasha Mittal, EECS

SUPPORT STAFF

Elizabeth Green, Senior Administrative Assistant

Elizabeth Kubicki, Administrative Assistant

SELECTED PUBLICATIONS

H. Wang, K. Wang, J. Yang, L. Shen, N. Sun, H.-S. Lee, and S. Han, "GCN-RL Circuit Designer: Transferable Transistor Sizing with Graph Neural Networks and Reinforcement Learning" *2020 57th ACM/IEEE Design Automation Conference (DAC)*, Jul. 2020.

T. Jeong, A. Chandrakasan, and H.-S. Lee, "S2ADC: A 12-bit, 1.25MS/s Secure SAR ADC with Power Side-Channel Attack Resistance," *Proceedings of IEEE 2020 Custom Integrated Circuits Conference*, March 2020.

J. Seo, H.-S. Lee, and C. Sodini, "Non-invasive Evaluation of a Carotid Arterial Pressure Waveform Using Motion-Tolerant Ultrasound Measurements During Valsalva Maneuver," *IEEE Journal of Biomedical and Health Informatics*, vol. 25, pp. 163-174, Jan. 2021

T. Jeong, A. Chandrakasan, and H.-S. Lee, "S2ADC: A 12-bit, 1.25MS/s Secure SAR ADC with Power Side-Channel Attack Resistance," *IEEE J. Solid-State Circuits*, vol. SC-53, pp. 844-854 Mar. 2021.

H.-S. Lee and D. Daly, "Push-pull dynamic amplifier circuits," *U.S. Patent 10,951,184*, Mar.16, 2021.

Luqiao Liu

Associate Professor

Department of Electrical Engineering & Computer Science

Spintronics; spin based logic and memory device; nanoscale magnetic material for information storage and microwave application; fabrication technique of magnetic nanodevices; spin related phenomena in semiconductor, topological insulator, superconductors and low dimensional material; magnetic dynamics.

Rm. 39-553a | 617-253-0019 | luqiao@mit.edu

GRADUATE STUDENTS

Josh Chou, Physics

Jiahao Han, EECS

Justin Hou, EECS

Zhongqiang Hu, EECS

Brooke C. McGoldrick, EECS

Taqiyyah Safi, EECS

Pengxiang Zhang, EECS

Y. Fan, J. Finley, M. E. Holtz, P. Quarterman, A. J. Grutter, J. Han, P. Zhang, T. S. Safi, J. T. Hou, and L. Liu, "Resonant spin transmission mediated by magnons in a magnetic insulator," *Advanced Materials*, 2008555: 2021.

SUPPORT STAFF

Steven O'Hearn, Administrative Assistant

SELECTED PUBLICATIONS

J. Han, P. Zhang, Z. Bi, Y. Fan, T. S. Safi, J. Xiang, J. Finley, L. Fu, R. Cheng, and L. Liu, "Birefringence-like spin transport via linearly polarized antiferromagnetic magnons," *Nature Nanotechnology*, 15, 563: 2020.

M. Huang, J. Xiang, C. Feng, H. Huang, P. Liu, Y. Wu, A. T. N'Diaye, G. Chen, J. Liang, H. Yang, J. Liang, X. Cui, J. Zhang, Y. Lu, K. Liu, D. Hou, L. Liu, and B. Xiang, "Direct Evidence of Spin Transfer Torque on Two-Dimensional Cobalt-Doped MoS₂ Ferromagnetic Material," *ACS Applied Electronic Materials* 2, 1497: 2020.

J. Finley and L. Liu, "Spintronics with compensated ferrimagnets," *Applied Physics Letters* 116, 110501: 2020.

Y. Fan, P. Quarterman, J. Finley, J. Han, P. Zhang, J. T. Hou, M. D. Stiles, A. J. Grutter, and L. Liu, "Manipulation of Coupling and Magnon Transport in Magnetic Metal-Insulator Hybrid Structures," *Physical Review Applied* 13, 061002: 2020.

T. S. Safi, P. Zhang, Y. Fan, Z. Guo, J. Han, E. R. Rosenberg, C. Ross, Y. Tserkovnyak, and L. Liu, "Variable spin-charge conversion across metal-insulator transition," *Nature Communications* 11, 476: 2020.

D. D. Awschalom, C. H. R. Du, R. He, J. Heremans, A. Hoffmann, J. Hou, H. Kurebayashi, Y. Li, L. Liu, V. Novosad, J. Sklenar, S. Sullivan, D. Sun, H. Tang, V. Tyberkevych, C. Trevillian, A. W. Tsen, L. Weiss, W. Zhang, X. Zhang, L. Zhao, and C. W. Zollitsch, "Quantum engineering with hybrid magnonics systems and materials," *IEEE Transactions on Quantum Engineering*, 1-1: 2021.

Scott R. Manalis

Viterbi Professor

Departments of Biological and Mechanical Engineering

Development of quantitative and real-time techniques for biomolecular detection and single cell analysis. We use conventional silicon processing techniques to fabricate fluidic devices and exploit the unique physical properties associated with micro and nanoscale dimensions for developing precision measurement methods.

Rm. 76-261 | 617-253-5039 | srm@mit.edu

POSTDOCTORAL ASSOCIATES

Chuyi Chen, KI

Georgios (Yorgos) Katsikis, KI

Scott Knudsen, BE

Teemu Miettinen, KI

Peter Winter, KI

Jiaquan (Jason) Yu, KI

Ye Zhang, KI

GRADUATE STUDENTS

Sarah Duquette, BE

Adam Langenbacher, CSB

Alex Miller, HST

Felicia Rodriguez, BE

Weida (Richard) Wu, BE

UNDERGRADUATE STUDENTS

Mitali Chowdhury, BE

Athena Nguyen, BE

Zak Zhang, BE

RESEARCH STAFF

Christina Bray, KI

Sarah Ishamuddin, KI

Lin Lin, KI

Mahnoor Mirza, KI

Nola Mulugeta, KI

Jennifer Yoon, KI

SUPPORT STAFF

Mariann Murray, Administrative Assistant

SELECTED PUBLICATIONS

J. H. Kang, G. Katsikis, M. A. Stockslager, D. Lim, M. B. Yaffe, S. R. Manalis, and T. P. Miettinen, "Monitoring and Modeling of Lymphocytic Leukemia Cell Bioenergetics Reveals Decreased ATP Synthesis During Cell Division," *Nature Communications*, 11(1), 2020.

L. Mu, J. H. Kang, S. Olcum, K. R. Payer, N. L. Calistri, R. J. Kimmerling, S. R. Manalis, and T. P. Miettinen, "Mass Measurements During Lymphocytic Leukemia Cell Polyploidization Decouple Cell Cycle and Cell Size-dependent Growth," *PNAS*, 117(27), 2020.

M. Urbanska, H. E. Muñoz, J. S. Bagnall, O. Otto, S. R. Manalis, D. D. Carlo, and J. Guck, "A Comparison of Microfluidic Methods for High-throughput Cell Deformability Measurements," *Nature Methods*, 17(6), 2020.

M. Gagino, G. Katsikis, S. Olcum, L. Viroto, M. Cochet, A. Thuaire, S. R. Manalis, and V. Agache, "Suspended Nanochannel Resonators Arrays with Piezoresistive Sensors for High-throughput Weighing of Nanoparticles in Solution," *ACS Sensors*, 5(4), 2020.

M. A. Stockslager, S. Olcum, S. M. Knudsen, R. J. Kimmerling, N. Cermak, K. Payer, V. Agache, and S. R. Manalis, "Rapid and High-precision Sizing of Single Particles Using Parallel Suspended Microchannel Resonator Arrays and Deconvolution," *Review of Scientific Instruments*, 90(8), 2019.

J. H. Kang, T. P. Miettinen, L. Chen, S. Olcum, G. Katsikis, P. S. Doyle, and S. R. Manalis, "Noninvasive Monitoring of Single-cell Mechanics by Acoustic Scattering," *Nature Methods*, 16(3):263-269, 2019.

B. Hamza, S. R. Ng, S. M. Prakadan, F. F. Delgado, C. R. Chin, E. M. King, L. F. Yang, S. M. Davidson, K. L. DeGouveia, N. Cermak, A. W. Navia, P. S. Winter, T. Tammela, C. M. Li, T. Papagiannakopoulos, A. J. Gupta, J. S. Bagnall, S. M. Knudsen, M. G. Vander Heiden, S. C. Wasserman, T. Jacks, A. K. Shalek, and S. R. Manalis, "An Optofluidic Real-Time Cell Sorter for Longitudinal CTC Studies in Mouse Models of Cancer," *PNAS*, 116(6), 2019.

M. R. Luskin, M. A. Murakami, S. R. Manalis, and D. M. Weinstock, "Targeting Minimal Residual Disease: a Path to Cure?" *Nature Reviews Cancer*, 18(4): 255-63, 2018.

N. L. Calistri, R. J. Kimmerling, S. W. Malinowski, M. Touat, M. M. Stevens, S. Olcum, K. L. Ligon, and S. R. Manalis, "Microfluidic Active Loading of Single Cells Enables Analysis of Complex Clinical Specimens," *Nature Communications*, 9, 2018.

A. E. Cetin, M. M. Stevens, N. L. Calistri, M. Fulciniti, S. Olcum, R. J. Kimmerling, N. C. Munshi, and S. R. Manalis, "Determining Therapeutic Susceptibility in Multiple Myeloma by Single-cell Mass Accumulation," *Nature Communications*, 8, 2017.

N. Cermak, J. W. Becker, S. M. Knudsen, S. W. Chisholm, S. R. Manalis, and M. F. Polz, "Direct Single-cell Biomass Estimates for Marine Bacteria via Archimedes' Principle," *ISME Journal*, 11(3): 825-8, 2017.

Farnaz Niroui

Assistant Professor

Department of Electrical Engineering & Computer Science

Nanofabrication techniques with a focus on achieving nanometer precision and resolution, utilizing emerging nanomaterials. Surfaces, interfaces and forces at the nanoscale. Active devices with applications in electromechanical systems, optoelectronics, and quantum technologies.

Rm. 13-3005B | 617-253-0085 | fniroui@mit.edu

GRADUATE STUDENTS

Patricia Jastrzebska-Perfect, EECS, NSF Fellow

Peter Satterthwaite, EECS, NSF Fellow

Spencer (Weikun) Zhu, ChemE

SUPPORT STAFF

Catherine Bourgeois, Administrative Assistant

SELECTED PUBLICATIONS

F. Niroui, M. Saravanapavanantham, J. Han, J. J. Patil, T. M. Swager, J. H. Lang, and V. Bulovic, "Hybrid Approach to Fabricate Uniform and Active Molecular Junctions," *Nano Lett.*, vol. 21, pp. 1606-1612, 2021.

V. Jamali, F. Niroui, L. W. Taylor, O. S. Dewey, B. A. Koscher, M. Pasquali, and A. P. Alivisatos, "Perovskite-Carbon Nanotube Light-Emitting Fibers," *Nano Lett.*, vol. 20, pp. 3178-3184, 2020.

S. Fathipour, S. F. Almeida, Z. A. Ye, B. Saha, F. Niroui, T. King Liu, and J. Wu, "Reducing Adhesion Energy of Nanoelectromechanical Relay Contacts by Self-assembled Perfluoro(2,3-Dimethylbutan-2-ol) Coating," *AIP Advances*, vol. 9, 055329, 2019.

F. Niroui, M. Saravanapavanantham, T. M. Swager, J. H. Lang, and V. Bulovic, "Fabrication of Nanoscale Structures with Nanometer Resolution and Surface Uniformity," *IEEE International Conference on Micro Electro Mechanical Systems*, pp. 659-662, 2017.

G. D. Han, K. H. Tu, F. Niroui, W. Xu, S. Zhou, X. Wang, V. Bulovic, C. A. Ross, J. H. Warner, and J. H. Grossman, "Photoluminescent Arrays of Nanopatterned Monolayer MoS₂," *Adv. Funct. Mater.*, vol. 27, 1703688, 2017.

R. Brenes, D. Guo, A. Osherov, N. K. Noel, C. Eames, E. M. Hutter, S. K. Pathak, F. Niroui, R. H. Friend, M. S. Islam, H. J. Snaith, V. Bulovic, T. J. Savenijie, and S. D. Stranks, "Metal Halide Perovskite Polycrystalline Films Exhibiting Properties of Single Crystals," *Joule*, vol. 1, pp. 155-167, 2017.

B. Osoba, B. Saha, L. Dougherty, J. Edgington, C. Qian, F. Niroui, J. H. Lang, V. Bulovic, J. Wu, and T. K. Liu, "Sub-50 mV NEM Relay Operation Enabled by Self-assembled Molecular Coating," *International Electron Devices Meeting*, pp. 655-658, 2016.

F. Niroui, A. I. Wang, E. M. Sletten, Y. Song, J. Kong, E. Yablonovitch, T. M. Swager, J. H. Lang, and V. Bulovic, "Tunneling Nanoelectromechanical Switches based on Compressible Molecular Thin Films," *ACS Nano*, vol. 9, pp. 7886-7894, 2015.

F. Niroui, E. M. Sletten, P. B. Deotare, A. I. Wang, T. M. Swager, J. H. Lang, and V. Bulovic, "Controlled Fabrication of Nanoscale Gaps using Stiction," *IEEE International Conference on Micro Electro Mechanical Systems*, pp. 85-88, 2015.

F. Niroui, P. B. Deotare, E. M. Sletten, A. I. Wang, E. Yablonovitch, T. M. Swager, J. H. Lang, and V. Bulovic, "Nanoelectromechanical Tunneling Switches based on Self-assembled Molecular Layers," *IEEE International Conference on Micro Electro Mechanical Systems*, pp. 1103-1106, 2014.

Jelena Notaros

Assistant Professor of Electrical Engineering & Computer Science
Department of Electrical Engineering & Computer Science

Integrated photonics platforms, devices, and systems for applications including displays, sensing, communications, quantum, and biology.
Rm. 26-343 | 617-253-3073 | notaros@mit.edu

GRADUATE STUDENTS

Sabrina Corsetti, EECS, MIT Presidential Fellow & NSF Fellow

Milica Notaros, EECS, MIT Presidential Fellow & NSF Fellow

Tal Sneh, EECS, MIT Presidential Fellow

UNDERGRADUATE STUDENT

Abigail Shull, EECS & Physics

SUPPORT STAFF

Dianne Lior, Administrative Assistant

RECENT PUBLICATIONS

J. Notaros, M. Notaros, M. Raval, C. V. Poulton, M. J. Byrd, N. Li, Z. Su, E. S. Magden, E. Timurdogan, T. Dyer, C. Baiocco, T. Kim, P. Bhargava, V. Stojanovic, and M. R. Watts, "Integrated Optical Phased Arrays for LiDAR, Augmented Reality, and Beyond," in *Proceedings of Applied Industrial Optics (AIO)* (OSA, 2021). (Invited Talk)

U. Chakraborty, J. Carolan, G. Clark, D. Bunandar, G. Gilbert, J. Notaros, M. R. Watts, and D. R. Englund, "Cryogenic operation of silicon-photonics modulators based on the DC Kerr effect," *Optica* 7(10), 1385-1390 (2020).

J. Notaros, M. Notaros, M. Raval, C. V. Poulton, M. J. Byrd, N. Li, Z. Su, E. S. Magden, E. Timurdogan, T. Dyer, C. Baiocco, T. Kim, P. Bhargava, V. Stojanovic, and M. R. Watts, "Integrated Optical Phased Arrays for LiDAR, Communications, Augmented Reality, and Beyond," in *Proceedings of Frontiers in Optics (FiO)* (OSA, 2020), paper FM5B.3. (Invited Talk)

J. Notaros, M. Notaros, M. Raval, C. V. Poulton, M. J. Byrd, N. Li, Z. Su, E. S. Magden, E. Timurdogan, T. Dyer, C. Baiocco, T. Kim, P. Bhargava, V. Stojanovic, and M. R. Watts, "Integrated Optical Phased Arrays: LiDAR, Communications, Augmented Reality, and Beyond," in *Proceedings of Photonics Networks and Devices (NETWORKS)* (OSA, 2020), paper NeTu3B.1. (Invited Talk)

N. Mehta, Z. Su, E. Timurdogan, J. Notaros, R. Wilcox, C. V. Poulton, C. Baiocco, N. Fahrenkopf, S. Kruger, T. Ngai, Y. Timalisina, M. R. Watts, and V. Stojanovic, "An Optically Sampled ADC in 3D Integrated Silicon-Photonics/65nm CMOS," in *Proceedings of the 2020 IEEE Symposium on VLSI Technology (VLSI)* (IEEE, 2020). (Technology Highlight)

U. Chakraborty, J. Carolan, G. Clark, D. Bunandar, J. Notaros, M. R. Watts, and D. R. Englund, "Cryogenic Operation of Silicon Photonic Electro-Optic Modulators based on DC Kerr Effect," in *Proceedings of the APS March Meeting* (APS, 2020), paper L27.4.

J. Notaros, M. Notaros, M. Raval, C. V. Poulton, M. J. Byrd, N. Li, Z. Su, E. S. Magden, E. Timurdogan, T. Dyer, C. Baiocco, T. Kim, P. Bhargava, V. Stojanovic, and M. R. Watts, "Integrated optical phased arrays: LiDAR, augmented reality, and beyond," in *Proceedings of Photonics West* (SPIE, 2020), paper 11285-18. (Invited Talk)

N. Li, M. Xin, Z. Su, E. S. Magden, N. Singh, J. Notaros, E. Timurdogan, Purnawirman, J. D. B. Bradley, and M. R. Watts, "A Silicon Photonic Data Link with a Monolithic Erbium-Doped Laser," *Scientific Reports* 10, 1114 (2020).

William D. Oliver

Professor of Electrical Engineering and Computer Science, Physics
Laboratory Fellow of Lincoln Laboratory
Director of Center for Quantum Engineering
Associate Director of Research Laboratory of Electronics

The materials growth, fabrication, design, measurement of superconducting qubits. The development of cryogenic packaging and control William electronics involving cryogenic CMOS and single-flux quantum digital logic.

Rm. 13-3050 | 617-258-6018 | william.oliver@mit.edu

RESEARCH SCIENTIST

Joel I. J. Wang, RLE

POSTDOCTORAL ASSOCIATES

Jochen Braumüller, RLE
Agustin Di Paolo, RLE
Patrick Harrington, RLE
Antti Vepsäläinen, RLE
Roni Winik, RLE

GRADUATE STUDENTS

Aziza Almanakly, EECS, Paul and Daisy Soros Fellow
Junyoung An, EECS, Kfas Fellow
Will Banner, EECS, JACOBS Fellow
Leon Ding, Physics, IBM Fellow
Qi (Andy) Ding, EECS
Ami Greene, EECS, Google PhD Fellow
Bharath Kannan, EECS, NDSEG Fellow
Amir Karamlou, EECS, NSF GRFP Fellow
Benjamin Lienhard, EECS
Chris McNally, EECS, CQA/NSA Fellow
Sarah Muschinske, EECS, NASA Fellow
Yanjie (Jack) Qiu, EECS
David Rower, Physics, MIT SOS Fellow
Gabriel O. Samach, EECS, Lincoln Laboratory Fellow
Youngkyu Sung, EECS, Kfas Fellow

UNDERGRADUATE STUDENTS

Sebastian N Alberdi, EECS
Matthew Baldwin, Physics
Franck N Belemkoabga, EECS
Thomas Bergamaschi, Physics
Grecia Castelazo, Physics
Thao Dinh, Physics
Lauren Li, Physics and Mathematics
Elaine Pham, EECS
Daniela A Zaidenberg, Physics

VISITING STUDENTS

Charlotte Böttcher, Harvard University, Yacoby/IBM
PhD Fellow
Tim Menke, Harvard University

SUPPORT STAFF

Chihiro Watanabe, Administrative Assistant

SELECTED PUBLICATIONS

B. Kannan, D. L. Campbell, F. Vasconcelos, R. Winik, D. K. Kim, M. Kjaergaard, P. Krantz, A. Melville, B. M. Niedzielski, J. L. Yoder, T. P. Orlando, S. Gustavsson, W. D. Oliver, "Generating Spatially Entangled Itinerant Photons with Waveguide Quantum Electrodynamics," *Science Advances* 6, 41, eabb8780, Oct. 2020.

A. P. Vepsäläinen, A. H. Karamlou, J. L. Orrell, A. S. Dogra, A. Loer, F. Vasconcelos, D. K. Kim, A. J. Melville, B. M. Niedzielski, J. L. Yoder, S. Gustavsson, J. A. Formaggio, B. A. VanDevender, W. D. Oliver, "Impact of Ionizing Radiation on Superconducting Qubit Coherence," *Nature* 584, 551-556, Aug. 2020.

B. Kannan, M. Ruckriegel, D. Campbell, A. F. Kockum, J. Braumüller, D. Kim, M. Kjaergaard, P. Krantz, A. Melville, B. M. Niedzielski, A. Vepsäläinen, R. Winik, J. Yoder, F. Nori, T. P. Orlando, S. Gustavsson, W. D. Oliver, "Waveguide Quantum Electrodynamics with Giant Superconducting Artificial Atoms," *Nature* 583, 775-779, Jul. 2020.

D. Rosenberg, S. Weber, D. Conway, D. Yost, J. Mallek, G. Calusine, R. Das, D. Kim, M. Schwartz, W. Woods, J. L. Yoder, W. D. Oliver, "Solid-State Qubits: 3D Integration and Packaging," *IEEE Microwave Magazine* 21:8, 72-85, Aug. 2020.

C. W. Yost, M. E. Schwartz, J. Mallek, D. Rosenberg, C. Stull, J. L. Yoder, G. Calusine, M. Cook, R. Das, A. L. Day, E. B. Golden, D. K. Kim, A. Melville, B. M. Niedzielski, W. Woods, A. J. Kerman, W. D. Oliver, "Solid-State Qubits Integrated with Superconducting Through-Silicon Vias," *npj Quantum Information* 6, 59, Jul. 2020.

M. Kjaergaard, M. E. Schwartz, J. Braumüller, P. Krantz, J. I-J. Wang, S. Gustavsson, W. D. Oliver, "Superconducting Qubits: Current State of Play," *Annual Reviews of Condensed Matter Physics* 11, 369-395, 2020.

Tomás Palacios

Professor

Department of Electrical Engineering & Computer Science

Design, fabrication, and characterization of novel electronic devices and systems based on wide bandgap semiconductors & 2-D materials, polarization & bandgap engineering, transistors for high voltage, sub-mm wave power & digital applications.

Rm. 39-567A | 617-324-2395 | tpalacios@mit.edu

POSTDOCTORAL ASSOCIATES

Marek Hempel, MTL

Ahmad Zubair, MTL

GRADUATE STUDENTS

Nadim Chowdhury, EECS

Kevin Limanta, EECS

Yiyue Luo, EECS, CSAIL

Elaine McVay, EECS

John Niroula, EECS

Joshua Perozek, EECS

Pao-Chuan Shih, EECS

Qingyun Xie, EECS

Mantian Xue, EECS

Mengyang Yuan, EECS

Jiadi Zhu, EECS

UNDERGRADUATE STUDENTS

Adina Golden, UROP

Alisa Hathaway, UROP

Jaeyoung Jung, SuperUROP

Sarah Spector, SuperUROP

VISITORS

Anthony Taylor, Edwards Vacuum

Kohei Yoshizawa, DOWA

SUPPORT STAFF

Joseph Baylon, Administrative Assistant

SELECTED PUBLICATIONS

E. McVay, T. Palacios, et al., "Impact of Al_2O_3 Passivation on the Photovoltaic Performance of Vertical WSe_2 Schottky Junction Solar Cells," *ACS Applied Materials & Interfaces*, 2020.

B. Han, T. Palacios, et al., "Deep-Learning-Enabled Fast Optical Identification and Characterization of 2D Materials," *Advanced Materials*, Vol. 32, Issue 29, pg. 2000953, 2020.

M. M. Tavakoli, T. Palacios, et al., "Synergistic Roll-to-Roll Transfer and Doping of CVD-Graphene Using Parylene for Ambient-Stable and Ultra-Lightweight Photovoltaics," *Adv. Functional Materials*, Vol. 30, Issue 31, pg. 2001924, 2020.

S. Warnock, T. Palacios, et al., "InAlN/GaN-on-Si HEMT with 4.5 W/mm in a 200-mm CMOS-Compatible MMIC Process for 3D Integration," *2020 IEEE/MTT-S International Microwave Symposium (IMS)*, pg. 289-292, 2020.

S. J. Bader, T. Palacios, et al., "Prospects for wide bandgap and ultrawide bandgap CMOS devices," *IEEE Transactions on Electron Devices*, Vol. 67, Issue 10, pg. 4010-4020, 2020.

K. H. Teo, T. Palacios, et al., "Recent Development in 2D and 3D GaN devices for RF and Power Electronics Applications," *2020 IEEE International Symposium on Radio-Frequency Integration Technology (RFIT)*, pg. 22-24, 2020.

N. Chowdhury, T. Palacios, et al., "Field-induced Acceptor Ionization in Enhancement-mode GaN p-MOSFETs," *2020 IEEE International Electron Devices Meeting (IEDM)*, pg. 5.5.1-5.5.4, 2020.

W. Chern, T. Palacios, et al., "Demonstration of a ~40 kV Si Vacuum Transistor as a Practical High Frequency and Power Device," *2020 IEEE International Electron Devices Meeting (IEDM)*, pg. 5.2.1-5.2.4, 2020.

P.-C. Shih, T. Palacios, et al., "Self-Align-Gated GaN Field Emitter Arrays Sharpened by a Digital Etching Process," in *IEEE Electron Device Letters*, vol. 42, no. 3, pp. 422-425, 2021.

Y. Zhang, T. Palacios, et al., "GaN FinFETs and trigate devices for power and RF applications: review and perspective," *Semicond. Sci. Technol.* 36 054001, 2021.

L. Zhou, T. Palacios, et al., "Liquid-vapor Growth of Atomically Thin Metal Tellurides with Controllable Polymorphism," *Research Square*, pg. 1-17, 2021.

L. G. Pimenta Martins, T. Palacios, et al., "Hard, transparent, sp³-containing 2D phase formed from few-layer graphene under compression," *Carbon*, Vol. 173, pg. 744-757, 2021.

R. Li, T. Palacios, et al., "Flexible and high-performance electrochromic devices enabled by self-assembled 2D TiO_2 /MXene heterostructures," *Nature Communications*, Vol. 12, Issue 1, pg. 1-11, 2021.

Y. Lin, T. Palacios, et al., "Towards High-Performance Monolayer Semiconductor Transistors with Semimetallic Ohmic Contact," *American Physical Society*, 2021.

Y. Luo, T. Palacios, et al., "Learning human-environment interactions using conformal tactile textiles," *Nature Electronics*, pg.1-1, 2021.

Negar Reiskarimian

X-Window Consortium Career Development Assistant Professor
Department of Electrical Engineering & Computer Science

Integrated circuits and systems and applied electromagnetics with a focus on analog, RF, millimeter-Wave (mm-Wave) and optical integrated circuits, metamaterials and systems for a variety of applications.

Rm. 39-427A | 617-253-0726 | negarr@mit.edu

GRADUATE STUDENTS

Soroush Araei, EECS

Shahabeddin Mohin, EECS

SUPPORT STAFF

Jami L. Mitchell, Administrative Assistant

SELECTED PUBLICATIONS

N. Reiskarimian, M. Khorshidian and H. Krishnaswamy, "Inductorless, Widely Tunable N-Path Shekel Circulators Based on Harmonic Engineering," *IEEE Journal of Solid-State Circuits (JSSC)* (invited), vol. 56, no. 4, Apr. 2021.

A. Nagulu, N. Reiskarimian and H. Krishnaswamy, "Non-reciprocal Electronics Based on Temporal Modulation," *Nature Electronics*, May 2020.

N. Reiskarimian, M. Khorshidian and H. Krishnaswamy, "Inductorless, Widely-Tunable N-Path Shekel Circulators Based on Harmonic Engineering," in *IEEE Radio Frequency Integrated Circuits Symposium (RFIC)*, pp. 39-42, Jun. 2020.

M. Khorshidian, N. Reiskarimian, and H. Krishnaswamy, "A Compact Reconfigurable N-Path Low-Pass Filter Based on Negative Trans-Resistance with <1dB Loss and >21dB Out-of-Band Rejection," in *IEEE International Microwave Symposium (IMS)*, pp. 799-802, Jun. 2020.

M. Khorshidian, N. Reiskarimian, and H. Krishnaswamy, "High-Performance Isolators and Notch Filters based on N-Path Negative Trans-Resistance," in *IEEE International Solid-State Circuits Conference (ISSCC)*, Feb. 2020.

M. Baraani Dastjerdi, S. Jain, N. Reiskarimian, A. Natarajan, and H. Krishnaswamy, "Analysis and Design of Full-Duplex 2x2 MIMO Circulator-Receiver with High TX power handling Exploiting MIMO RF and Shared-delay Baseband Self-Interference Cancellation," *IEEE Journal of Solid State Circuits (JSSC)* (invited), vol. 54, no. 12, pp. 3525-3540, Dec. 2019.

N. Reiskarimian, M. Tymchenko, A. Alu, and H. Krishnaswamy, "Breaking Time-Reversal Symmetry Within Infinitesimal Dimensions Through Staggered Switched Networks," in *Metamaterials*, Sep. 2019.

N. Reiskarimian, A. Nagulu, T. Dinc, and H. Krishnaswamy, "Non-Reciprocal Devices: A Hypothesis Turned into Reality," *IEEE Microwave Magazine* (invited), vol. 20, no. 4, pp. 94-111, Apr. 2019.

N. Reiskarimian, T. Dinc, J. Zhou, T. Chen, M. Baraani Dastjerdi, J. Diakonikolas, G. Zussman, and H. Krishnaswamy, "A One-Way Ramp to a Two-Way Highway: Integrated Magnetic-Free Non-Reciprocal Antenna Interfaces for Full Duplex Wireless," in *IEEE Microwave Magazine* (invited), vol. 20, no. 2, pp. 56-75, Feb. 2019.

M. Baraani Dastjerdi, S. Jain, N. Reiskarimian, A. Natarajan, and H. Krishnaswamy, "Full-Duplex 2x2 MIMO Circulator-Receiver with High TX Power Handling Exploiting MIMO RF and Shared-Delay Baseband Self-Interference Cancellation," accepted and to appear in *IEEE International Solid-State Circuits Conference (ISSCC)*, Feb. 2019.

Jennifer L. M. Rupp

Professor of Electrochemical Materials
Department of Materials Science and Engineering
Department of Electrical Engineering and Computer Science

Electrochemical Materials.

Rm. 8-242 | 617-253-4477 | jrupp@mit.edu

POSTDOCTORAL ASSOCIATES

Moran Balaish, DMSE
Kunjoong Kim, DMSE
Haemin Paik, DMSE
Linping Kong, DMSE

GRADUATE STUDENTS

Drew Buzzel, EECS
Thomas Defferriere, DMSE
Willis O'Leary, DMSE
Sara Catherine Sand, DMSE
Philipp Simons, DMSE
Yuntong Zhu, DMSE
Hyunwon Chu, DMSE
Jesse Hinricher, DMSE

SELECTED PUBLICATIONS

M. Balaish, J. C. Gonzalez-Rosillo, K.J. Kim, Y. Zhu, Z.D. Hood, and J. L. M. Rupp, "Processing Thin but Robust Electrolytes for Solid-State Batteries," *Nature Energy*, 10.1038/s41560-020-00759-5, 2021.

K. J. Kim, M. Balaish, M. Wadaguchi, L. Kong, and J. L. M. Rupp, "Solid-State Li-Metal Batteries: Challenges and Horizons of Oxide and Sulfide Solid Electrolytes and Their Interfaces," *Advanced Energy Materials*, 202002689, 2021.

M. Balaish, and J. L. M. Rupp, "Widening the Range of Trackable Environmental and Health Pollutants for Li-Garnet-Based Sensors," *Advanced Materials*, in press, 2021.

T. Defferriere, D. Kalaev, J. L. M Rupp, and H. L. Tuller, "Impact of Oxygen Non-stoichiometry on Near-Ambient Temperature Ionic Mobility in Polaronic Mixed-Ionic-Electronic Conducting Thin Films," *Advanced Functional Materials*, 202005640, 2021.

J. Irvine, J.L.M. Rupp, G. Liu, X. Xu, S. Haile, X. Qian, A. Snyder, R. Freer, D. Ekren, S. Skinner, O. Celikbilek, S. Chen, S. Tao, T.H. Shin, R. O'Hayre, J. Huang, C. Duan, M. Papac, S. Li, A. Russel, V. Celorrio, B. Hayden, H. Nolan, X. Huang, G. Wang, I. Metcalfe, D. Neagu, and S. Martin, "Roadmap on Inorganic Perovskites For Energy Applications," *Journal of Physics: Energy*, in press, 2021.

E. Sediva, A. J. Carrillo, C. E. Halloran, and J. L. M. Rupp, "Evaluating the Redox Behavior of Doped Ceria for Thermochemical CO₂ Splitting Using Time-Resolved Raman Spectroscopy," *ACS Applied Energy Materials*, 4, 2, 1474–1483, 2021.

Y. Zhu, J. C. Gonzalez-Rosillo, M. Balaish, Z. D. Hood, K. J. Kim, and J. L. M. Rupp, "Lithium-Film Ceramics for Solid-State Lithionic Devices," *Nature Review Materials*, 6, 313–331, 2021.

Charles G. Sodini

LeBel Professor

Department of Electrical Engineering & Computer Science

Electronics and integrated circuit design and technology. Specifically, his research involves technology intensive integrated circuit and systems design, with application toward medical electronic devices for personal monitoring of clinically relevant physiological signals.

Rm. 39-527B | 617-253-4938 | sodini@mit.edu

COLLABORATORS

Sam Fuller, Analog Devices, Inc

Thomas O'Dwyer, MTL Research Affiliate

Joohyun Seo, Analog Devices, Inc.

POSTDOCTORAL ASSOCIATE

Anand Chandraksekhar, MTL

GRADUATE STUDENT

Jeanne Harabedian, MTL

SUPPORT STAFF

Kathleen Brody, Administrative Assistant

SELECTED PUBLICATIONS

J. Seo, H.-S. Lee, and C. G. Sodini, "Non-Invasive Evaluation of a Carotid Arterial Pressure Waveform Using Motion-Tolerant Ultrasound Measurements During the Valsalva Maneuver," *IEEE Journal Of Biomedical And Health Informatics*, vol. 25, no. 1, Jan. 2021.

H. Lai, G. Saavedra-Peña, C. G. Sodini, V. Sze, and T. Heldt, "Measuring Saccade Latency Using Smartphone Cameras," *IEEE Journal of Biomedical and Health Informatics*, vol. 24, no. 3, pp. 885-897, Mar. 2020.

J. Liu, C.G. Sodini, Y. Ou, B. Yan, Y.T. Zhang, N. Zhao, "Feasibility of Fingertip Oscillometric Blood Pressure Measurement: Model-based Analysis and Experimental Validation," *IEEE Journal of Biomedical and Health Informatics (JBHI)*, May, 2019

M. Delano and C. Sodini, "Evaluating Calf Bioimpedance Measurements for Fluid Overload Management in a Controlled Environment," *Physiological Measurement*, vol. 39, no. 12, p. 125009, 2018.

Vivienne Sze

Associate Professor of Electrical Engineering & Computer Science
Department of Electrical Engineering & Computer Science

Joint design of signal processing algorithms, architectures, VLSI and systems for energy-efficient implementations. Applications include computer vision, machine learning, autonomous navigation, image processing and video coding.
Rm. 38-260 | 617-324-7352 | sze@mit.edu

GRADUATE STUDENTS

Jamie Koerner, EECS (co-advised with Thomas Heldt)
Hsin-Yu Lai, EECS (co-advised with Thomas Heldt)
Yi-Lun Liao, EECS,
Peter Li, EECS (co-advised with Sertac Karaman)
Soumya Sudhakar, AeroAstro (co-advised with Sertac Karaman)
Yannan Nellie Wu, EECS (co-advised with Joel Emer)
Tien-Ju Yang, EECS

UNDERGRADUATE STUDENTS

Michael Gilbert, EECS
Keshav Gupta, EECS
Fan Francis Wang, EECS
Howard Zhong, EECS

SUPPORT STAFF

Janice L. Balzer, Administrative Assistant

SELECTED PUBLICATIONS

V. Sze, Y.-H. Chen, T.-J. Yang, and J. S. Emer, "Efficient Processing of Deep Neural Networks," *Synthesis Lectures on Computer Architecture - Morgan & Claypool Publishers*, 2020.

T.-J. Yang, Y.-L. Liao, and V. Sze, "NetAdapt v2: Efficient Neural Architecture Search with Fast Super-Network Training and Architecture Optimization," *Conference on Computer Vision and Pattern Recognition (CVPR)*, Jun. 2021.

F. Wang, Y. Wu, M. Woicik, V. Sze, and J. S. Emer, "Architecture-Level Energy Estimation for Heterogeneous Computing Systems," *IEEE International Symposium on Performance Analysis of Systems and Software (ISPASS)*, Mar. 2021.

Y. Wu, P. Tsai, A. Parashar, V. Sze, and J. Emer, "Sparseloop: An Analytical, Energy-Focused Design Space Exploration Methodology for Sparse Tensor Accelerators," *IEEE International Symposium on Performance Analysis of Systems and Software (ISPASS)*, Mar. 2021

J. Ray, A. Brahmakshatriya, R. Wang, S. Kamil, A. Reuther, V. Sze, and S. Amarasinghe, "Domain-Specific Language Abstractions for Compression," *Data Compression Conference (DCC)*, Mar. 2021

L. Bernstein, A. Sludds, R. Hamerly, V. Sze, J. Emer, and D. Englund, "Freely-scalable, reconfigurable optical hardware for deep learning," *Scientific Reports*, vol. 11, no. 3144, Feb. 2021.

V. Sze, Y.-H. Chen, T.-Y. Yang, and J. S. Emer, "How to Evaluate Deep Neural Network Processors: TOPS/W (Alone) Considered Harmful," *IEEE Solid-State Circuits Magazine*, vol. 12, no. 3, pp. 28-41, Summer 2020.

Z. Zhang, T. Henderson, S. Karaman, and V. Sze, "FSMI: Fast computation of Shannon Mutual Information for information-theoretic mapping," *International Journal of Robotics Research (IJRR)*, Vol. 39, No. 9, pp. 1155-1177, Aug. 2020.

J. Noraky, and V. Sze, "Low Power Depth Estimation of Rigid Objects for Time-of-Flight Imaging," *IEEE Transactions on Circuits and Systems for Video Technology (TCSVT)*, Vol. 30, No. 6, pp. 1524-1534, Jun. 2020.

S. Sudhakar, S. Karaman, V. Sze, "Balancing Actuation and Computing Energy in Motion Planning," *IEEE International Conference on Robotics and Automation (ICRA)*, May 2020.

T. Henderson, V. Sze, S. Karaman, "An Efficient and Continuous Approach to Information-Theoretic Exploration," *IEEE International Conference on Robotics and Automation (ICRA)*, May 2020.

Y. N. Wu, V. Sze, J. S. Emer, "An Architecture-Level Energy and Area Estimator for Processing-In-Memory Accelerator Designs," *IEEE International Symposium on Performance Analysis of Systems and Software (ISPASS)*, Apr. 2020.

H.-Y. Lai, G. Saavedra Peña, C. Sodini, V. Sze, T. Heldt, "Measuring Saccade Latency Using Smartphone Cameras," *IEEE Journal of Biomedical and Health Informatics (JBHI)*, Vol. 24, No. 3, pp. 885-897, Mar. 2020.

Carl V. Thompson

Stavros Salapatas Professor of Materials Science and Engineering
Department of Materials Science & Engineering
Director of Materials Research Laboratory

Optimization of processing and properties of thin films and nanostructures for applications in electronic, microelectromechanical, and electrochemical devices and systems. Interconnect and device reliability.

Rm. 13-2098 | 617-253-7652 | cthomp@mit.edu

RESEARCH SCIENTIST

Wardhana Sasangka, SMART

POSTDOCTORAL ASSOCIATES

Michael Chon, MRL

Pushpendra Kumar, SMART

Hui Teng Tan, SMART

An Tao, SMART

Baoming Wang, MRL

Gao Yu, SMART

GRADUATE STUDENTS

Michael Dubrovsky, ASP

Misong Ju, DMSE

Maxwell L'Etoile, DMSE

Jinghui Miao, DMSE

Yoon Ah Shin, DMSE

Lin Xu, DMSE

UNDERGRADUATE STUDENTS

Udochukwu D. Eze, DMSE

Brian A. Mills, Physics

SUPPORT STAFF

Sarah Ciriello, Administrative Assistant

SELECTED PUBLICATIONS

J. Miao, B. Wang, and C. V. Thompson, "First-order Amorphous-to-Amorphous Phase Transitions During Lithiation of Silicon Thin Films," *Phys. Rev. Materials*, volume 4, pp. 043608, 2020.

J. Miao, B. Wang, and C. V. Thompson, "Kinetic Study of Lithiation-Induced Phase Transitions in Amorphous Germanium Thin Film," *J. Electrochem. Soc.*, volume 167, pp. 090557, 2020.

L. Xu and C.V. Thompson, "Mechanisms of the Cyclic (de)lithiation of RuO₂," *J. Mater. Chem. A*, volume 8, pp. 21872, 2020.

Y. A. Shin and C.V. Thompson, "Templated Fingering During Solid State Dewetting," *Acta Materialia*, volume 207, pp.16669, 2021.

Luis Fernando Velásquez-García

Principal Research Scientist
Microsystems Technology Laboratories

Micro- and nano-enabled, multiplexed, scaled-down systems that exploit high electric field phenomena; powerMEMS; additively manufactured MEMS/NEMS. Actuators, cold cathodes, ionizers, microfluidics, microplasmas, CubeSat hardware, portable mass spectrometry, pumps, sensors, X-ray sources.
Rm. 39-415B | 617-253-0730 | lfvelasq@mit.edu

GRADUATE STUDENTS

Ashley L. Beckwith, MechE
Alejandro Diaz, EECS
Alex Kashkin, MechE
Nicholas Klugman, EECS
Hyeonseok Kim, MechE
Yosef S. Kornbluth, MechE
Zackary Pitcher, EECS

UNDERGRADUATE STUDENTS

Andrea Garcia, MechE
Maisha Prome, BioEng
Jordan Street, Wellesley

VISITOR

Javier Izquierdo Reyes, Tecnológico de Monterrey

SUPPORT STAFF

Jami L. Mitchell, Administrative Assistant

SELECTED PUBLICATIONS

L. F. Velásquez-García and Y. Kornbluth, "Biomedical Applications of Metal 3D Printing," accepted for publication, *Annual Review of Biomedical Engineering*, 2021.

A. L. Beckwith, J. Borenstein, and L. F. Velásquez-García, "Tunable Plant-based Biomaterials via in vitro Cell Culture using a Zinnia elegans Model," *Journal of Cleaner Production*, vol. 288, 125571 (10pp), Mar. 2021.

D. Melo Máximo and L. F. Velásquez-García, "Additively Manufactured Electrohydrodynamic Ionic Liquid Pure-Ion Sources for Nanosatellite Propulsion", *Additive Manufacturing*, vol. 36, 101719 (11pp), Dec. 2020.

Y. Kornbluth, R. H. Mathews, L. Parameswaran, L. Racz, and L. F. Velásquez-García, "Nano-Additively Manufactured Gold Thin Films with High Adhesion and Near-Bulk Electrical Resistivity via Jet-Assisted, Nanoparticle-Dominated, Room-Temperature Microsputtering," *Additive Manufacturing*, vol. 36, 101679 (11pp), Dec. 2020.

A. Fusova, S. Konev, L. F. Velásquez-García, Z. Sun, E. Nikolaev, "Study on the Thermal Expansion Effects of the 3D Printed Space Instrument", *Technical digest 15th International Manufacturing Science and Technology Conference*, Sep. 3, 2020; MSEC2020-8293.

A. P. Taylor, J. Izquierdo Reyes, and L. F. Velásquez-García, "Compact, Magnetically Actuated, Additively Manufactured Pumps for Liquids and Gases," *Journal of Physics D – Applied Physics*, vol. 53, no. 35, 355002 (13pp) Aug. 2020.

Y. Kornbluth, L. F. Velásquez-García, I. Ehrenberg, D. Carter, and K. J. Russell, "Atmospheric Microplasma-Sputtered Micro and Nanowires for Advanced THz Interconnects," *technical digest 33rd International Vacuum Nanoelectronics Conference (IVNC 2020)*, July 6-10, 2020.

Joel Voldman

Clarence J. Lebel Professor of Electrical Engineering
Faculty Head, Electrical Engineering
Department of Electrical Engineering & Computer Science

Microtechnology for basic cell biology, applied cell biology, Immunology, and human health.

Rm. 36-824 | 617-253-2094 | voldman@mit.edu

POSTDOCTORAL ASSOCIATES

Dohyun Lee, RLE
Sarvesh Varma, RLE

GRADUATE STUDENTS

Kru Kikkeri, EECS
Wei Liao, EECS
Dousabel May Yi Tay, ChemE

VISITOR

Mahdi Aeinehvand, Tec de Monterrey

SUPPORT STAFF

Chadwick Collins, Administrative Assistant

SELECTED PUBLICATIONS

D. Wu and J. Voldman, "An integrated model for bead-based immunoassays," *Biosens Bioelectron*, vol. 154, p. 112070, Apr. 15, 2020.

D. Wu and J. Voldman, "An integrated and automated electronic system for point-of-care protein testing," in *41st Annual International Conference of the IEEE Engineering in Medicine and Biology Society Berlin, Germany*, 2019.

C. P. Tostado, J. W. J. Heng, L. X. D. Ong, R. DasGupta, J. Voldman, and Y.-C. Toh, "Automation and integration of computer vision image analysis for cancer immunotherapy research with on-chip cell trapping," in *Micro Total Analysis Systems 2019*, Basel, Switzerland, 2019.

D.-H. Lee, B. Jundi, H. Ryu, R. M. Baron, J. Han, B. D. Levy, and J. Voldman, "Electrical profiling of septic neutrophils using microfluidics," in *Biomedical Engineering Society Annual Meeting*, Philadelphia, Pennsylvania, 2019.

D.-H. Lee, H. Jeon, B. Jundi, R. M. Baron, B. D. Levy, J. Han, and J. Voldman, "Rapid monitoring of sepsis by integration of spiral inertial microfluidics and isodielectric separation," in *Micro Total Analysis Systems 2019*, Basel, Switzerland, 2019.

B. Jundi, H. Ryu, D.-H. Lee, R.-E. E. Abdunnour, B. D. Engstrom, M. G. Duvall, A. Higuera, M. Pinilla-Vera, M. E. Benson, J. Lee, N. Krishnamoorthy, R. M. Baron, J. Han, J. Voldman, and B. D. Levy, "Leukocyte function assessed via serial microlitre sampling of peripheral blood from sepsis patients correlates with disease severity," *Nature Biomedical Engineering*, vol. 3, pp. 961-973, 2019.

R. Yuan, M. B. Nagarajan, J. Lee, J. Voldman, P. S. Doyle, and Y. Fink, "Designable 3d microshapes fabricated at the intersection of structured flow and optical fields," *Small*, vol. 14, p. e1803585, Dec. 2018.

R. Yuan, J. Lee, H.-W. Su, E. Levy, T. Khudiyev, J. Voldman, and Y. Fink, "Microfluidics in structured multimaterial fibers," *Proc Natl Acad Sci, U S A*, vol. 115, pp. E10830-E10838, 2018.

D. Wu, D. Rios-Aguirre, M. Chounlakone, S. Camacho-Leon, and J. Voldman, "Sequentially multiplexed amperometry for electrochemical biosensors," *Biosensors and Bioelectronics*, vol. 117, pp. 522-529, 2018.

S. Varma, G. Garcia-Cardena, and J. Voldman, "Unraveling endothelial cell phenotypic regulation by spatial hemodynamic flows with microfluidics," in *Micro Total Analysis Systems*, Kaohsiung, Taiwan, 2018.

A. Jaffe and J. Voldman, "Multi-frequency dielectrophoretic characterization of single cells," *Microsystems & Nanoengineering*, vol. 4, p. 23, 2018.

N. Apichitsopa and J. Voldman, "Large-area cell-tracking intrinsic cytometry with digital holographic imaging," in *Micro Total Analysis Systems*, Kaohsiung, Taiwan, 2018.

N. Apichitsopa, A. Jaffe, and J. Voldman, "Multiparameter cell-tracking intrinsic cytometry for single-cell characterization," *Lab on a Chip*, vol. 18, pp. 1430-1439, 2018.

S. Varma, A. Fendyur, A. Box, and J. Voldman, "Multiplexed cell-based sensors for assessing the impact of engineered systems and methods on cell health," *Analytical Chemistry*, vol. 89, pp. 4663-4670, 2017.

M. Carminati, G. Ferrari, M. D. Vahey, J. Voldman, and M. Sampietro, "Miniaturized impedance flow cytometer: Design rules and integrated readout," *IEEE Trans Biomed Circuits Syst*, vol. PP, pp. 1-12, Sep. 22, 2017.

N. Apichitsopa, A. Jaffe, and J. Voldman, "Multiparameter cell-tracking intrinsic cytometry for the characterization of single cells," in *Micro Total Analysis Systems*, Savannah, GA, 2017, pp. 225-7.

Evelyn N. Wang

Department Head, Gail E. Kendall Professor
Department of Mechanical Engineering

Heat and mass transport at the micro- and nano-scales, nanoengineered surfaces, and thermal microdevices for applications in thermal management, solar thermal energy conversion, and water desalination.

Rm. 3-174 | 617-253-3523 | enwang@mit.edu

POSTDOCTORAL ASSOCIATES

Xiangyu Li, MechE
Hyeongyun Cha, MechE

GRADUATE STUDENTS

Samuel Cruz, MechE
Carlos Daniel Diaz Marin, MechE
Cody Jacobucci, MechE
Arny Leroy, MechE
Adela Li, MechE
Jay Sircar, MechE
Youngsup Song, MechE
Geoffrey Vaartstra, MechE
Chad Wilson, MechE
Lenan Zhang, MechE
Yajing Zhao, MechE
Yang Zhong, MechE

UNDERGRADUATE STUDENT

Minna Wyttenbach, MechE

SUPPORT STAFF

Alexandra Cabral, Administrative Assistant

SELECTED PUBLICATIONS

Y. Song, S. Gong, G. Vaartstra, and E. N. Wang, "Microtube Surfaces for Simultaneous Enhancement of Efficiency and Critical Heat Flux During Pool Boiling," *ACS Applied Materials and Interfaces*, 1, 2021.

L. Li, L. Zhang, L. Zhang, Y. Zhong, E. N. Wang, Z. Chen, and L. Guo, "Sub-Picosecond Optical Response of Metals Due to Non-Thermalized Electron Dynamics," *ES Energy & Environment*, 1, p. 19-27, 2021.

S. M. Mirvakili, A. Leroy, D. Sim, and E. N. Wang, "Solar-Driven Soft Robots," *Advanced Science*, p. 2004235, 2021.

L. Zhang, R. Iwata, L. Zhao, S. Gong, Z. Lu, Z. Xu, Y. Zhong, J. Zhu, S. Cruz, K.L. Wilke, P. Cheng, and E.N. Wang, "Nucleation Site Distribution Probed by Phase-Enhanced Environmental Scanning Electron Microscopy," *Cell Report Physical Science*, 1(12), p. 100262, 2020.

S. Gong, L. Zhang, P. Cheng, and E. N. Wang, "Understanding Triggering Mechanisms for Critical Heat Flux In Pool Boiling Based On Direct Numerical Simulations," *International Journal of Heat and Mass Transfer*, 163, p. 120546, 2020.

Y. Song, L. Zhang, and E. N. Wang, "Criteria for Antibubble Formation From Drop Pairs Impinging On A Free Surface," *Physical Review Fluids*, 5(12), p. 123601, 2020.

D. S. Antao, K. L. Wilke, J. H. Sack, S. Lee, Z. Xu, D. J. Preston, and E. N. Wang, "Jumping Droplet Condensation in Internal Convective Vapor Flow," *International Journal of Heat and Mass Transfer*, 163, p. 120398, 2020.

Z. Lu, L. Zhang, R. Iwata, E. N. Wang, and J. C. Grossman, "Transport-Based Modeling of Bubble Nucleation on Gas Evolving Electrodes," *Langmuir*, 36(49), p. 15112-15118, 2020.

L. Zhao, B. Bhatia, L. Zhang, E. Strobach, A. Leroy, M. K. Yadav, S. Yang, T. A. Cooper, L.A. Weinstein, A. Modi, S. B. Kedare, G. Chen, and E. N. Wang, "A Passive High-Temperature High-Pressure Solar Steam Generator for Medical Sterilization," *Joule*, 4, p. 1-13, 2020.

K. L. Wilke, D. S. Antao, S. Cruz, R. Iwata, Y. Zhao, A. Leroy, D. J. Preston, and E. N. Wang, "Polymer Infused Porous Surfaces for Robust, Thermally Conductive, Self-Healing Coatings for Dropwise Condensation," *ACS Nano*, 2020.

H. Kim, S. Rao, A. LaPotin, S. Lee, and E. N. Wang, "Thermodynamic Analysis and Optimization of Adsorption-Based Atmospheric Water Harvesting," *International Journal of Heat and Mass Transfer*, 161, p. 120253, 2020.

A. LaPotin, Y. Zhong, L. Zhang, L. Zhao, A. Leroy, H. Kim, S. Rao, and E. N. Wang, "Dual-stage atmospheric water harvesting device for scalable solar-driven water production," *Joule*, 4, p. 1-17, 2020.

J. Zhu, L. Zhang, X. Li, K. L. Wilke, E. N. Wang, and L. L. Goddard, "Quasi-Newtonian Environmental Scanning Electron Microscopy (QN-ESEM) for Monitoring Material Dynamics in High-Pressure Gaseous Environments," *Advanced Science*, 7(19), p. 2001268, 2020.

G. Vaartstra, L. Zhang, Z. Lu, C. D. Diaz-Marin, J. C. Grossman, and E. N. Wang, "Capillary-Fed, Thin Film Evaporation Devices," *Journal of Applied Physics*, 128(13), p. 130901, 2020.

L. Zhang, W. Li, L. Zhang, Y. Zhong, X. Guo, L. Li, E. N. Wang, and L. Guo, "Framework For Analyzing The Thermoreflectance Spectra Of Metal Thermal Transducers With Spectrally Tunable Time-Domain Thermoreflectance," *Journal of Applied Physics*, 128(5), p. 055107, 2020.

Theses Awarded

Theses Awarded

S.M.

- **Maitreyi Ashok** (A. CHANDRAKASAN)
Hardware Security with Electromagnetic Side Channels
- **Kaustav Brahma** (A. CHANDRAKASAN)
Efficient CNNs and Energy Efficient SRAM Design for Ubiquitous Medical Devices
- **Ruicong Chen** (H.-S. LEE)
Activity-Scaling SAR with Direct Hybrid Encoding for Signed Expressions for AIoT Applications
- **Nicholas Klugman** (J. LANG)
Modeling and Design of Magnetic Flux Compression Generators
- **Kyungmi Lee** (A. CHANDRAKASAN)
Improved Methodology for Evaluating Adversarial Robustness in Deep Neural Networks
- **Rishabh Mittal** (A. CHANDRAKASAN)
A Sampling Jitter Tolerant Continuous-time Pipeline ADC
- **Vipasha Mittal** (A. CHANDRAKASAN/H.-S. LEE)
Design of a Bandgap-Less Temperature Sensor for Achieving High Untrimmed Accuracy
- **Yanjie Shao** (J. A. DEL ALAMO)
Design and Fabrication of III-V Broken-Band Vertical Nanowire Esaki Diodes
- **Elise Uyehara** (Q. HU)
Phase-locking Terahertz Quantum Cascade Lasers for High Dynamic Range Heterodyne Imaging
- **Drew Weninger** (A. M. AGARWAL)
Materials and Devices for Optoelectronic Packaging
- **Jongchan Woo** (A. CHANDRAKASAN)
Physical-Security for Wireless with Orbital Angular Momentum Wave
- **Fan Yang** (J. HU)
Achromatic and Wide Field-of-View Metalens Design
- **Pengxiang Zhang** (L. LIU)
Quantitative Study on Current Induced Effect in Antiferromagnet Insulator/Pt Bilayer
- **Wang Zhang** (L. DANIEL)
Modeling Internal Combustion Engine Three-Piece Oil Control Ring Coupling Reduced Order Oil Transport based on Neural Network

M. ENG.

- **Ebrahim Al Johany** (J. A. DEL ALAMO)
Surface Transfer Doping of Diamond for Power Electronics

- **Benjamin Cary** (J. LANG)
Design of Surgically Viable Umbo Microphone For Implantable Assistive Hearing Devices
- **Gloria (Yu-Liang) Fang** (A. CHANDRAKASAN)
Instruction-Level Power Consumption Simulator for Modeling Simple Timing and Power Side Channels in a 32-bit RISC-V Micro-Processor
- **Katharina Gschwind** (S. HAN)
Model Compression and AutoML for Efficient Click-Through Rate Prediction
- **Keshav Gupta** (V. SZE/S. KARAMAN)
Efficient Computation of Map-scale Continuous Mutual Information on Chip in Real Time
- **Damien Martin** (D. BONING/J. LANG)
Fault Detection in Manufacturing Equipment Using Unsupervised Deep Learning
- **Brooke McGoldrick** (L. LIU)
Ising Machine Based on Electrically Coupled Spin Hall Oscillators
- **Haripriya Mehta** (A. CHANDRAKASAN)
Secure Inference of Quantized Neural Networks
- **Jeet Mohapatra** (L. DANIEL)
Neural Network Robustness: Se-mantic Perturbations and Random-ized Smoothing Costs
- **Phoebe Piercy** (J. LANG)
Low Power Circuits with Integrated Magnetics for Sensors and Energy Harvesting Systems
- **Joanna Sands** (A. CHANDRAKASAN)
Modular device for wireless optically controlled neuromodulation in free behaving models
- **Daniel Sheen** (J. LANG)
A UHF Multimode Array Feed for the Westford Radio Telescope

PH.D.

- **Mohamed Abdelhamid** (A. CHANDRAKASAN)
Low Power Adaptive Wireless Circuits for the Internet of Things and In-body implants
- **Nicha Apichitsopa** (J.VOLDMAN)
Large-area cell-tracking cytometry for biophysical measurements of single cells
- **Utsav Banerjee** (A. CHANDRAKASAN)
Efficient Algorithms, Protocols and Hardware Architectures for Next-Generation Cryptography in Embedded Systems
- **Mindy Bishop** (M. SHULAKER)
Progress in Nanosystems for Computing and Health

PH.D. (CONTINUED)

- **Hongge Chen** (D. BONING)
Robust Machine Learning Models and Their Applications
- **Chanyeol Choi** (J. KIM)
Memristor-based AI Hardware for Reliable and Reconfigurable Neuromorphic Computing
- **Skylar Deckoff-Jones** (J. HU)
Chalcogenide Glass on Layered van der Waals Crystals for Integrated Photonic Devices
- **Joseph Finley** (L. LIU)
Spintronics Using Low Magnetization Materials
- **Matthew Flavin** (J. HAN)
Electrochemical Modulation of Neural Tissue Using ion-Selective Electrodes
- **Jinchi Han** (J. LANG)
Active Micro-/Nano-Structures for Electromechanical Actuation
- **Jack Holloway** (R. HAN)
Energy Efficient sub-Terahertz Electrical Interconnect
- **Ali Khalatpour** (Q. HU)
New Frontiers in THz Quantum Cascade Lasers
- **Harneet Khurana** (A. CHANDRAKASAN/H.-S. LEE)
Energy Efficient SAR ADC with Resolution Enhancement for Sensor Signals
- **Zheng Li** (J. LANG)
Computational Raman Imaging and Thermography
- **Ji Lin** (S. HAN)
Efficient Algorithms and Systems for Tiny Deep Learning
- **Sirma Orguc** (A. CHANDRAKASAN)
Programmable Interfaces for Biomedical and Neuroscience Applications
- **Pin-Chun Shen** (J. KONG)
Ohmic Contact to Monolayer Semiconductors
- **Robin Singh** (A. AGARWAL)
Integrated Bio-Photonic Devices: Sensors, Imagers, and Beyond
- **Haozhe Wang** (J. KONG)
Graphene-metal Interactions Beyond Van der Waals Force
- **Dan Wu** (J. VOLDMAN)
Microfluidic and Electronic Detection of Protein Biomarkers
- **Jin Xue** (R. RAM)
A Small, Bright Silicon Light-Emitting Diode Directly Integrated with Microelectronics
- **Tien-Ju Yang** (V. SZE)
Hardware-Aware Efficient Deep Neural Network Design
- **Yifei Zhang** (J. HU)
Reconfigurable Photonics based on Broadband Low Loss Optical Phase Change Materials

Glossary

TECHNICAL ACRONYMS

ADC	Analog-to-Digital Converters
CMOS	Complementary Metal–Oxide–Semiconductor
CNT	Carbon Nanotubes
ECP	Electro-chemical Plating
FET	Field-effect Transistor
HSQ	Hydrogen Silsesquioxane
InFO	Integrated Fan Out
MOSFET	Metal–Oxide–Semiconductor Field-effect Transistor
nTRON	Nanocryotron
RDL	Re-distribution Layers
RIE	Reactive ion etching
SNSPDs	Superconducting nanowire single photon detectors
SS	Subthreshold swing
TMAH	Tetramethylammonium Hydroxide
TREC	Thermally regenerative electrochemical cycle

MIT ACRONYMS & SHORTHAND

BE	Department of Biological Engineering
Biology	Department of Biology
ChemE	Department of Chemical Engineering
CICS	Center for Integrated Circuits and Systems
CMSE	Center for Materials Science and Engineering
↑ IRG	Interdisciplinary Research Group
DMSE	Department of Materials Science & Engineering
EECS	Department of Electrical Engineering & Computer Science
ISN	Institute for Soldier Nanotechnologies
KI	David H. Koch Institute for Integrative Cancer Research
LL	Lincoln Laboratory
MAS	Program in Media Arts & Sciences
MechE	Department of Mechanical Engineering
MEDRC	Medical Electronic Device Realization Center
MIT-CG	MIT/MTL Center for Graphene Devices and 2D Systems
MITEI	MIT Energy Initiative
MIT-GaN	MIT/MTL Gallium Nitride (GaN) Energy Initiative

MISTI	MIT International Science and Technology Initiatives
MIT-SUTD	MIT-Singapore University of Technology and Design Collaboration Office
MIT Skoltech	MIT Skoltech Initiative
MTL	Microsystems Technology Laboratories
NSE	Department of Nuclear Science & Engineering
Physics	Department of Physics
Sloan	Sloan School of Management
SMA	Singapore-MIT Alliance
↑ SMART	Singapore-MIT Alliance for Research and Technology Center
↑ SMART-LEES	SMART Low Energy Electronic Systems Center
SUTD-MIT	MIT-Singapore University of Technology and Design Collaboration Office
UROP	Undergraduate Research Opportunities Program

U.S. GOVERNMENT ACRONYMS

AFOSR	U.S. Air Force Office of Scientific Research
↑ FATE-MURI	Foldable and Adaptive Two-dimensional Electronics Multidisciplinary Research Program of the University Research Initiative
AFRL	U.S. Air Force Research Laboratory
ARL	U.S. Army Research Laboratory
↑ ARL-CDQI	U.S. Army Research Laboratory Center for Distributed Quantum Information
ARO	Army Research Office
ARPA-E	Advanced Research Projects Agency - Energy (DOE)
DARPA	Defense Advanced Research Projects Agency
↑ DREaM	Dynamic Range-enhanced Electronics and. Materials
DoD	Department of Defense
DoE	Department of Energy
↑ EFRC	U.S. Department of Energy: Energy Frontier Research Center (Center for Excitonics)
DTRA	U.S. DoD Defense Threat Reduction Agency
IARPA	Intelligence Advanced Research Projects Activity
↑ RAVEN	Rapid Analysis of Various Emerging Nanoelectronics
NASA	National Aeronautics and Space Administration
↑ GSRP	NASA Graduate Student Researchers Project
NDSEG	National Defense Science and Engineering Graduate Fellowship
NIH	National Institutes of Health
↑ NCI	National Cancer Institute
NNSA	National Nuclear Security Administration

NRO	National Reconnaissance Office
NSF	National Science Foundation
↑ CBMM	NSF Center for Brains, Minds, and Machines
↑ CIQM	Center for Integrated Quantum Materials
↑ CSNE	NSF Center for Sensorimotor Neural Engineering
↑ E3S	NSF Center for Energy Efficient Electronics Science
↑ GRFP	Graduate Research Fellowship Program
↑ IGERT	NSF The Integrative Graduate Education and Research Traineeship
↑ NEEDS	NSF Nano-engineered Electronic Device Simulation Node
↑ SEES	NSF Science, Engineering, and Education for Sustainability
↑ STC	NSF Science-Technology Center
ONR	Office of Naval Research
↑ PECASE	Presidential Early Career Awards for Scientists and Engineers

OTHER ACRONYMS

CNRS Paris	Centre National de la Recherche Scientifique
CONACyT	Consejo Nacional de Ciencia y Tecnología (Mexico)
IEEE	Institute of Electrical and Electronics Engineers
IHP Germany	Innovations for High Performance Microelectronics Germany
KIST	Korea Institute of Science and Technology
KFAS	Kuwait Foundation for the Advancement of Sciences
MASDAR	Masdar Institute of Science and Technology
NTU	Nanyang Technological University
NUS	National University of Singapore
NYSCF	The New York Stem Cell Foundation
SRC	Semiconductor Research Corporation
↑ NEEDS	NSF/SRC Nano-Engineered Electronic Device Simulation Node
SUTD	Singapore University of Technology and Design
TEPCO	Tokyo Electric Power Company
TSMC	Taiwan Semiconductor Manufacturing Company



**IN APPRECIATION OF OUR
MICROSYSTEMS INDUSTRIAL GROUP
MEMBER COMPANIES:**

Analog Devices, Inc.	IBM
Applied Materials	Lam Research
Draper	NEC
Edwards	TSMC
HARTING	Texas Instruments
Hitachi High-Tech Corporation	

AND MIT.NANO CONSORTIUM MEMBER COMPANIES:

Agilent Technologies	IBM
Analog Devices, Inc.	Lam Research
Dow	NCSOFT
Draper	NEC
DSM	Oxford Instruments Asylum Research
Edwards	Raith
Fujikura	Waters